AD-A118 165 NAVAL OCEAN RESEARCH AND DEVELOPMENT ACTIVITY NSTL S--ETC F/G 20/1
VOLUME REVERBERATION MEASUREMENTS IN THE EASTERN CARRIBEAN SEA.(U)
NOV 81 C LEVENSON, R A LOVE, M A WILSON

UNCLASSIFIED NORDA-TN-128 NL

1 OF 2
AD A
118165

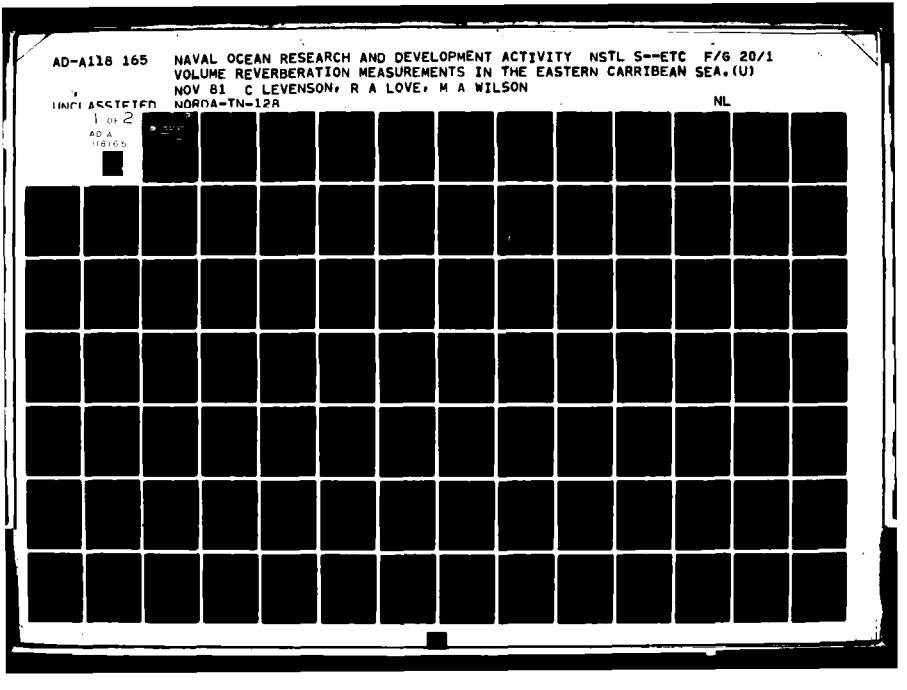

AD A118165

NORDA Technical Note 128

Naval Ocean Research
and Development Activity
NSTL Station, Mississippi 39529

Volume Reverberation Measurements in the Eastern Caribbean Sea

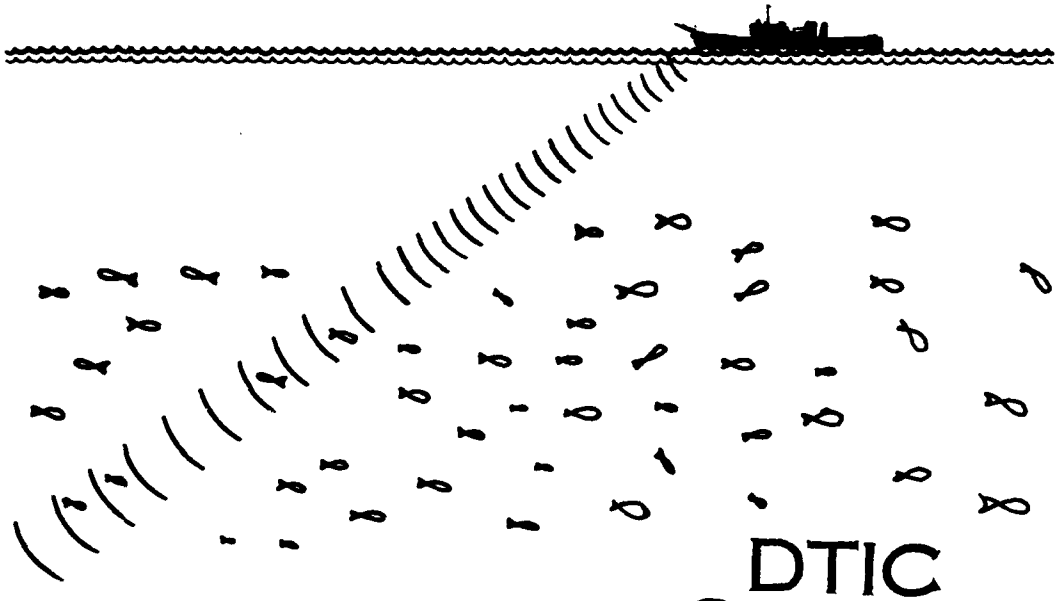

DTIC FILE COPY

DTIC
ELECTE
AUG 13 1982
S D
D

Coleman Levenson
Richard H. Love
Marcia A. Wilson
Robert A. Fisher

Ocean Acoustics Division
Ocean Science and Technology Laboratory

November 1981

DISTRIBUTION STATEMENT A
Approved for public release;
Distribution Unlimited

82 08 13 062

ABSTRACT

Volume reverberation measurements were made utilizing explosive sources and an omnidirectional receiver in the Caribbean Sea along the Aves Ridge during June 1974 and February through March 1977. This report presents results of those measurements in the form of scattering strength profiles and column strengths for one-third octave bands. Comparisons are made between the two sets of data and previous data taken in the same area. Discrete biological net tows at one station are also compared to peak scattering depths.

Accession For	
NTIS GRA&I	☒
DTIC TAB	☐
Unannounced	☐
Justification	
By	
Distribution/	
Availability Codes	
Dist	Avail and/or Special
A	

DTIC COPY INSPECTED 2

ACKNOWLEDGEMENTS

This work has been partially supported by the Naval Material Command Marine Biosciences Program administered by the Naval Ocean Systems Center.

CONTENTS

TABLES

ILLUSTRATIONS

I. INTRODUCTION

When sound is propagated in an ocean medium, any inhomogeneities will scatter a portion of the sound. This scattered sound is termed volume reverberation and is primarily caused by biological scatterers. Owing to movement, growth and proclivity of these organisms, volume reverberation varies with season, geographic location, time of day, depth, and acoustic frequency.

Measurements of volume reverberation levels were made for the Caribbean Sea Acoustic Project (CARIBCAP)* along the Aves Ridge during June 1974 (CARIBCAP I) and February through March 1977 (CARIBCAP II). Figure 1 shows station locations. Stations 4 through 8 were occupied in 1974 and Stations 1 through 7 in 1977. Day and night acoustic measurement sequences were conducted at each station. Limited biological sampling was conducted at Station 4 of CARIBCAP I. Table I gives dates and locations of each measurement sequence.

Volume reverberation measurements were made in one-third octave bands from 1.0 to 20.0 kHz utilizing surface vented explosive sources and an omnidirectional receiver. This report presents results of those measurements, examines geographic and seasonal variations in reverberation levels and relates these data to previous acoustic measurements made in the same general areas.

II. ACOUSTIC THEORY

The fundamental quantity of volume reverberation is the backscattering coefficient of a unit volume of ocean, M, which is the ratio of scattered intensity at a unit distance from the unit volume to the incident intensity [1]. M is generally assumed, at least for purposes of calculation, to be only a function of depth, z. The scattering strength of a unit volume of ocean at depth, z, $S_v(z)$, is then defined as

$$S_v(z) = 10 \log M(z). \tag{1}$$

Integrated scattering strength as a function of depth, $S_c(z)$, is defined as

$$S_c(z) = 10 \log \left[\int_0^z M(z)dz \right]. \tag{2}$$

Integrated scattering strength of the complete water column, or column scattering strength, S_c, is defined as

$$S_c = 10 \log \left[\int_0^d M(z)dz \right], \tag{3}$$

where d is the depth of deepest scatterers. In MKS units, $S_v(z)$, $S_c(z)$ and S_c are scattering strengths in decibels of volumes which are 1 m^3, 1 m^2 x z m and 1 m^2 x d m, respectively.

*CARIBCAP is an unofficial designation for these measurements that was adopted for convenience when discussing this Caribbean Sea Acoustic Project. This designation will be used throughout this report.

The parameter measured in experiments employing an omnidirectional source and receiver is the integrated scattering strength, $S_c(z)$, which can be calculated from:

$$S_c(z) = 20 \log p(t) + 30 \log t - 10 \log E + \alpha ct - k, \tag{4}$$

where t is time after detonation, p(t) is received pressure level in analysis bandwidth at time t, E is source energy in analysis bandwidth, α is an absorption coefficient, c is speed of sound and k is a constant which depends on experimental configuration and units of the various terms [2]. Two equations were utilized to calculate α; Thorpe's [3] for frequencies from 1.0 to 4.0 kHz and Schulkin and Marsh's [4] for frequencies from 5.0 to 20.0 kHz.

Estimates of $S_v(z)$ can be obtained from $S_c(z)$ by utilizing a numerical differentiation procedure [5]. At any depth z_1,

$$S_c(z_1) = 10 \log \left[\int_0^{z_1} M(z)dz \right] . \tag{5}$$

If it is assumed that M(z) is constant over $0 \leq z \leq z_1$ and $M(z) = \overline{M(z_1)}$, where the bar denotes the average over depth, then the integration in equation 5 can be performed to give

$$S_c(z_1) = 10 \log \overline{M(z_1)} z_1 , \tag{6}$$

from which the value of $\overline{M(z_1)}$ can be determined. Similarly, if over the interval $z_1 \leq z \leq z_2$, it is assumed that $M(z) = \overline{M(z_2)}$, then

$$S_c(z_2) = 10 \log \left[\int_0^{z_2} M(z)dz \right]$$

$$= 10 \log \left\{ \overline{M(z_2)} \ [z_2 - z_1] + \overline{M(z_1)} z_1 \right\} , \tag{7}$$

and the value of $\overline{M(z_2)}$ can be determined. In general then,

$$S_c(z_n) = 10 \log \sum \overline{M(z_n)} \left[z_n - z_{n-1} \right] \tag{8}$$

Thus, $\overline{M(z_n)}$ can be determined and

$$S_v(z_n) = 10 \log \overline{M(z_n)} . \tag{9}$$

III. DATA COLLECTION

Each explosive source volume reverberation measurement sequence consisted of approximately six shots, at about ten minute intervals near midday or midnight. Sources were 0.25 kg blocks of TNT electrically detonated at a depth of 0.5 m.

(Source levels of these blocks at this depth were measured by the Naval Ordnance Laboratory [6].) Scattered acoustic signals were received on a broadband omnidirectional F-50 hydrophone at a depth of 10 m. Hydrophones were obtained from the Naval Research Laboratory Underwater Sound Reference Division, where their free-field voltage sensitivities were calibrated both before and after measurements. Horizontal distances between source and receiver were approximately 10 m. Acoustic signals received by the hydrophone were filtered, amplified and analog recorded on a magnetic tape on three separate channels with an approximate 10 dB per channel difference in amplification. Recorded data were simultaneously monitored on a logarithmic graphic level recorder.

During each acoustic sequence, weather, wind, and sea conditions were noted and the temperature profile measured with an expendable bathythermograph (XBT). Salinity, temperature, depth (STD) profiles were also obtained at each station. Biological sampling was conducted at station 4 of CARIBCAP I using a 3m Isaacs-Kidd midwater trawl with a four-chambered, discrete-depth, cod-end sampler.

IV. DATA PROCESSING

A block diagram of the computer data analysis process is shown in Figure 2. Three channels of high, medium, and low amplification analog data were played into the A/D converter of a PDP-11 computer and digitized onto a fixed head disc. A total of 3.2 seconds of data, including approximately 0.4 seconds of ambient noise, was digitized at 42.0 kHz per channel. Figure 3 shows a typical three-channel broadband display of digitized voltage versus time, with each data point representing a 12.5 msec sample. The first peak in the figure is the direct signal, which is followed by reverberation. The second peak is bottom return. Broadband data were filtered into fourteen one-third octave bands between 1.0 and 20.0 kHz by passage through a discrete Fourier transform processor. Filtered data were then recorded on digital tape. The transform processor produced one data point every 25 msec. Calibration signals underwent similar processing.

Results of this processing are calibrated one-third octave plots of voltage versus time. This voltage is total voltage V_T, which is the sum of signal, V_S, and ambient noise voltage, V_N, and

$$V_T^2 = V_S^2 + V_N^2. \tag{10}$$

V_N is obtained by averaging a portion of the noise recorded prior to the direct signal.

In order to determine pressure at the hydrophone due to the scattered signal V_S was calculated for each data point utilizing equation 10 and p(t) was calculated as

$$20 \log p(t) = 20 \log V_S(t) - FFVS, \tag{11}$$

where FFVS is the hydrophone free-field voltage sensitivity. Results of these calculations were then plotted versus time. An example of such a plot is shown in Figure 4. Integrated scattering strength profiles, $S_C(z)$, were then calculated for each frequency band, channel, and shot of a sequence utilizing equation 4. Figure 5 shows a typical result. The increased level above 100 m is primarily due to the direct signal and surface reverberation. A shallow area will also show increased levels on these plots which is caused by bottom return. To be exact the $S_C(z)$ profiles contain both surface and bottom reverberation, however, for convenience the complete profile will be called the $S_C(z)$ profile. Three channels of

data were recorded to increase dynamic range of the recording system so that at short ranges, when the high-gain channel was clipped lower gain channels would not be. In most cases, the high-gain channel was used for analysis. Wide variations seen in the low gain channel below 800 m are caused when V_T approaches V_N.

After this processing, all shots in a sequence were compared and, after discarding any anomalous shots, averaged. Anomalies usually were caused by wave action, which infrequently would cause a shot to be detonated very near the surface. Average $S_C(z)$ profiles were then numerically differentiated utilizing the procedure given in equations 5 through 9 to produce $S_V(z)$ profiles. Since in theory integrated curves cannot decrease with depth, small negative changes in $S_C(z)$ profiles were smoothed by considering only points of increasing $S_C(z)$. Figure 6 shows an example of an $S_V(z)$ profile and the smoothed $S_C(z)$ profile from which it was calculated.

IV. RESULTS

A. OCEANOGRAPHIC CONDITIONS

This area is generally dominated by the Caribbean current, which flows from the southeast at speeds from 0.5 to 1.0 knot [7]. Bathythermograph (BT) and salinity, depth, temperature (STD) profiles indicate surface temperatures of 25° to 26° and salinities of around 36 parts per thousand, with little change throughout the area.

Figure 7 is a typical example of ray trace diagrams constructed from oceanographic data obtained at each station. These indicate no appreciable bending of rays or shadow zones occurred over the ranges analyzed.

B. SCATTERING STRENGTHS

Average $S_C(z)$ profiles for each station, time of day, and one-third octave band frequency between 1.0 and 20.0 kHz are shown in Appendix A. $S_V(z)$ profiles and smoothed $S_C(z)$ profiles from which they were obtained are shown in Appendix B. At some stations, in some frequency bands, the signal (V_T) approached ambient noise (V_N) very rapidly, and it was not possible to determine valid $S_C(z)$ values. In these cases $S_C(z)$ calculated profiles are shown in Appendix A but $S_V(z)$ profiles were not calculated. In all cases, $S_V(z)$ results were not calculated below 2.0 kHz due to very low scattering levels at these frequencies. Continual slow increases or decreases in some $S_C(z)$ profiles are caused by errors in measurements of ambient noise level (V_N).

The $S_C(z)$ and $S_V(z)$ profiles indicate layer strengths, depths, and diel changes for each frequency band and station. Although these profiles give a comprehensive description of volume scattering for each station, they are, by virtue of the large amount of data contained in them, cumbersome to use when making comparisons of scattering strengths at different frequencies and stations. In order to make these comparisons in a concise manner the column scattering strength, S_C, will be utilized. In addition, the depth of scatterers which contribute to S_C will be discussed. This is the depth d in equation 3. Due to the logarithmic nature of the $S_C(z)$ profiles, exact values of d are difficult to determine; however, small variations are not significant, and only general trends are considered.

Day and night S_C versus frequency curves for Stations 4 through 8 of CARIBCAP I are shown in Figures 8 through 12. S_C curves for Station 4 are shown in Figure 8. Night values are greater than day values at all frequencies where comparisons can

be made. Differences of 9 to 10 dB occur at 5.0 kHz and below. Above 5.0 kHz both curves are essentially similar with a maximum difference of 3 dB at 6.3 kHz. The day curve increases with frequency from 3.15 to 5.0 kHz and then remains generally constant. The night curve is flat to 3.15 kHz, rises to a peak at 5.0 kHz and then decreases slightly. Smoothed $S_c(z)$ and derived $S_v(z)$ curves in Appendix B show daytime scattering at depths from less than 100 m to about 700 m. Peak scattering occurs between 400 and 700 m in all but the 3.15 and 20.0 kHz bands. Nighttime scattering occurs to about 400 m with peaks generally above 200 m.

At Station 5 (Fig. 9) day and night curves show a maximum diel difference of 13 dB at 2.5 kHz. This difference decreases with frequency, until at 10.0 kHz, day S_c values become greater than night, with differences of 3 to 4 dB above 10.0 kHz. The day curve shows constant low values to 3.15 kHz, increases to a peak at 10.0 kHz and then remains essentially flat. The night curve increases to 3.15 kHz, remains fairly constant to 8.0 kHz, and then decreases. Profiles in Appendix B show that between 4.0 and 6.3 kHz day scattering occurs to between 700 and 800 m with peaks at 600 m. This deep layer fades at higher frequencies. Night scattering occurs above 300 m at all frequencies with peaks above 200 m.

Station 6 (Fig. 10) day S_c curve shows the same general shape as Station 5, increasing with frequency to a maximum at 10.0 kHz and then remaining fairly constant. The night S_c curve also shows generally the same shape as Station 5, with a range of 5 dB and a slight peak at 4.0 kHz. A maximum day-night difference of 16 dB occurs at 2.5 kHz. Profiles in Appendix B show day scattering occurs to 600 m at 3.15 kHz, 800 m from 4.0 to 6.3 kHz, and above 500 m at higher frequencies. At night, scattering is above 300 m at all frequencies.

At Station 7 (Fig. 11) the day S_c curve increases with frequency to a peak at 12.5 kHz and then decreases to 20.0 kHz. The night S_c curve has generally the same shape as those at Stations 5 and 6, with peaks occurring between 3.15 and 5.0 kHz and values for the entire curve having a range of 6 dB. A maximum day-night difference of 18 dB occurs at 3.15 kHz. Appendix B profiles show day scattering extending to between 700 and 800 m at frequencies between 6.3 and 12.5 kHz. Night scattering occurs to 300 m at all frequencies except 12.5 kHz, where it extends to 400 m.

Station 8 day-night curves (Fig. 12) show the same features as previous stations with the exception of a maximum day peak at 20.0 kHz. Above 10.0 kHz day values are slightly higher than night values. Day values remain constant to 5.0 kHz where they begin a gradual increase to 20.0 kHz. Night values are almost constant at all frequencies with a maximum 4 dB range between highest and lowest values. A maximum day-night difference of 11 dB occurs at 4.0 kHz. Appendix B profiles show day scattering extending to 700 m for frequencies of 4.0 kHz and above. At night, scattering extends to about 300 m at all frequencies.

CARIBCAP II day and night S_c versus frequency curves are shown in Figures 13 to 19. Station 1 curves (Fig. 13) show night S_c values greater than day values at all frequencies, with a maximum difference of 19 dB at 3.15 kHz. The day curve increases 11 dB from 3.15 to 5.0 kHz and then varies by no more than 3 dB at higher frequencies. Night values vary by a maximum of 5 dB throughout the frequency range. Profiles in Appendix B indicate day scattering at frequencies above 3.15 kHz generally extends to between 600 and 900 m, with peak scattering between 400 and 600 m. At night, scattering extends to between 300 and 500 m, with peak scattering above 200 m.

Station 2 (Fig. 14) shows day S_c values increase slowly from 4.0 to 20.0 kHz. The night S_c curve peaks at 8.0 kHz with an 8 dB range. Night S_c values are higher than day below 12.5 kHz; at higher frequencies there is little difference. Appendix B profiles show scattering extends as deep as 1200 m, with peak scattering between 400 and 600 m. Night scattering extends rather deep at this station, extending to almost 1000 m at 5.0 kHz. Peak night scattering is generally between 100 and 300 m.

At Station 3 (Fig. 15) the day S_c curve increases from 4.0 to 8.0 kHz and then remains fairly constant to 20.0 kHz. The night S_c curve increases from 2.0 kHz to a maximum at 5.0 kHz with a range of 11 dB between 2.0 and 20.0 kHz. Maximum day-night difference of 14 dB occurs at 4.0 kHz. At frequencies above 6.3 kHz differences are 3 dB or less. At frequencies above 4.0 kHz, Appendix B profiles show that day scattering extends to about 800 m, with peak scattering between 400 and 700 m. At night, scattering extends as deep as 600 m, with peak scattering above 300 m.

Station 4 (Fig. 16) shows day S_c values varying by a maximum 3 dB from 5.0 to 20.0 kHz with a maximum at 20.0 kHz. Night S_c values increase with frequency to a peak at 6.3 kHz and then vary by no more than 4 dB to 20.0 kHz. Maximum day-night difference is 9 dB at 5.0 kHz. Appendix B profiles show day scattering extending to 1000 m at 10.0 to 16.0 kHz and to 800 m at other frequencies. Peak day scattering is between 500 and 800 m. At night, scattering is above 500 m for frequencies below 10.0 kHz and extends to almost 800 m at the highest frequencies. Peak night scattering occurs between 100 and 400 m.

Station 5 (Fig. 17) shows day S_c values from 2.0 to 20.0 kHz. This is the only station of CARIBCAP II for which low frequency day S_c values were calculated. The low S_c value at 2.0 kHz increases 15 dB to a maximum at 8.0 kHz and then decreases slightly at higher frequencies. Night S_c values increase with frequency to 4.0 kHz and then decrease to 20.0 kHz. A day-night maximum difference of 18 dB occurs at 3.15 kHz. Appendix B profiles show day scattering extends to about 700 to 800 m at frequencies between 4.0 and 16.0 kHz. Peak day scattering is between 600 and 800 m for frequencies between 4.0 and 10.0 kHz and between 400 and 600 m at higher frequencies. At night, scattering is above 250 m at all frequencies.

Figure 18 shows Station 6 day and night S_c curves. These curves are similar to Station 4. The day S_c curve increases with frequency to a small peak at 8.0 kHz. At frequencies above 8.0 kHz, S_c values are fairly constant. At night, S_c values increase to a maximum at 5.0 kHz and then gradually decrease to 20.0 kHz. The maximum range for all frequencies is 8 dB. Maximum day-night difference is 12 dB at 4.0 kHz. Profiles in Appendix B show day scattering occurs primarily at 400 to 600 m with some additional scattering to 800 m occurring at 16.0 and 20.0 kHz. At night, scattering is above 300 m at all frequencies.

Station 7 S_c curves are shown in Figure 19. The day S_c curve increases to a peak at 10.0 kHz and then varies by about 3 dB to 20.0 kHz. The night S_c curve peaks at 5.0 kHz with equally low values at both ends of the frequency spectrum. Maximum day-night difference is at 4.0 kHz. At 10.0 kHz and above, day-night differences are about 3 dB. Appendix B profiles indicate day scattering extends to between 500 and 700 m, with no consistent peak scattering depth. Night scattering extends to between 250 and 500 m, with peak scattering below 200 m at low frequencies and above 200 m at higher frequencies.

C. MIDWATER FISHES

Limited biological sampling was conducted at Station 4 of CARIBCAP I. Two day tows were completed with discrete depth samples obtained at approximately 300, 400, 500 and 600 m, and oblique samples were obtained between 500 and 600 m, 300 and 400 m, 0 and 500 m, and 0 and 300 m. Three night tows were completed with discrete depth samples obtained at approximately 100, 200, 300, 400 and 450 m and oblique samples obtained between 400 and 450 m, 200 and 300 m, 0 and 400 m, 0 and 200 m, and 0 and 100 m.

Catches were dominated by fish of the genus Cyclothone, which comprised 57% of individuals captured. These fish occurred below 300 m during both day and night. Cyclothone are relatively inefficient sound scatterers, since swimbladders are usually regressed or absent in adults. In large numbers, however, these fish could increase scattering levels at higher frequencies.

Primary scatterers from 2.0 to 20.0 kHz are swimbladder-bearing fishes. Principal swimbladdered species caught are listed in Table II. Myctophids were most abundant of these fishes. They were caught below 500 m during day and around 100 m at night. Gonostomatids and sternoptychids were other principal families of swimbladder fish caught. These were caught between 300 and 400 m during day and between 100 and 400 m at night.

Depths at which swimbladder-bearing species were caught agree well with depths of peak scattering at this station: between 400 and 700 m during the day and above 200 m at night.

VI. DISCUSSION

Figure 20 compares all CARIBCAP I day S_c versus frequency curves. Between 2.0 and 3.15 kHz, S_c values for all stations except Station 8 are below -60 dB. Above 10.0 kHz, S_c values for all stations except Station 7 are above -50 dB. Except for low frequencies at Station 8, S_c values at Stations 7 and 8 are generally less than those at Stations 4, 5, and 6. The range between highest and lowest S_c values for all stations at a given frequency is between 4 and 9 dB. However, the range for Stations 4, 5, and 6 is only 1 to 4 dB.

Night S_c versus frequency curves for CARIBCAP I are compared in Figure 21. All curves begin near -50 dB at 2.0 kHz, increase slightly to peaks around 4.0 kHz, generally decrease with increasing frequency back to about -50 dB at 16.0 kHz and then increase to 20.0 kHz. Above 4.0 kHz, S_c values at Stations 7 and 8 are slightly lower than Stations 4, 5, and 6. If Station 4 is excluded, there is little variation in shape or level of curves from station to station. The range between highest and lowest S_c values for all stations at a given frequency is between 3 and 6 dB. If Station 4 is excluded it is between 0 and 4 dB.

Conclusions that can be drawn for CARIBCAP I are that geographic variation in S_c values are small; Stations 5 and 6 are similar; and Stations 7 and 8, the northern stations, generally have slightly lower S_c values than other stations at frequencies above 4.0 kHz.

CARIBCAP II day S_c versus frequency curves are shown in Figure 22. These curves are all similar in shape, generally increasing with frequency to about 6.3 kHz and then remaining fairly constant to 20.0 kHz. Between 6.3 and 20.0 kHz, S_c values are generally between -50 and -55 dB, except for Station 2 which is several dB higher. The range between highest and lowest S_c values for all stations is

between 3 and 9 dB for frequencies of 4.0 kHz and higher. If Station 2 is excluded it is between 1 and 7 dB.

Figure 23 compares night S_c versus frequency curves of CARIBCAP II. These curves generally begin between -50 and -55 dB at 2.0 kHz, increase with frequency from -43 to -45 dB at 4.0 or 5.0 kHz, decrease back to between -50 and -55 dB at 16.0 kHz and then increase to 20.0 kHz. Station 2 is an exception in that it peaks at 8.0 kHz. The range between highest and lowest S_c values at a given frequency is between 3 and 7 dB.

The conclusion that can be drawn for CARIBCAP II is that geographic variations in S_c values are even smaller than for CARIBCAP I with only Station 2 being slightly atypical.

Figures 24 through 27 compare S_c versus frequency curves of CARIBCAP I and II Stations 4 through 7, respectively. Seasonal differences at night at all stations are quite small, with no difference greater than 4 dB and most 2 dB or less. During the day the summer S_c values (CARIBCAP I) are generally several dB higher than winter values (CARIBCAP II), particularly at frequencies above 6.3 kHz. A comparison of average curves of all CARIBCAP I and II stations (Fig. 28) indicates that this is valid, not only for individual stations, but all along the Aves Ridge.

Previous column strength data from the eastern Caribbean Sea were obtained by the Naval Oceanographic Office (NAVOCEANO) in January 1968 along 65.5°W at 12°N, 14.5°N, and 17°N [8]. The Canadian Defence Research Establishment Atlantic (DREA) obtained data somewhat to the west along 15°N at 70°W and 72°W [9]. These data are compared to CARIBCAP data in Figures 29 through 33. DREA values of S_c are several dB higher than CARIBCAP Station 4 values for both day and night at frequencies above 8.0 kHz (Figs. 31 and 32). NAVOCEANO values of S_c are increasingly higher than both DREA and CARIBCAP values at frequencies above 5.0 kHz during the day and above 8.0 kHz at night in all cases.

At about 15°N, S_c values at higher frequencies were lowest in February 1977, with increasingly higher values in June 1974, November 1969, and January 1968. These differences could be attributed to either seasonal, annual, or long-term variations, or some combination. If differences are seasonal, then January scattering levels are much higher than February, with June and November levels intermediate. If differences are due to a nine-year decrease in scattering levels, the decrease between January 1968 and November 1969 is more than that between November 1969 and February 1977 at 16.0 and 20.0 kHz. Differences are probably due to both seasonal and annual variations, with possibly some long-term decrease.

VII. SUMMARY

During June 1974 and February through March 1977 volume reverberation measurements were made along and across the Aves Ridge in the Caribbean Sea. Acoustic measurements were made utilizing surface-vented explosive sources and a shallow omnidirectional hydrophone. Signals were analog recorded on magnetic tape and digitized in the laboratory utilizing a PDP 11 computer. One-third octave band profiles of integrated scattering strength, $S_c(z)$, and corresponding column scattering strengths, S_c, were calculated. $S_c(z)$ profiles were then numerically differentiated to produce profiles of scattering strength per unit volume, $S_v(z)$. Results show very little geographic or seasonal change for both day and night scattering. Day S_c versus frequency curves generally increase with frequency to between 5.0 and 10.0 kHz and then remain relatively constant. Night curves do not vary greatly with frequency, with small peaks in the neighborhood of 5.0 kHz. Maximum diel

differences occur at low frequencies with little day-night spread in values above 8.0 kHz. Depths of peak scattering strengths are generally between 400 and 800 m during the day and above 300 m at night. Biological sampling at one station in 1974 showed that depths at which swimbladder-bearing mid-water fishes were abundant agreed well with depths of peak scattering strengths.

Comparison with previous data indicate differences which could be attributed to a combination of seasonal, annual, or long-term variations in scattering.

REFERENCES

[1] Machlup, S. and J. B. Hersey, Analysis of Sound-Scattering Observations from Non-Uniform Distributions of Scatterers in the Ocean, Deep Sea Res. 3, 1-22, 1955.

[2] Marshall, J. R. and R. P. Chapman, Reverberation from a Deep Scattering Layer Measured with Explosive Sound Sources, J. Acoust. Soc. Am. 36, 164-167, 1964.

[3] Thorpe, W. H., Analytic Description of Low Frequency Attenuation Coefficient, J. Acoust. Soc. Am. 42, 270, 1967.

[4] Shulkin, M. and H. W. Marsh, Sound Absorption in Sea Water, J. Acoust. Soc. Am. 34, 864-865, 1962.

[5] Love, R. H., Progress in the Correlation of Volume Scattering Strengths to Biological Data, in Oceanic Sound Scattering Prediction, N. R. Andersen and B. J. Zahuranec (EDS.), Plenum Press, New York, p. 631-646, 1977.

[6] Slifko, J. P., Naval Ordnance Lab. Letter, Ser. 243:JPS:caf, 13 Dec 1971.

[7] Bialek, E. L., Handbook of Oceanographic Tables, NAVOCEANO, Washington, D.C., SP-68, 1966.

[8] Farquhar, G. B., Biological Sound Scattering in the Oceans: A Review, in Oceanic Sound Scattering Prediction, N. R. Andersen and B. J. Zahuranec (EDS.) Plenum Press, New York, p. 493-527, 1977.

[9] Chapman, R. P., O. Z. Bluy, R. H. Adlington and A. E. Robinson, Deep Scattering Layer Spectra in the Atlantic and Pacific Oceans and Adjacent Seas, J. Acoust. Soc. Am., 56, 1772-1734, 1974.

TABLE I

STATION LOCATIONS

CARIBCAP I

STATION	DATE	LAT (N)	LONG (W)
4 Day	3 June 74	15°05'	63°58'
4 Night	4 " "	14°59'	63°55'
5 Day	6 " "	15°11'	63°10'
5 Night	6 " "	15°09'	63°00'
6 Day	7 " "	13°14'	63°47'
6 Night	7 " "	13°15'	63°44'
7 Day	11 " "	17°05'	64°05'
7 Night	10 " "	17°01'	63°57'
8 Day	12 " "	17°32'	65°25'
8 Night	12 " "	17°30'	65°20'

CARIBCAP II

1 Day	3 Mar 77	12°02'	63°02'
1 Night	3 " "	12°01'	63°03'
2 Day	2 " "	12°02'	64°00'
2 Night	2 " "	12°04'	64°01'
3 Day (1)	4 " "	13°15'	62°55'
3 Day (2)	5 " "	13°16'	62°54'
3 Night	4 " "	13°14.6'	62°55.4'
4 Day	28 Feb 77	15°00	63°48'
4 Night	27 " "	14°59.3'	63°50.6'
5 Day	27 " "	15°10.5'	63°00
5 Night	27 " "	15°14.6'	63°01.8'
6 Day	1 Mar 77	13°13.4'	63°47.2'
6 Night	1 " "	13°15'	63°45'
7 Day	26 Feb 77	17°00	64°00'
7 Night	25 Feb 77	16°58.9	64°00

TABLE II

PRINCIPAL SWIMBLADDER-BEARING MID-WATER FISH CAPTURED AT STATION 4 OF CARIBCAP I*

	Percentage of total swimbladder bearing individuals	Depths of Maximum Abundance	
		Day	Night
MYCTOPHIDAE			
Lepidophanes guentheri	23	600m	100m
Diaphus splendidus	15	500-600	100
Diaphus dumerilil	7	500-600	100
Myctophum affine	3	500-600	100
Hygophum macrochir	3	600	100
Notolychnus valdiviae	3	500	100
Diaphus brachycephalus	3	-	200
Ceratoscopelus warmingii	3	-	0-100
GONOSTOMATIDAE			
Valenciennellus tripunctulatus	10	400	400
Vinciguerria poweriae	3	-	100
STERNOPTYCHIDAE			
Argyropelecus aculeatus	7	400	200-300
Argyropelecus hemigymnus	2	300-400	400

*Species which comprise at least 2% of all swimbladder-bearing fish captured.

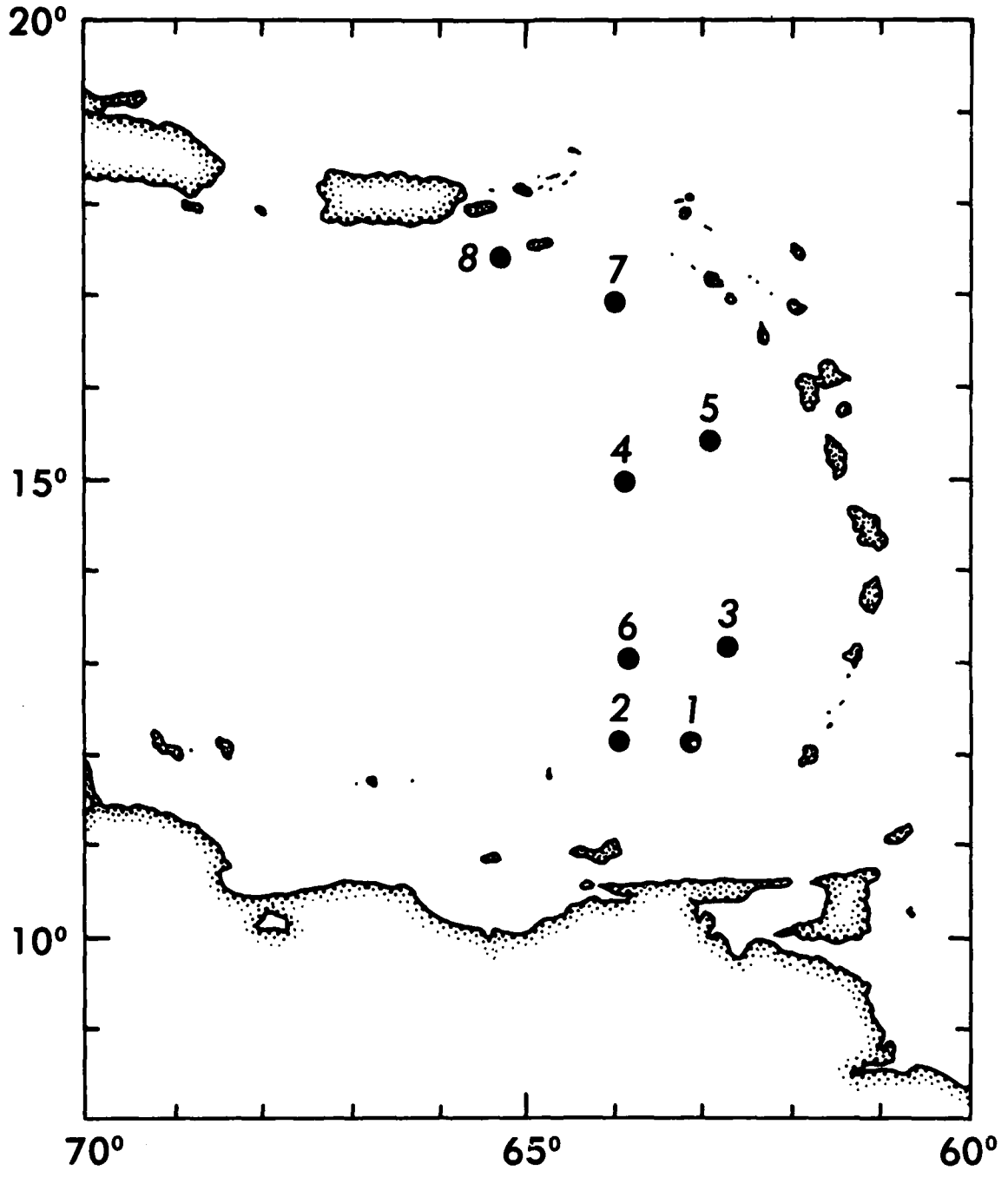

Figure 1. Station locations, CARIBCAP I and II

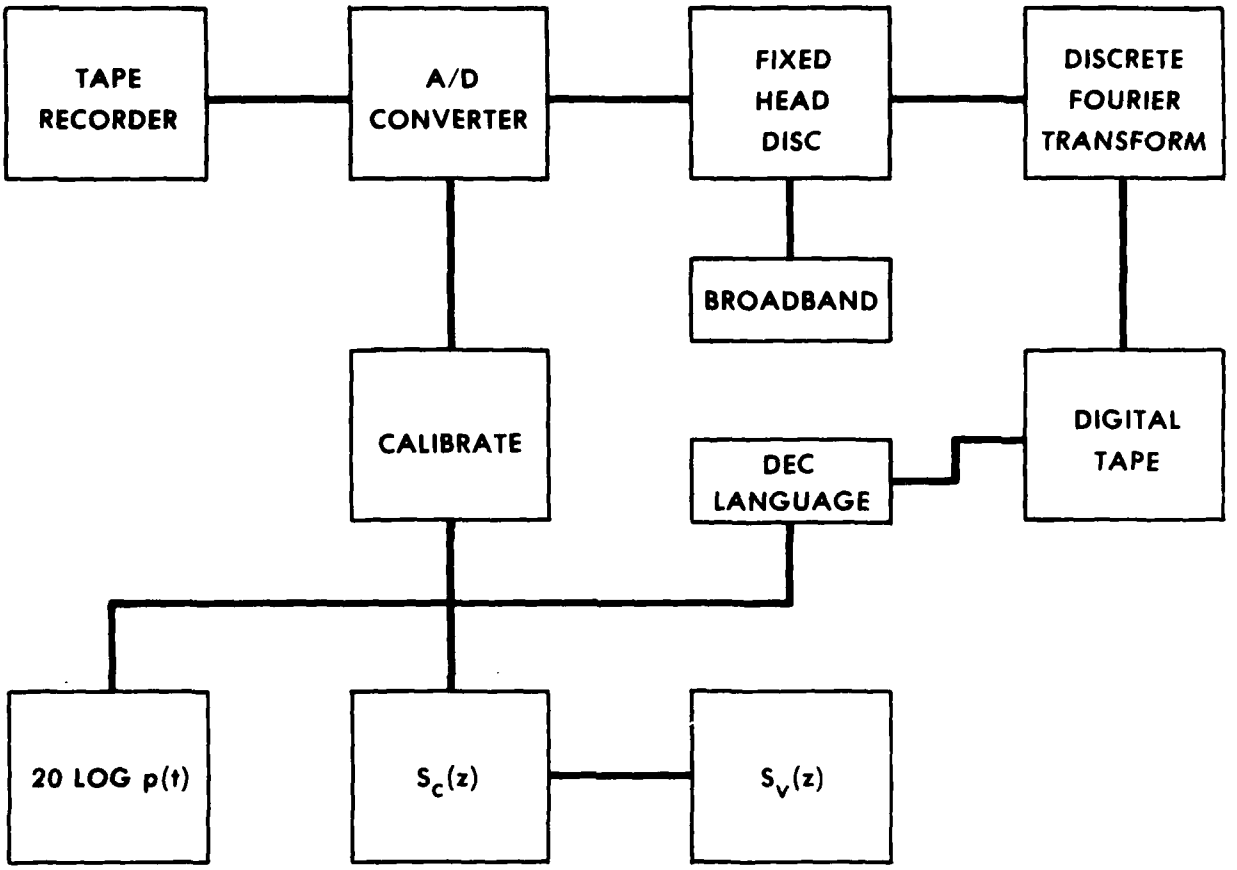

Figure 2. Block diagram of computer analysis

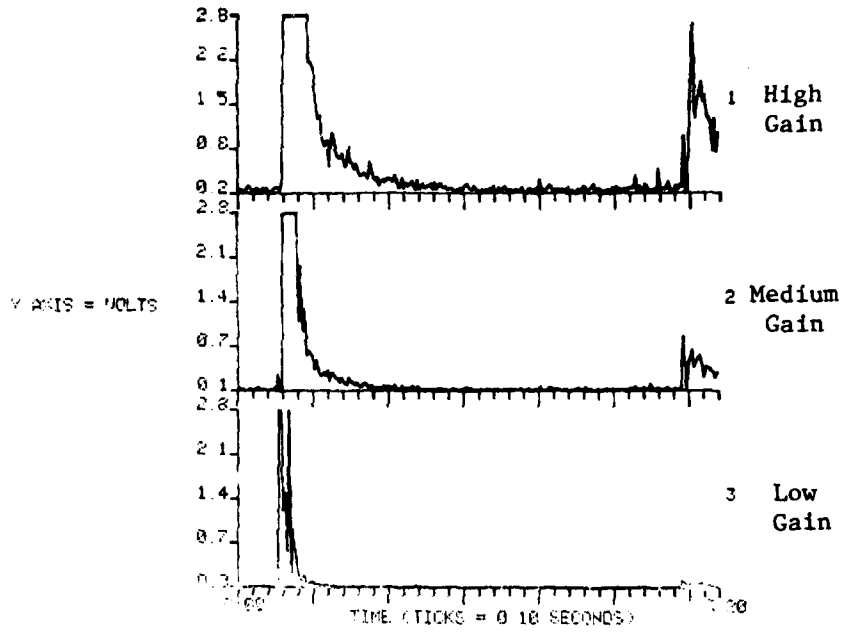

Figure 3. Typical three channel broadband display

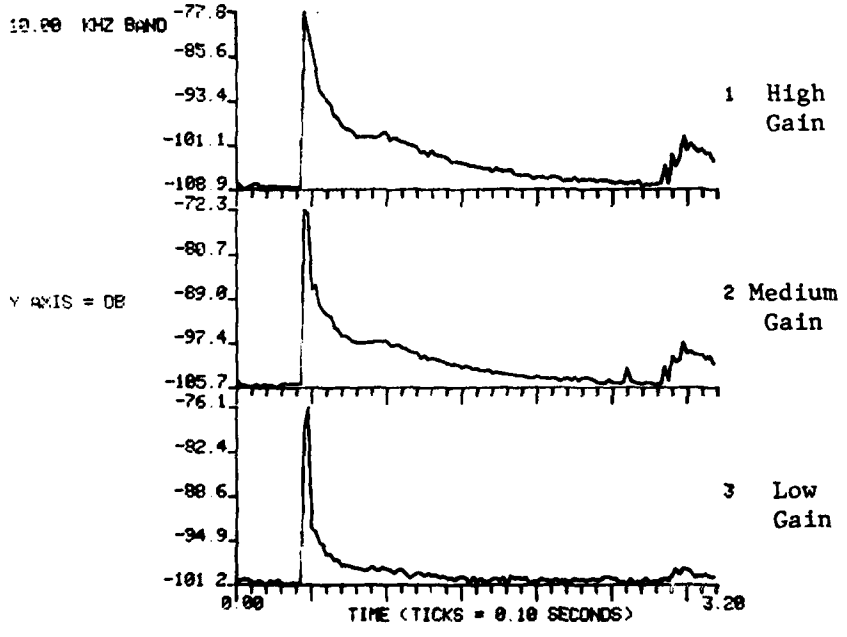

Figure 4. Example of calibrated shot in 10kHz band

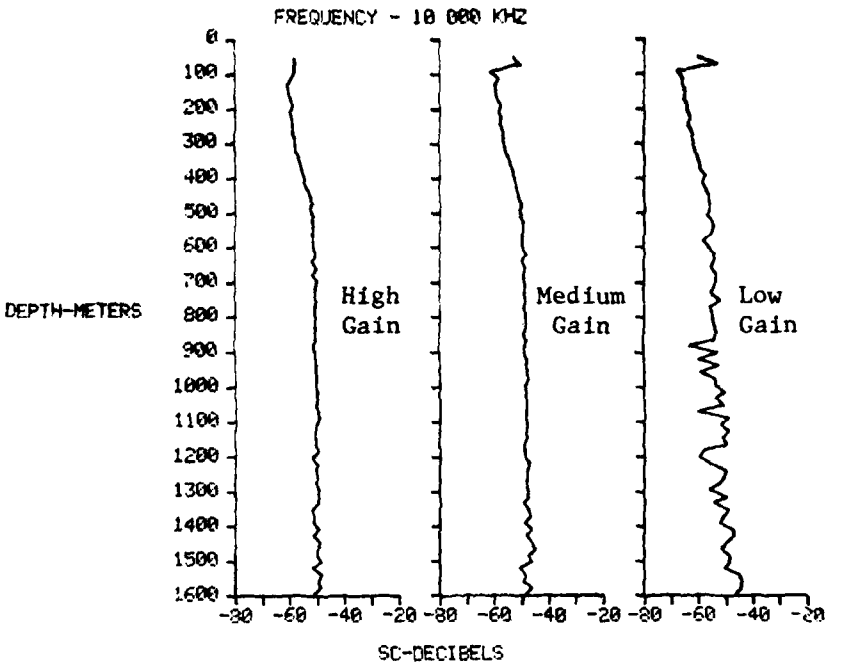

Figure 5. Example of average $S_c(z)$ with high, medium and low gain channels

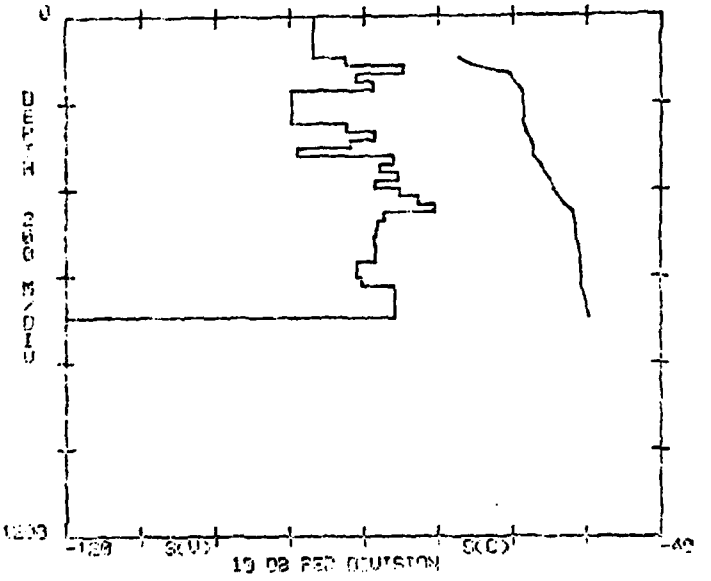

Figure 6. Example of average $S_v(z)$ and smoothed $S_c(z)$

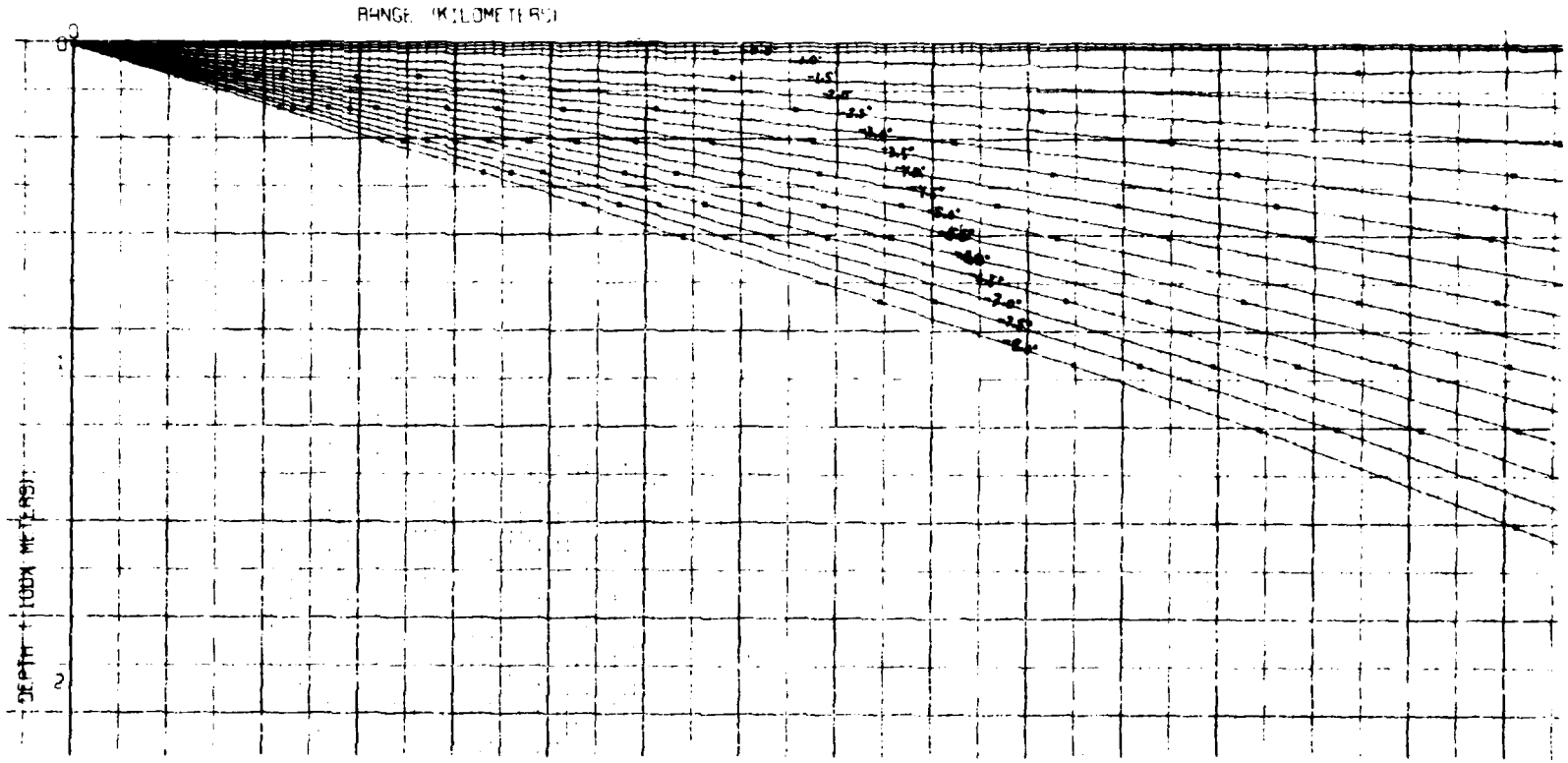

Figure 7. Typical ray trace diagram

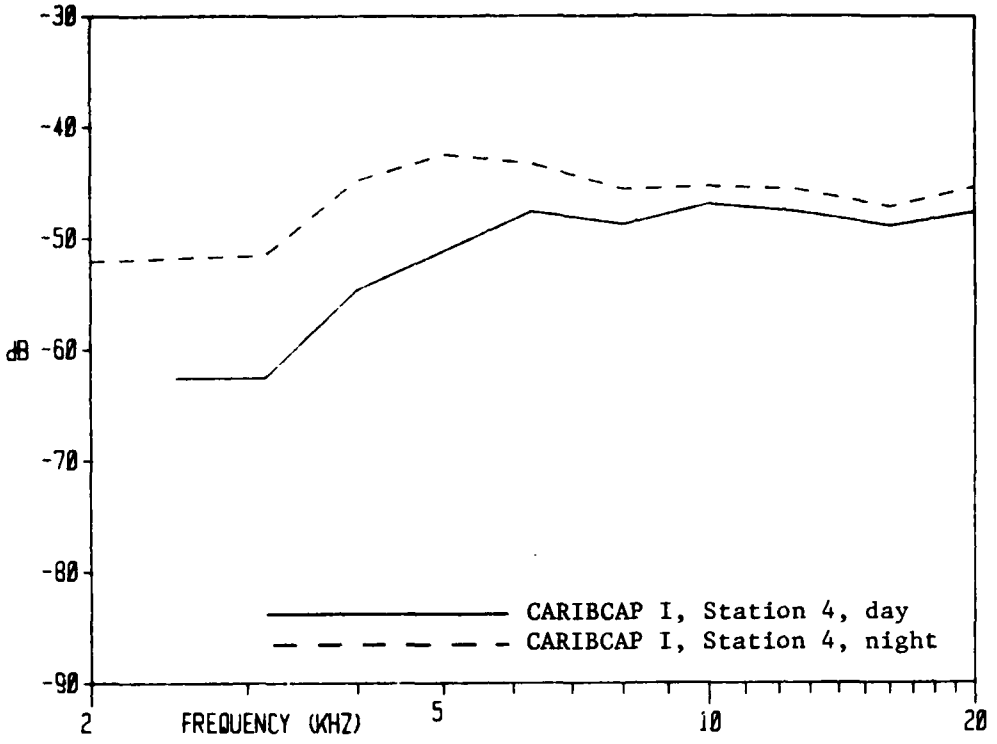

Figure 8. S_c vs. frequency, Station 4, day-night

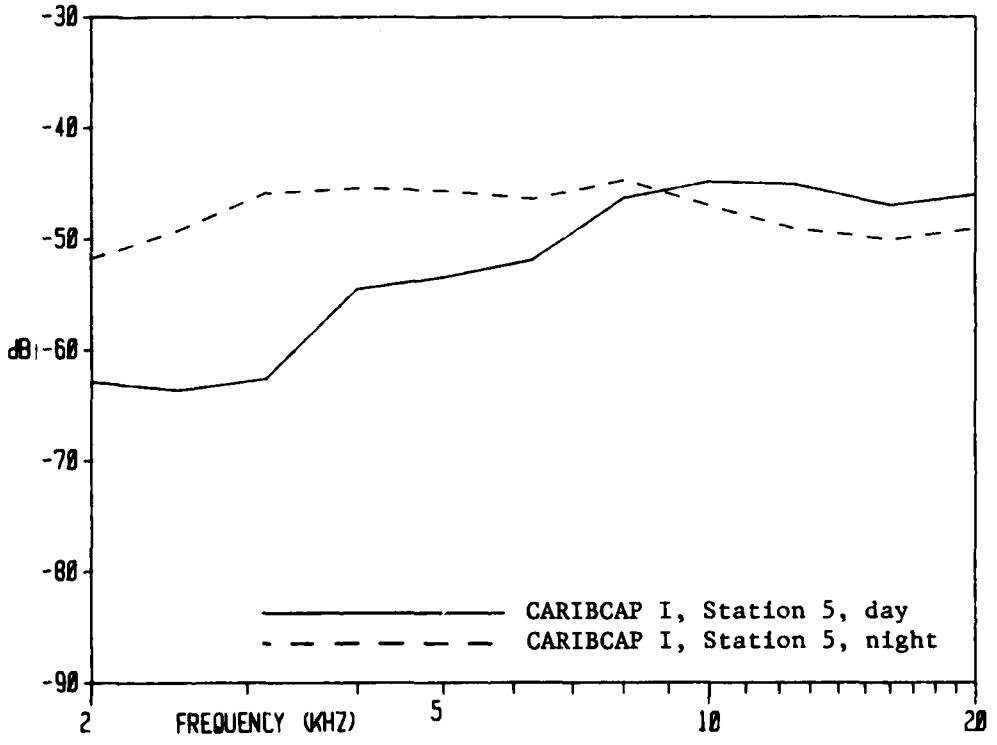

Figure 9. S_c vs. frequency, Station 5, day-night

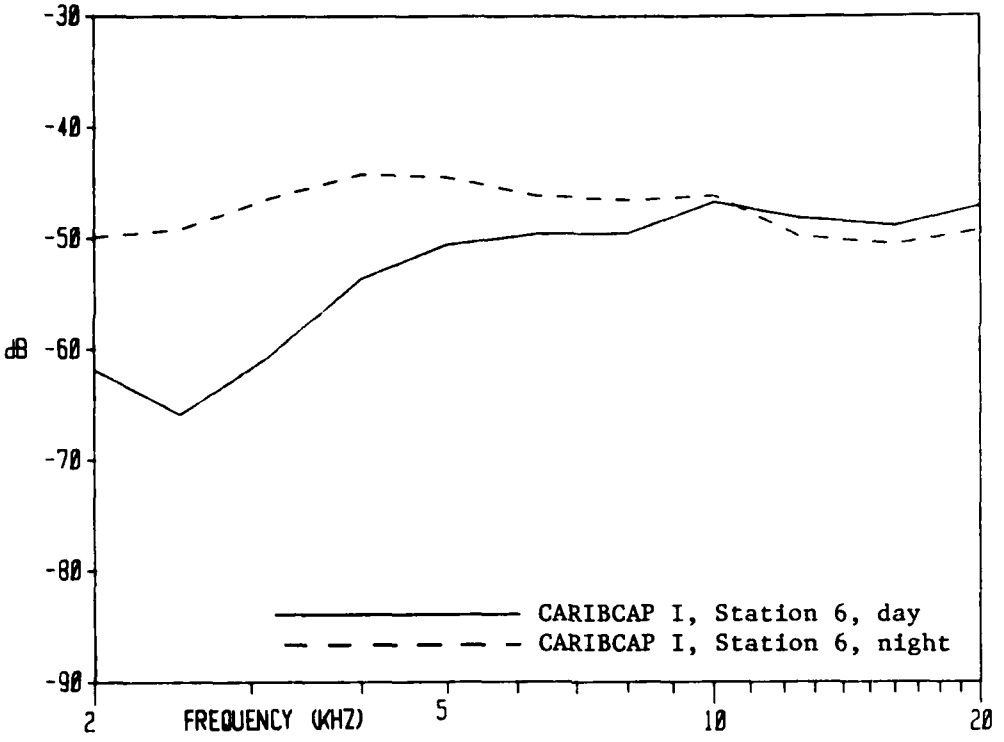

Figure 10. S_c vs. frequency, Station 6, day-night

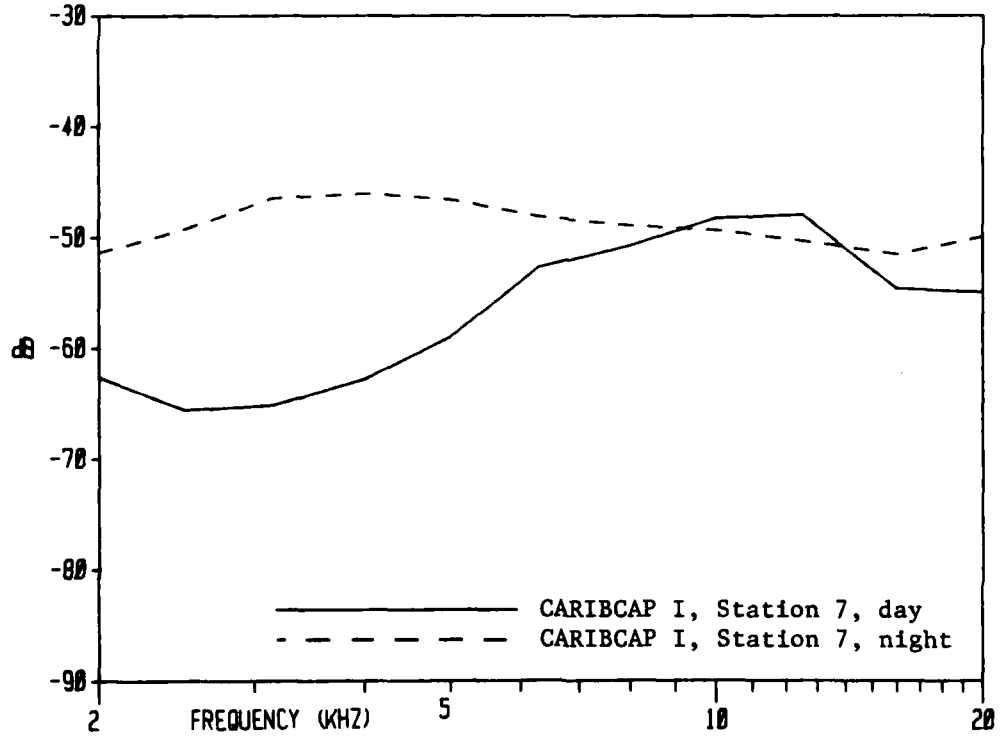

Figure 11. S_c vs. frequency, Station 7, day-night

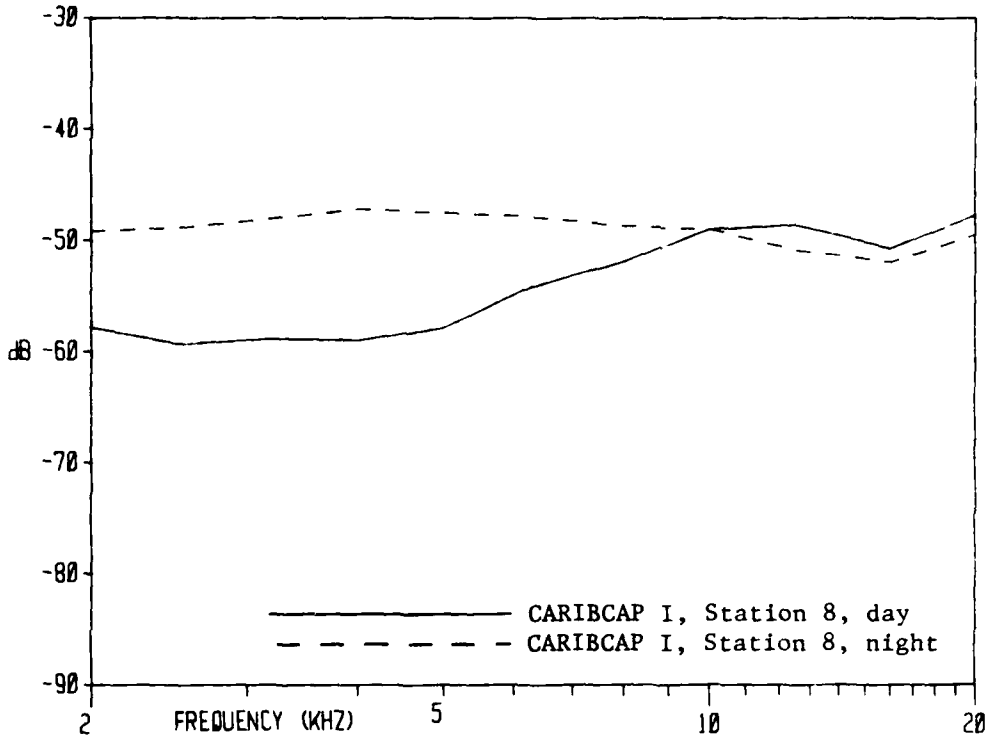

Figure 12. S_C vs. frequency, Station 8, day-night

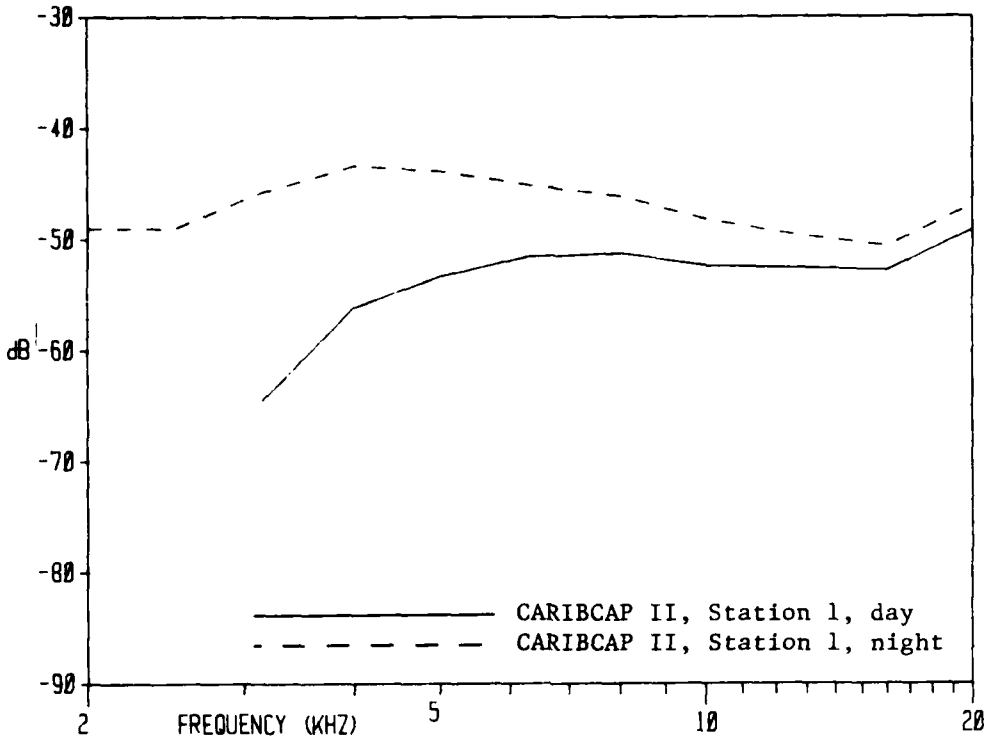

Figure 13. S_C vs. frequency, Station 1, day-night

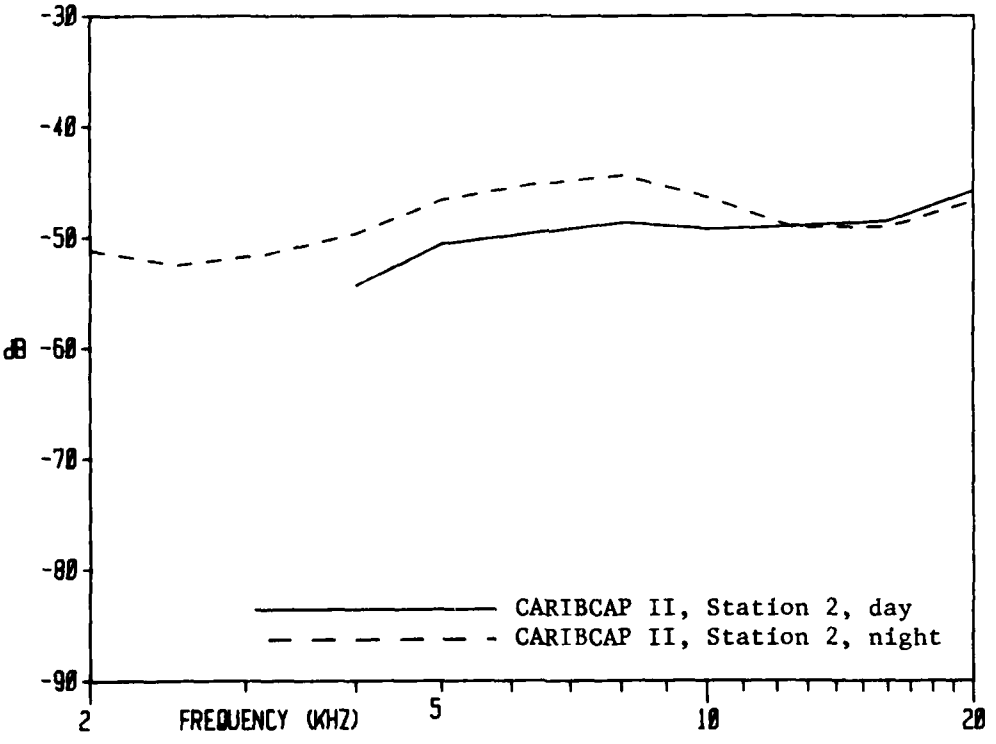

Figure 14. S_C vs. frequency, Station 2, day-night

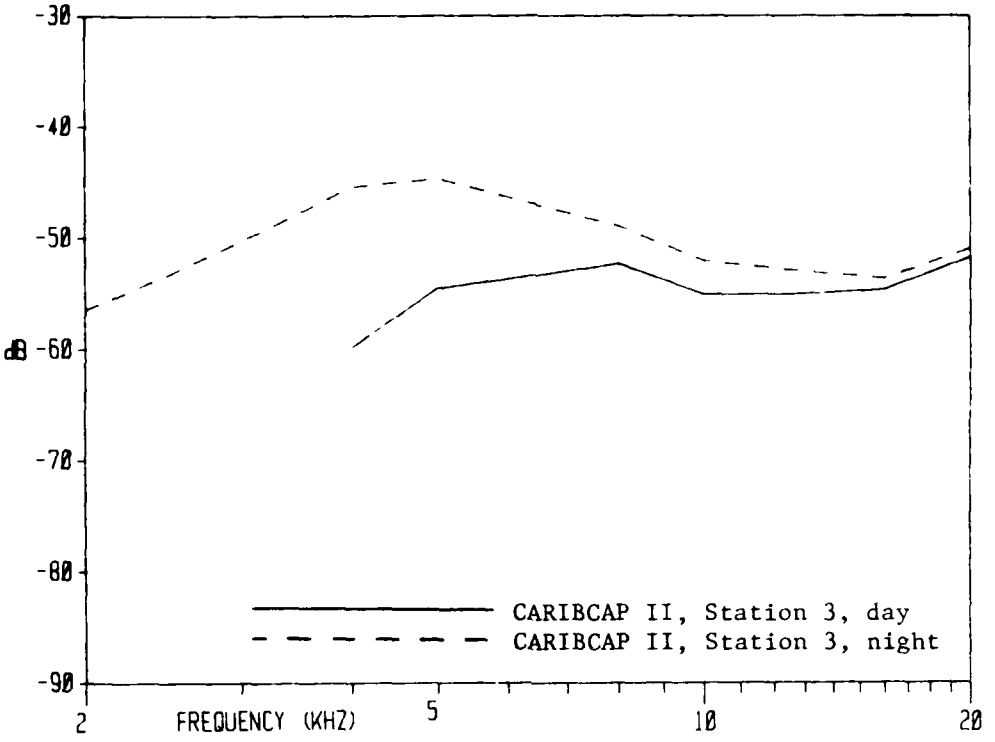

Figure 15. S_c vs. frequency, Station 3, day-night

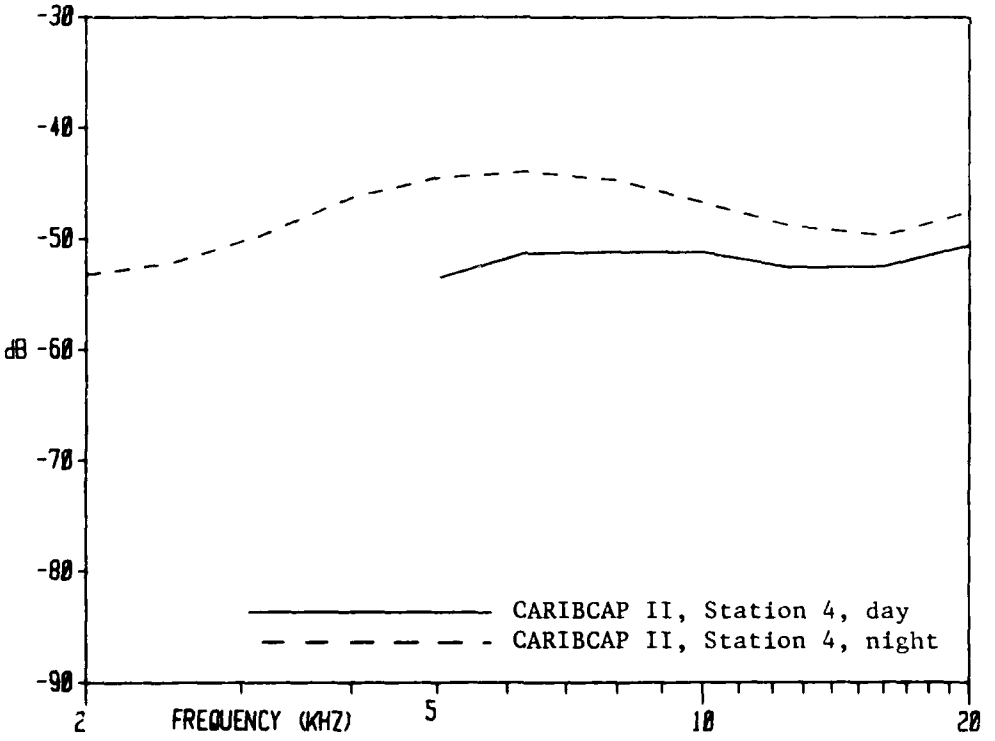

Figure 16. S_c vs. frequency, Station 4, day-night

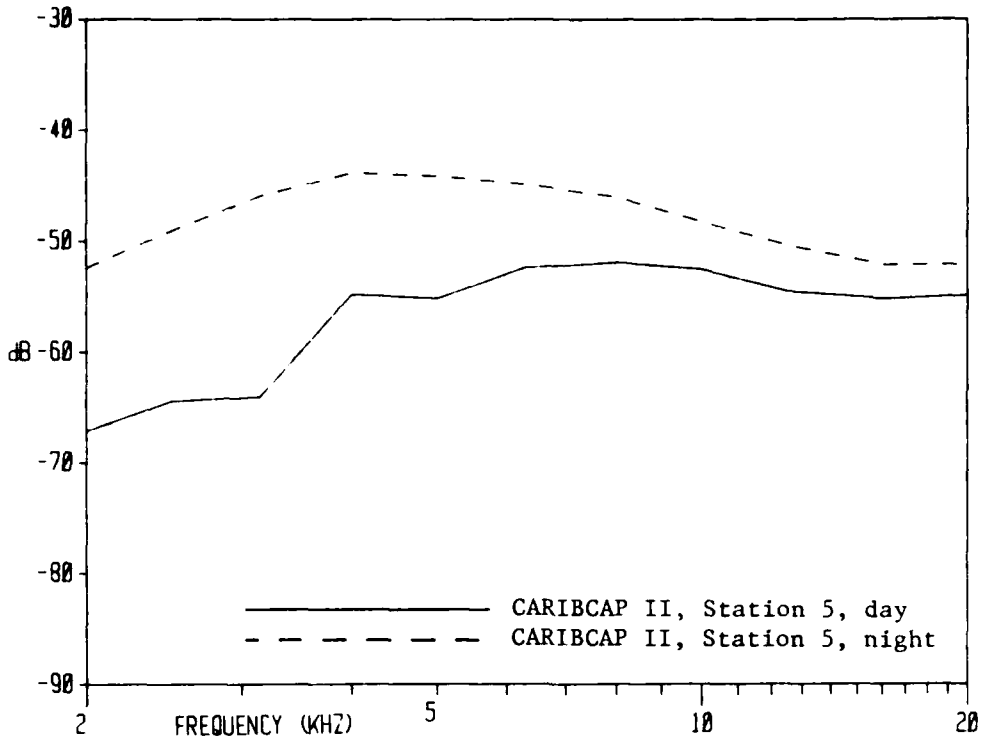

Figure 17. S_c vs. frequency, Station 5, day-night

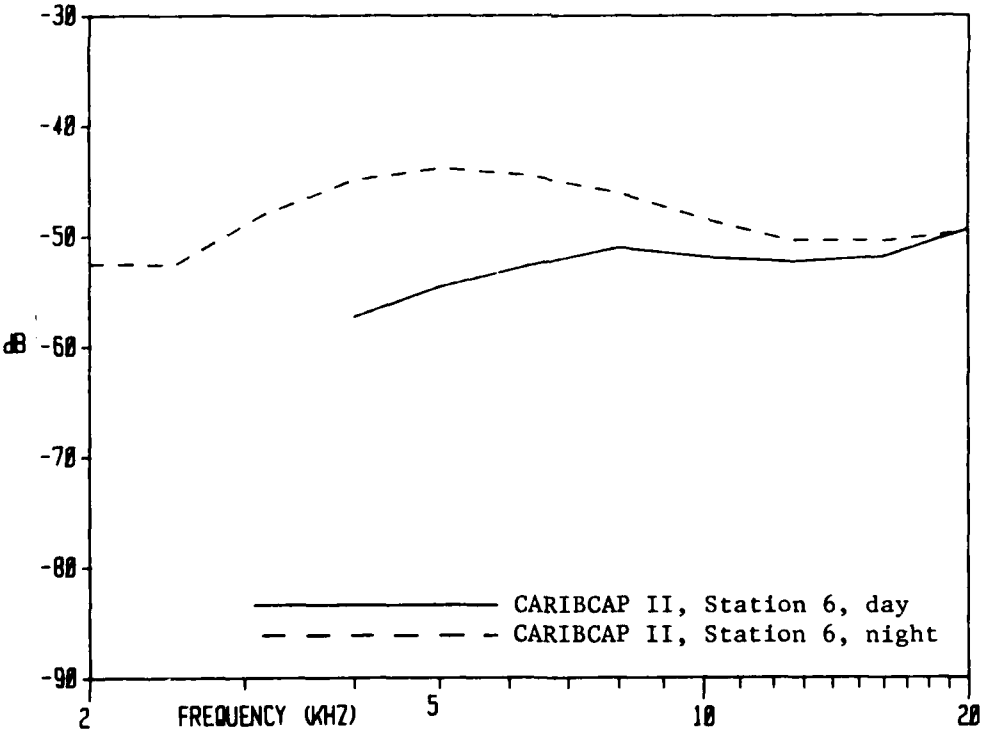

Figure 18. S_c vs. frequency, Station 6, day-night

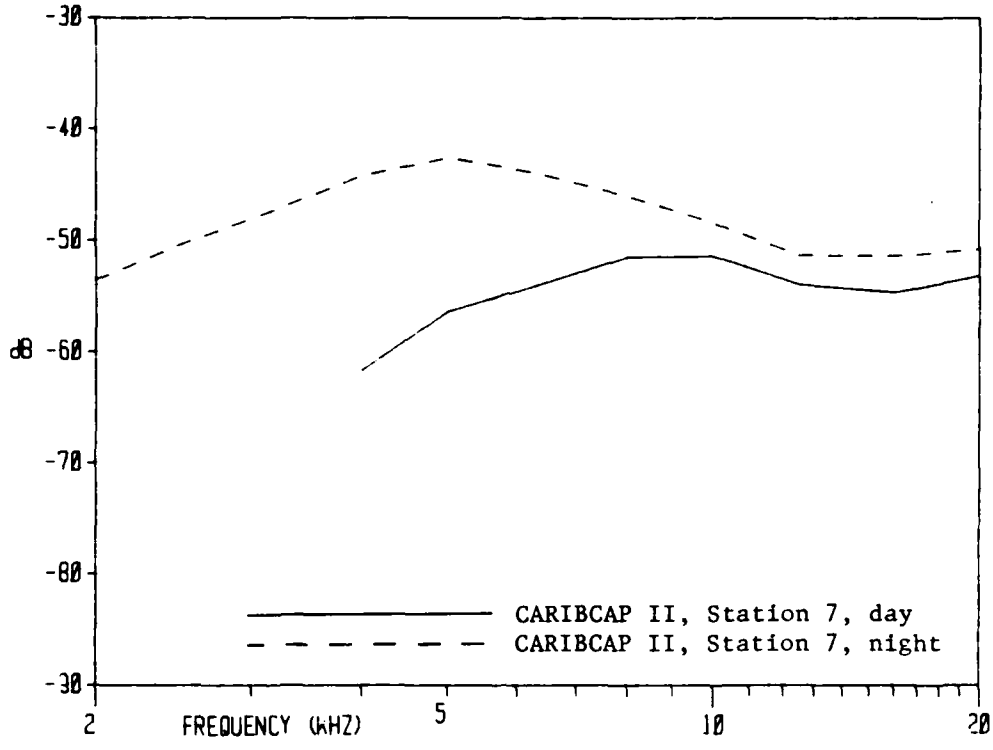

Figure 19. S_c vs. frequency, Station 7, day-night

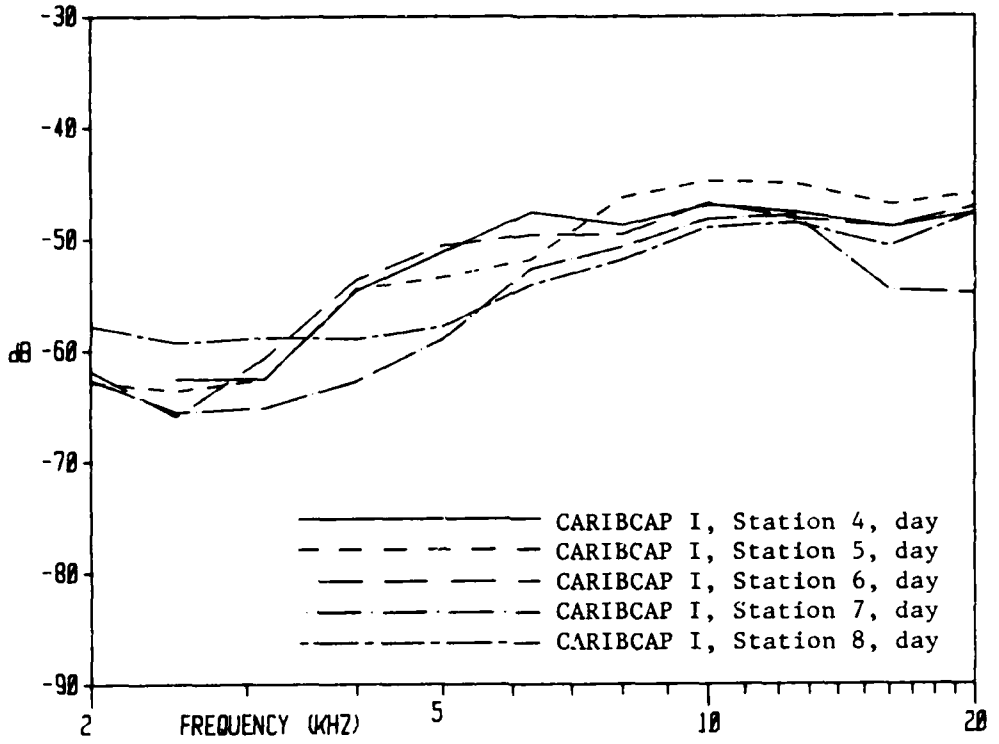

Figure 20. S_c vs. frequency, CARIBCAP I stations, day

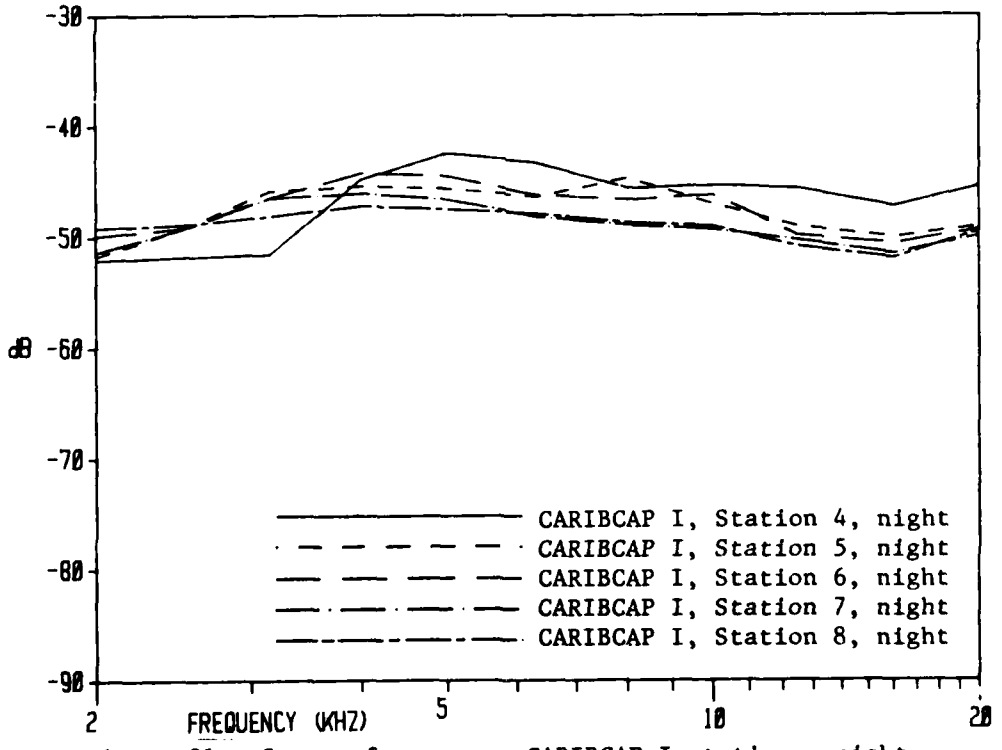

Figure 21. S_c vs. frequency, CARIBCAP I stations, night

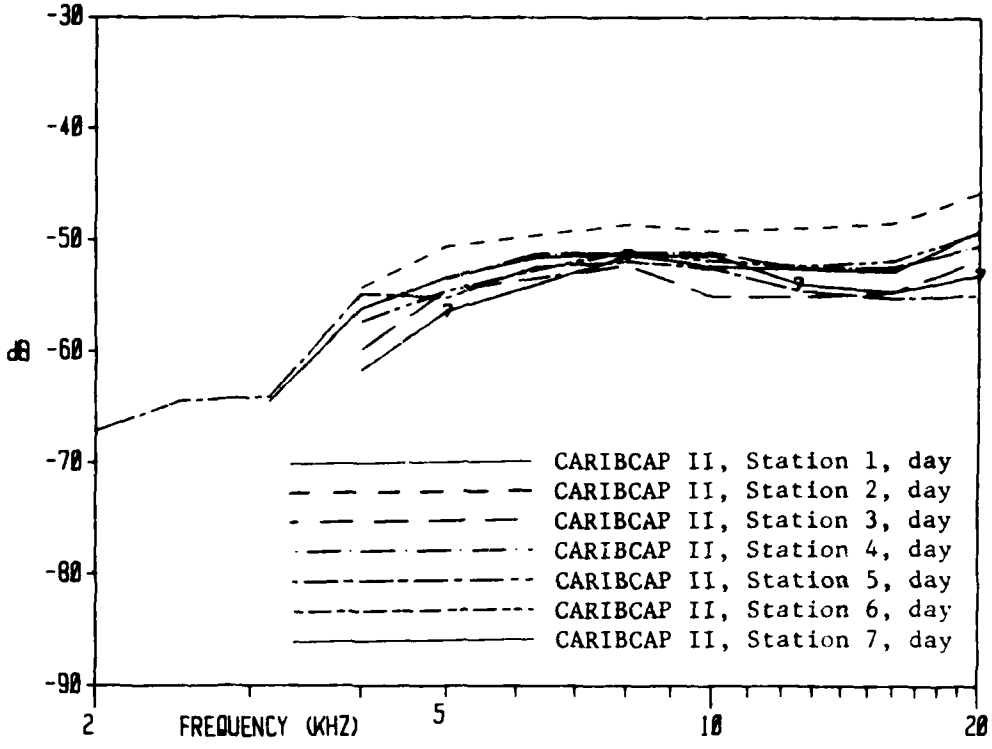

Figure 22. S_c vs. frequency, CARIBCAP II stations, day

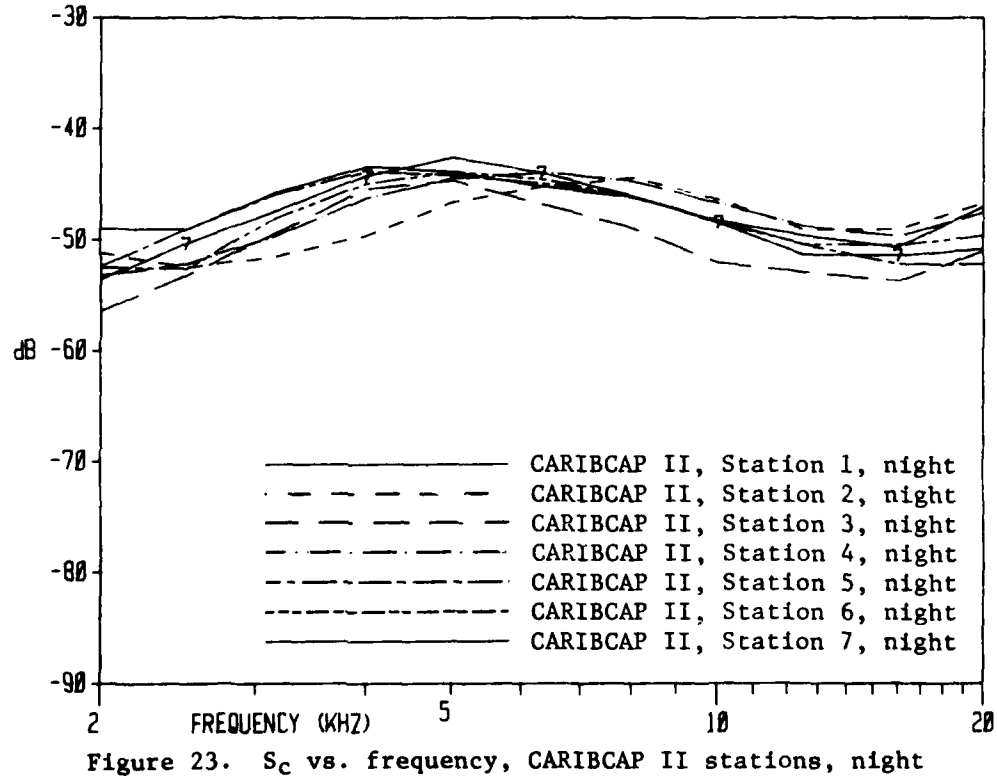

Figure 23. S_c vs. frequency, CARIBCAP II stations, night

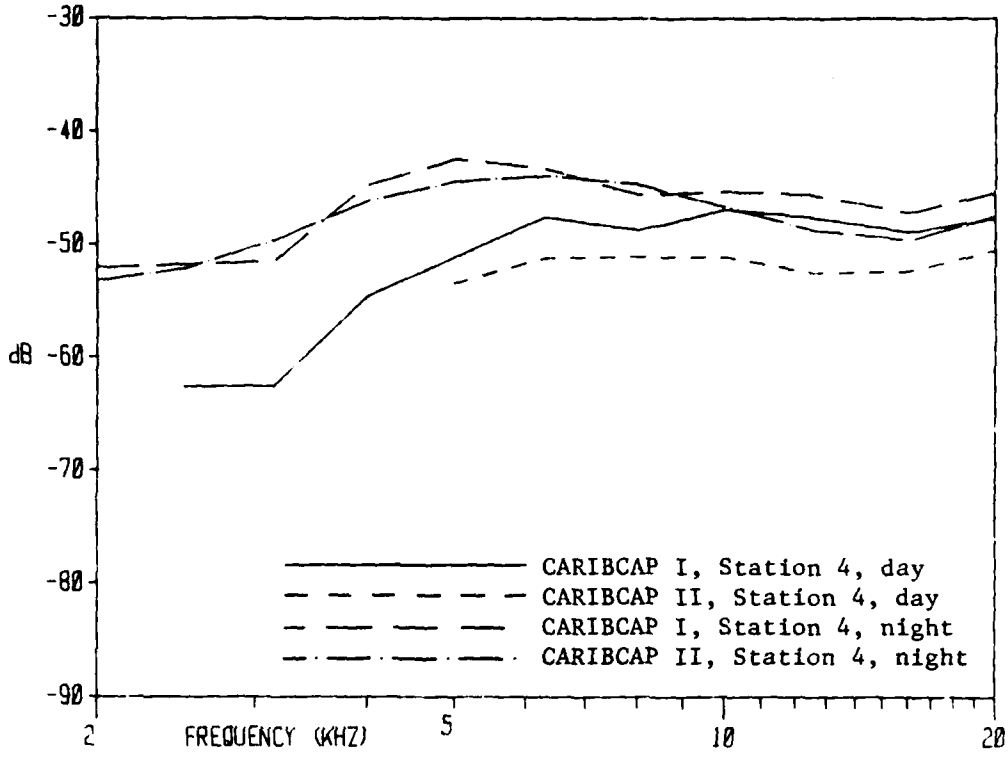

Figure 24. S_c vs. frequency, CARIBCAP I and II, Station 4, day and night

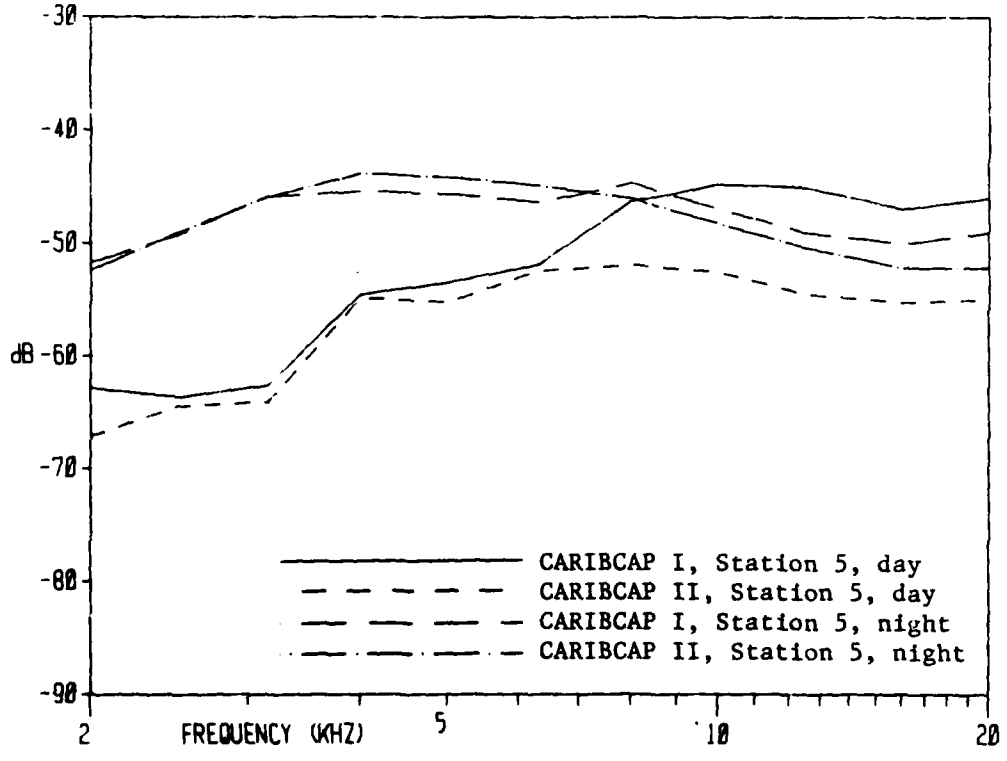

Figure 25. S_c vs. frequency, CARIBCAP I and II, Station 5, day and night

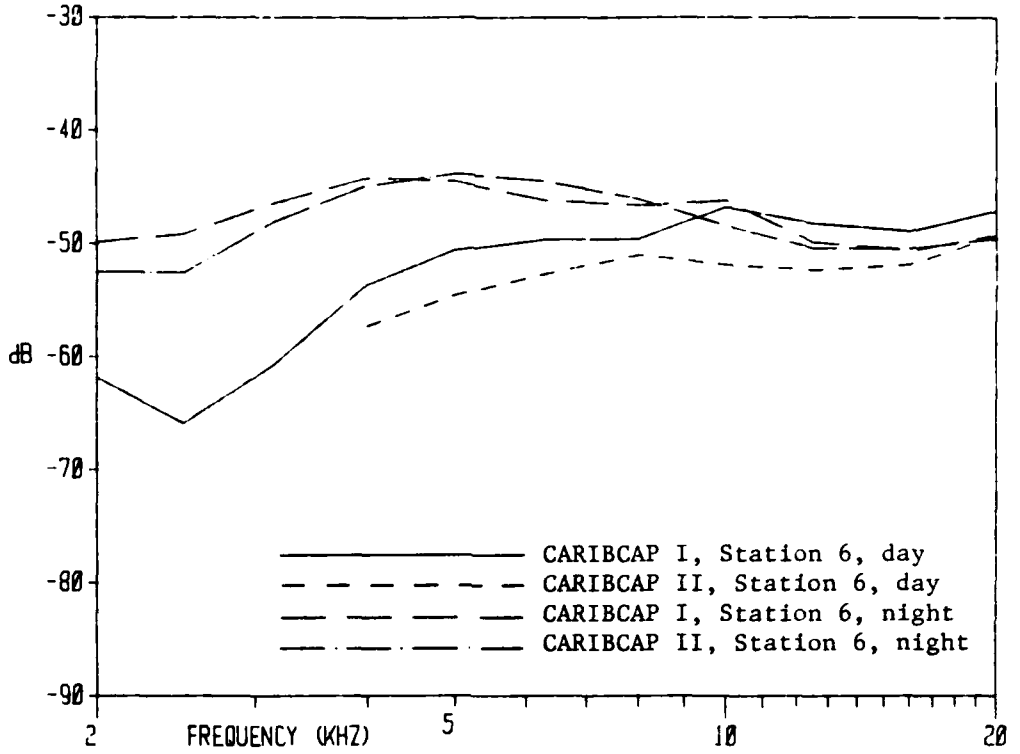

Figure 26. S_c vs. frequency, CARIBCAP I and II, Station 6, day and night

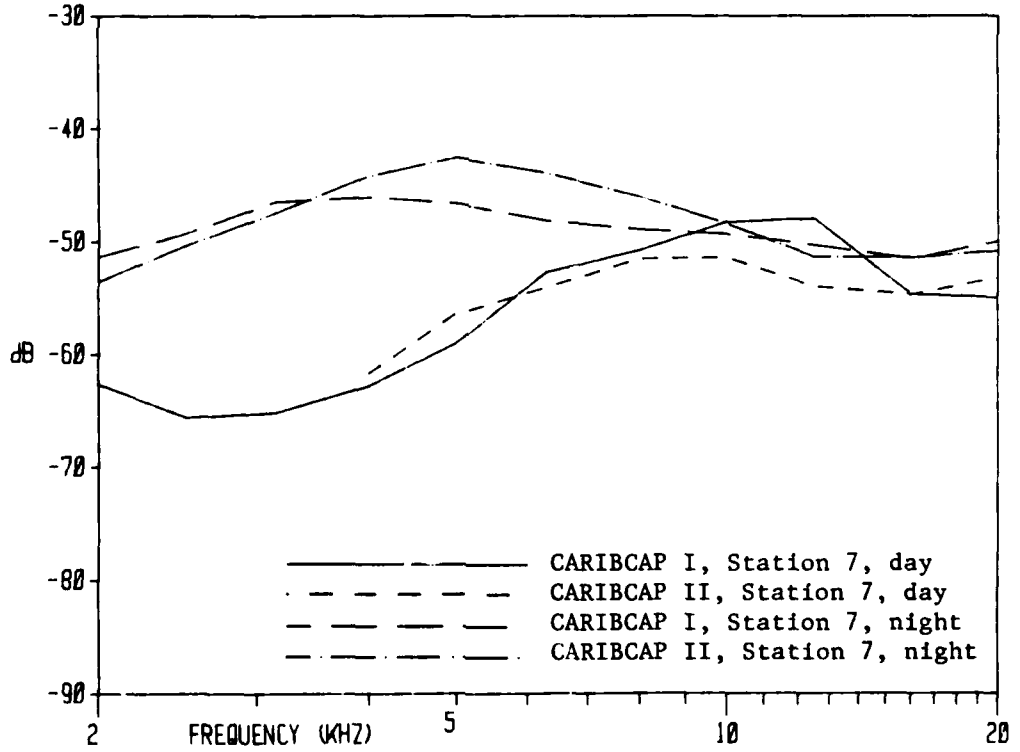

Figure 27. S_c vs. frequency, CARIBCAP I and II, Station 7, day and night

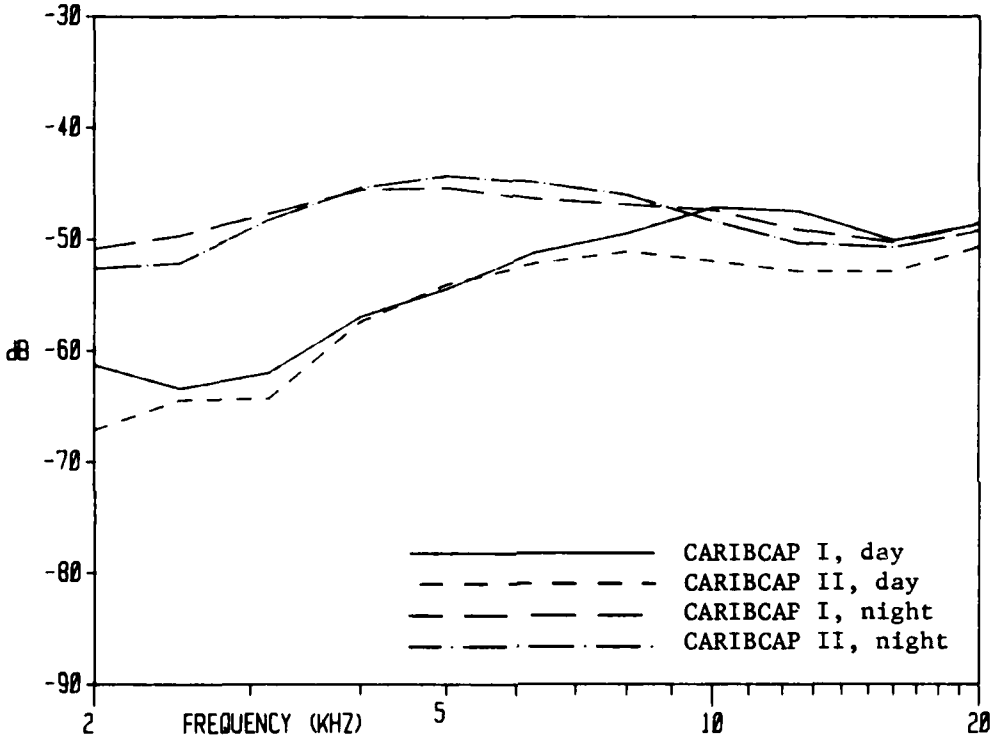

Figure 28. Mean S_c vs. frequency, CARIBCAP I and II, day-night

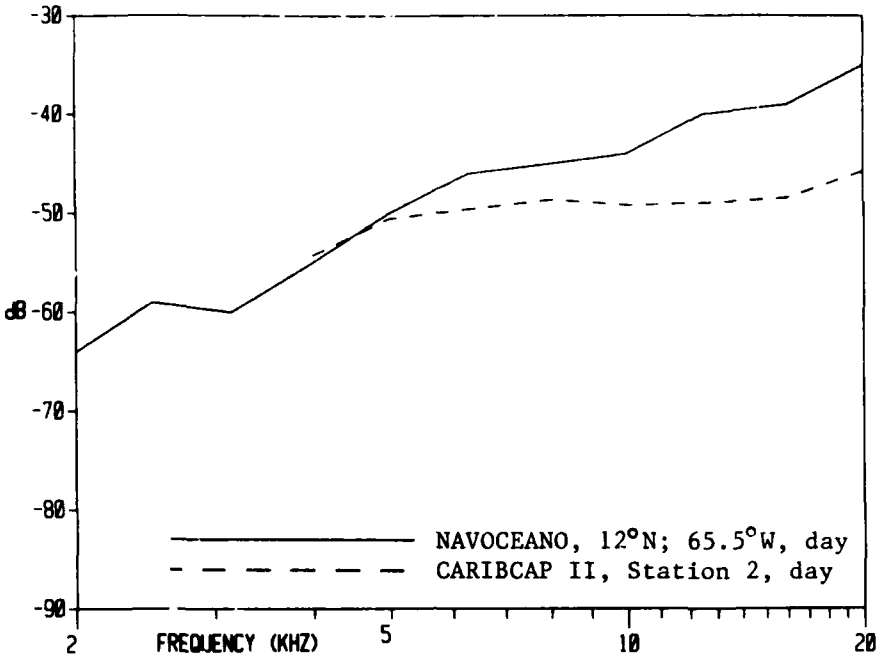

Figure 29. S_C vs. frequency. Comparison between CARIBCAP II, Station 2, day, and NAVOCEANO day data at 12°N; 65.5°W

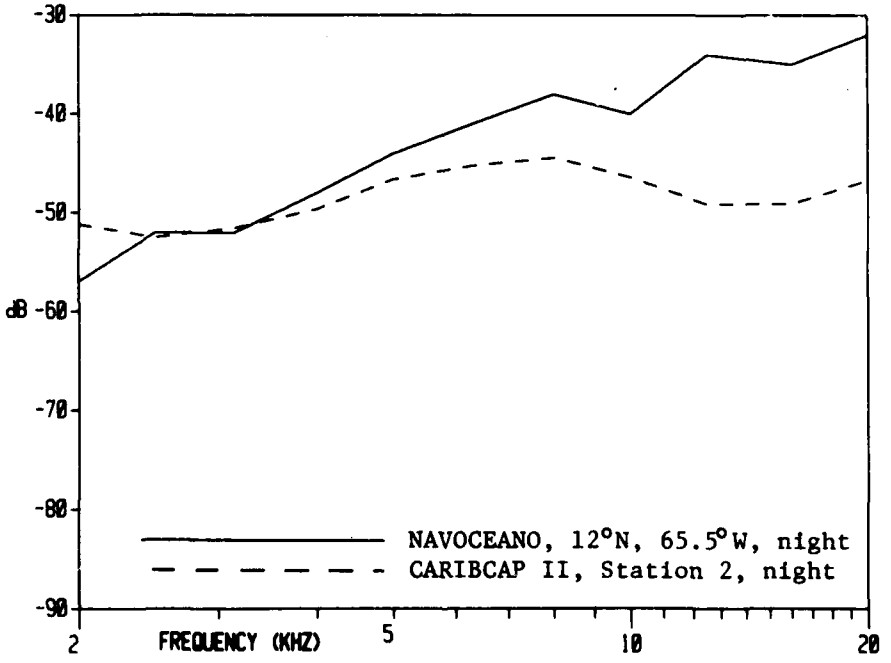

Figure 30. S_C vs. frequency. Comparison between CARIBCAP II, Station 2, night, and NAVOCEANO night data at 12°N; 65.5°W

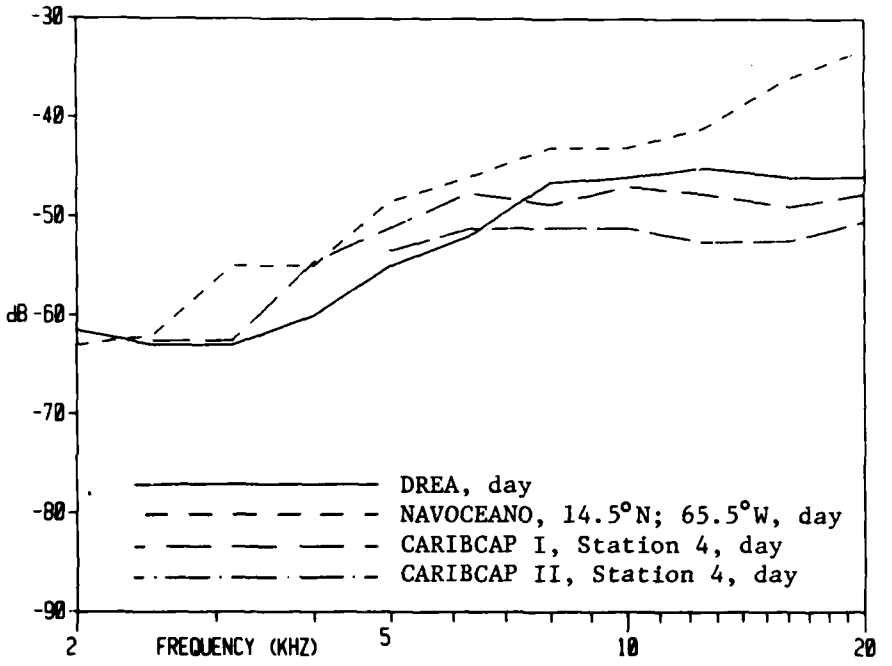

Figure 31. S_c vs. frequency. Comparison between DREA, NAVOCEANO and CARIBCAP I and II Station 4 day data

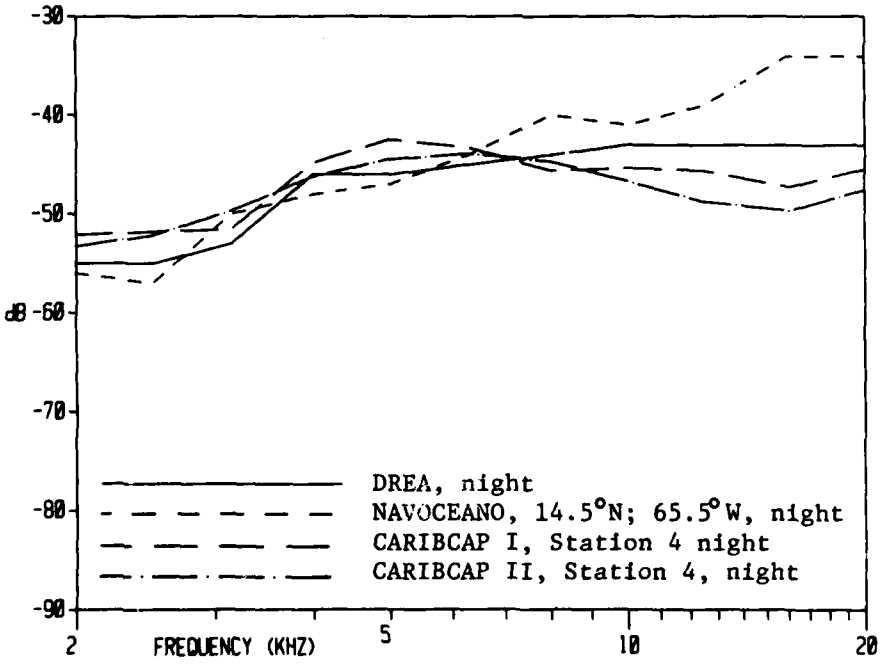

Figure 32. S_c vs. frequency. Comparison between DREA, NAVOCEANO and CARIBCAP I and II Station 4 night data

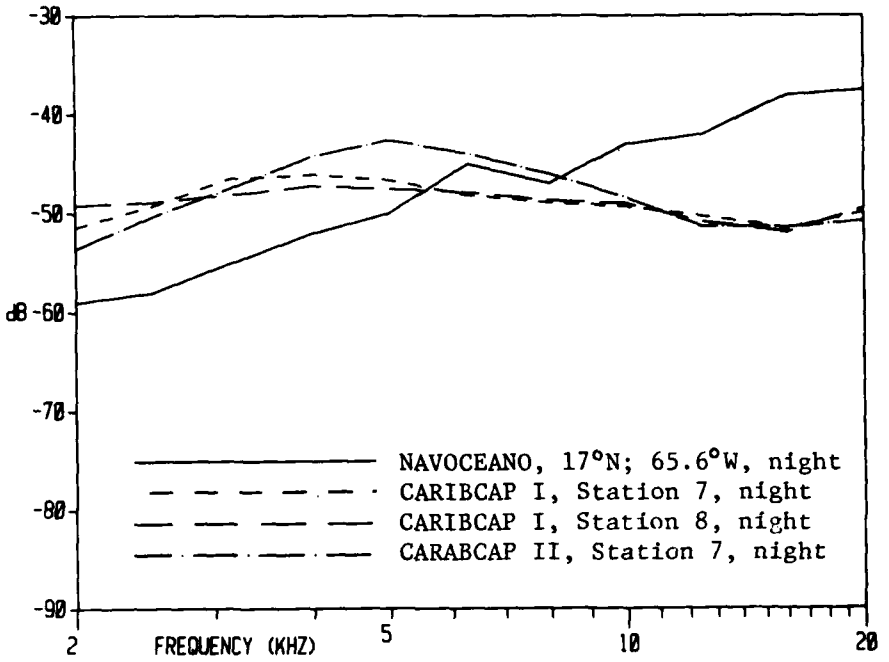

Figure 33. S_C vs. frequency. Comparison between NAVOCEANO night data at 17°N; 65.5°W and CARIBCAP I and II night data at Stations 7 and 8

Appendix A

Mean $S_c(z)$ Profiles

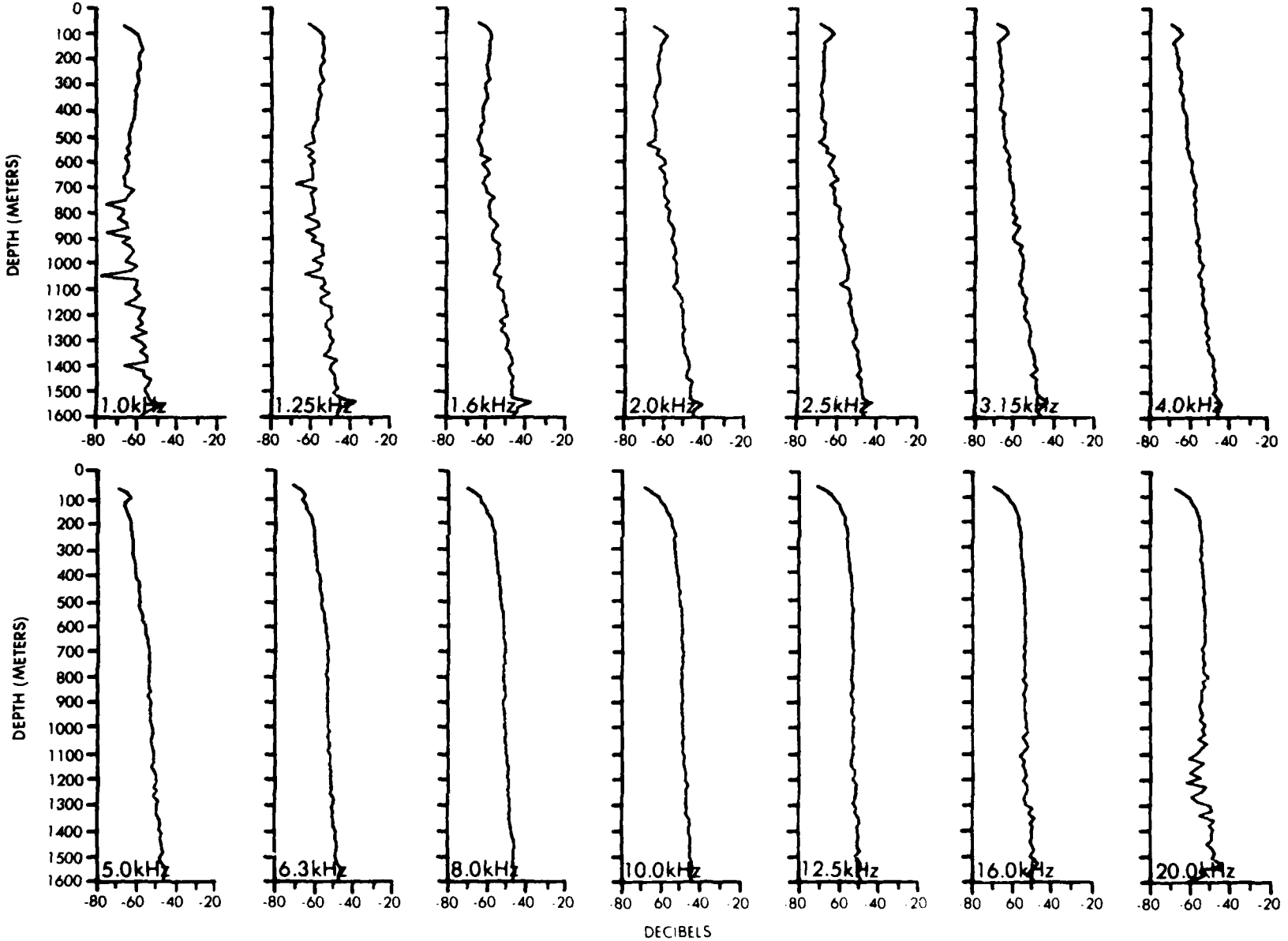

Figure A-1. $S_c(z)$, CARIBCAP I, Station 4, day

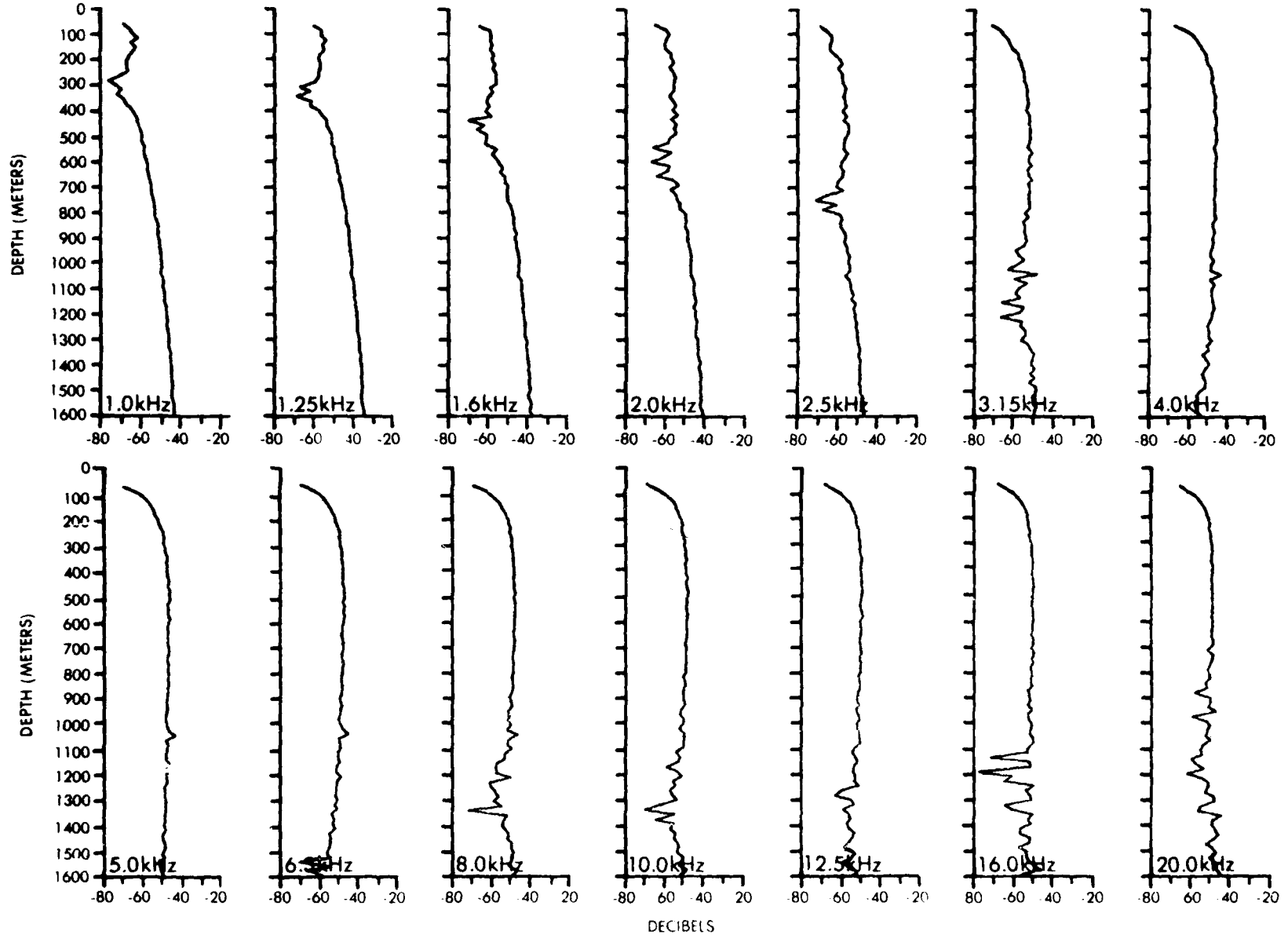

Figure A-2. $S_c(z)$, CARIBCAP I, Station 4, night

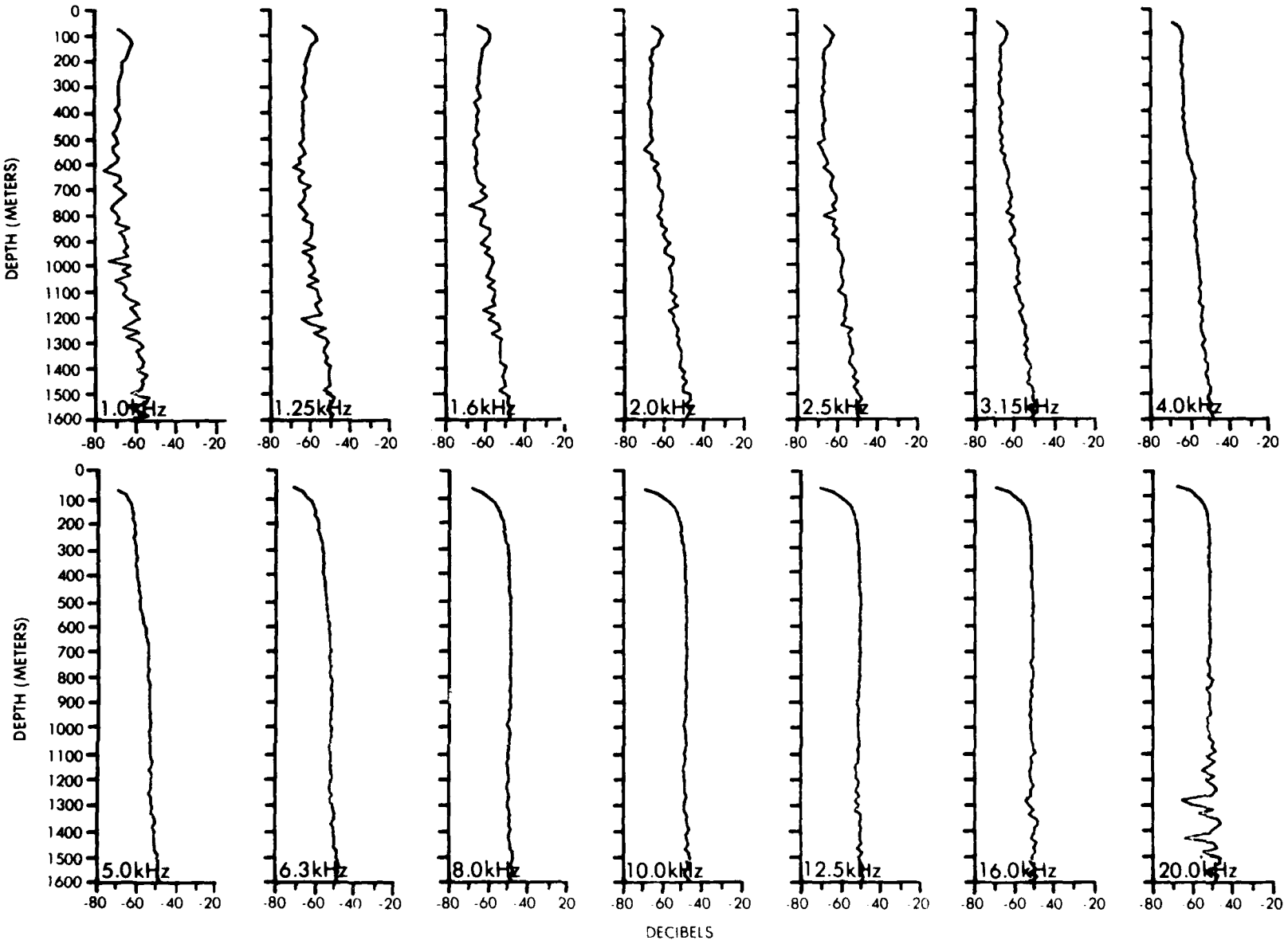

Figure A-3. $S_c(z)$, CARIBCAP I, Station 5, day

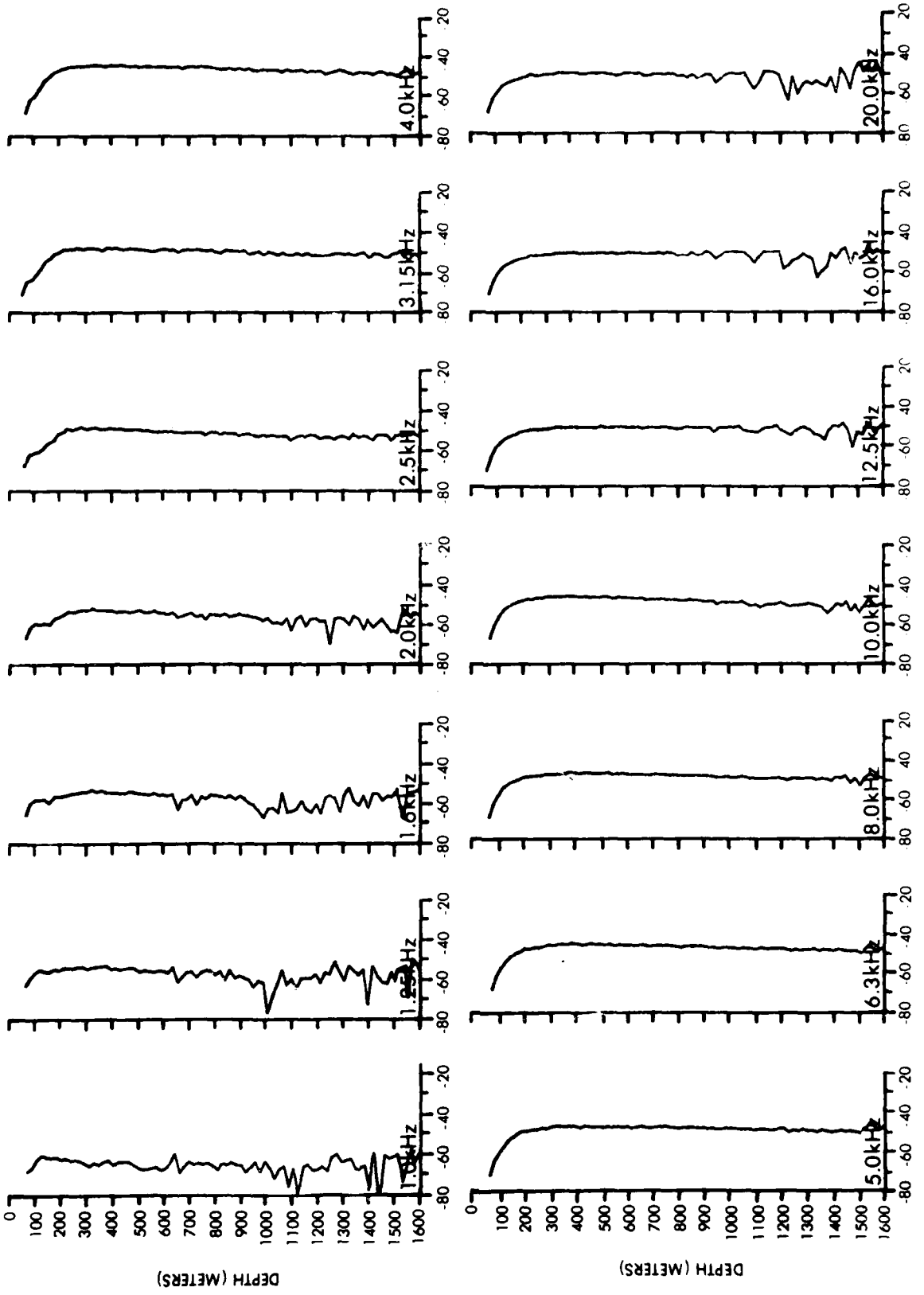

Figure A-4. $S_c(z)$, CARIBCAP I, Station 5, night

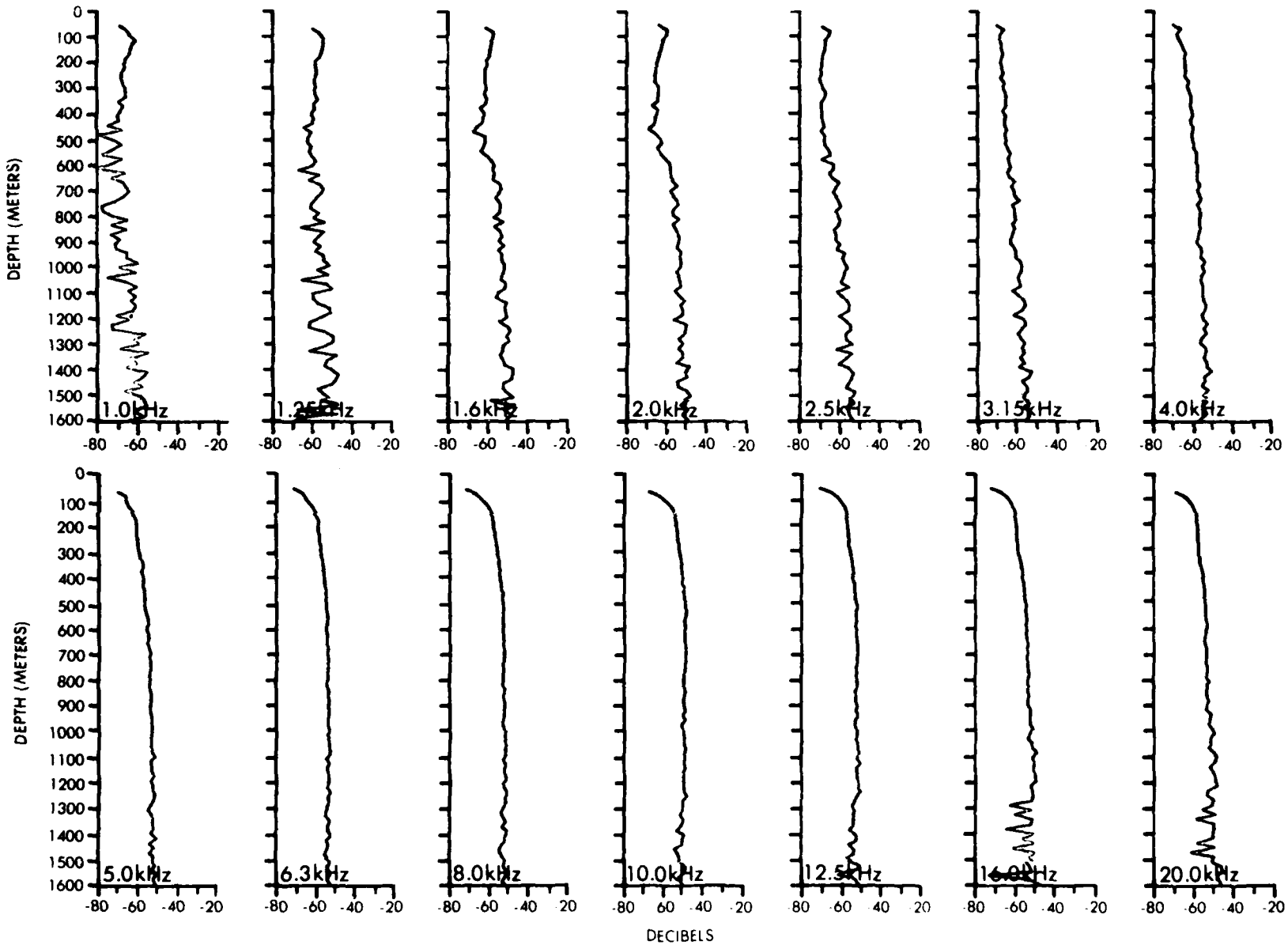

Figure A-5. $S_c(z)$, CARIBCAP I, Station 6, day

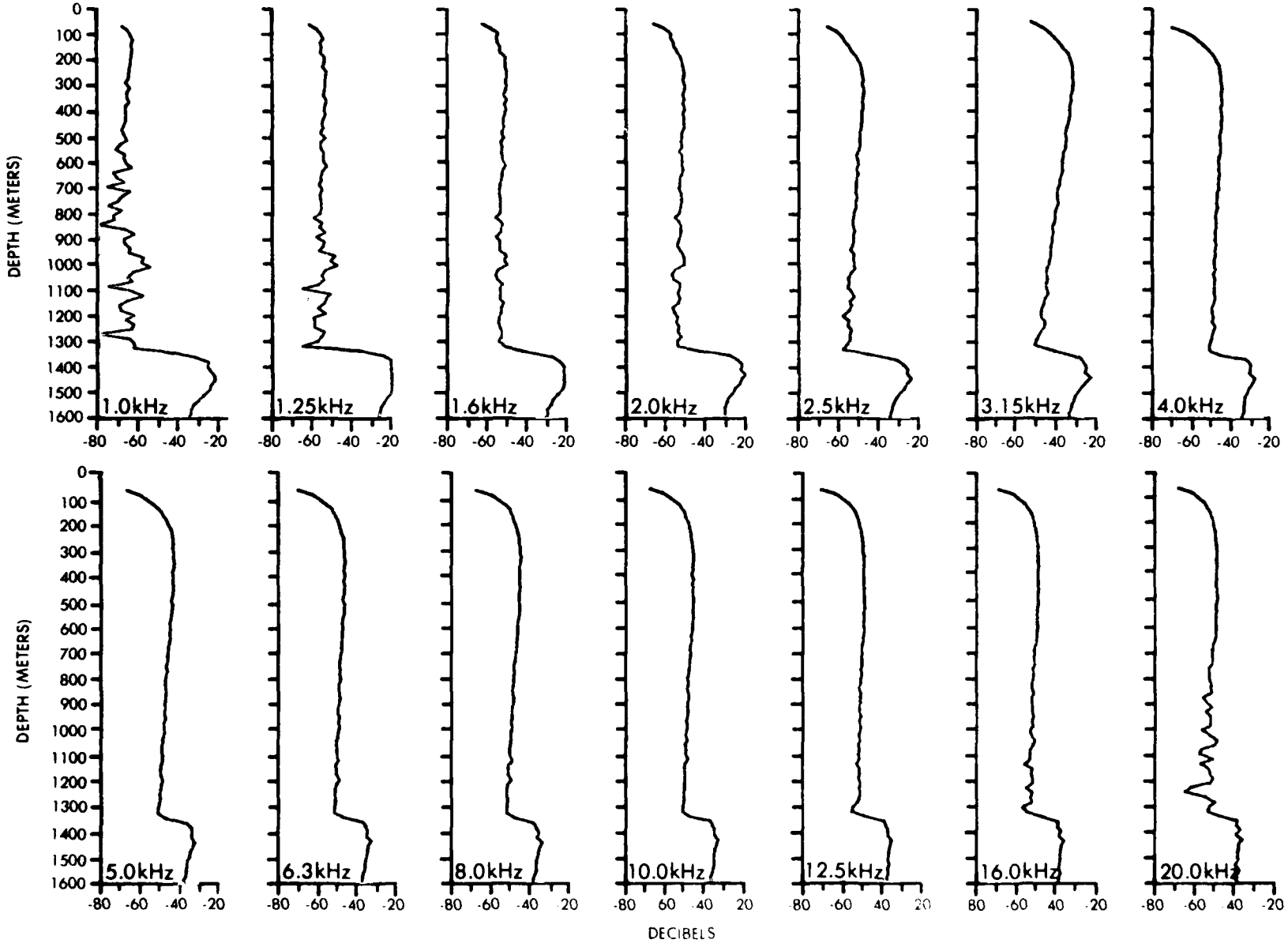

Figure A-6. $S_c(z)$, CARIBCAP I, Station 6, night

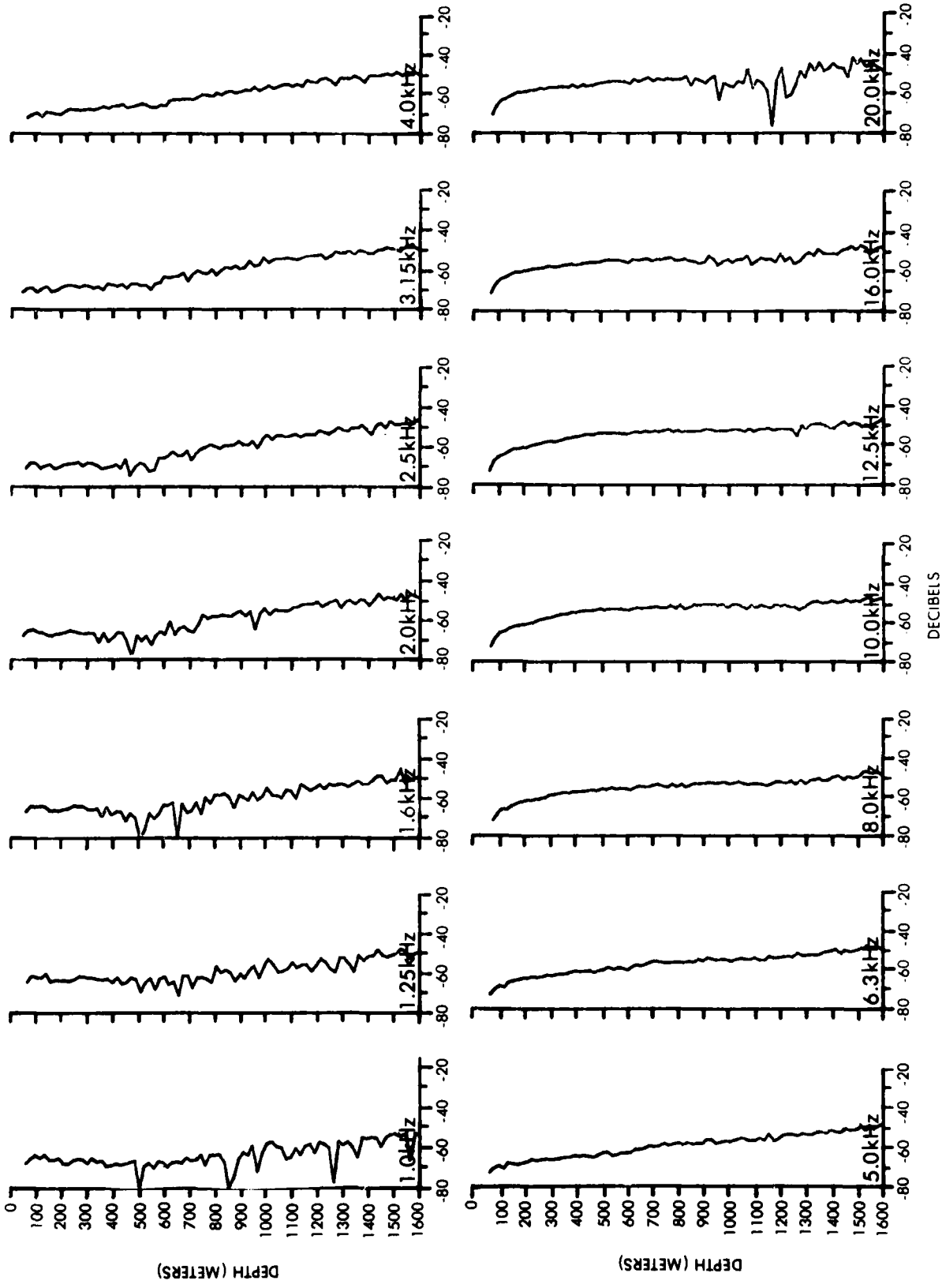

Figure A-7. $S_c(z)$, CARIBCAP I, Station 7, day

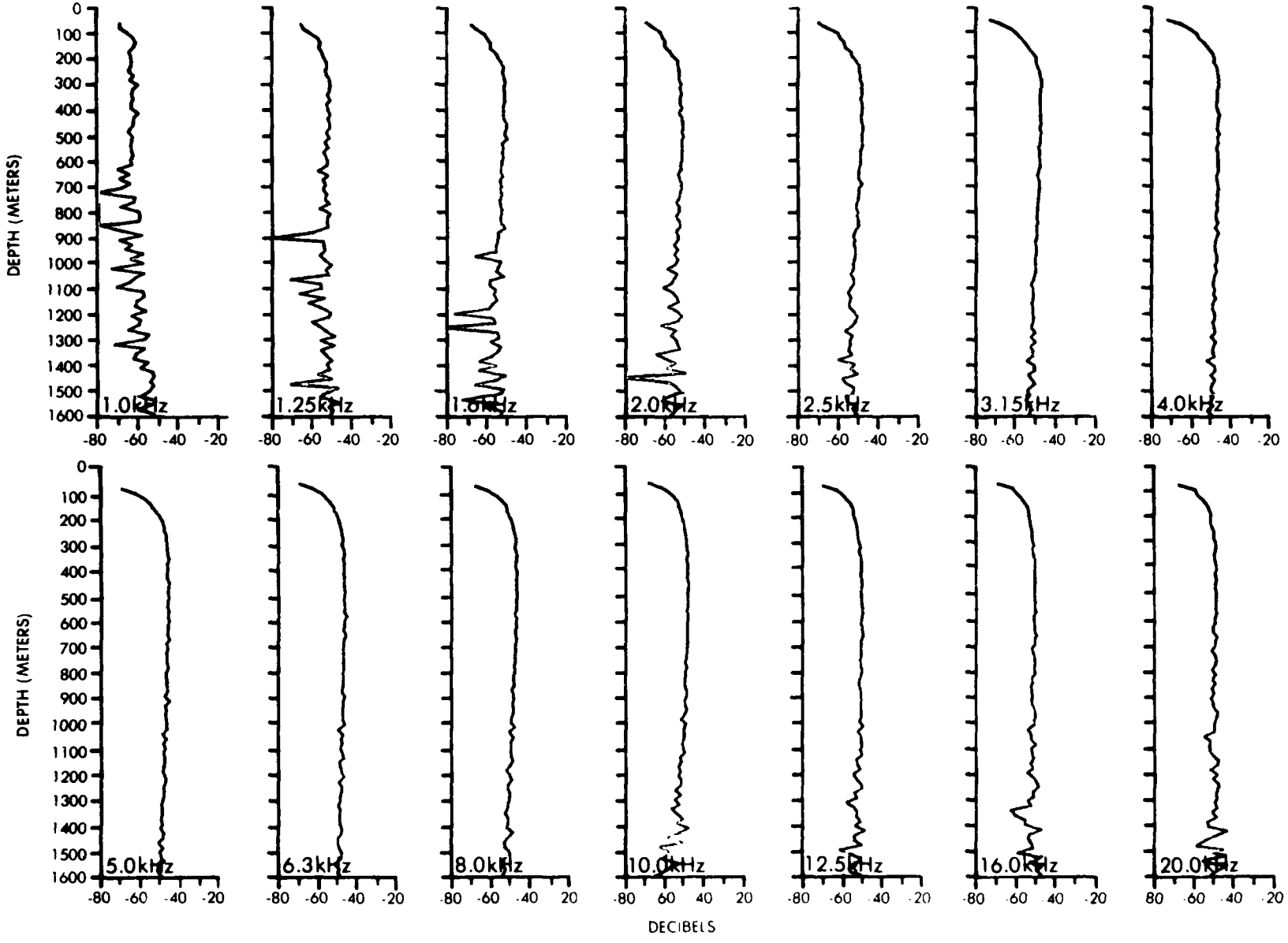

Figure A-8. $S_c(z)$, CARIBCAP I, Station 7, night

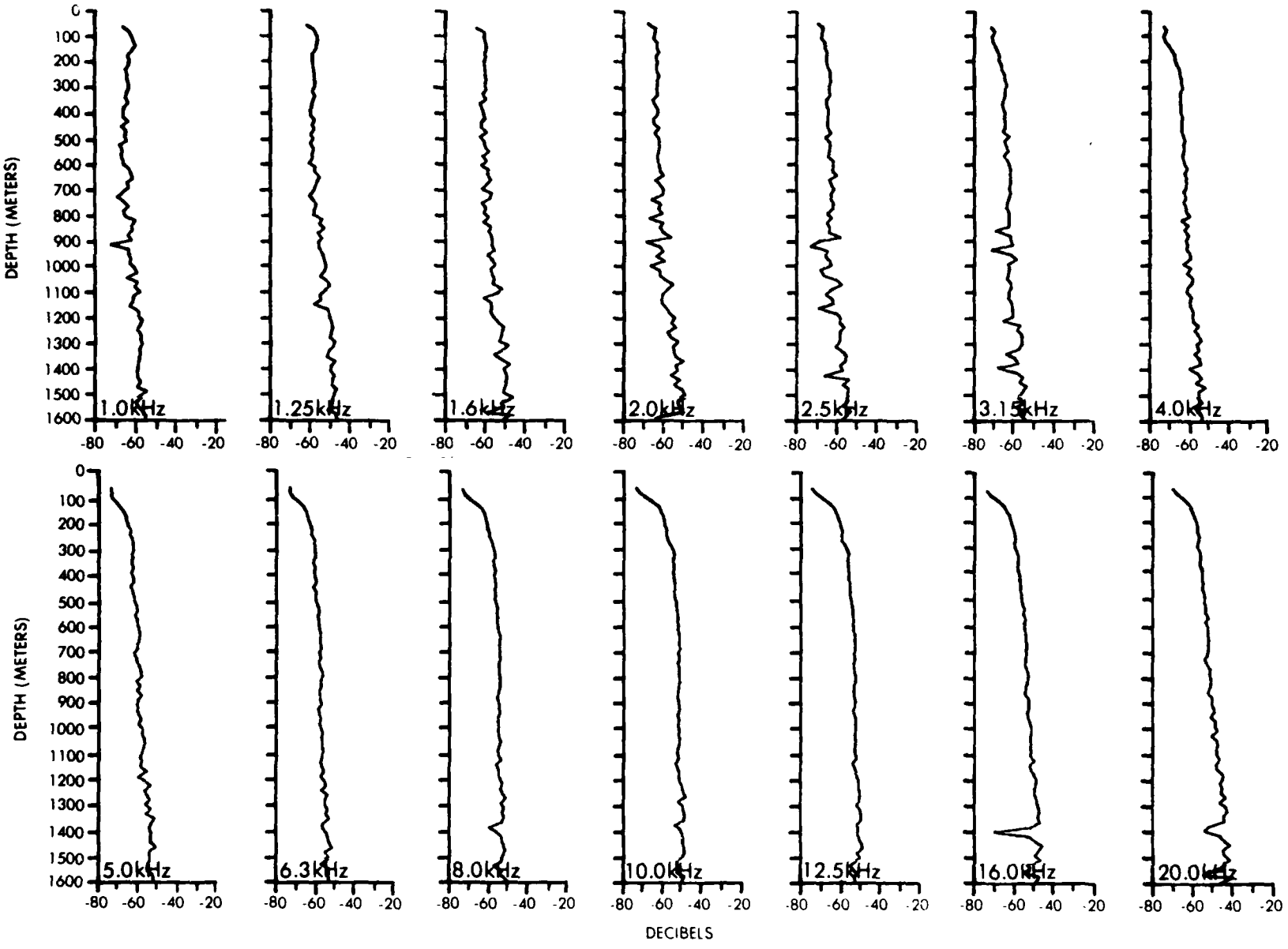

Figure A-9. $S_C(z)$, CARIBCAP I, Station 8, day

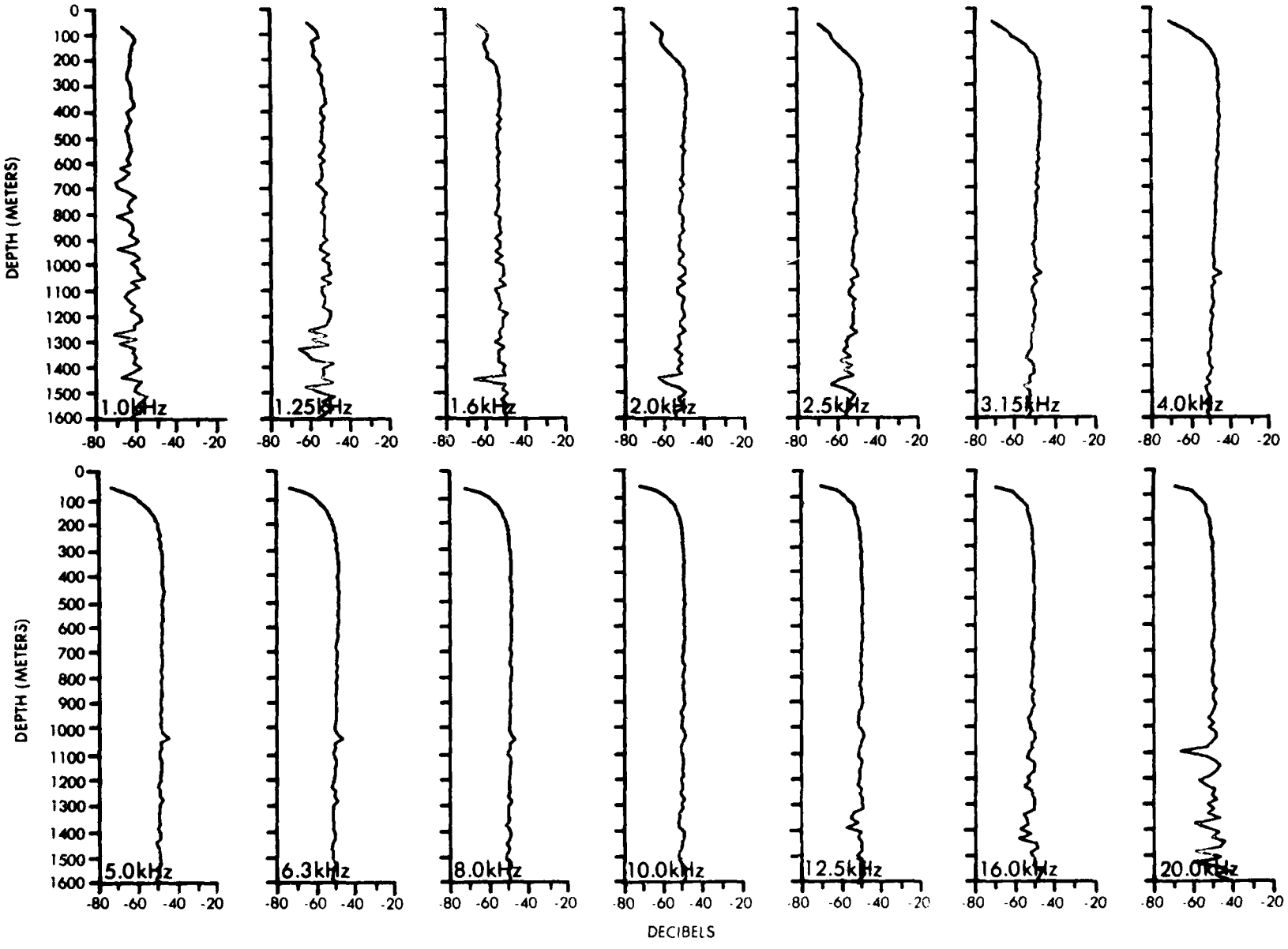

Figure A-10. $S_c(z)$, CARIBCAP I, Station 8, night

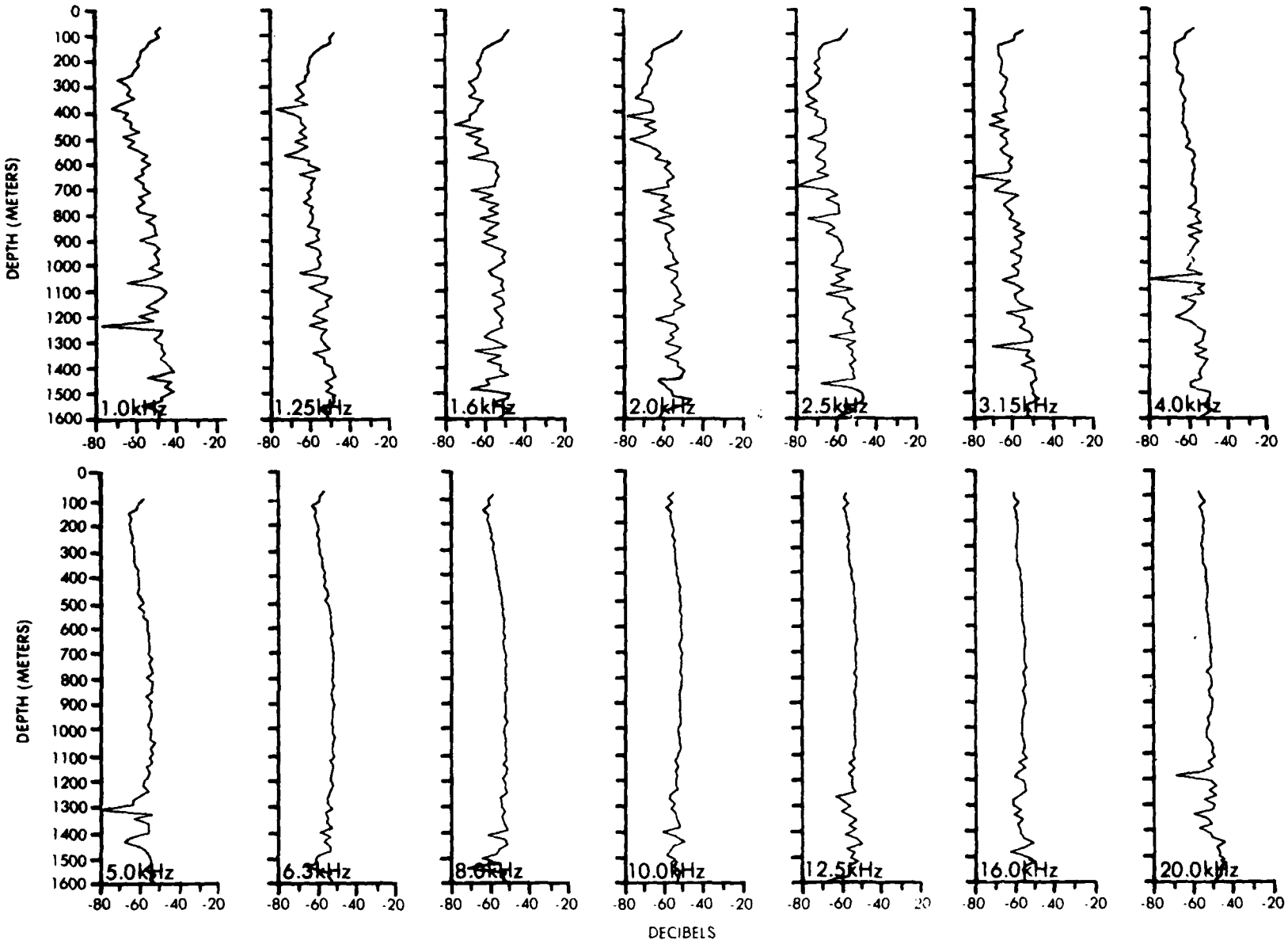

Figure A-11. $S_c(z)$, CARIBCAP II, Station 1, day

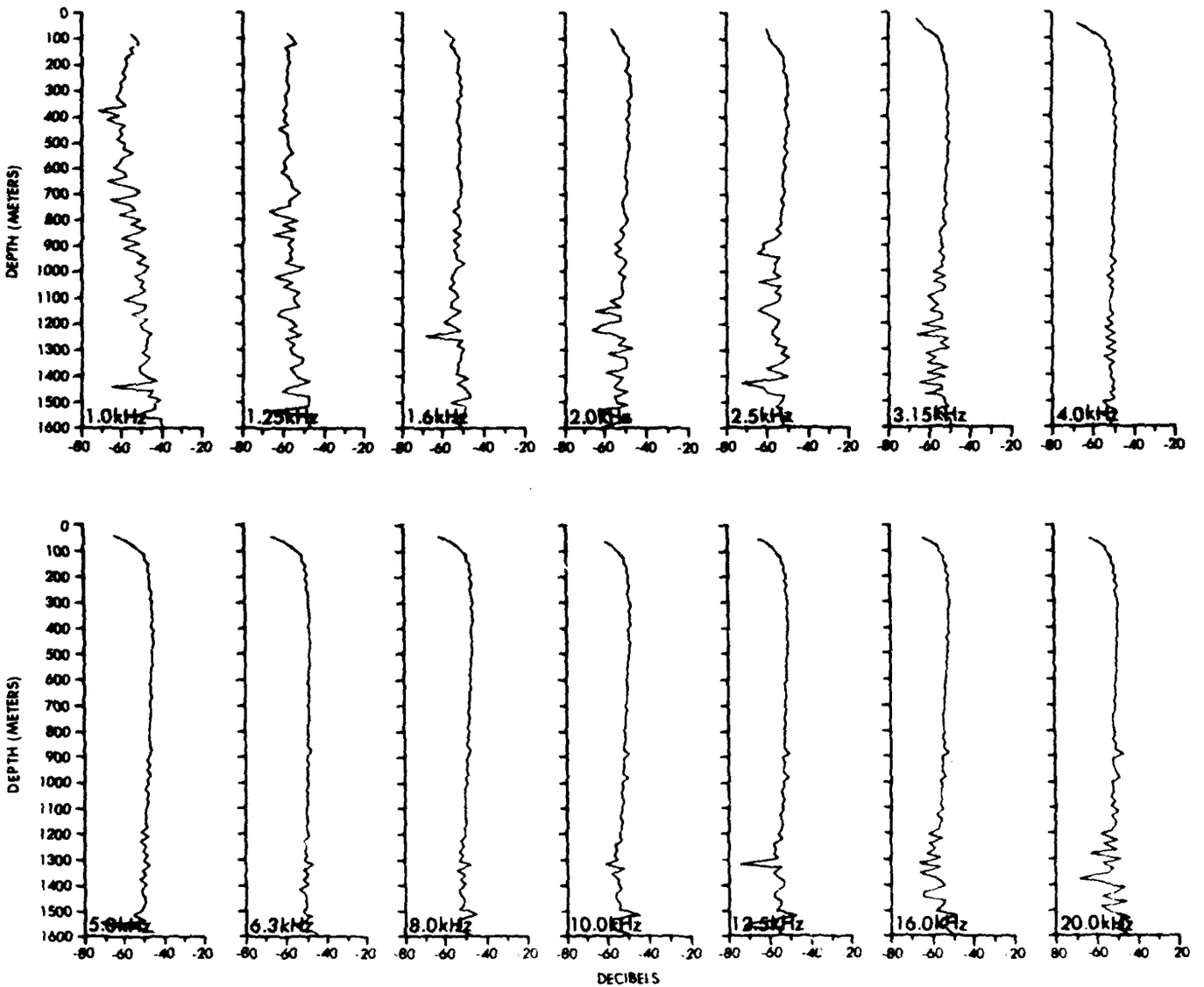

Figure A-12. $S_C(z)$, CARIBCAP II, Station 1, night

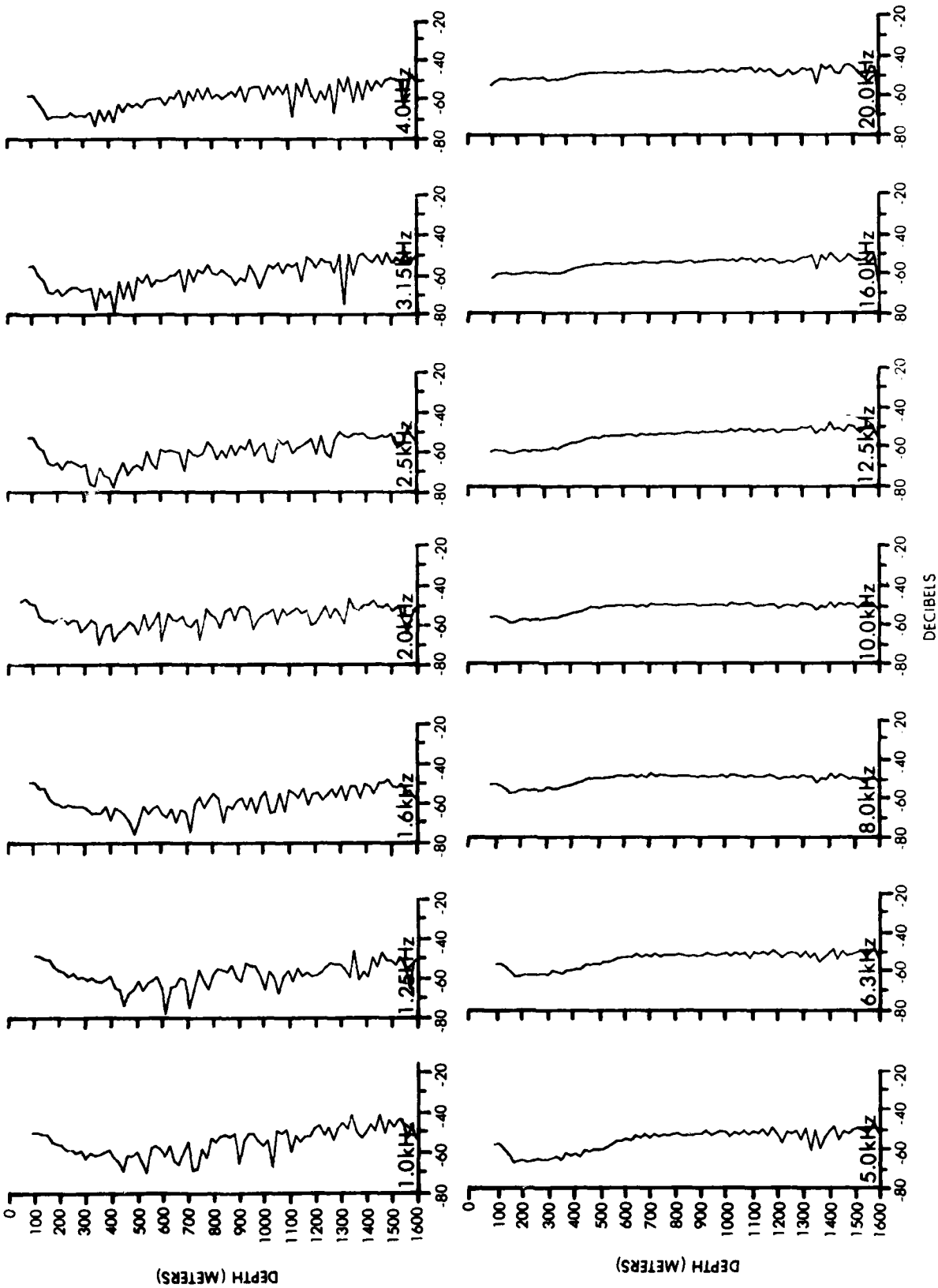

Figure A-13. $S_c(z)$, CARIBCAP II, Station 2, day

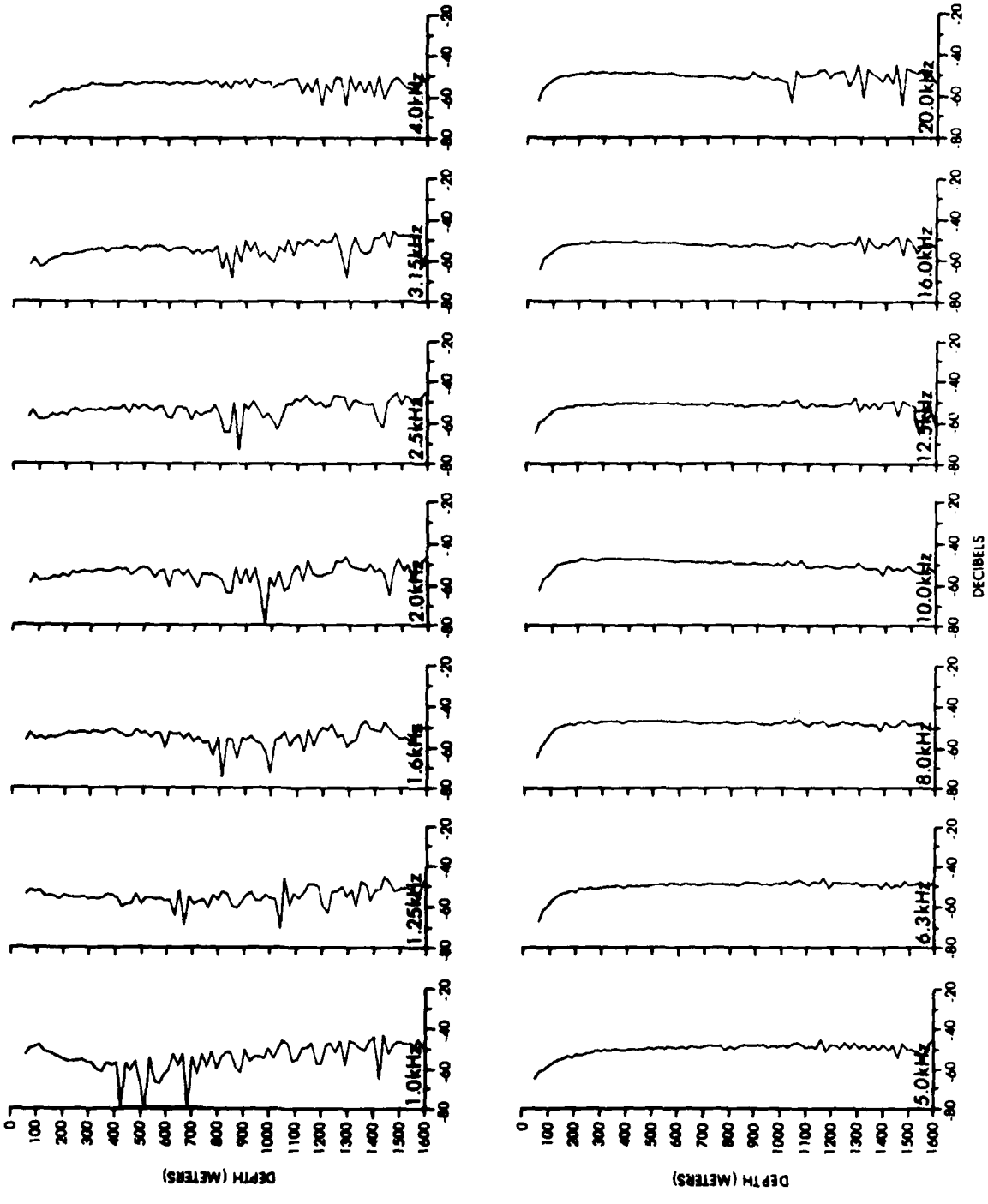

Figure A-14. $S_C(z)$, CARIBCAP II, Station 2, night

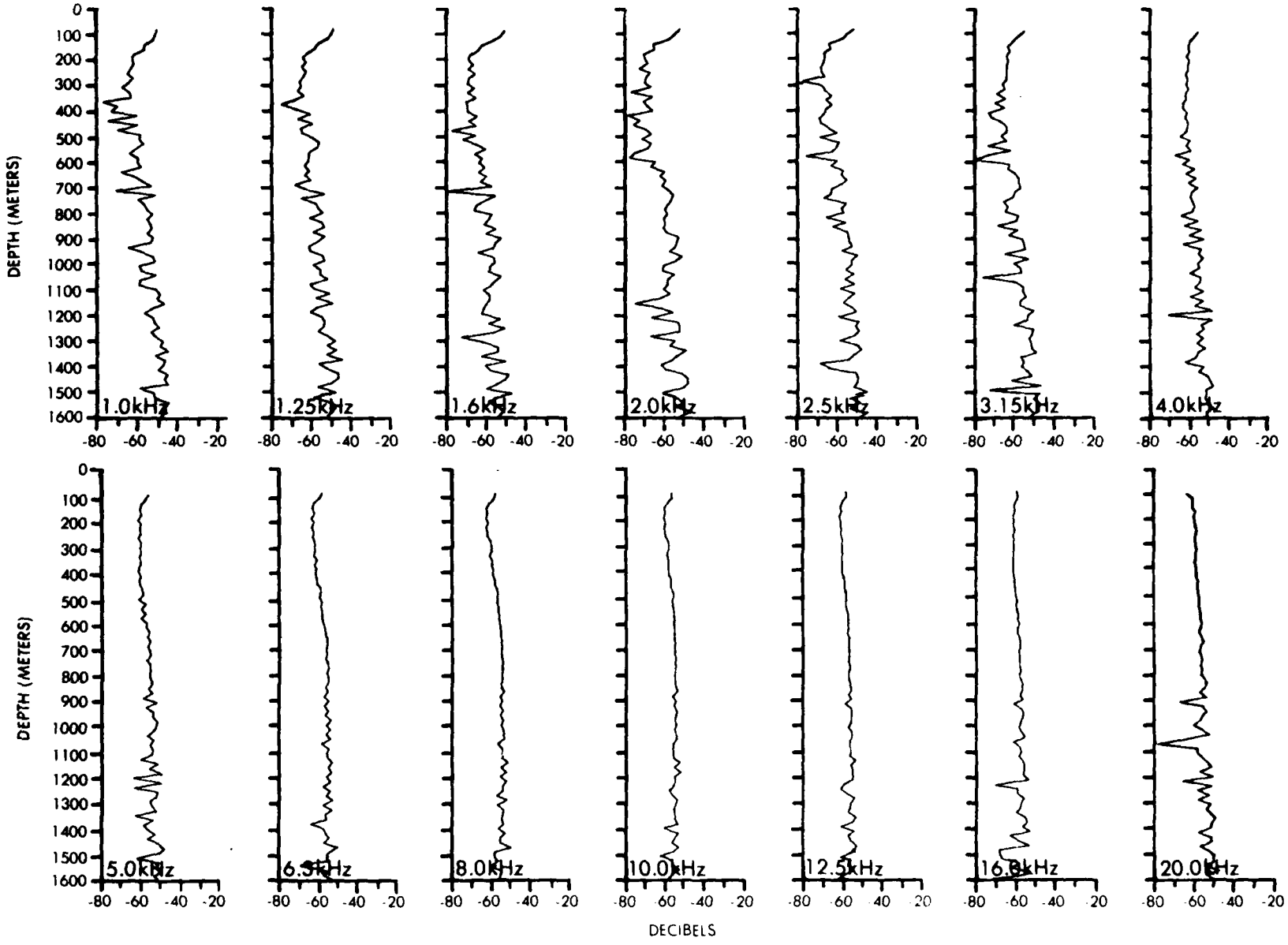

Figure A-15. $S_c(z)$, CARIBCAP II, Station 3, day

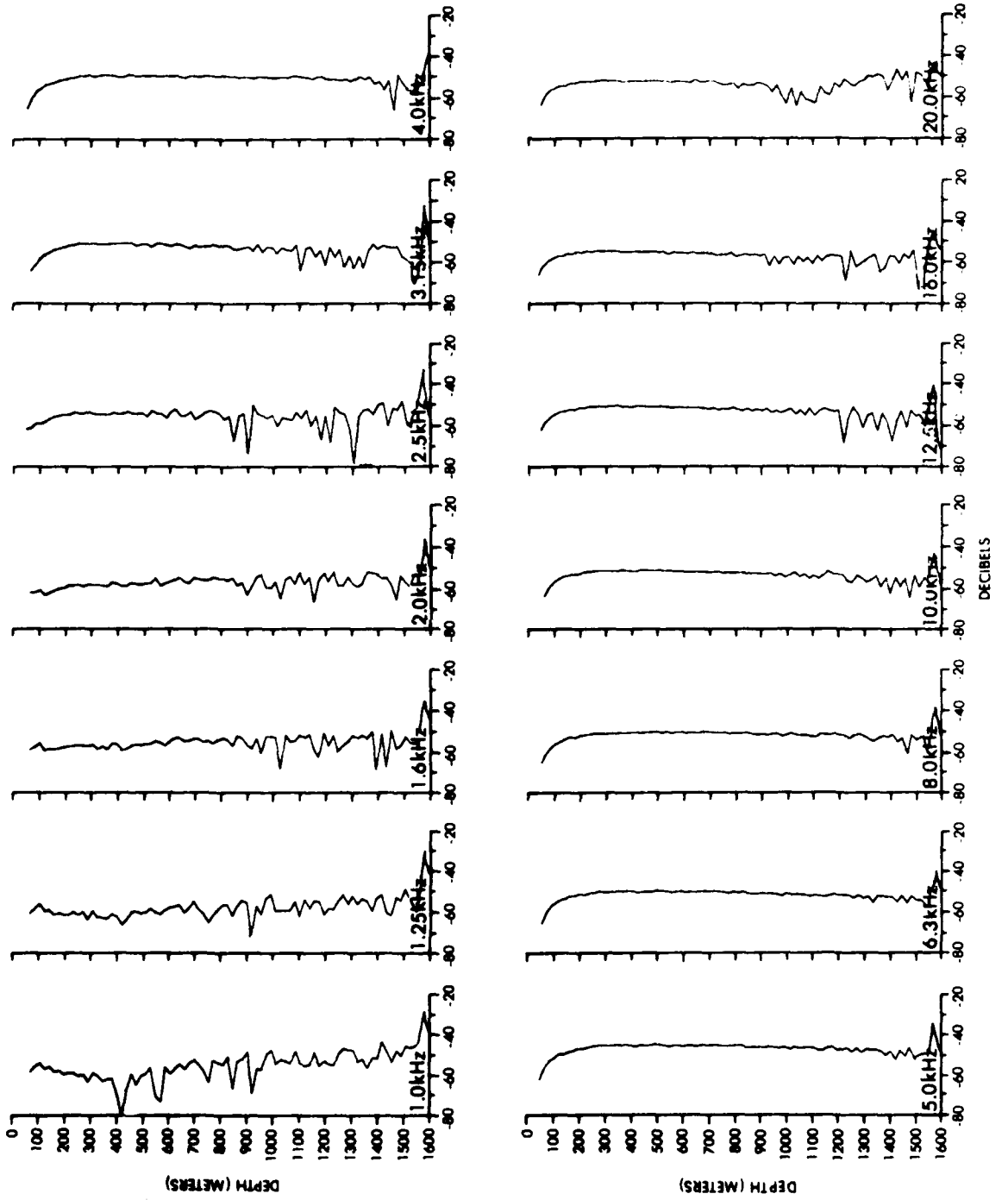

Figure A-16. $S_C(z)$, CARIBCAP II, Station 3, night

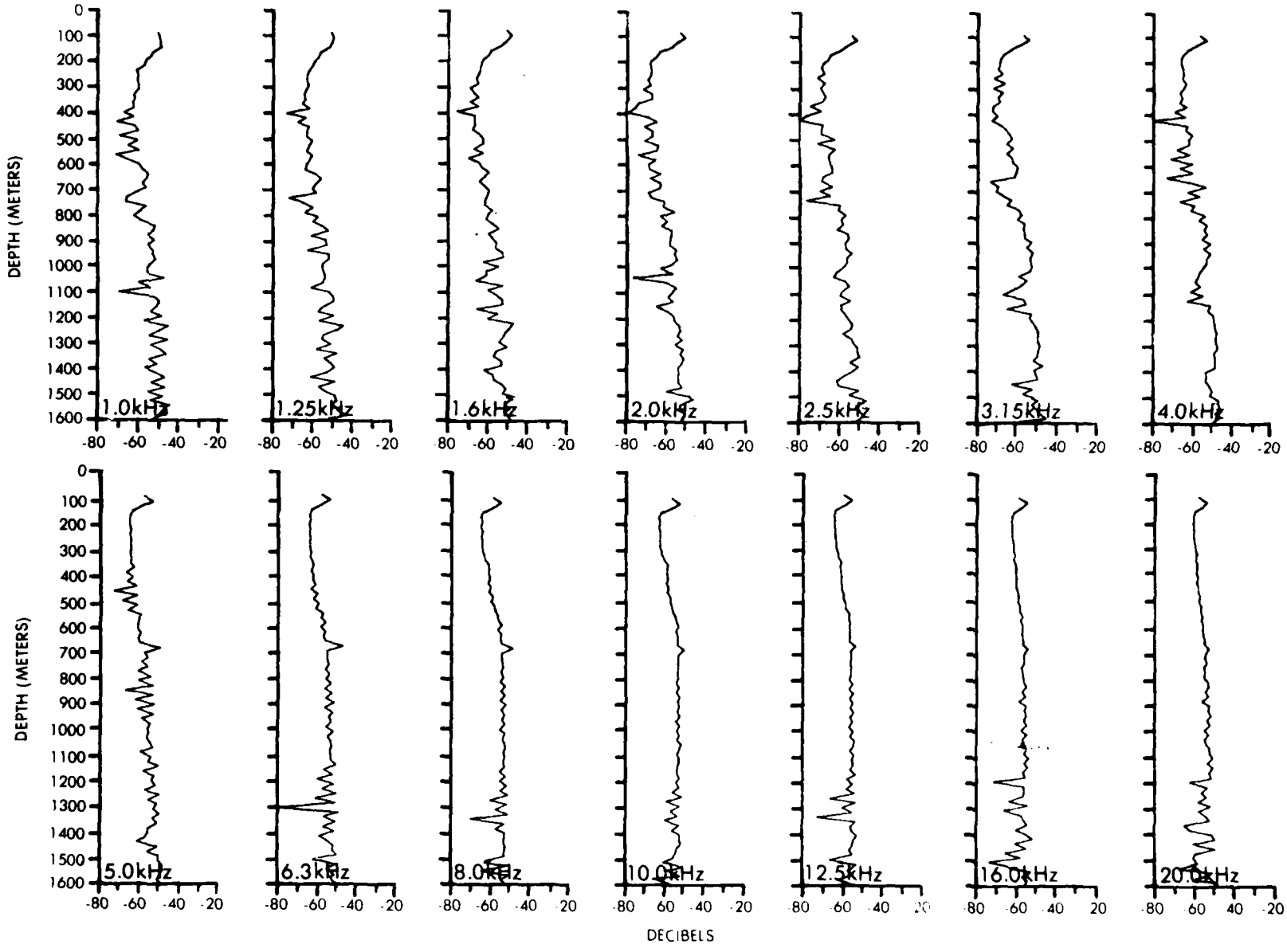

Figure A-17. $S_c(z)$, CARIBCAP II, Station 4, day

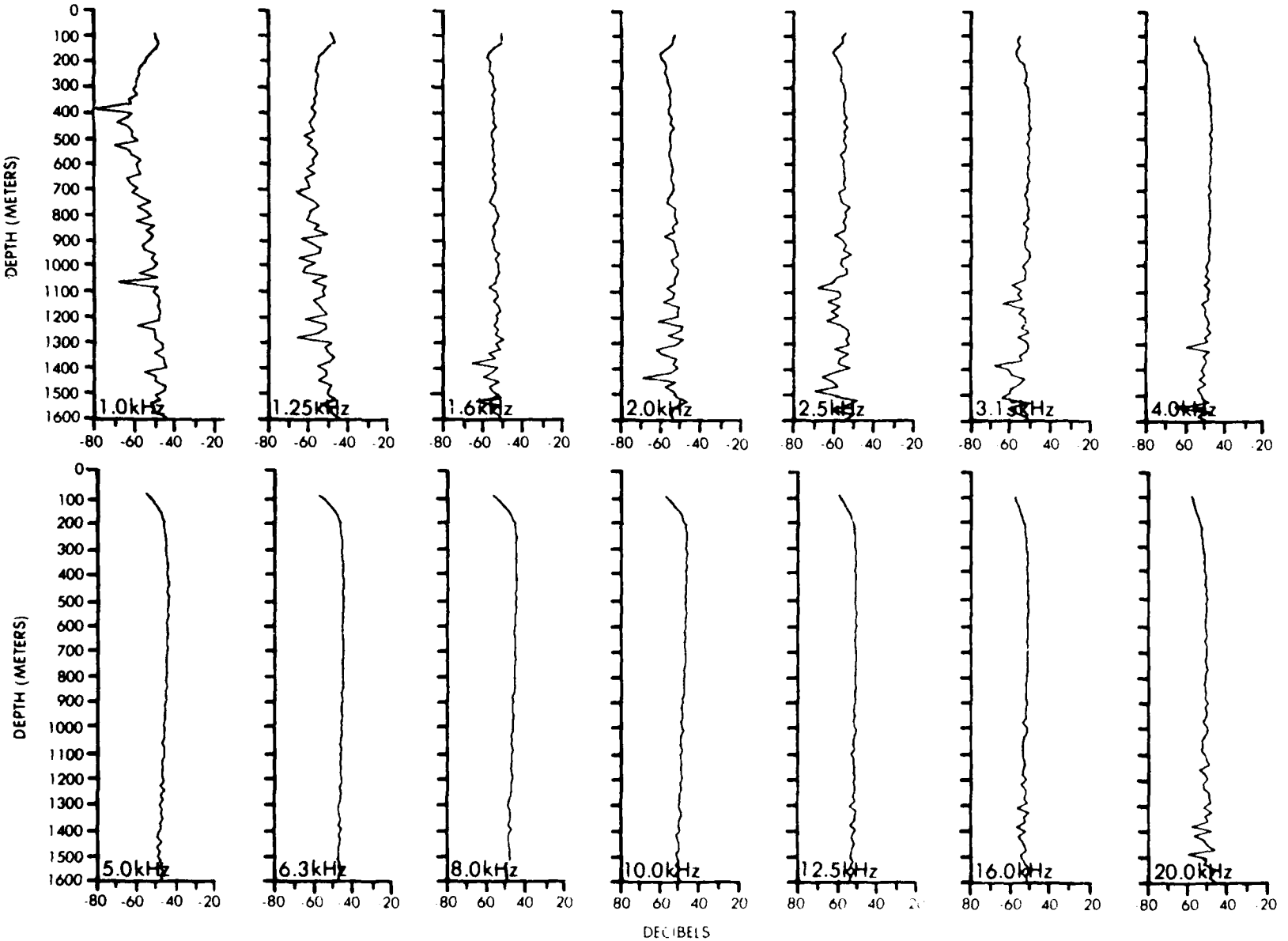

Figure A-18. $S_c(z)$, CARIBCAP II, Station 4, night

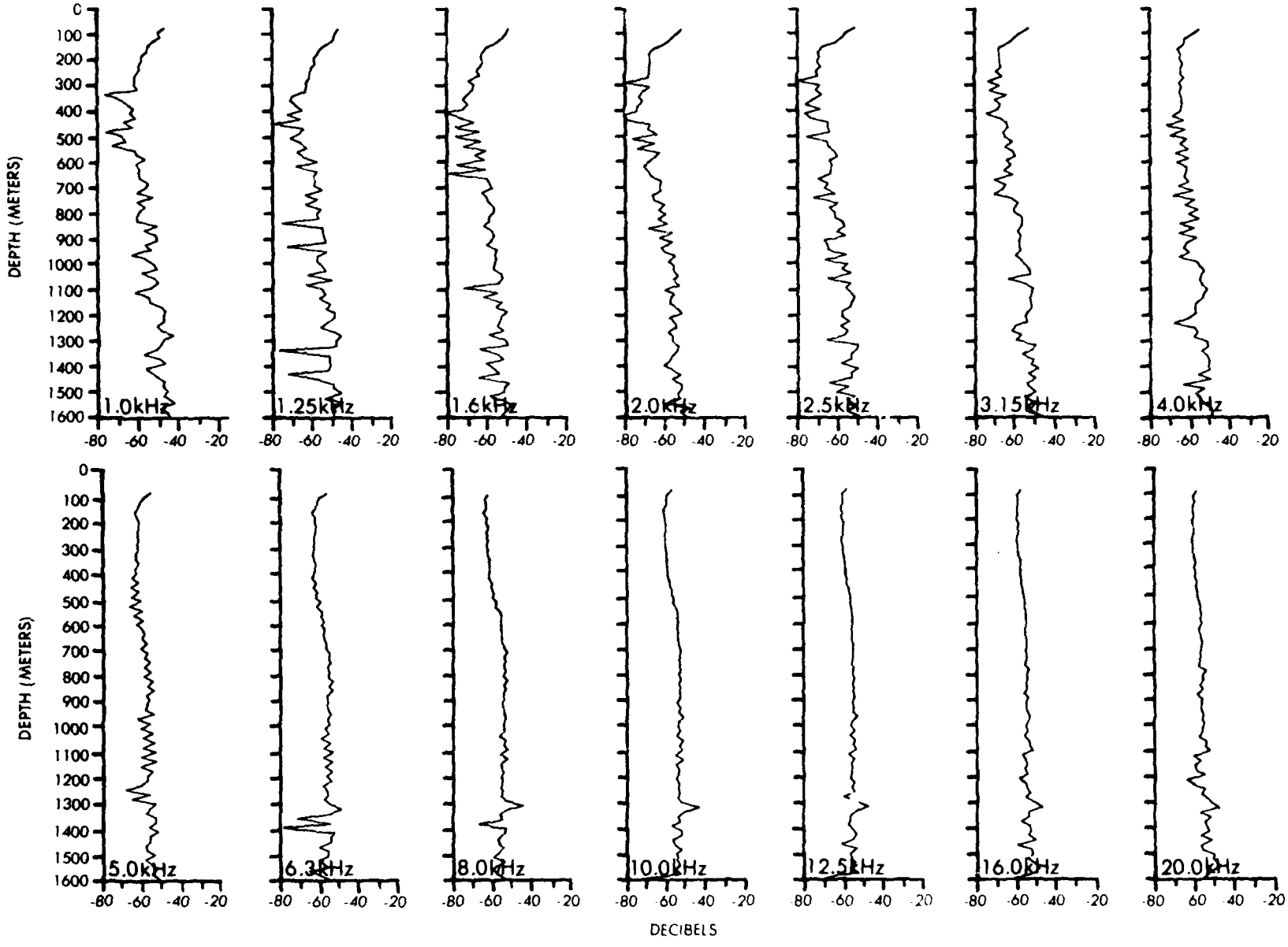

Figure A-19. $S_C(z)$, CARIBCAP II, Station 5, day

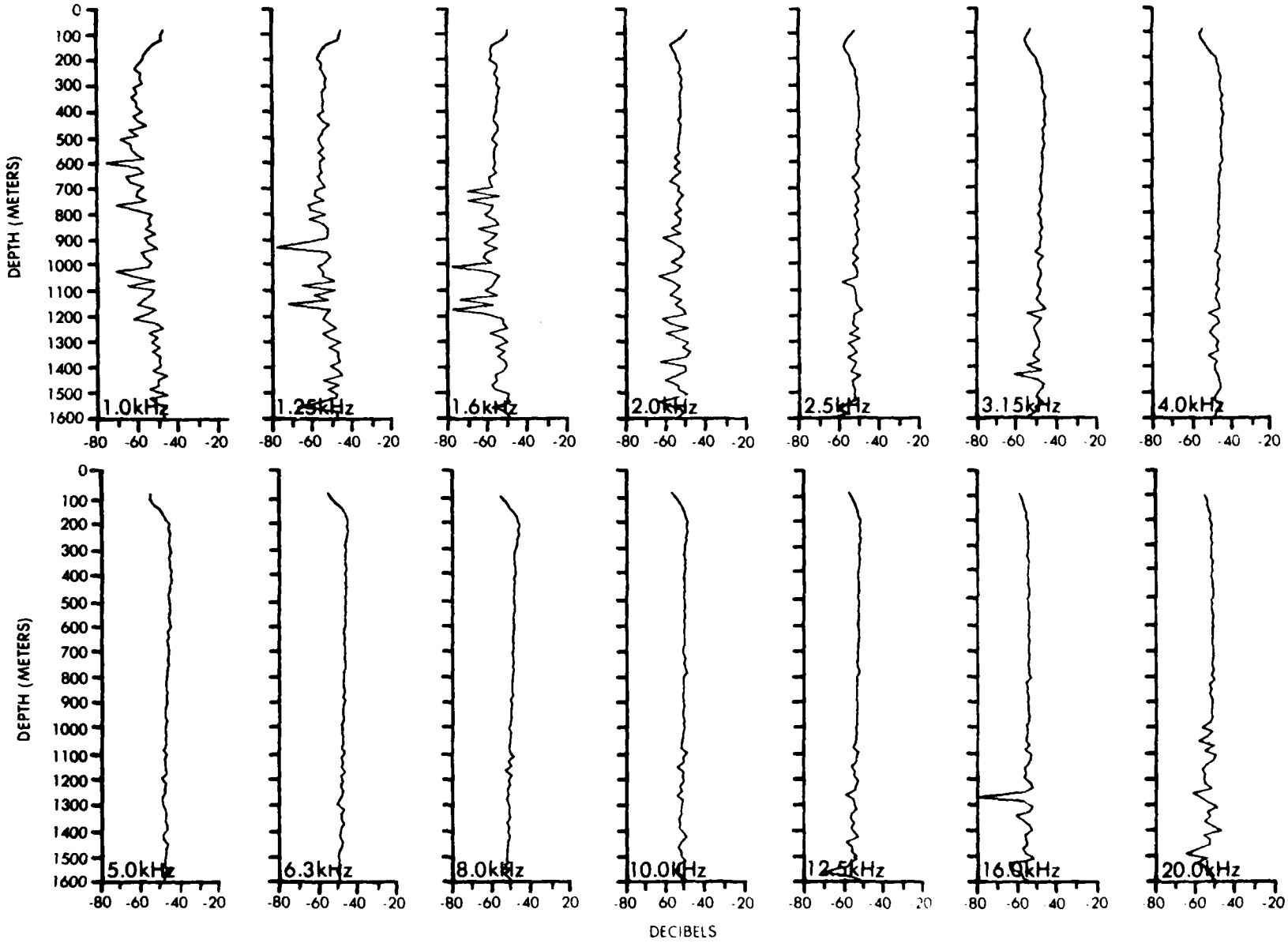

Figure A-20. $S_c(z)$, CARIBCAP II, Station 5, night

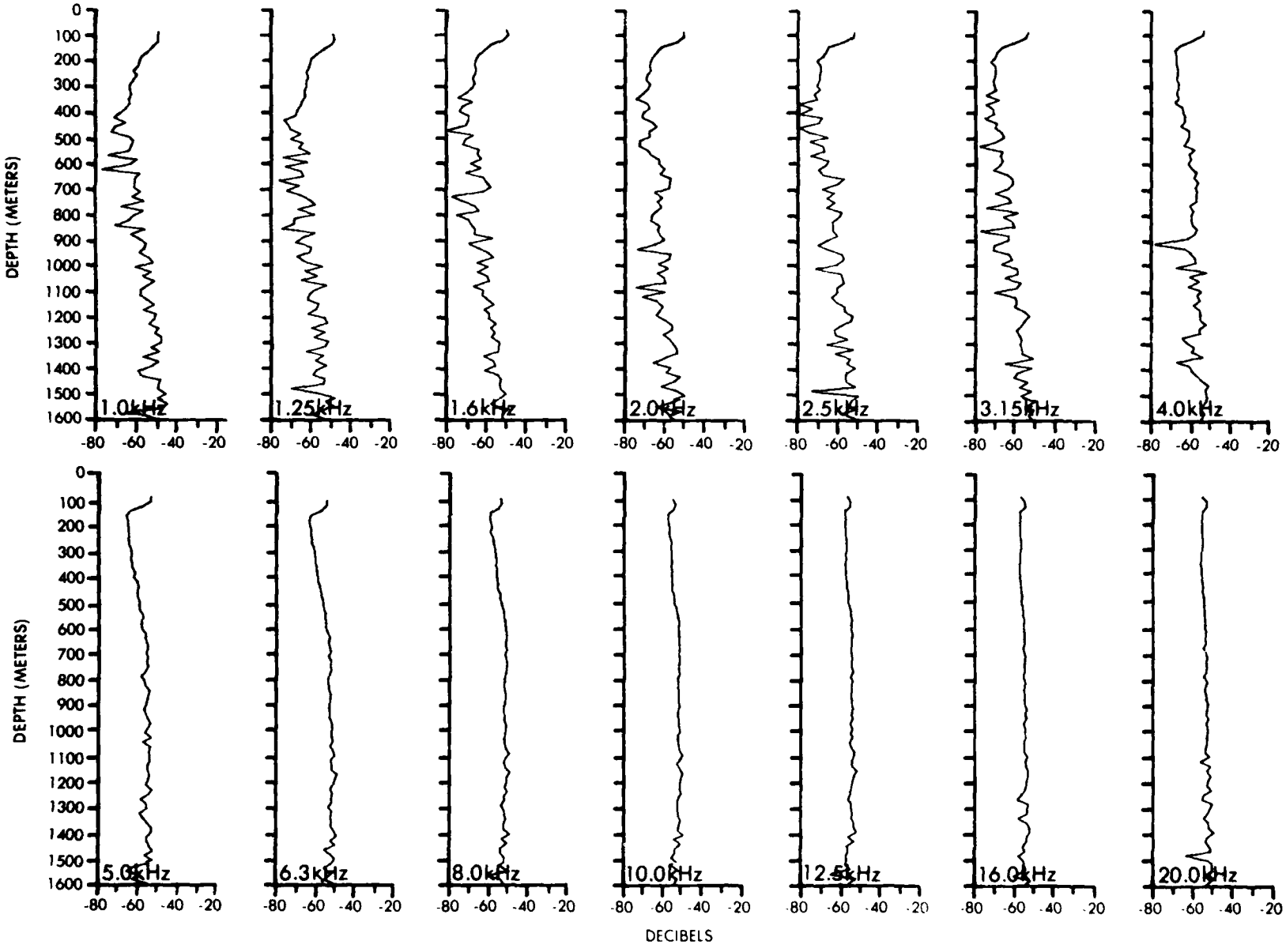

Figure A-21. $S_c(z)$, CARIBCAP II, Station 6, day

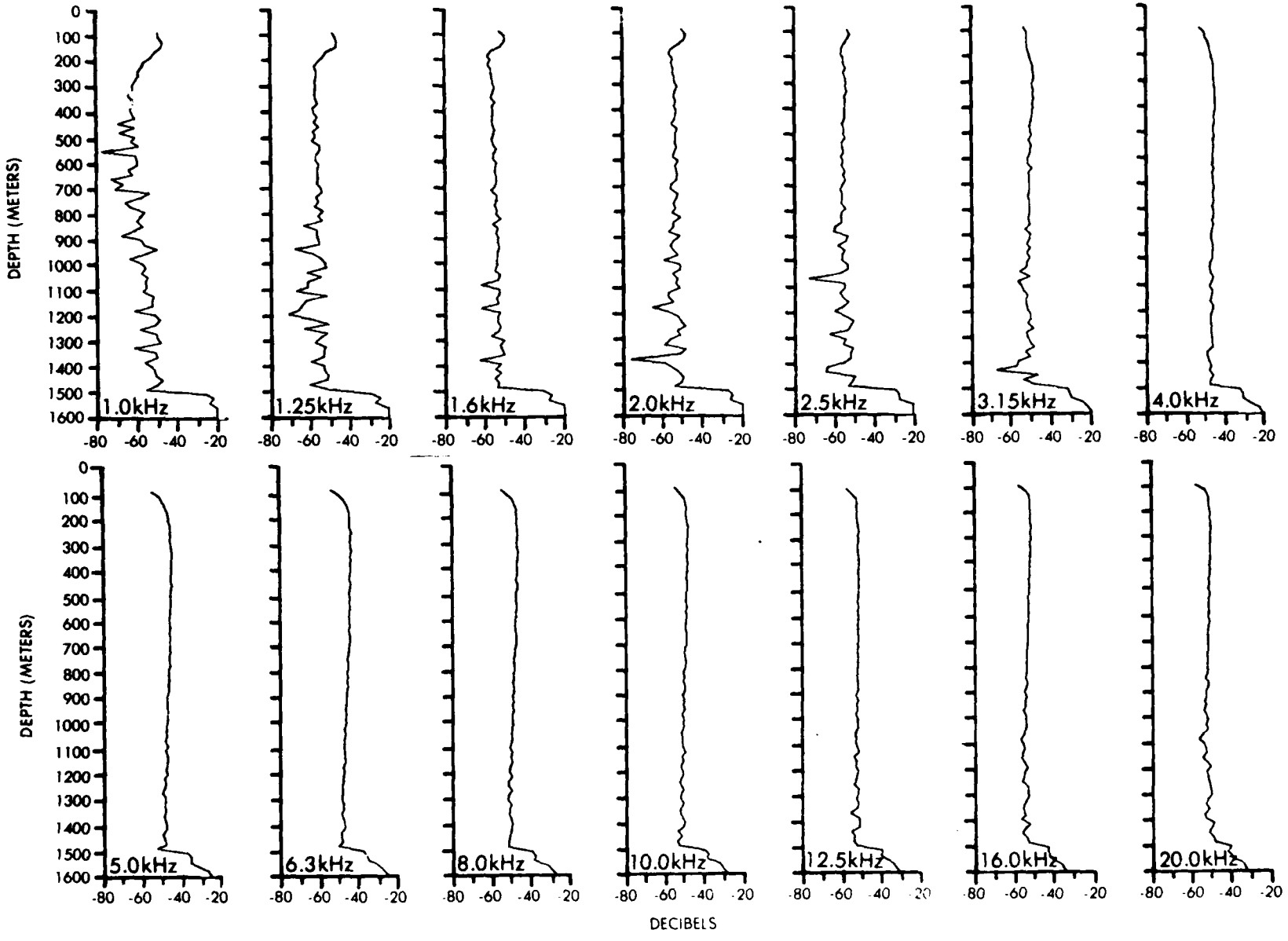

Figure A-22. $S_c(z)$, CARIBCAP II, Station 6, night

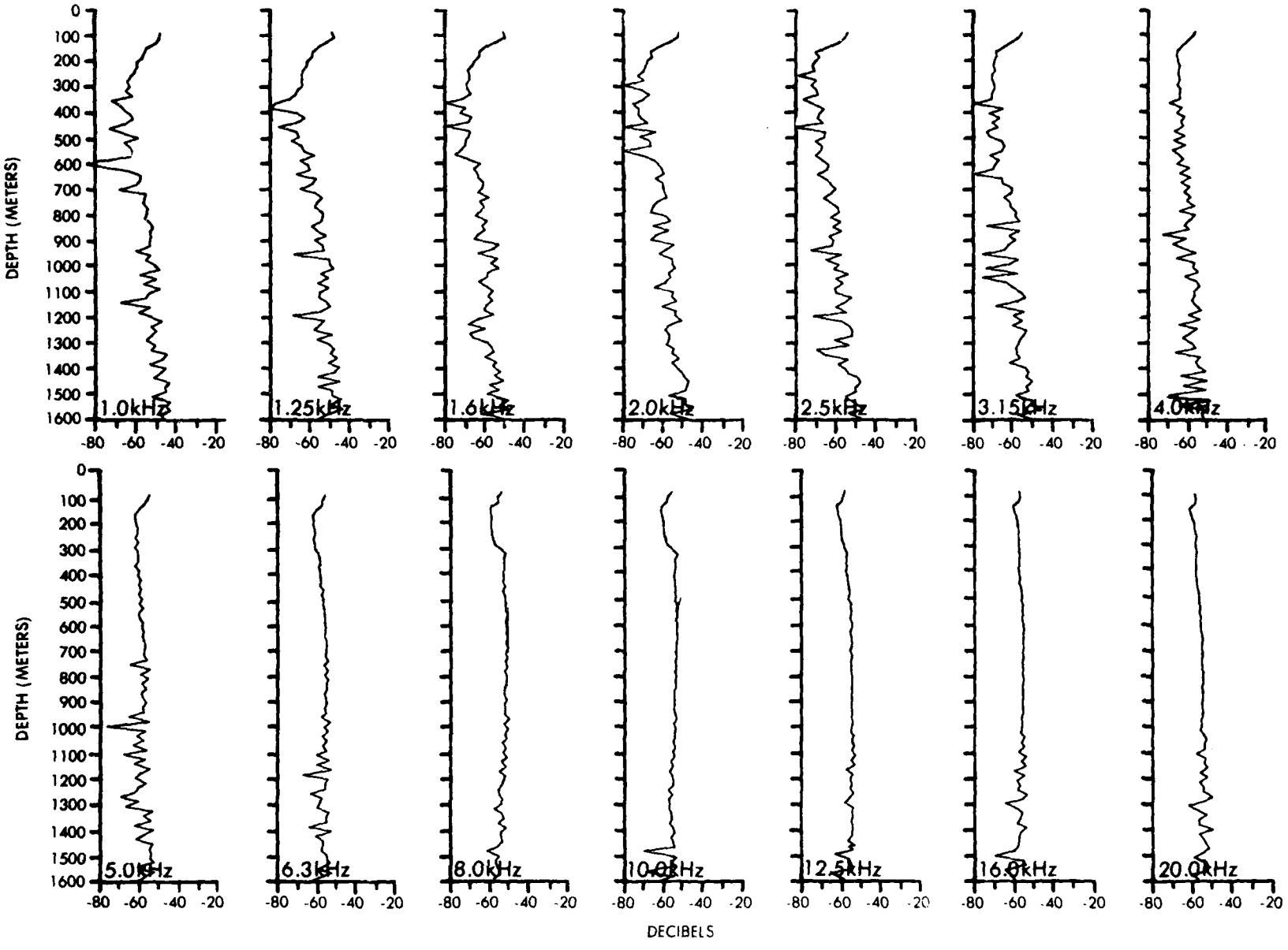

Figure A-23. $S_c(z)$, CARIBCAP II, Station 7, day

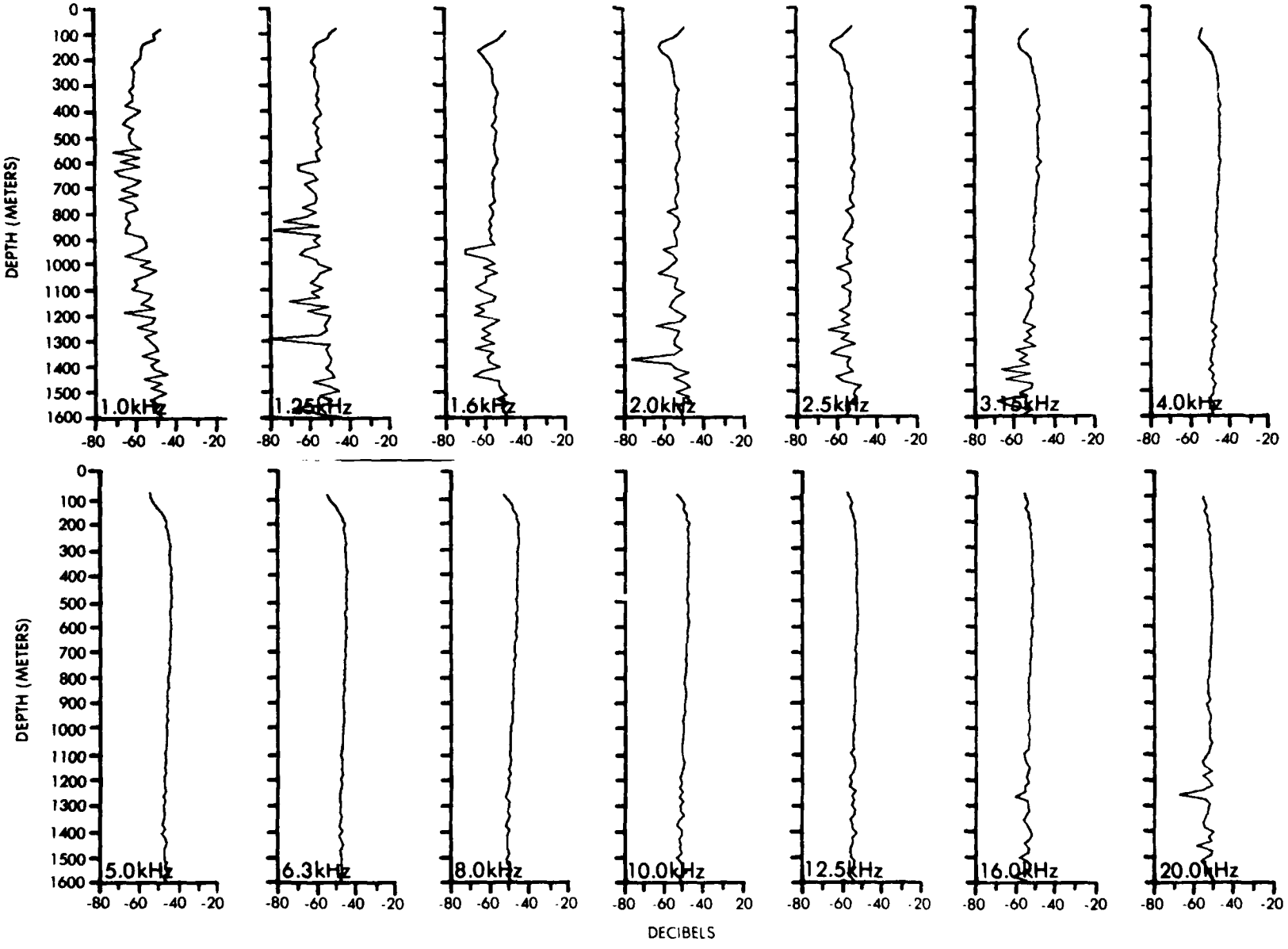

Figure A-24. $S_c(z)$, CARIBCAP II, Station 7, night

Appendix B

Mean $S_V(z)$ Profiles and Smoothed Mean $S_C(z)$ Profiles

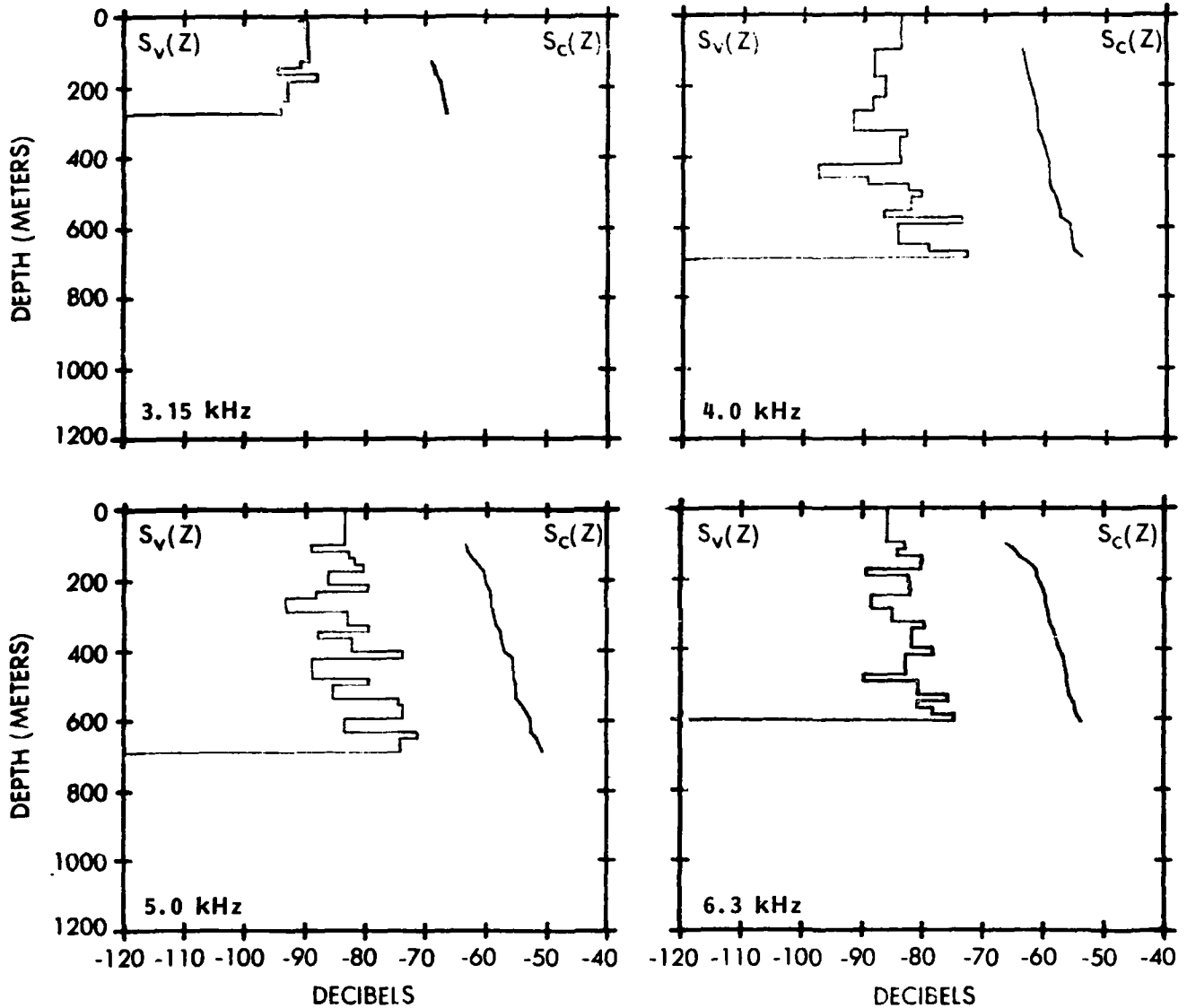

Figure B-1. CARIBCAP I, $S_v(z)$ and $S_c(z)$, 3.15 to 6.3 kHz, Station 4, day

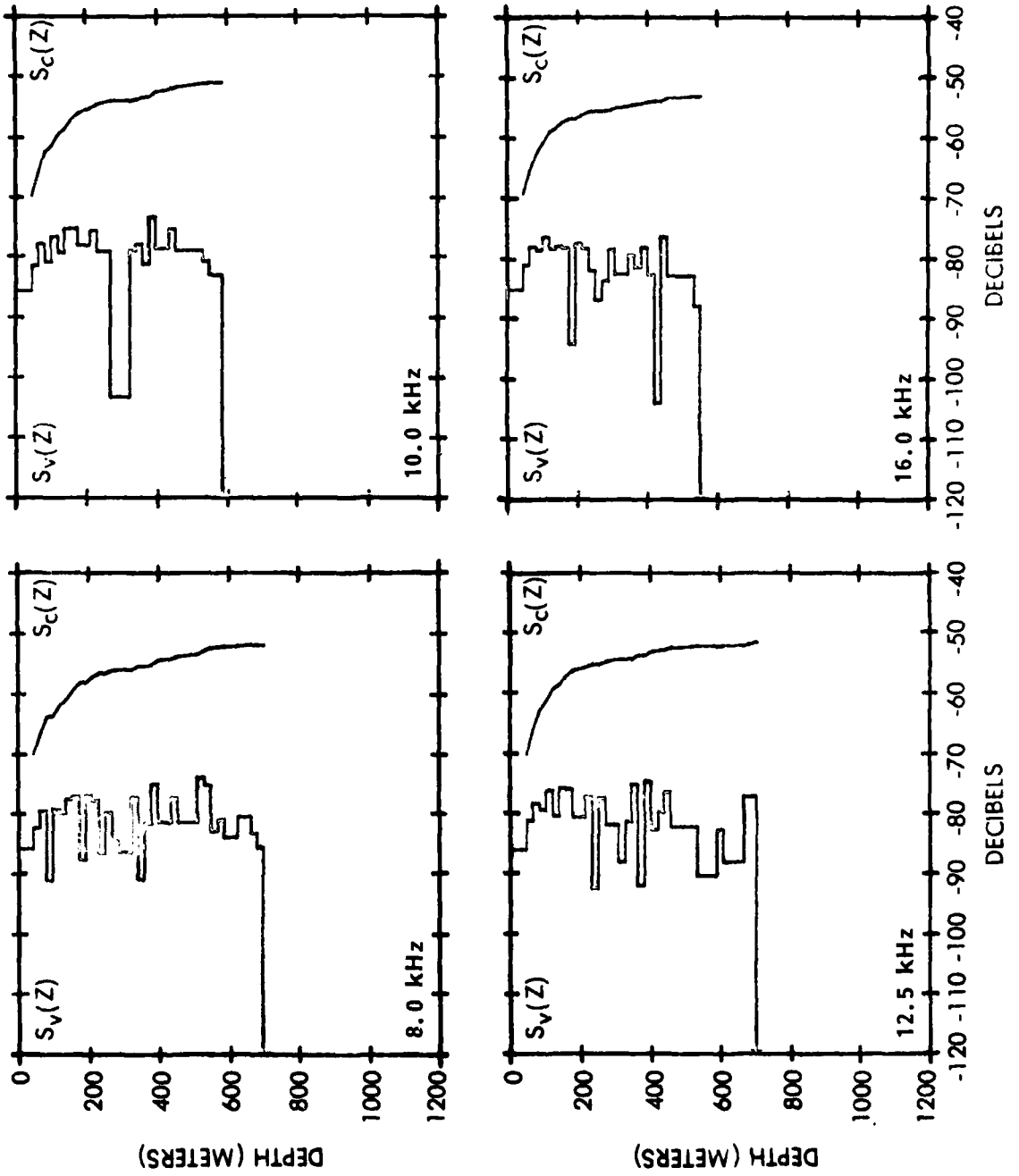

Figure B-2. CARIBCAP I, $S_v(z)$ and $S_c(z)$, 8 to 16 kHz, Station 4, day

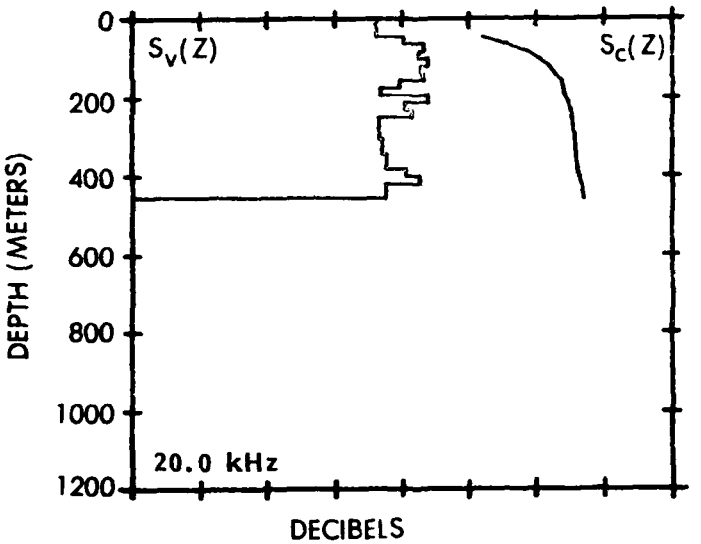

Figure B-3. CARIBCAP I, $S_v(z)$ and $S_c(z)$, 20 kHz, Station 4, day

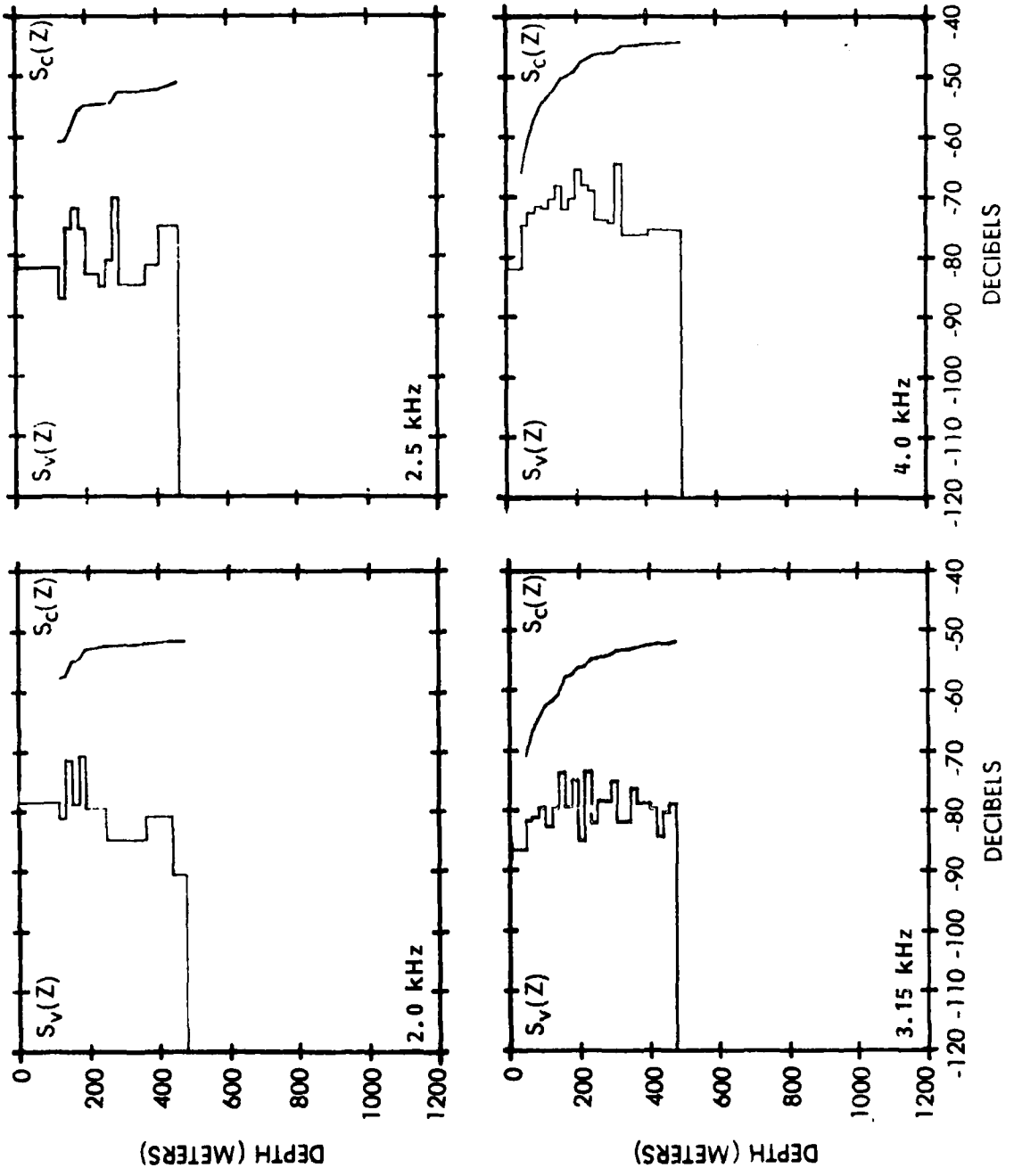

Figure B-4. CARIBCAP I, $S_v(z)$ and $S_c(z)$, 2 to 4 kHz, Station 4, night

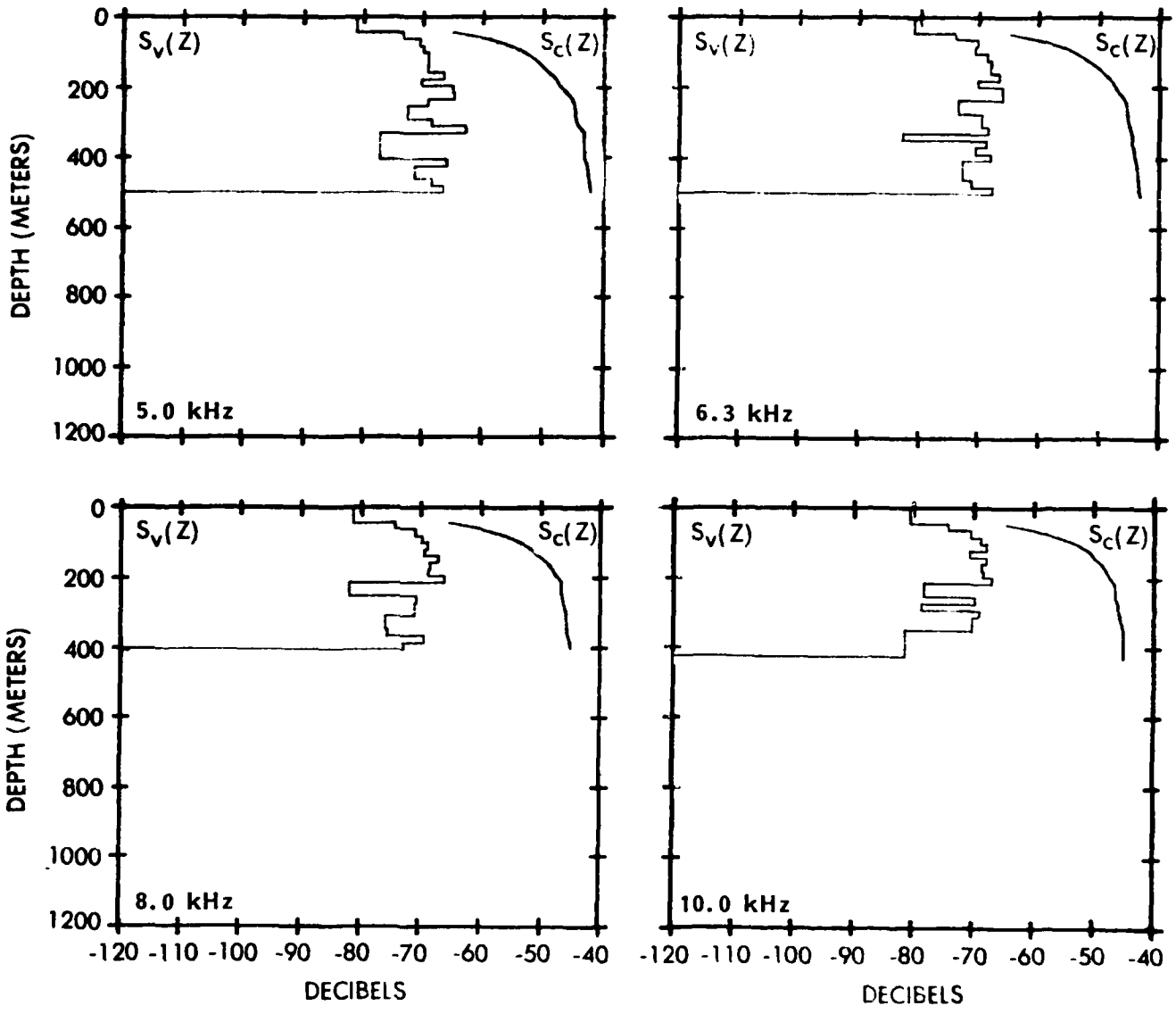

Figure B-5. CARIBCAP I, $S_v(z)$ and $S_c(z)$, 5 to 10 kHz, Station 4, night

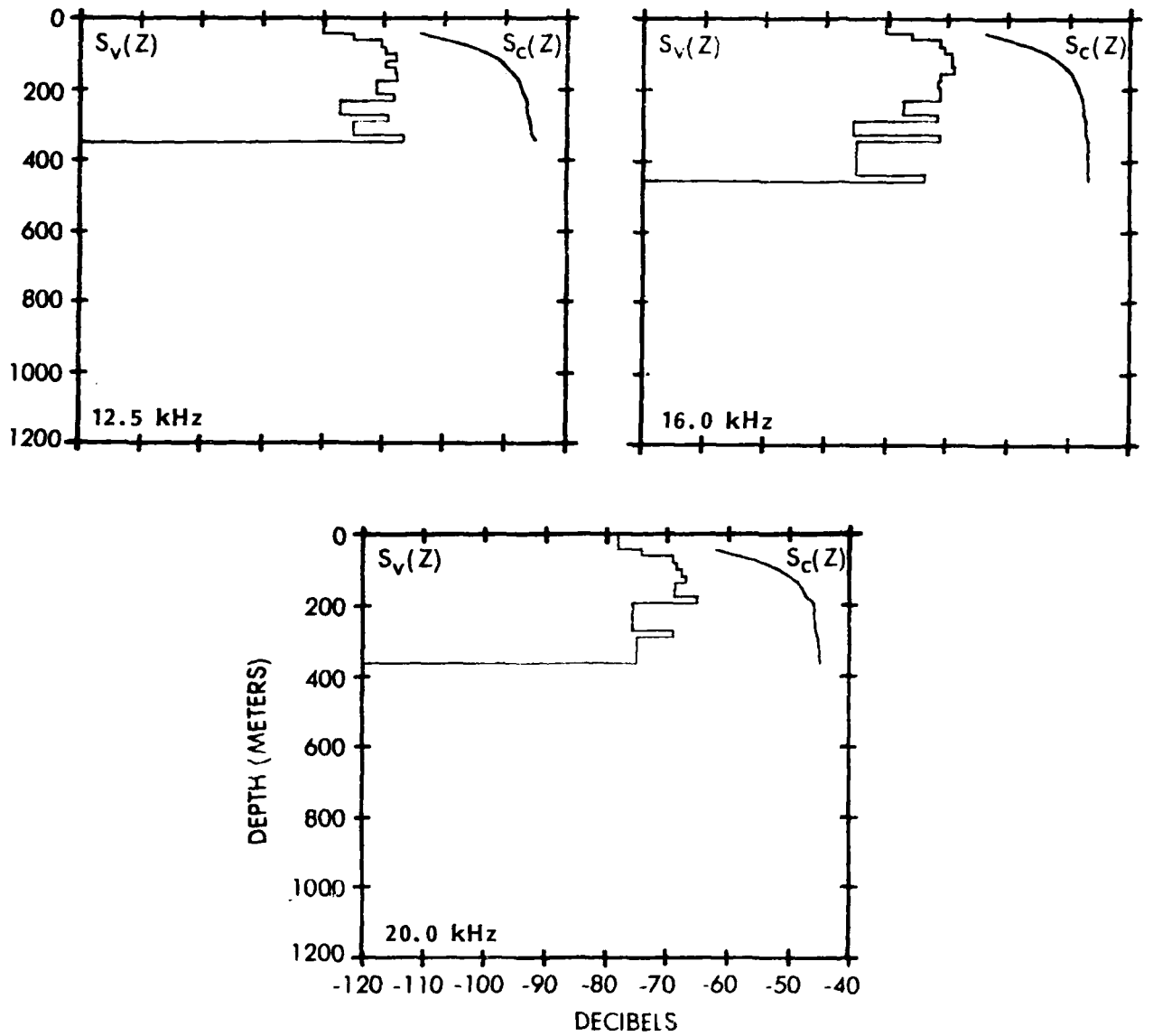

Figure B-6. CARIBCAP I, $S_v(z)$ and $S_c(z)$, 12.5 to 20 kHz, Station 4, night

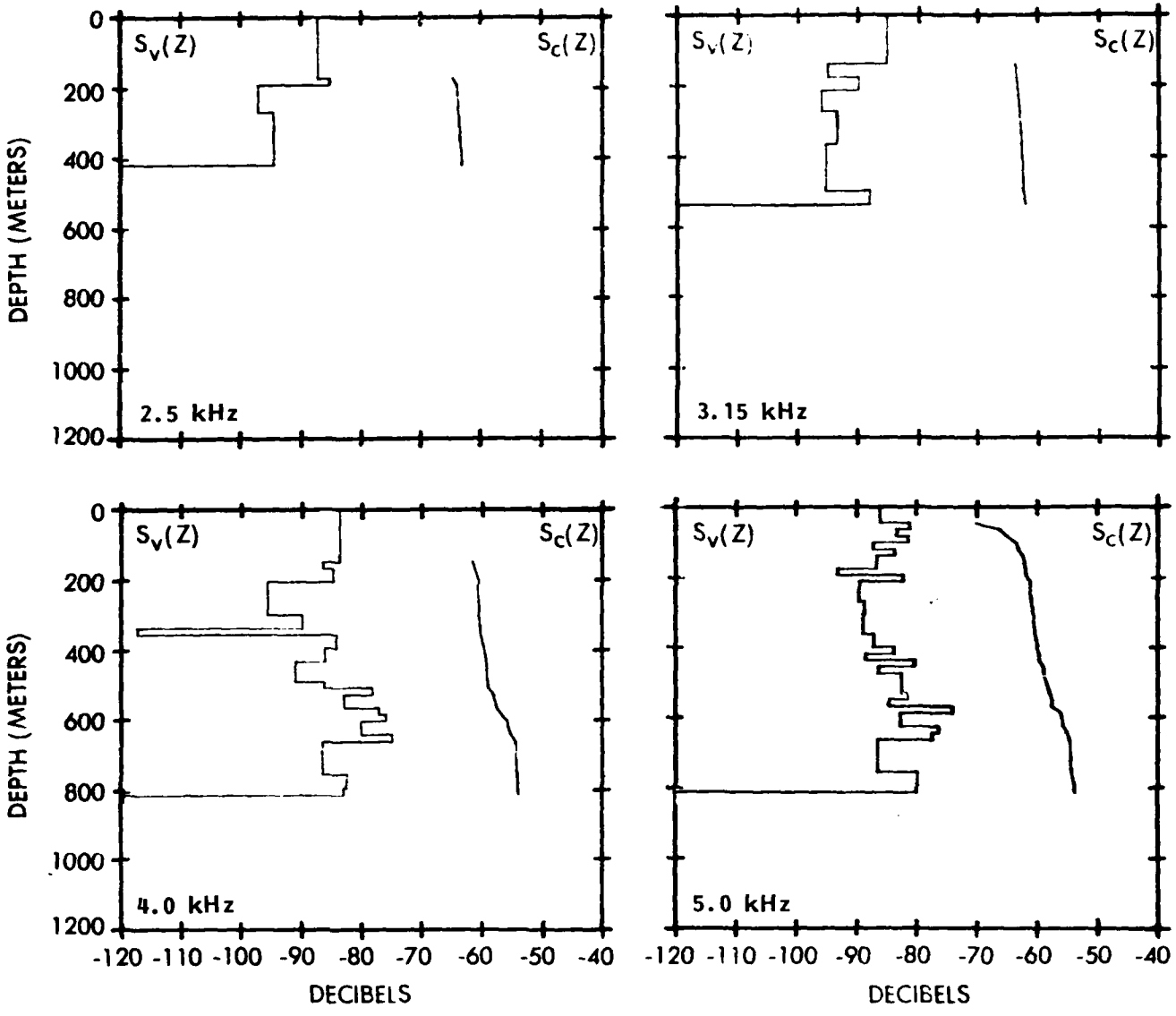

Figure B-7. CARIBCAP I, $S_v(z)$ and $S_c(z)$, 2.5 to 5 kHz, Station 5, day

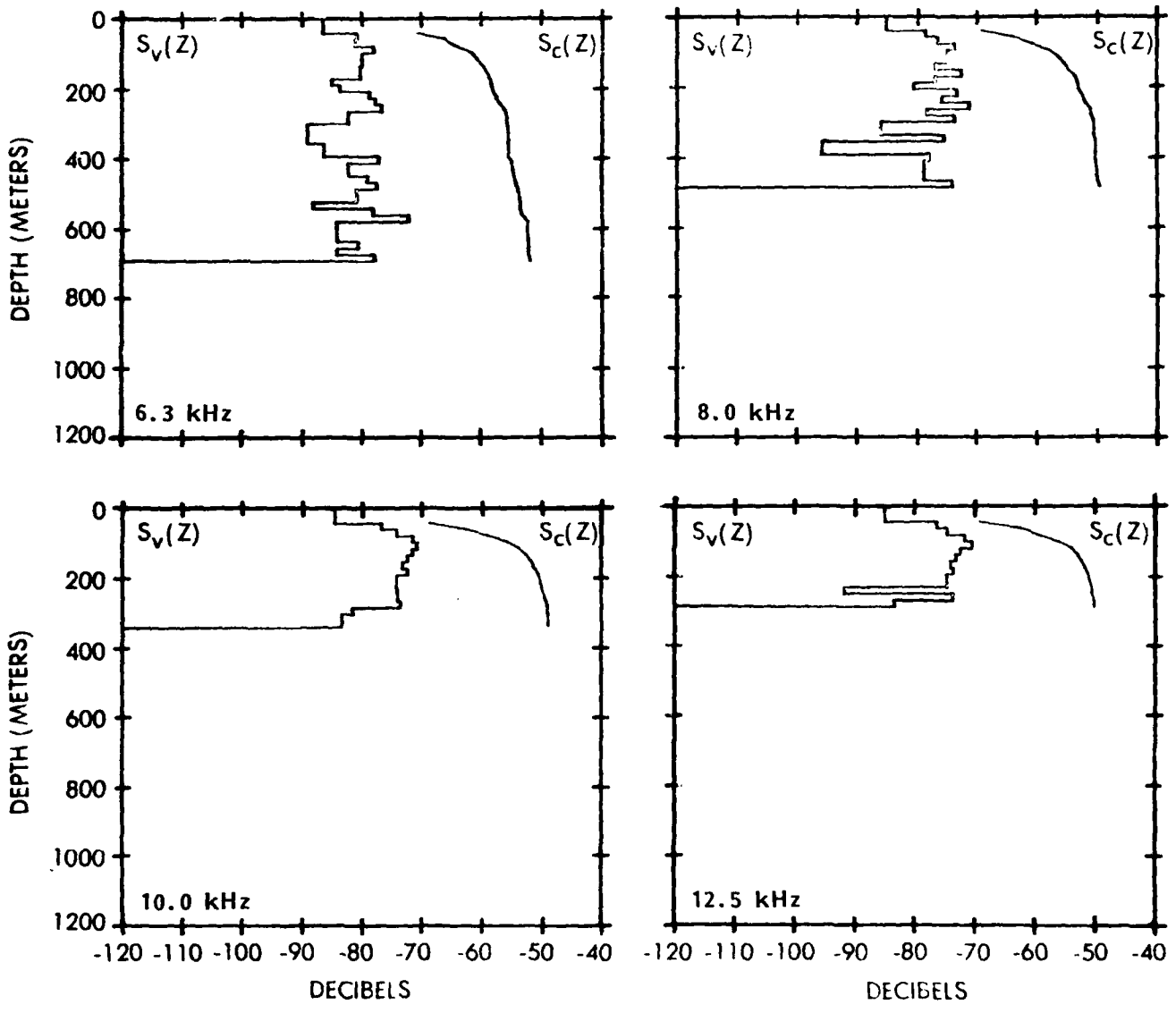

Figure B-8. CARIBCAP I, $S_v(z)$ and $S_c(z)$, 6.3 to 12.5 kHz, Station 5, day

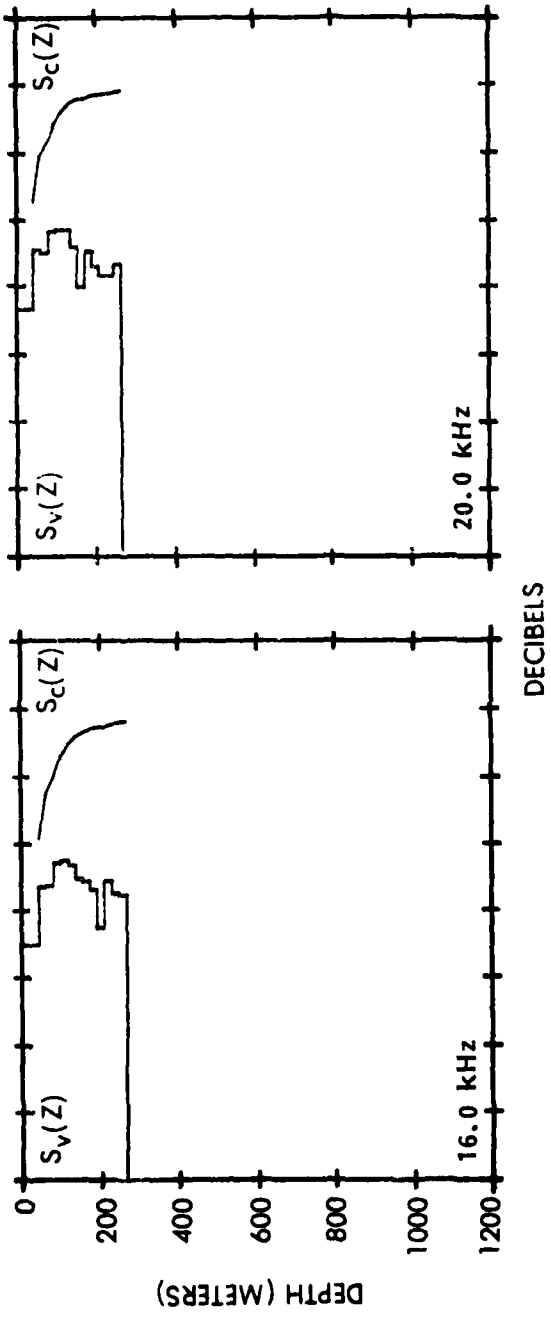

Figure B-9. CARIBCAP I, $S_v(z)$ and $S_c(z)$, 16 and 20 kHz, Station 5, day

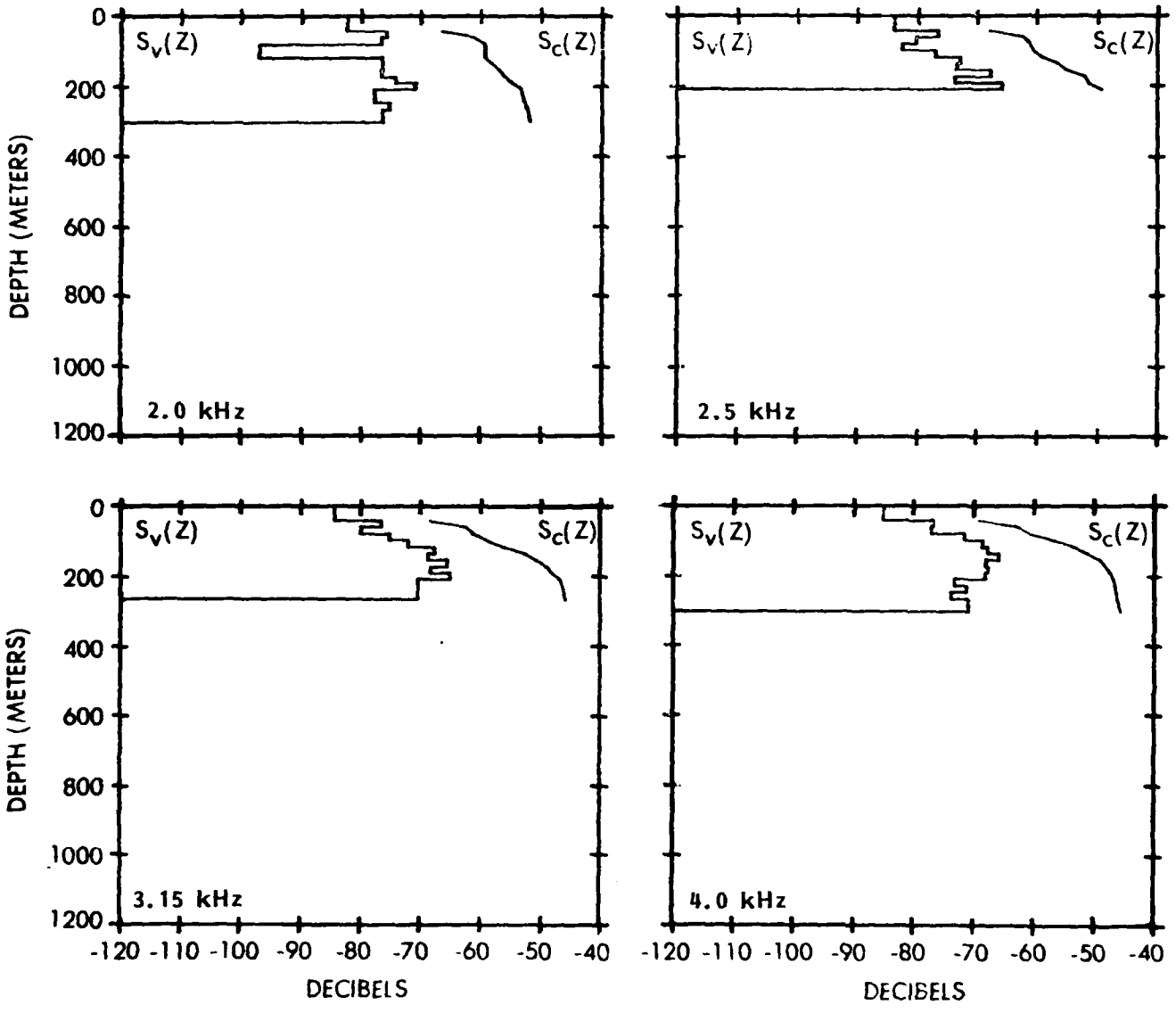

Figure B-10. CARIBCAP I, $S_v(z)$ and $S_c(z)$, 2 to 4 kHz, Station 5, night

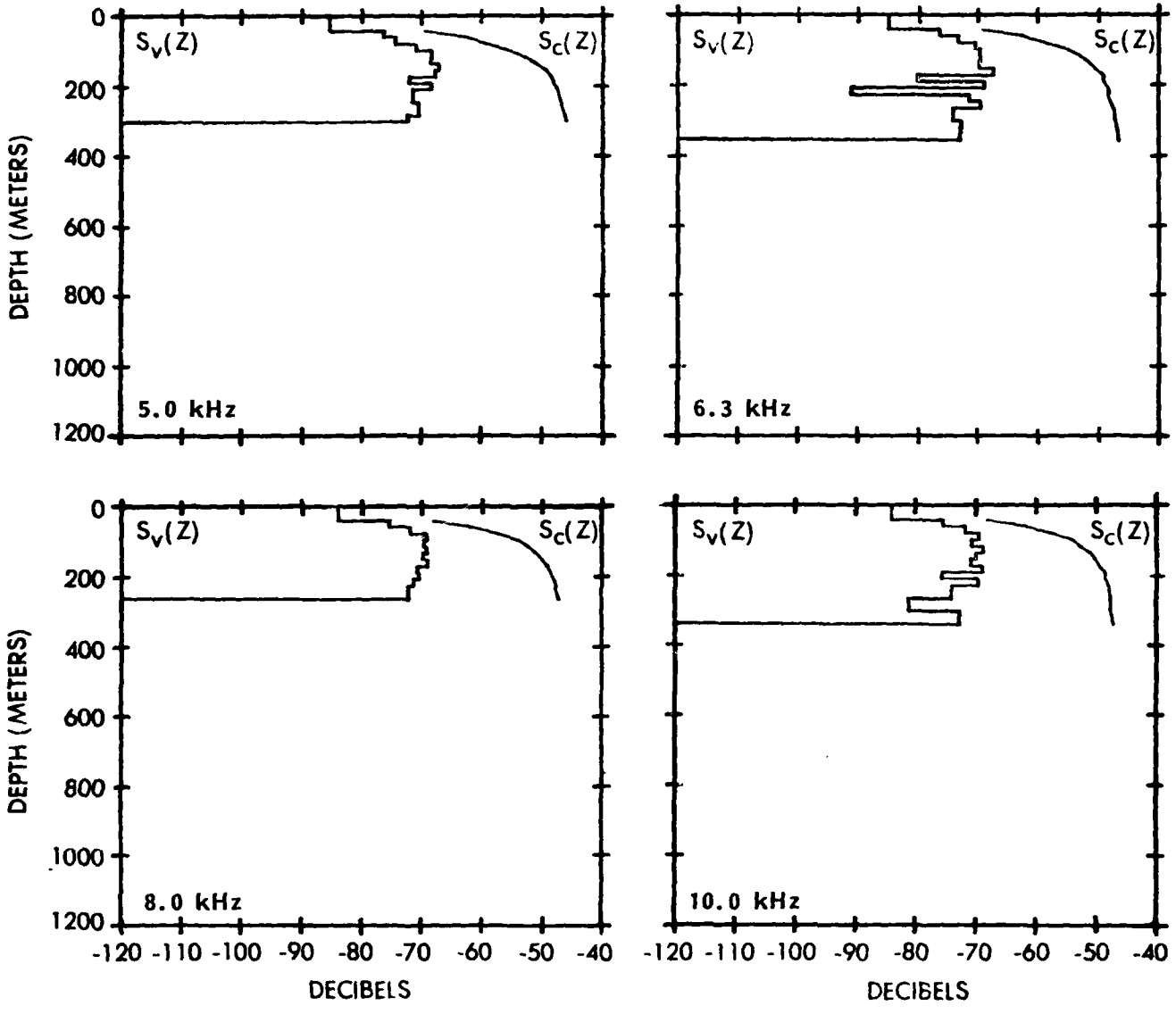

Figure B-11. CARIBCAP I, $S_v(z)$ and $S_c(z)$, 5 to 10 kHz, Station 5, night

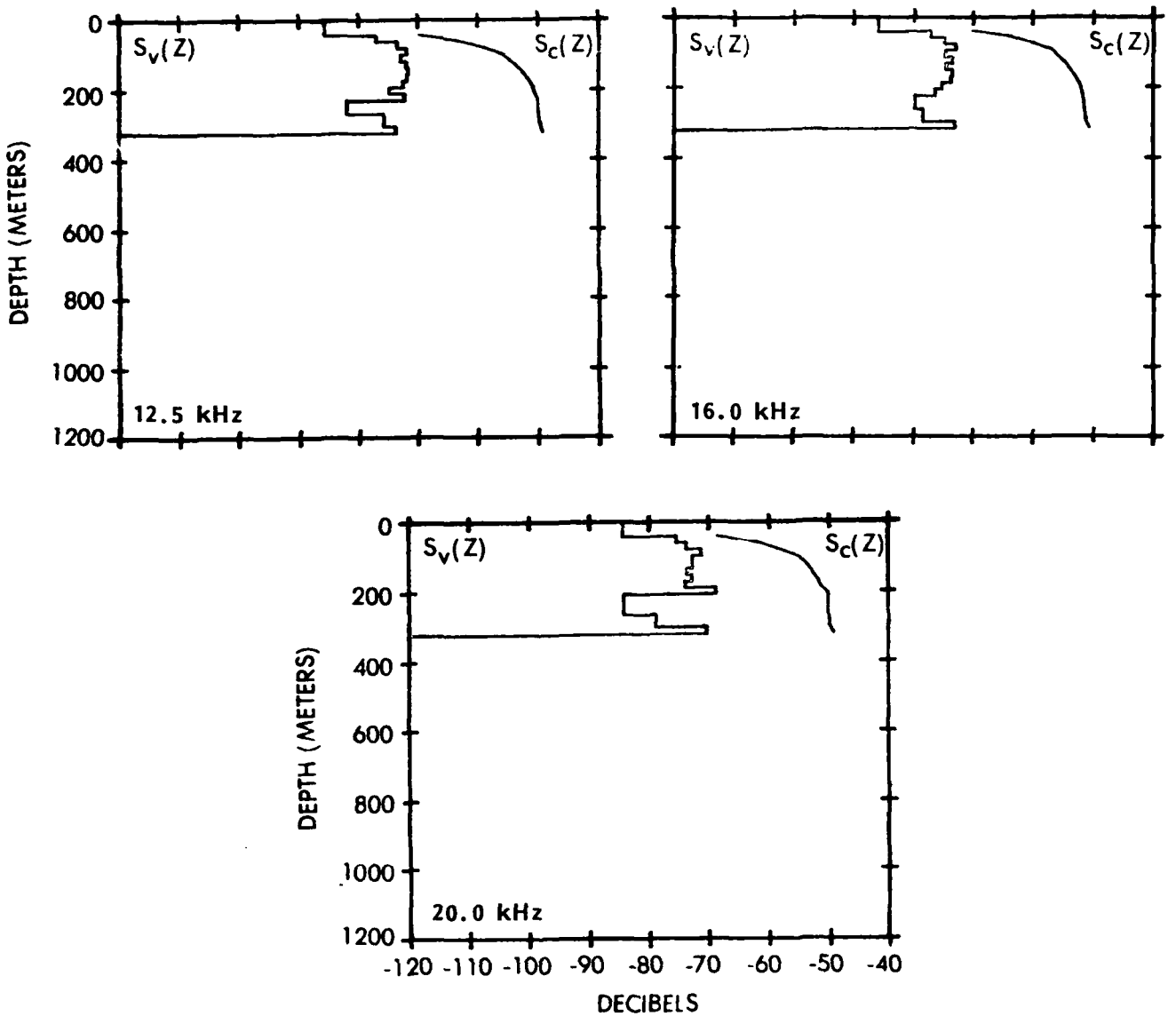

Figure B-12. CARIBCAP I, $S_v(z)$ and $S_c(z)$, 12.5 to 20 kHz, Station 5, night

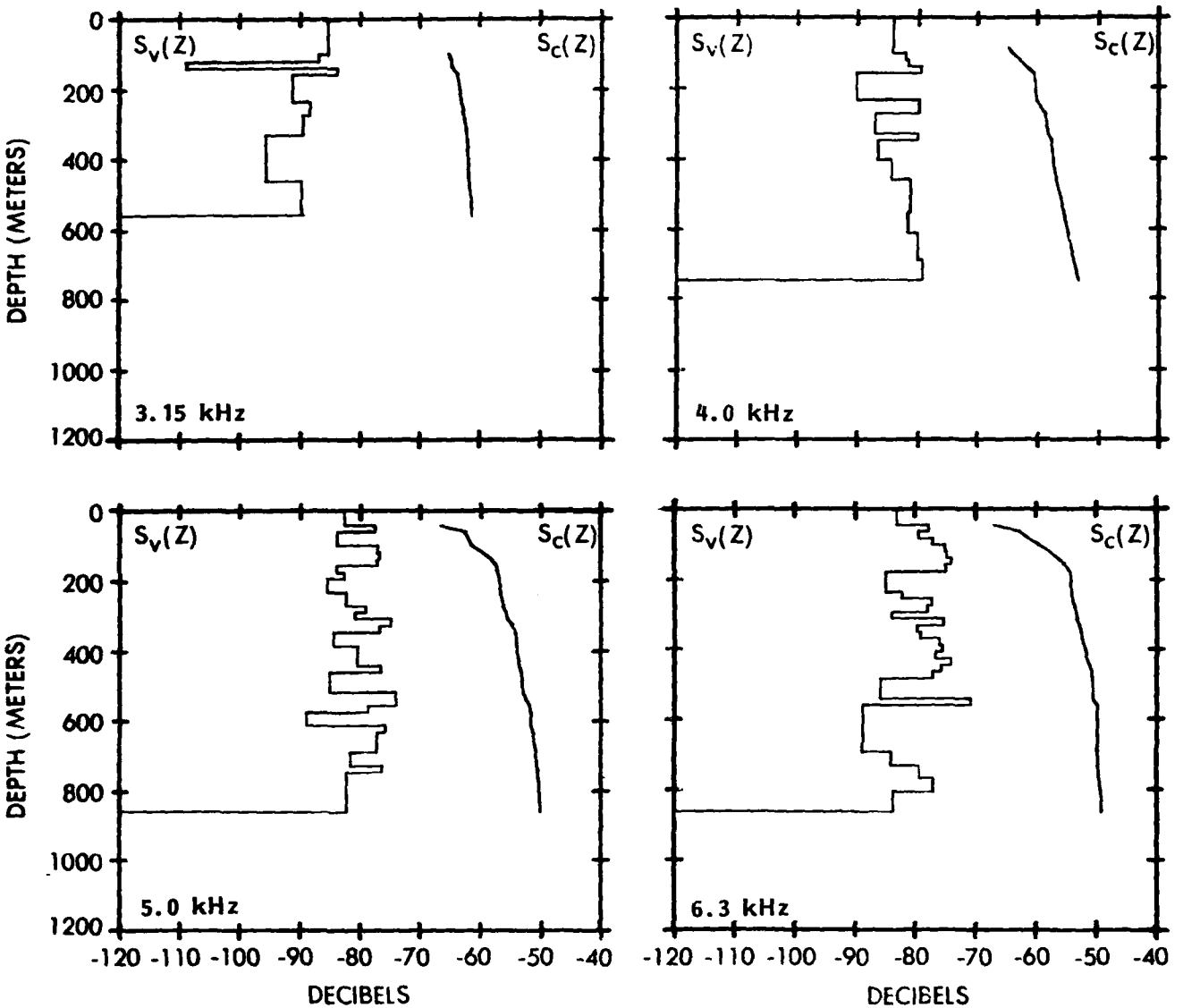

Figure B-13. CARIBCAP I, $S_v(z)$ and $S_c(z)$, 3.15 to 6.3 kHz, Station 6, day

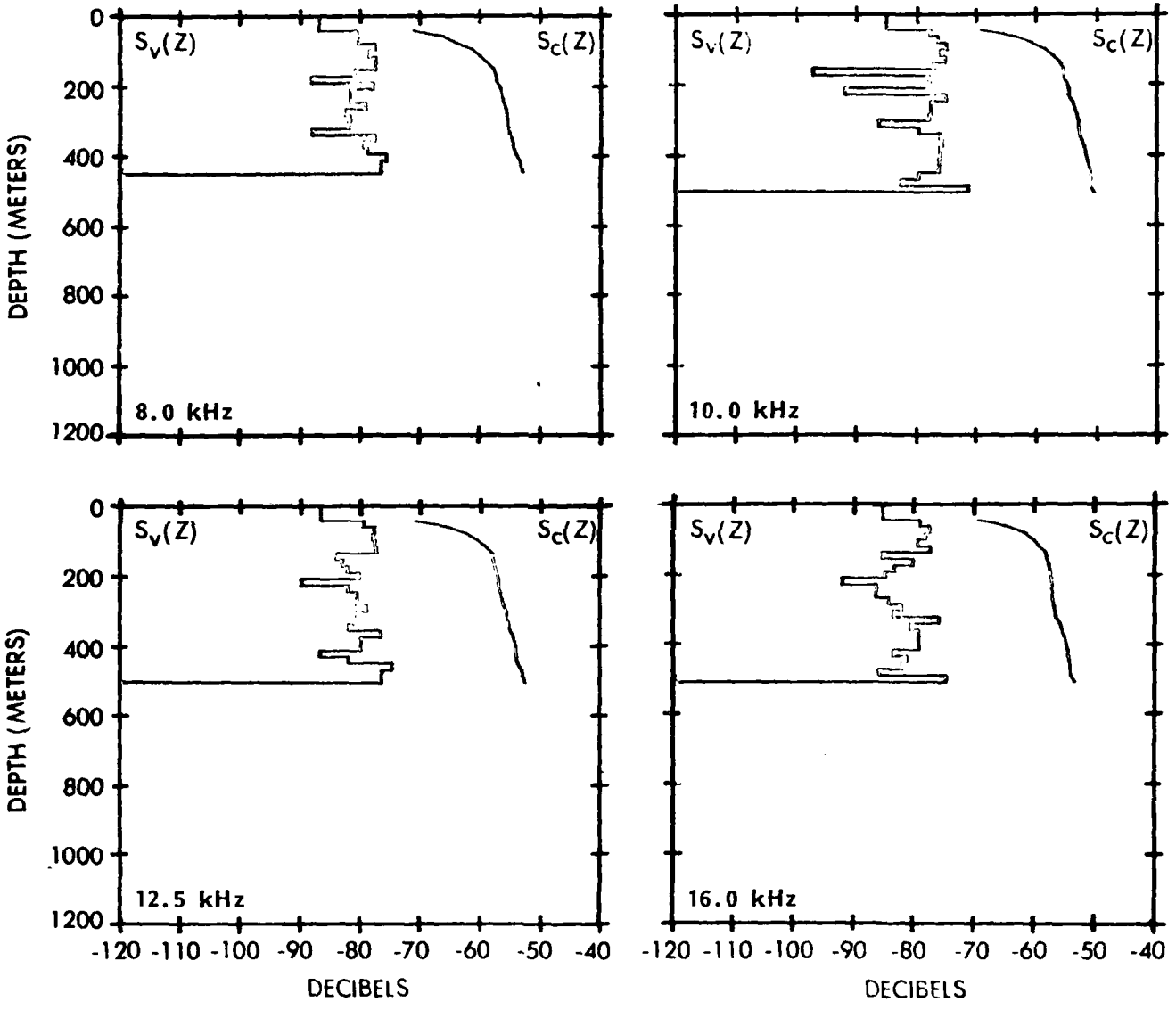

Figure B-14. CARIBCAP I, $S_v(z)$ and $S_c(z)$, 8 to 16 kHz, Station 6, day

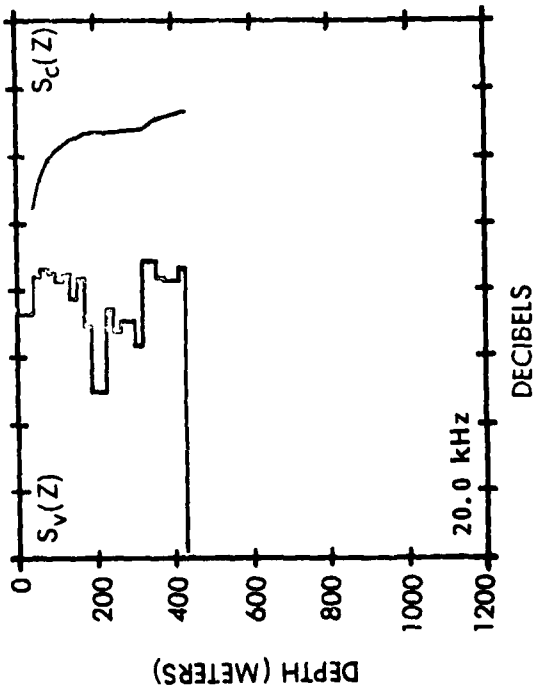

Figure B-15. CARIBCAP I, $S_v(z)$ and $S_c(z)$, 20 kHz, Station 6, day

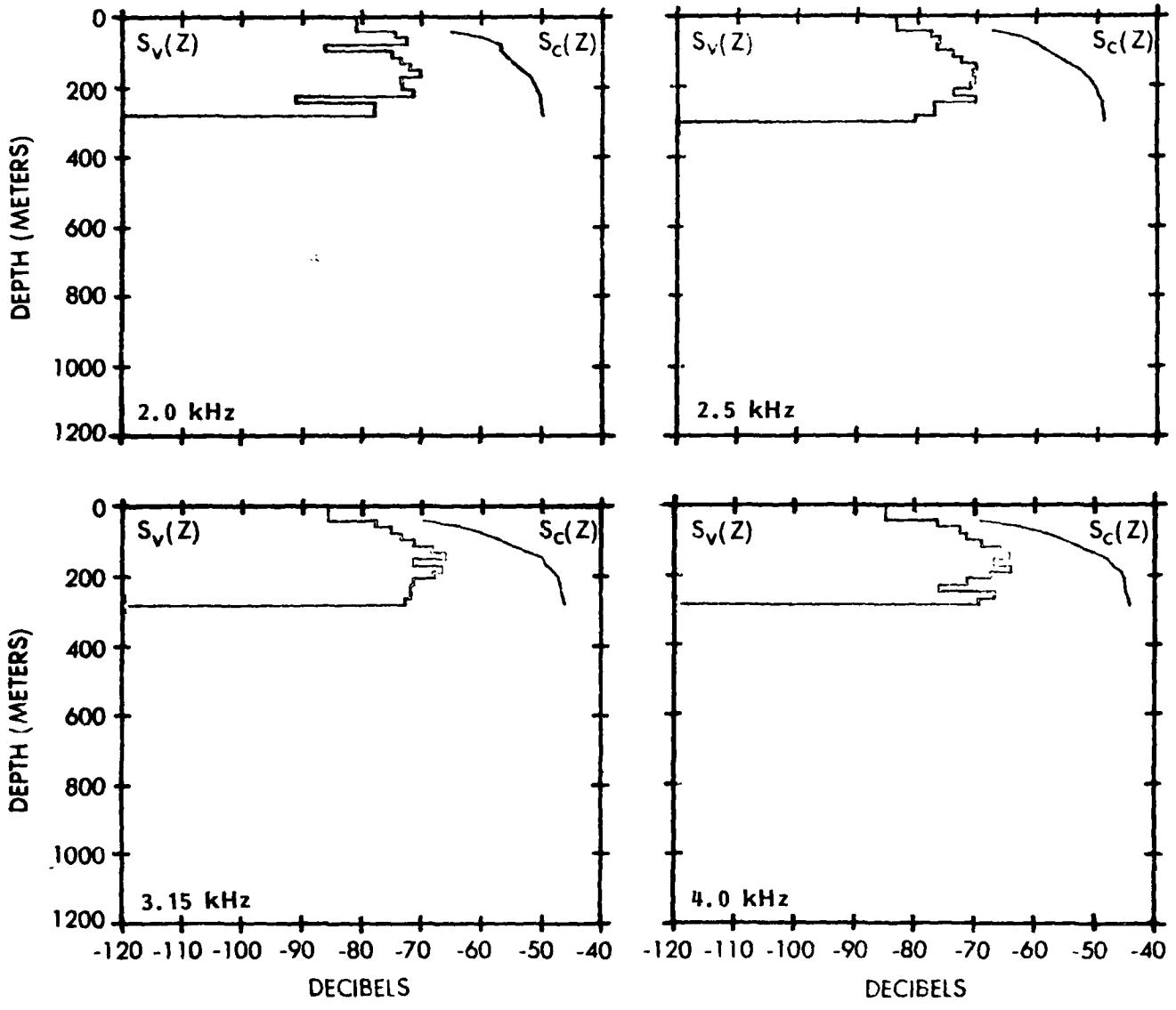

Figure B-16. CARIBCAP I, $S_V(z)$ and $S_C(z)$, 2 to 4 kHz, Station 6, night

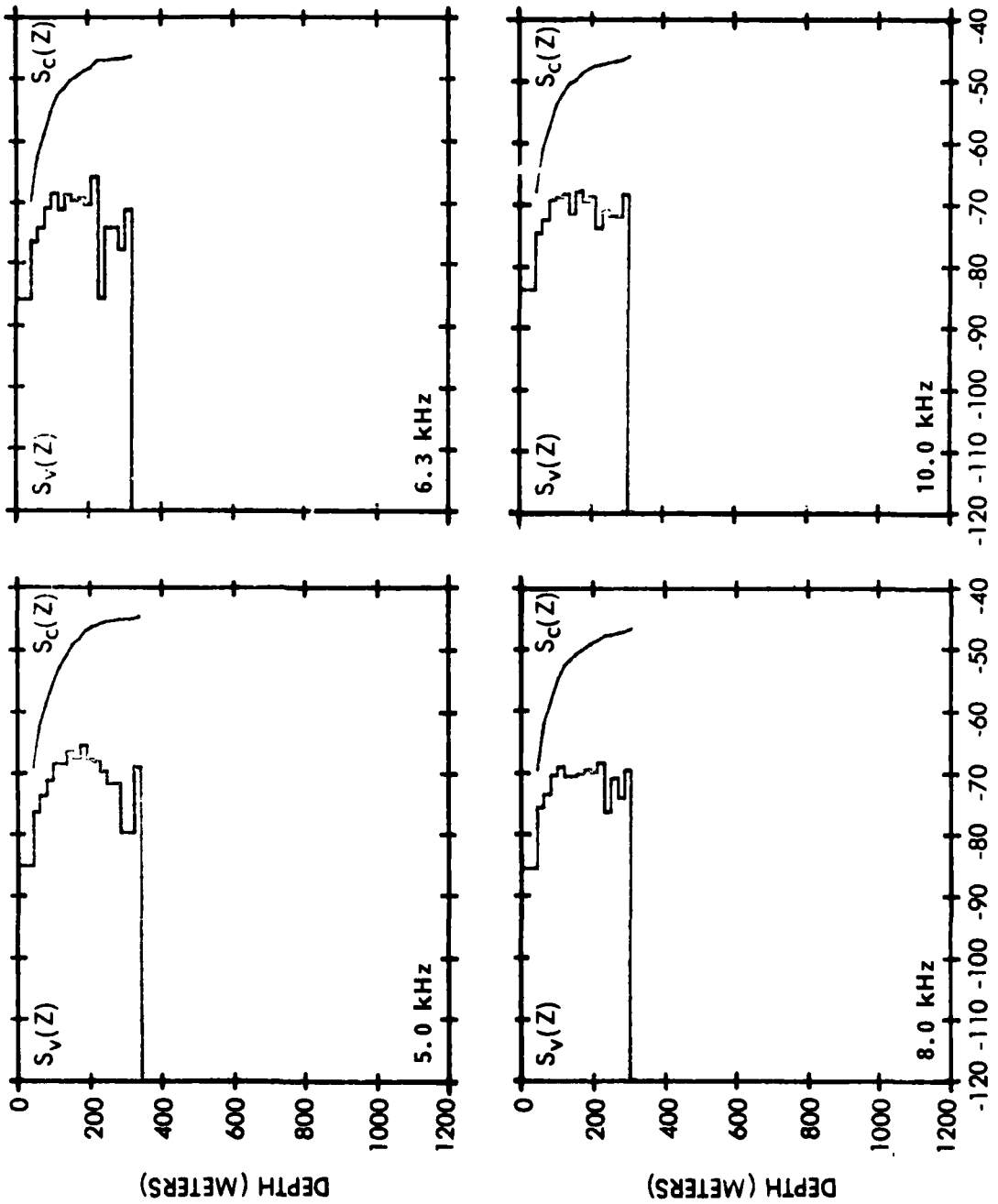

Figure B-17. CARIBCAP I, $S_v(z)$ and $S_c(z)$, 5 to 10 kHz, Station 6, night

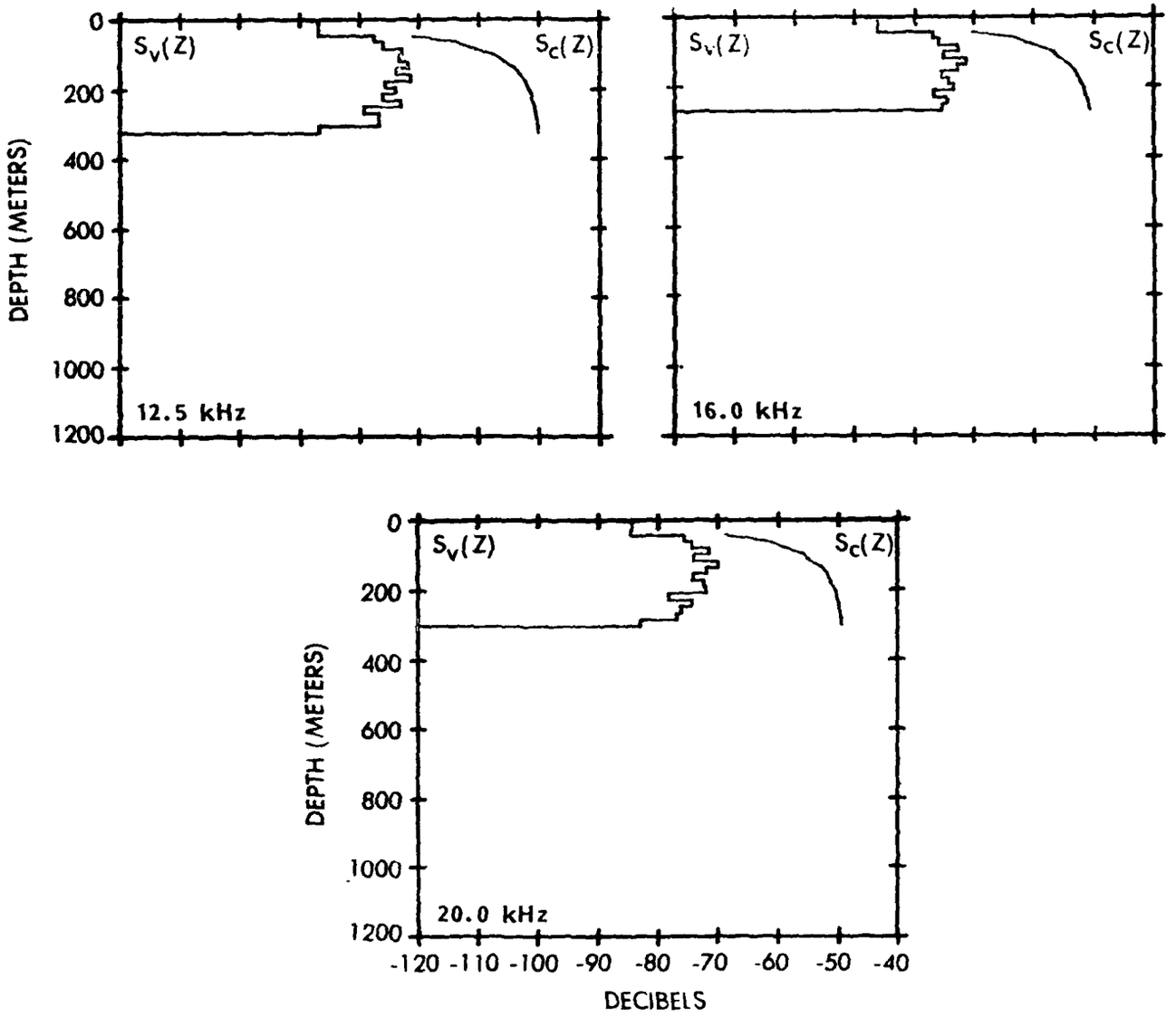

Figure B-18. CARIBCAP I, $S_v(z)$ and $S_c(z)$, 12.5 to 20 kHz, Station 6, night

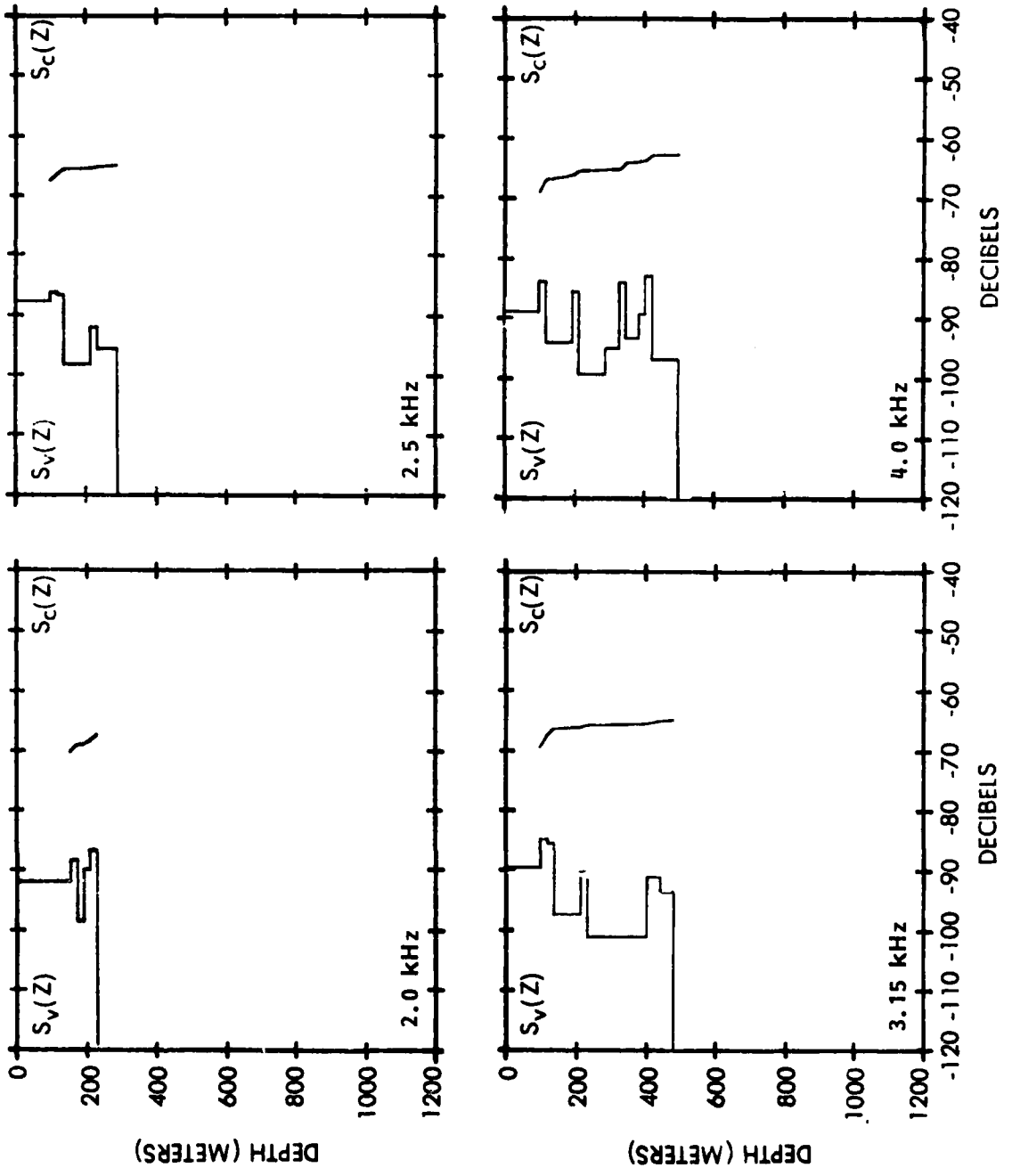

Figure B-19. CARIBCAP I, $S_v(z)$ and $S_c(z)$, 2 to 4 kHz, Station 7, day

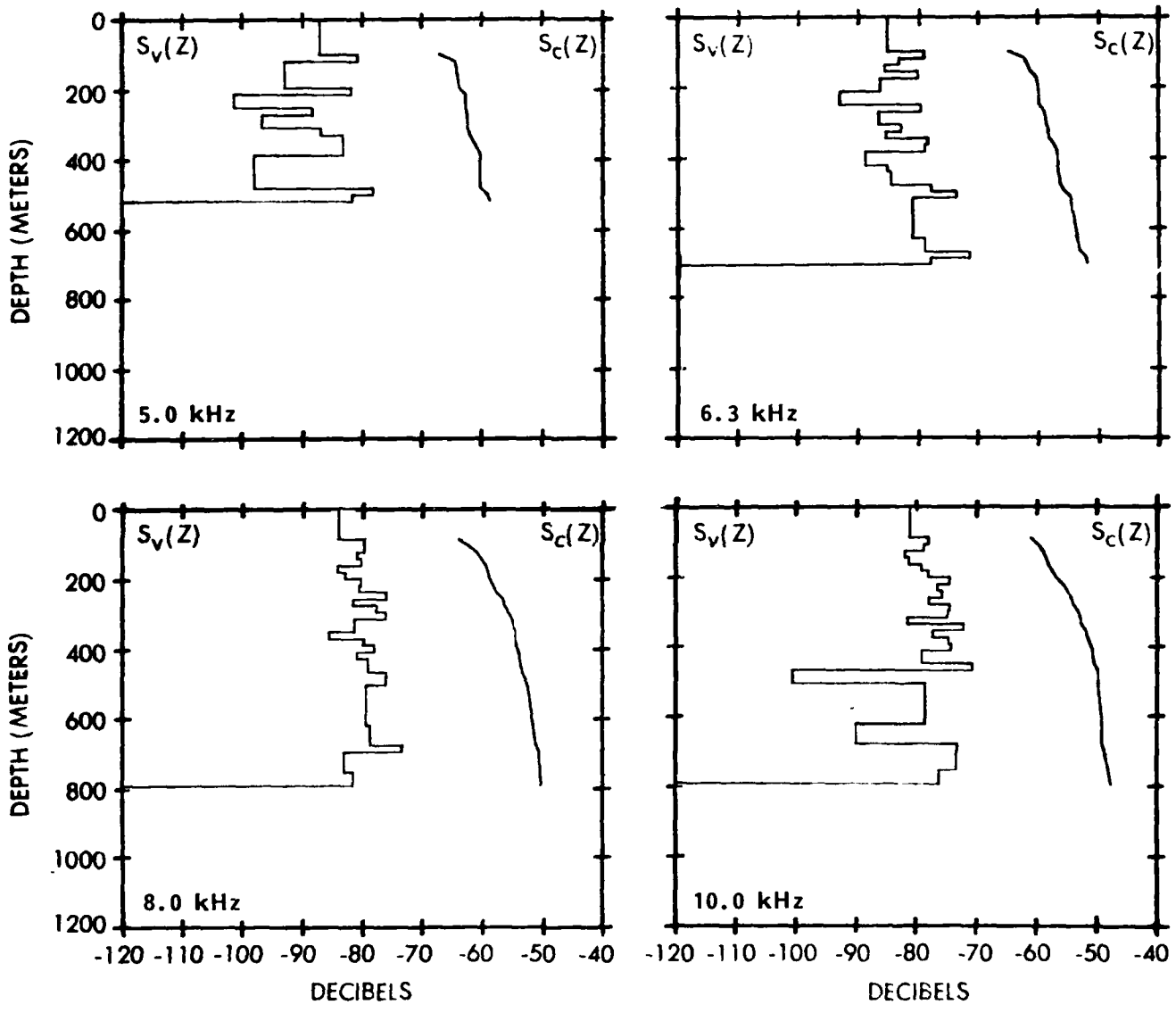

Figure B-20. CARIBCAP I, $S_V(z)$ and $S_C(z)$, 5 to 10 kHz, Station 7, day

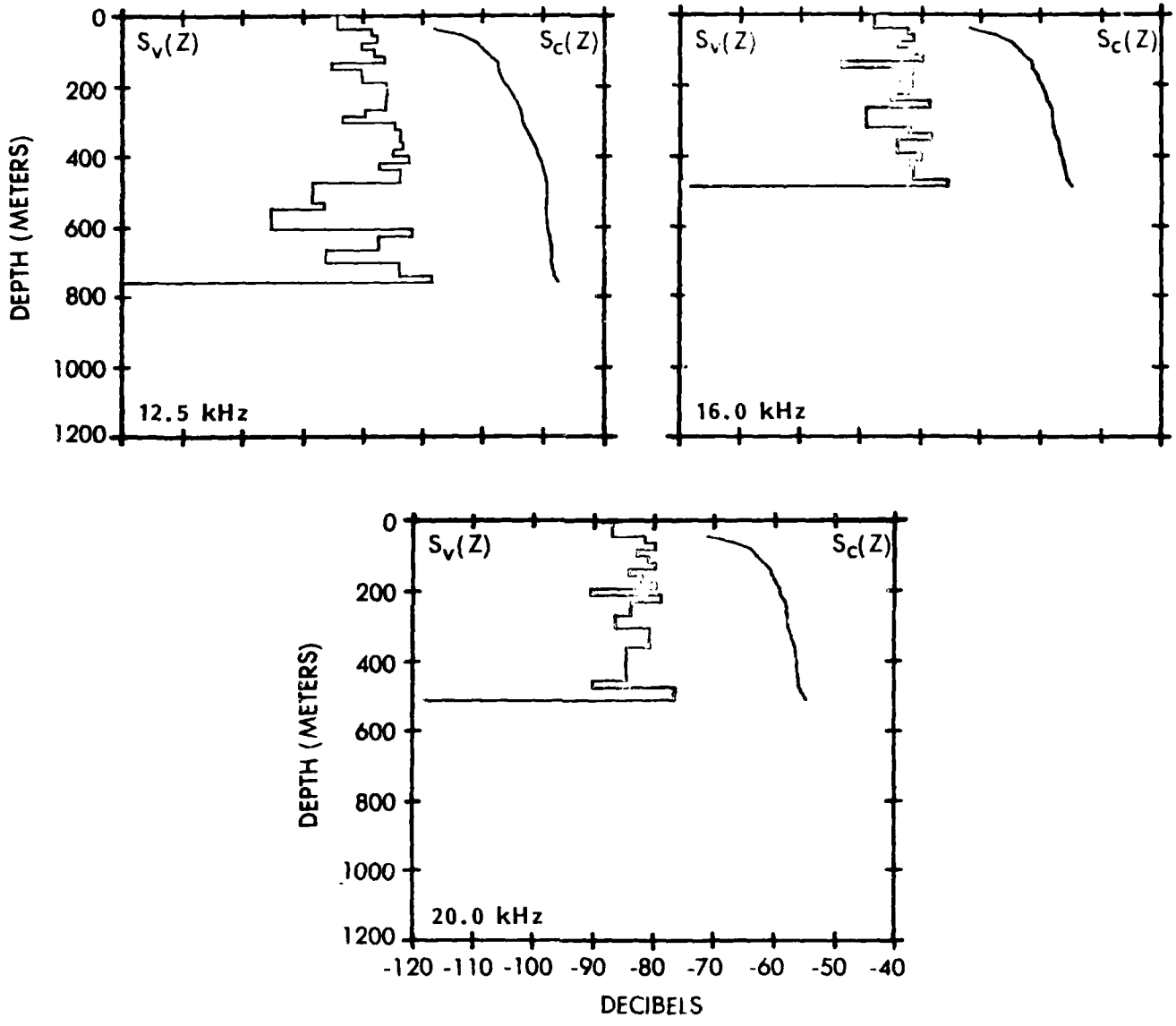

Figure B-21. CARIBCAP I, $S_v(z)$ and $S_c(z)$, 12.5 to 20 kHz, Station 7, day

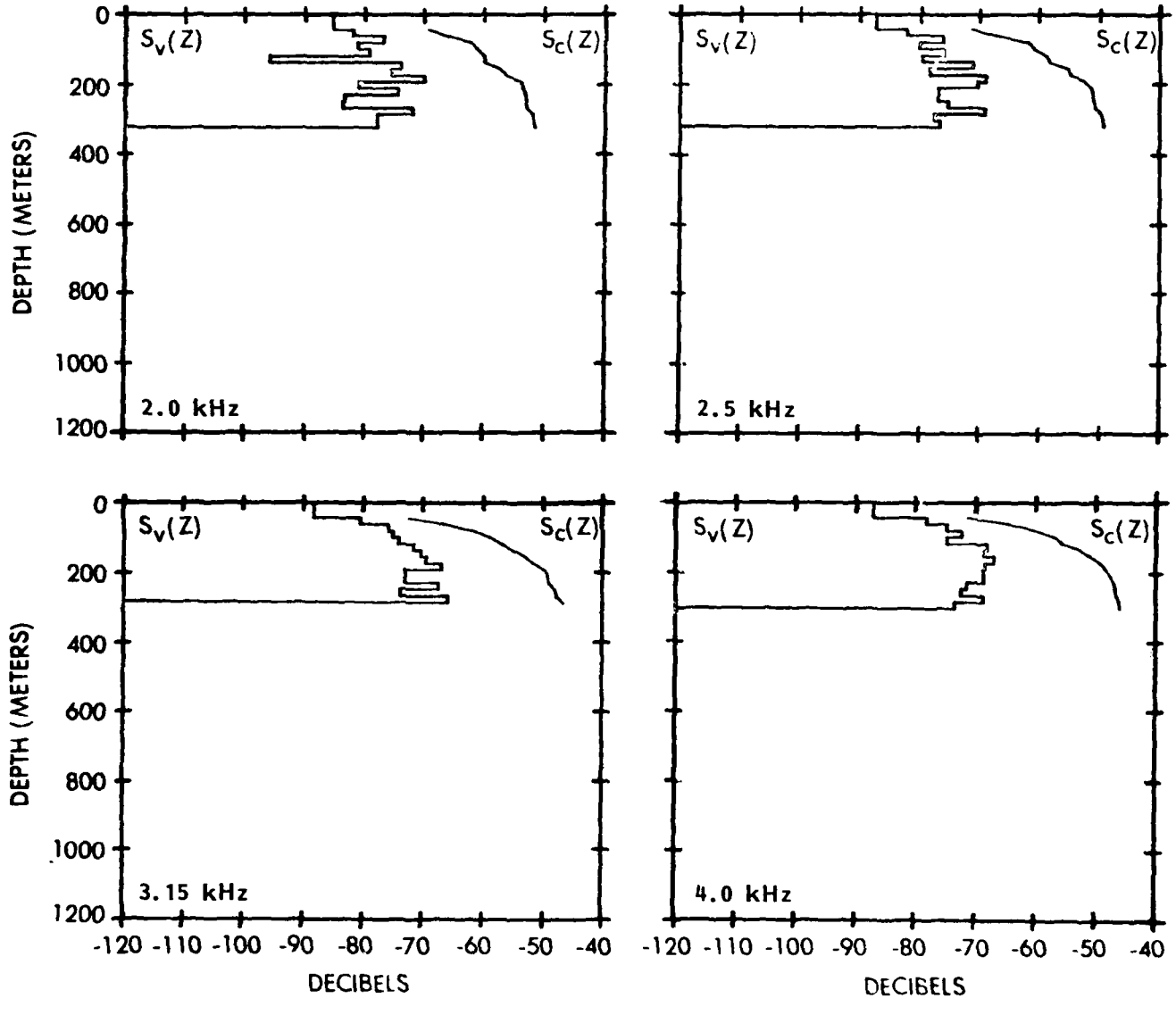

Figure B-22. CARIBCAP I, $S_v(z)$ and $S_c(z)$, 2 to 4 kHz, Station 7, night

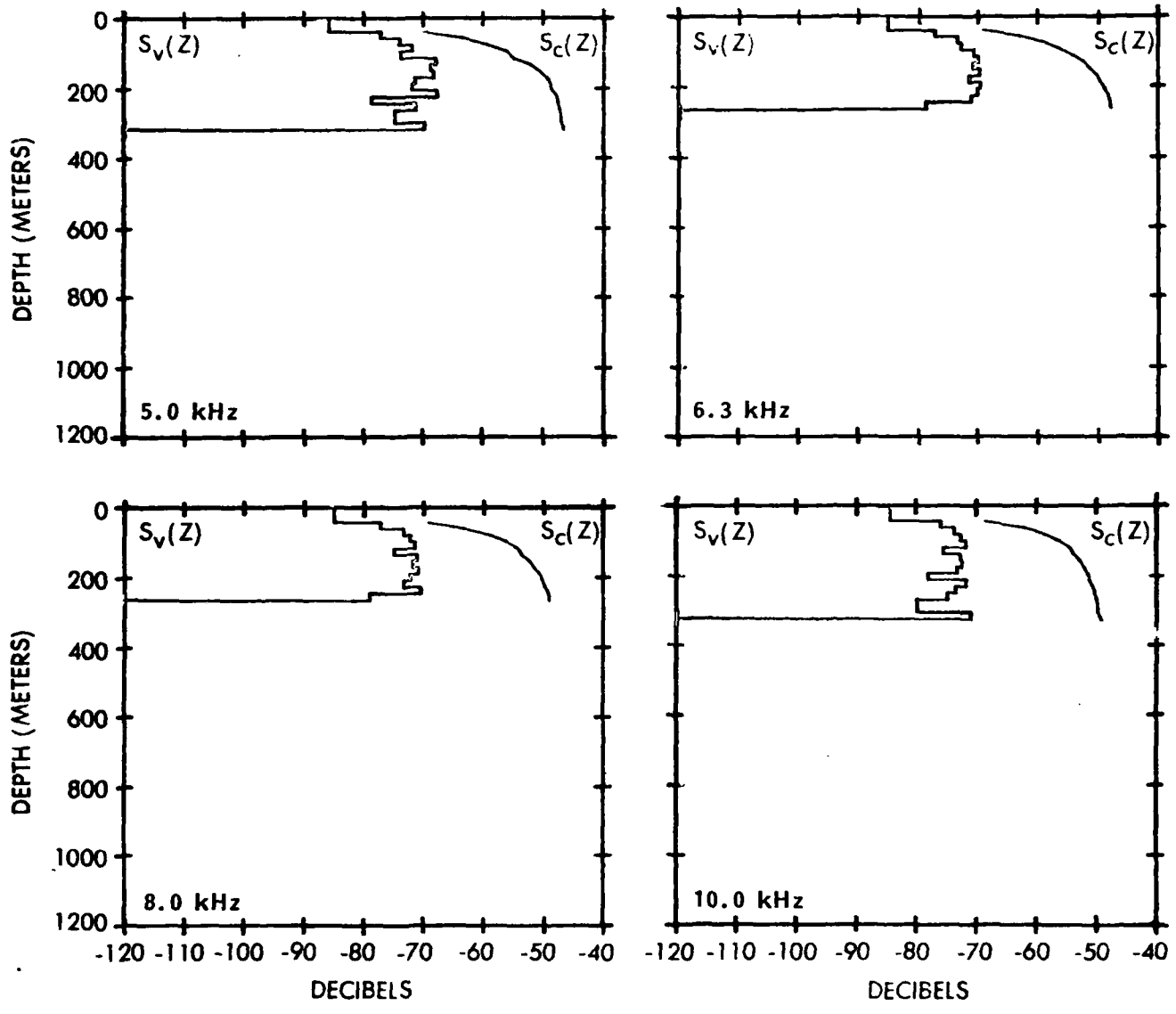

Figure B-23. CARIBCAP I, $S_V(z)$ and $S_C(z)$, 5 to 10 kHz, Station 7, night

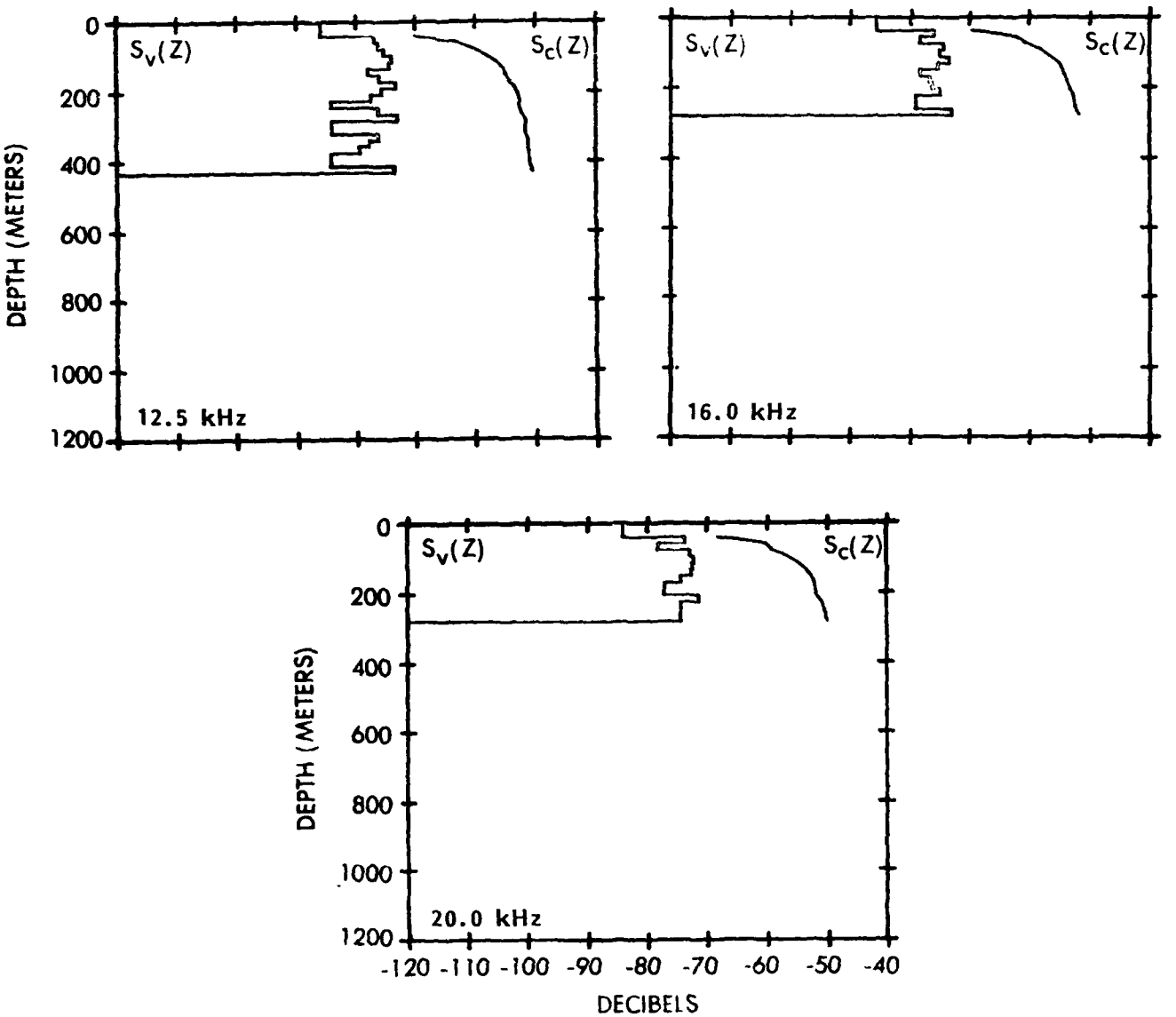

Figure B-24. CARIBCAP I, $S_V(z)$ and $S_C(z)$, 12.5 to 20 kHz, Station 7, night

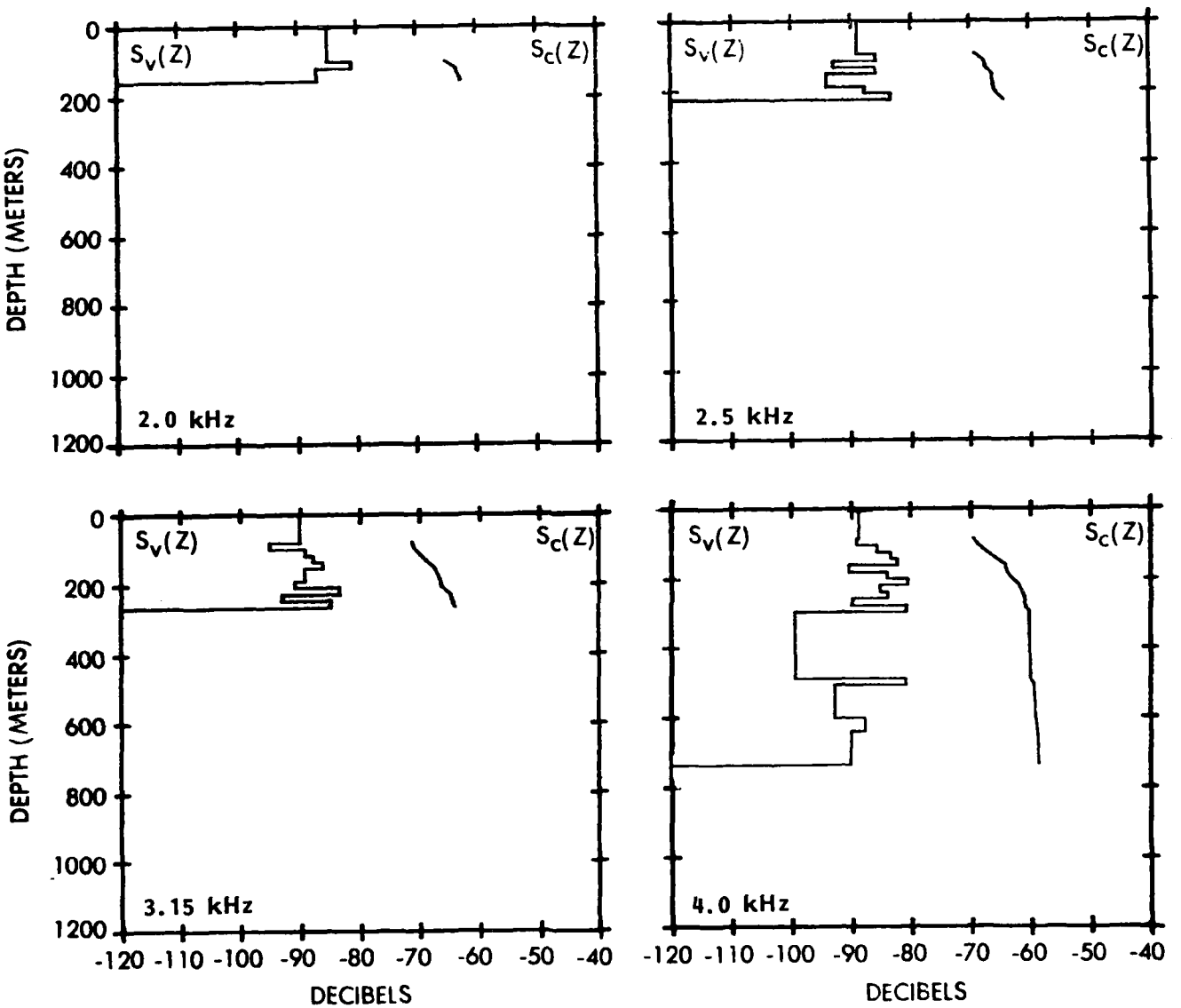

Figure B-25. CARIBCAP I, $S_v(z)$ and $S_c(z)$, 2 to 4 kHz, Station 8, day

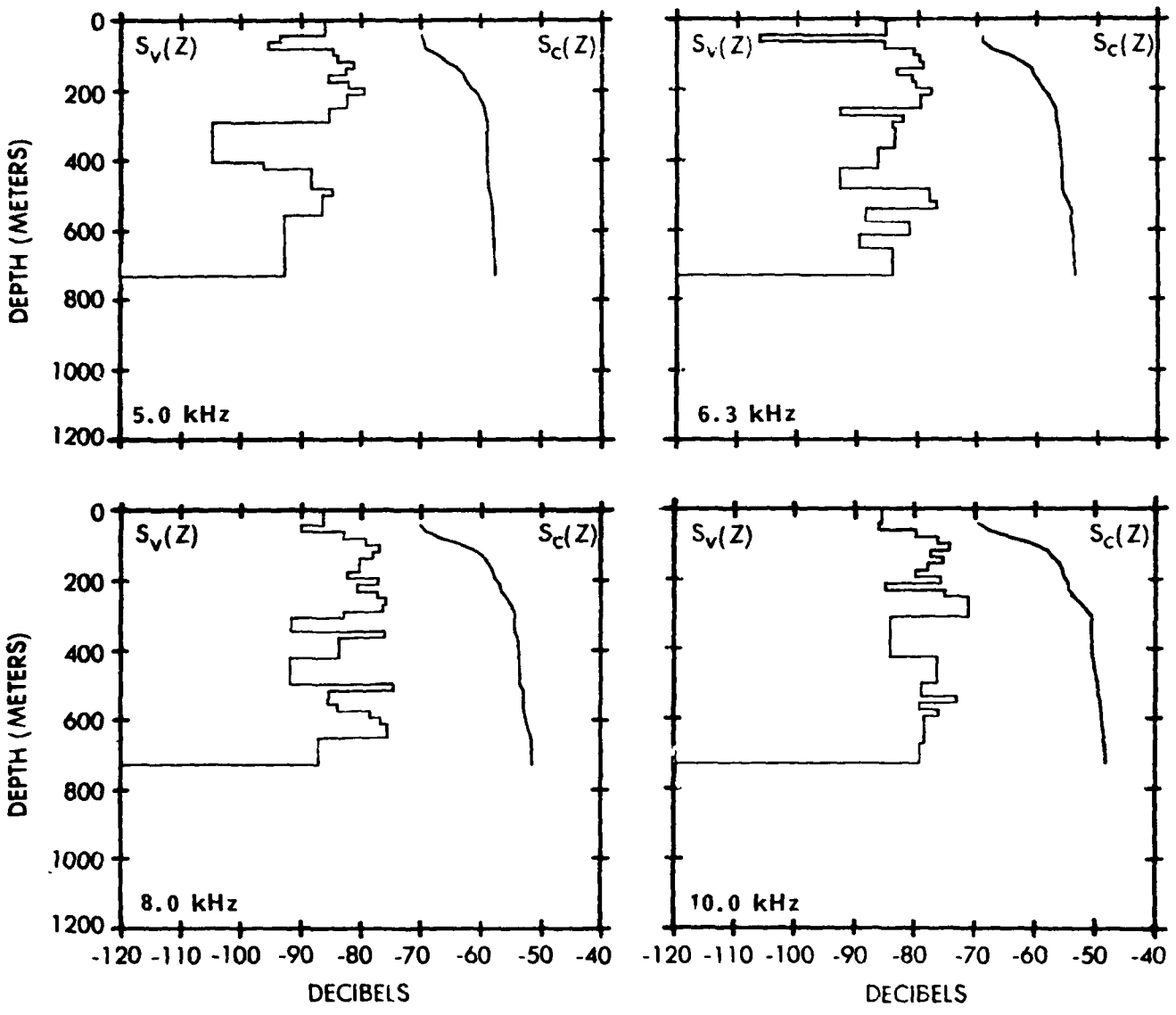

Figure B-26. CARIBCAP I, $S_v(z)$ and $S_c(z)$, 5 to 10 kHz, Station 8, day

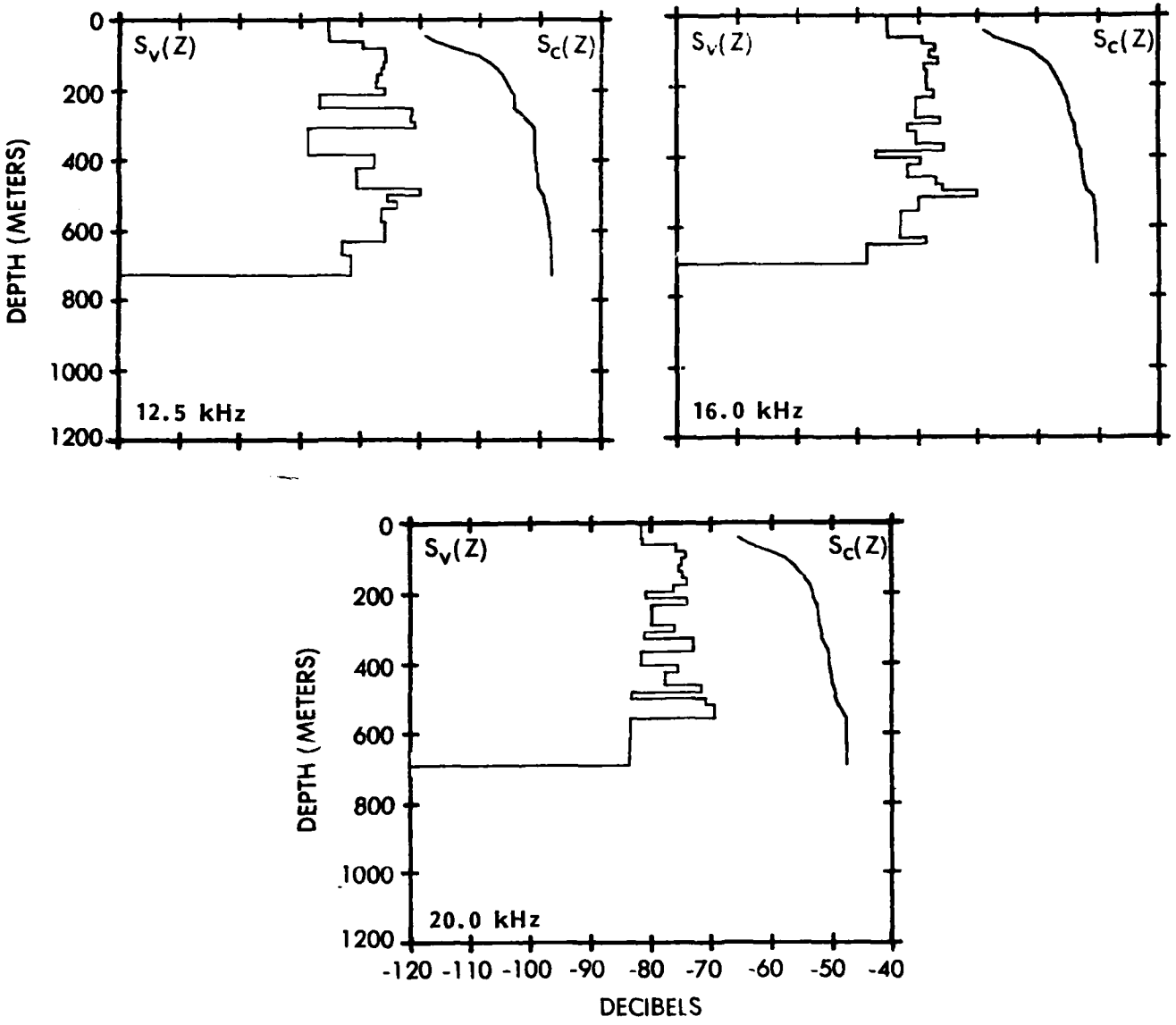

Figure B-27. CARIBCAP I, $S_v(z)$ and $S_c(z)$, 12.5 to 20 kHz, Station 8, day

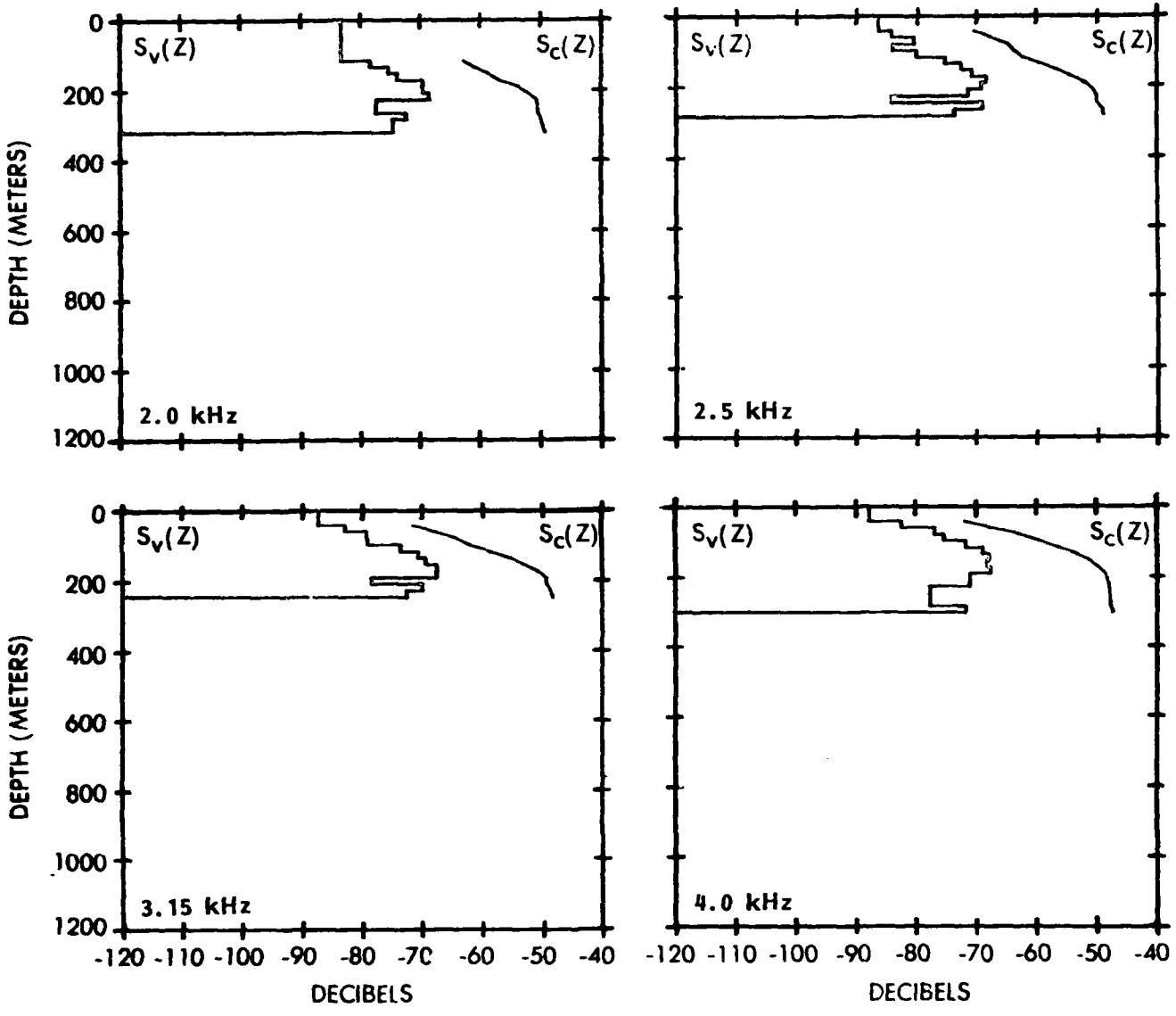

Figure B-28. CARIBCAP I, $S_v(z)$ and $S_c(z)$, 2 to 4 kHz, Station 8, night

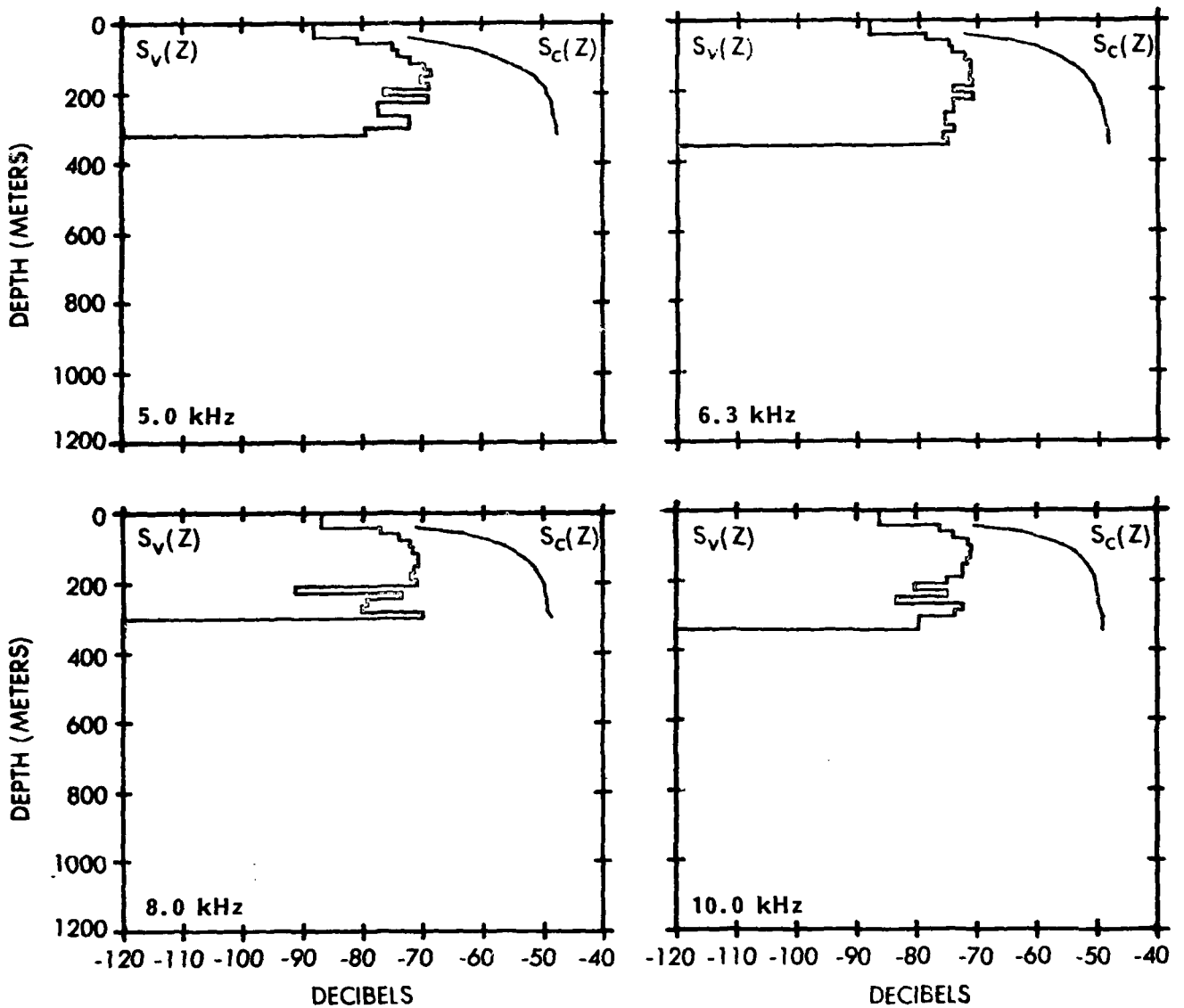

Figure B-29. CARIBCAP I, $S_V(z)$ and $S_C(z)$, 5 to 10 kHz, Station 8, night

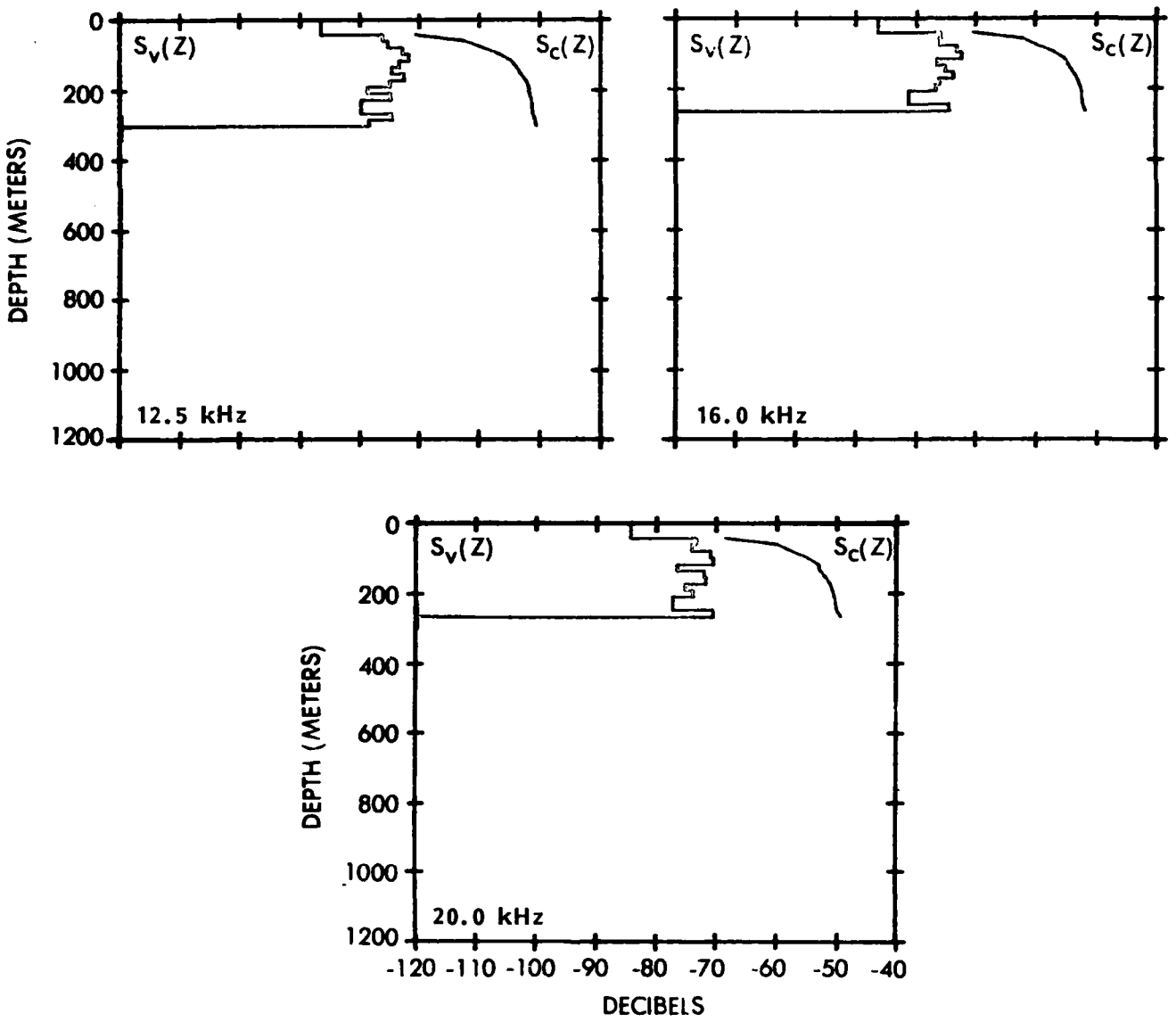

Figure B-30. CARIBCAP I, $S_V(z)$ and $S_C(z)$, 12.5 to 20 kHz, Station 8, night

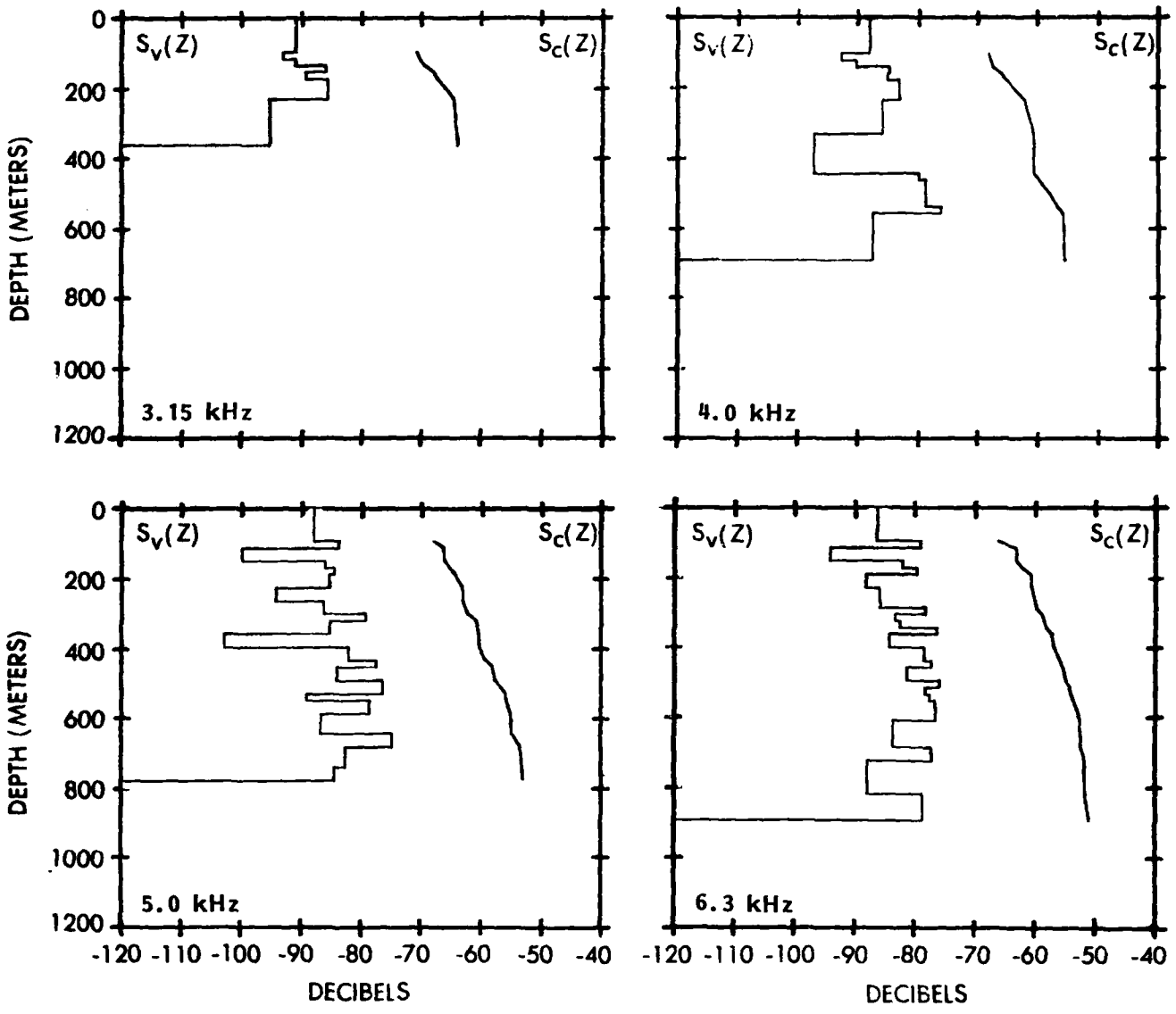

Figure B-31. CARIBCAP II, $S_v(z)$ and $S_c(z)$, 3.15 to 6.3 kHz, Station 1, day

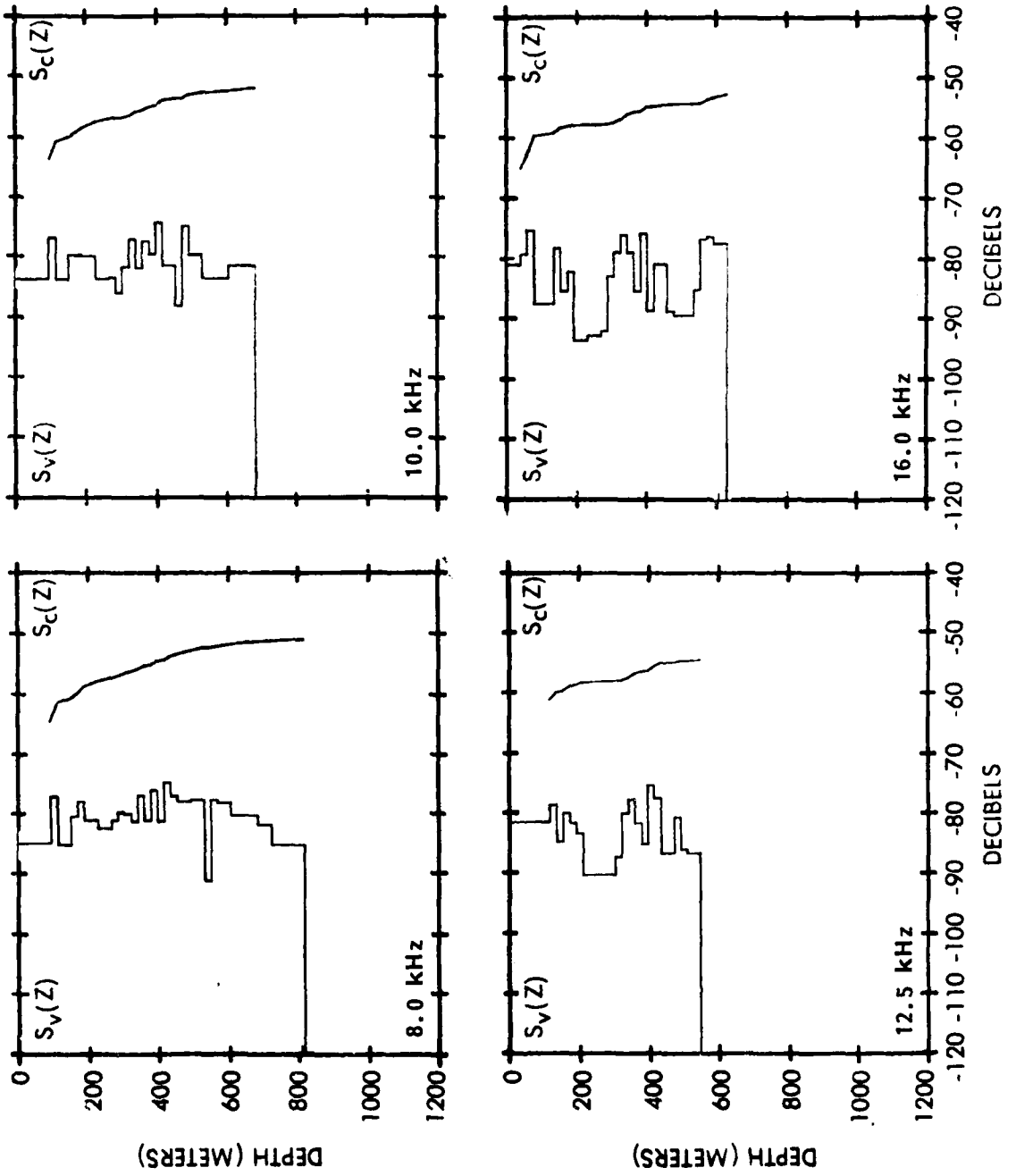

Figure B-32. CARIBCAP II, $S_v(z)$ and $S_c(z)$, 8 to 16 kHz, Station 1, day

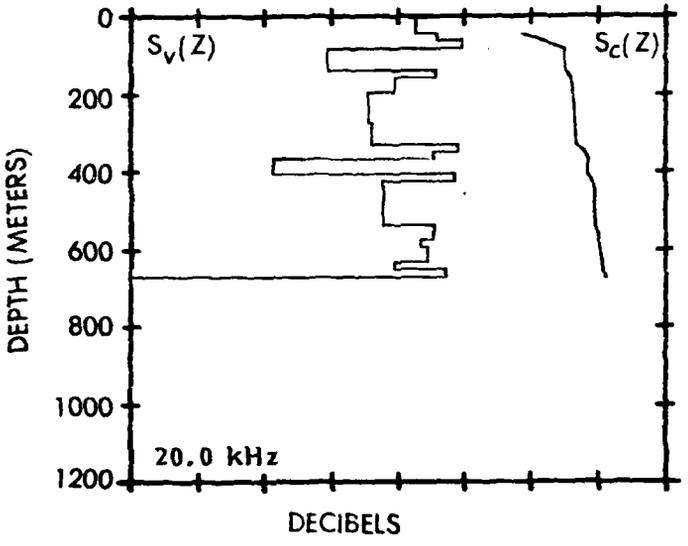

Fig. B-33. CARIBCAP II, $S_v(z)$ and $S_c(z)$, 20 kHz, Station 1, day

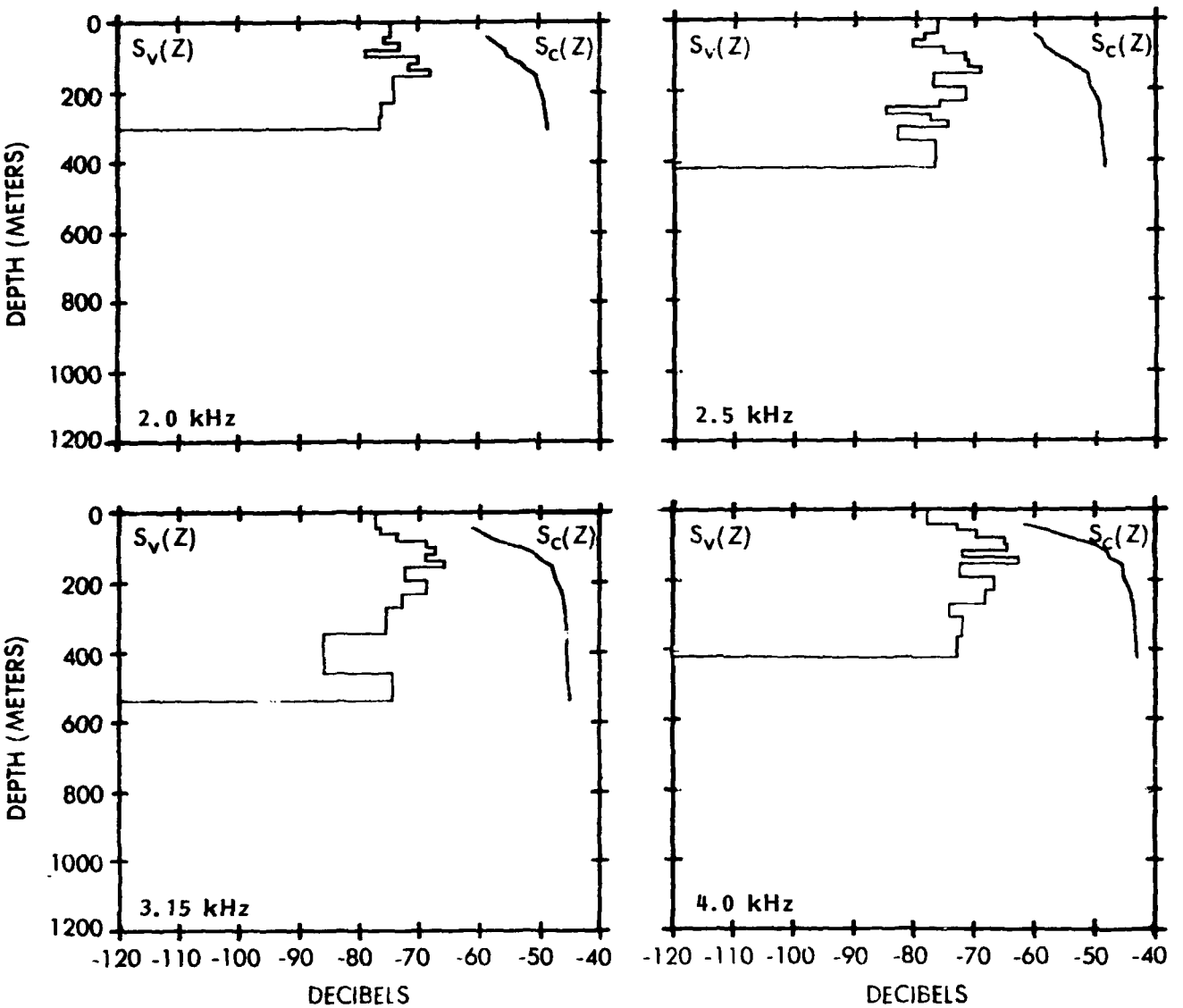

Figure B-34. CARIBCAP II, $S_v(z)$ and $S_c(z)$, 2 to 4 kHz, Station 1, night

AD-A118 165 NAVAL OCEAN RESEARCH AND DEVELOPMENT ACTIVITY NSTL S--ETC F/G 20/1
VOLUME REVERBERATION MEASUREMENTS IN THE EASTERN CARRIBEAN SEA.(U)
NOV 81 C LEVENSON, R A LOVE, M A WILSON

UNCLASSIFIED NORDA-TN-128 NL

2 OF 2
AD A
118165

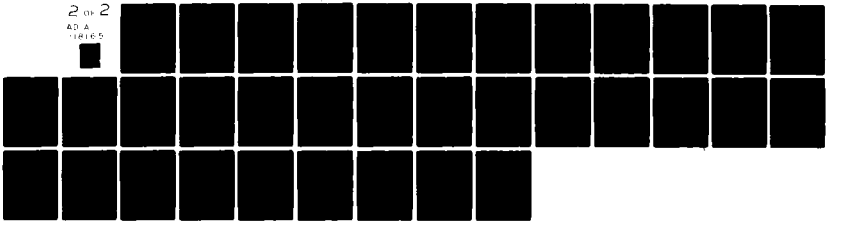

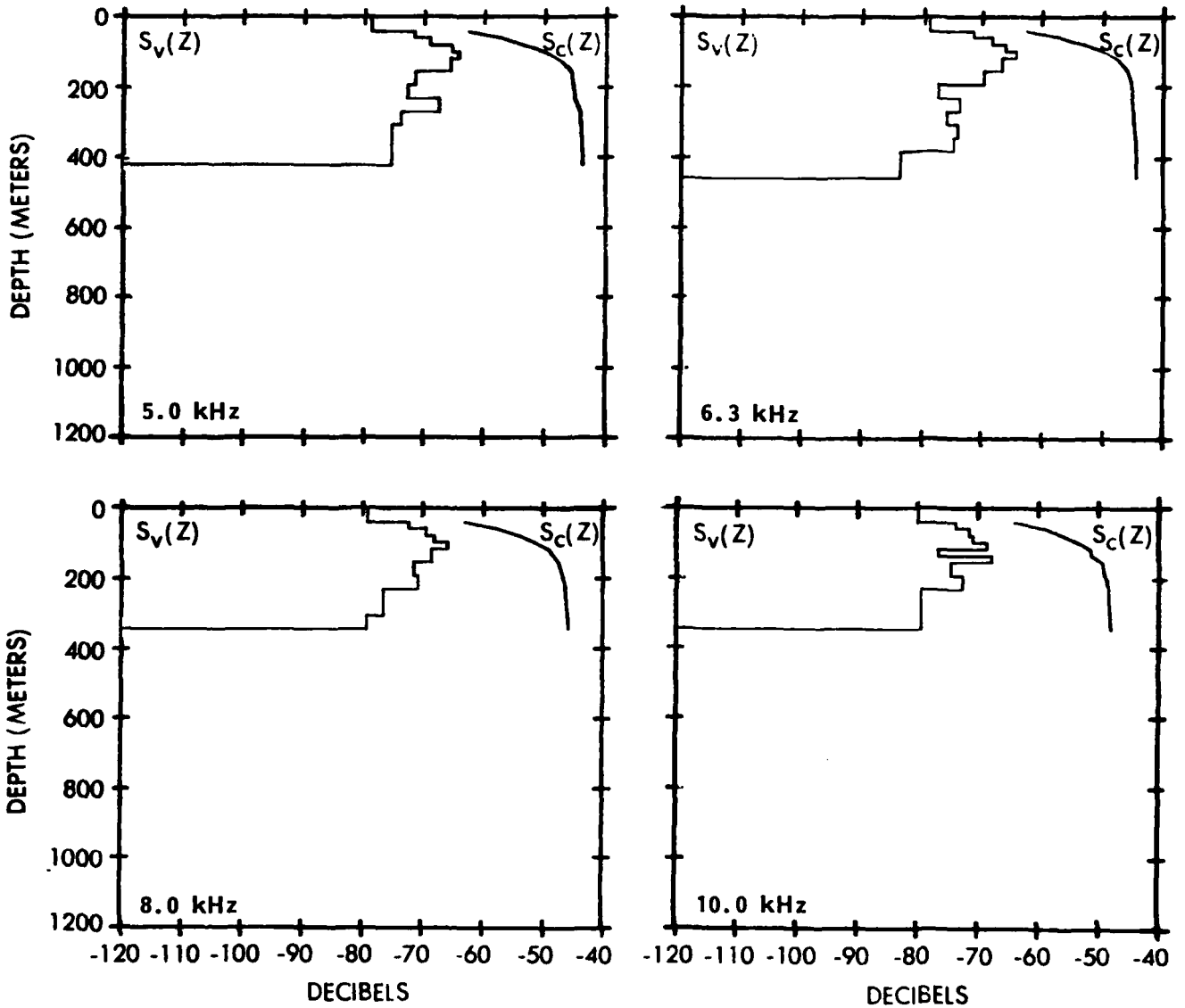

Figure B-35. CARIBCAP II, $S_v(z)$ and $S_c(z)$, 5 to 10 kHz, Station 1, night

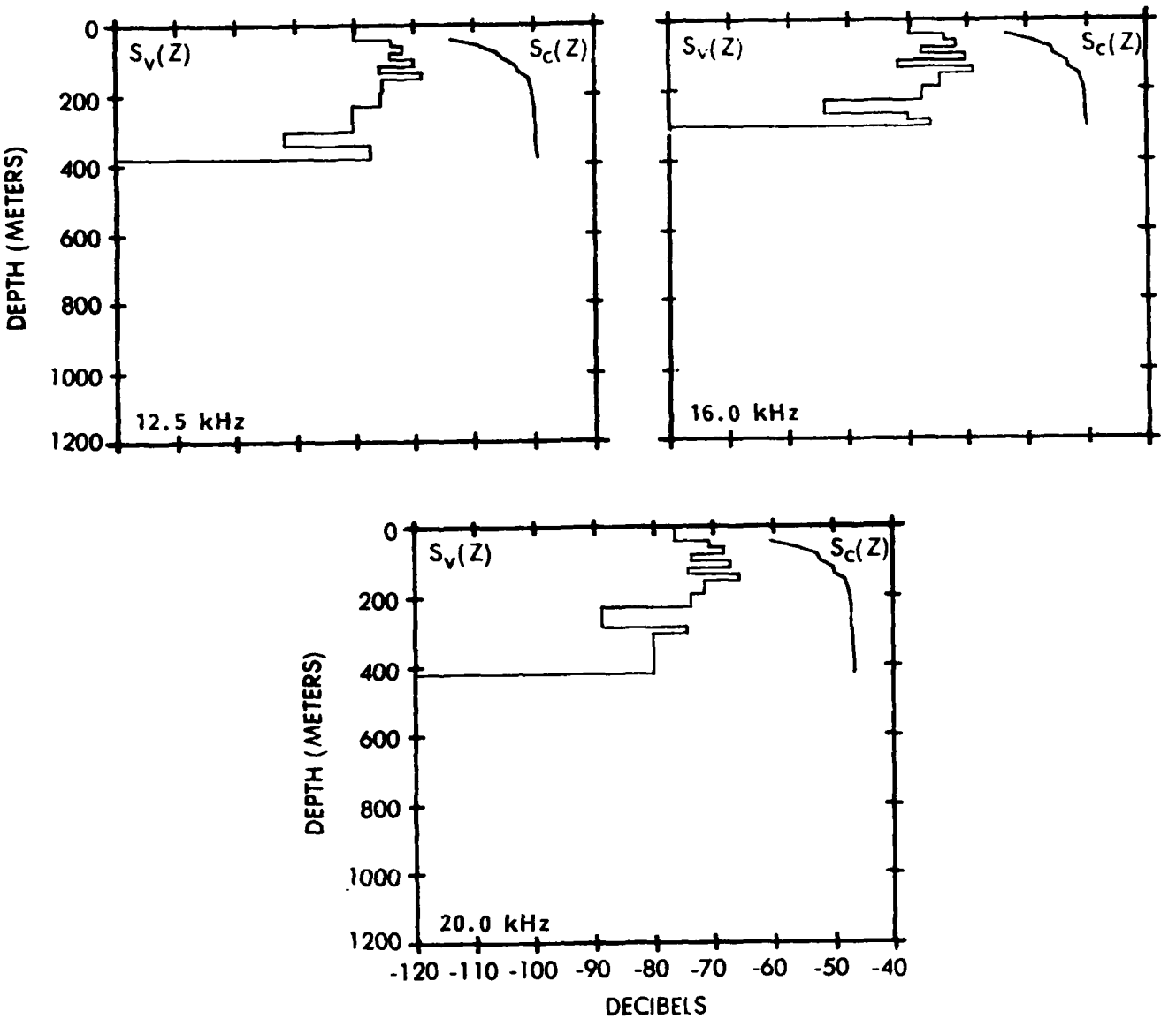

Figure B-36. CARIBCAP II, $S_v(z)$ and $S_c(z)$, 12.5 to 20 kHz, Station 1, night

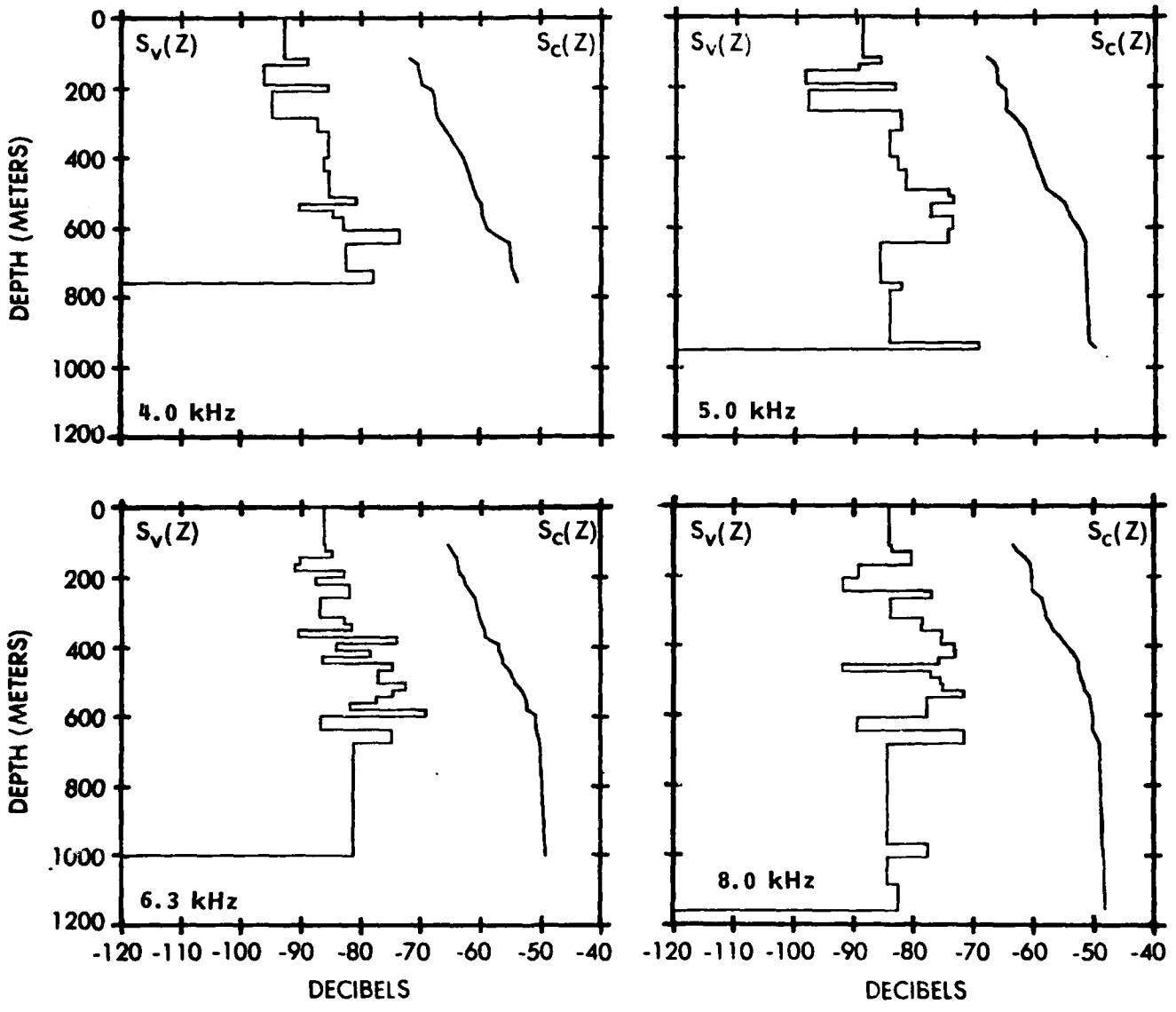

Figure B-37. CARIBCAP II, $S_v(z)$ and $S_c(z)$, 4 to 8 kHz, Station 2, day

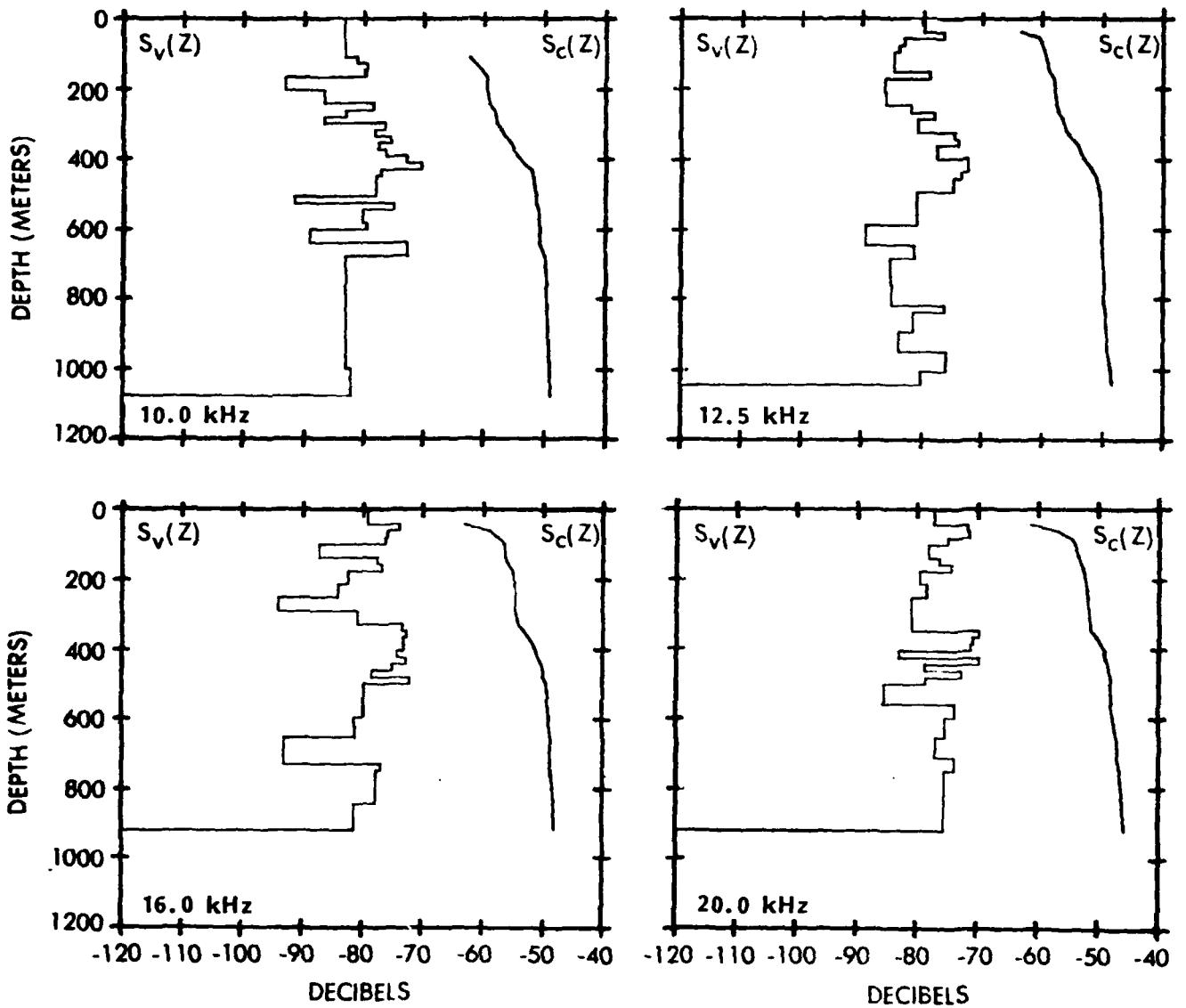

Figure B-38. CARIBCAP II, $S_v(z)$ and $S_c(z)$, 10 to 20 kHz, Station 2, day

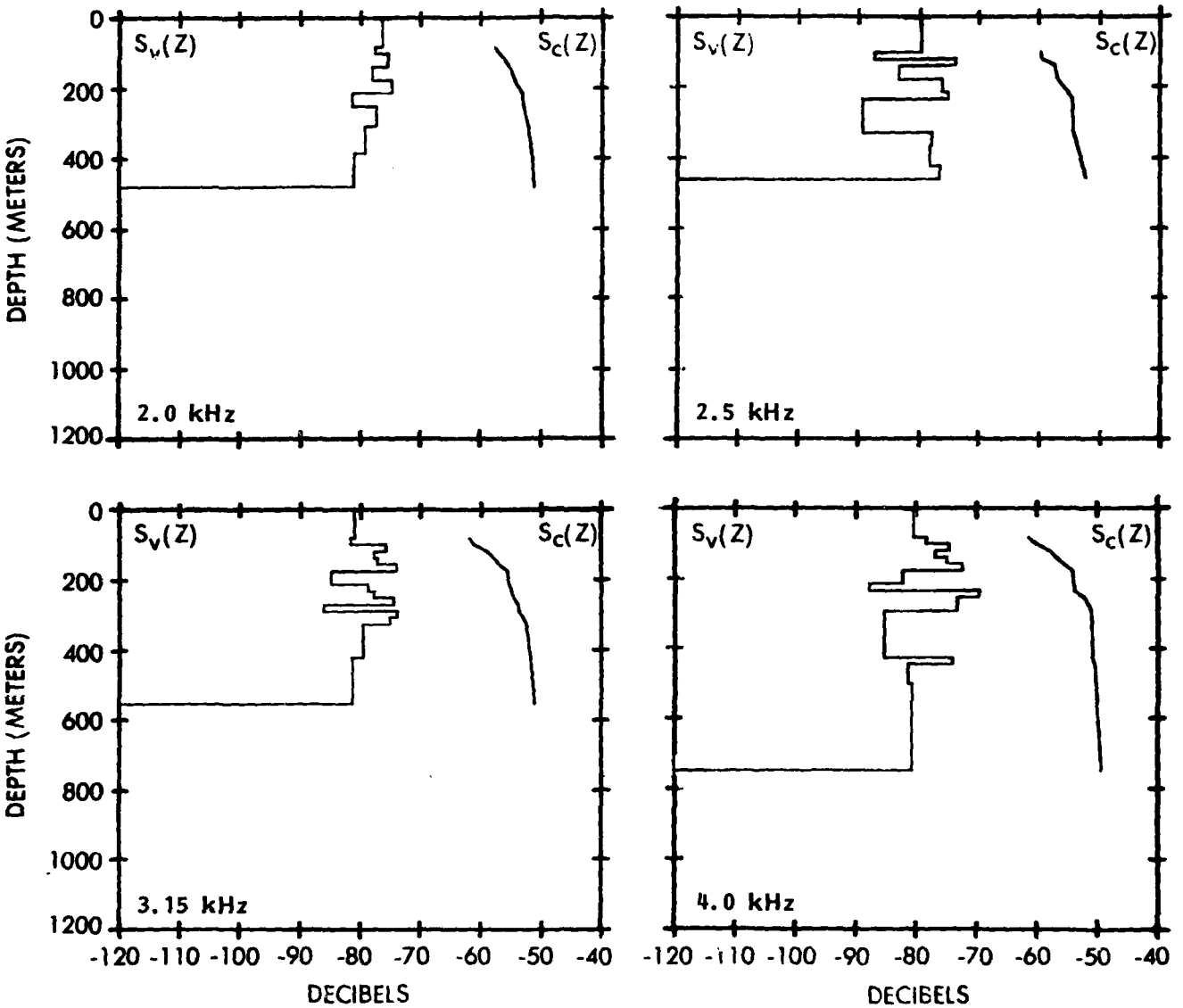

Figure B-39. CARIBCAP II, $S_v(z)$ and $S_c(z)$, 2 to 4 kHz, Station 2, night

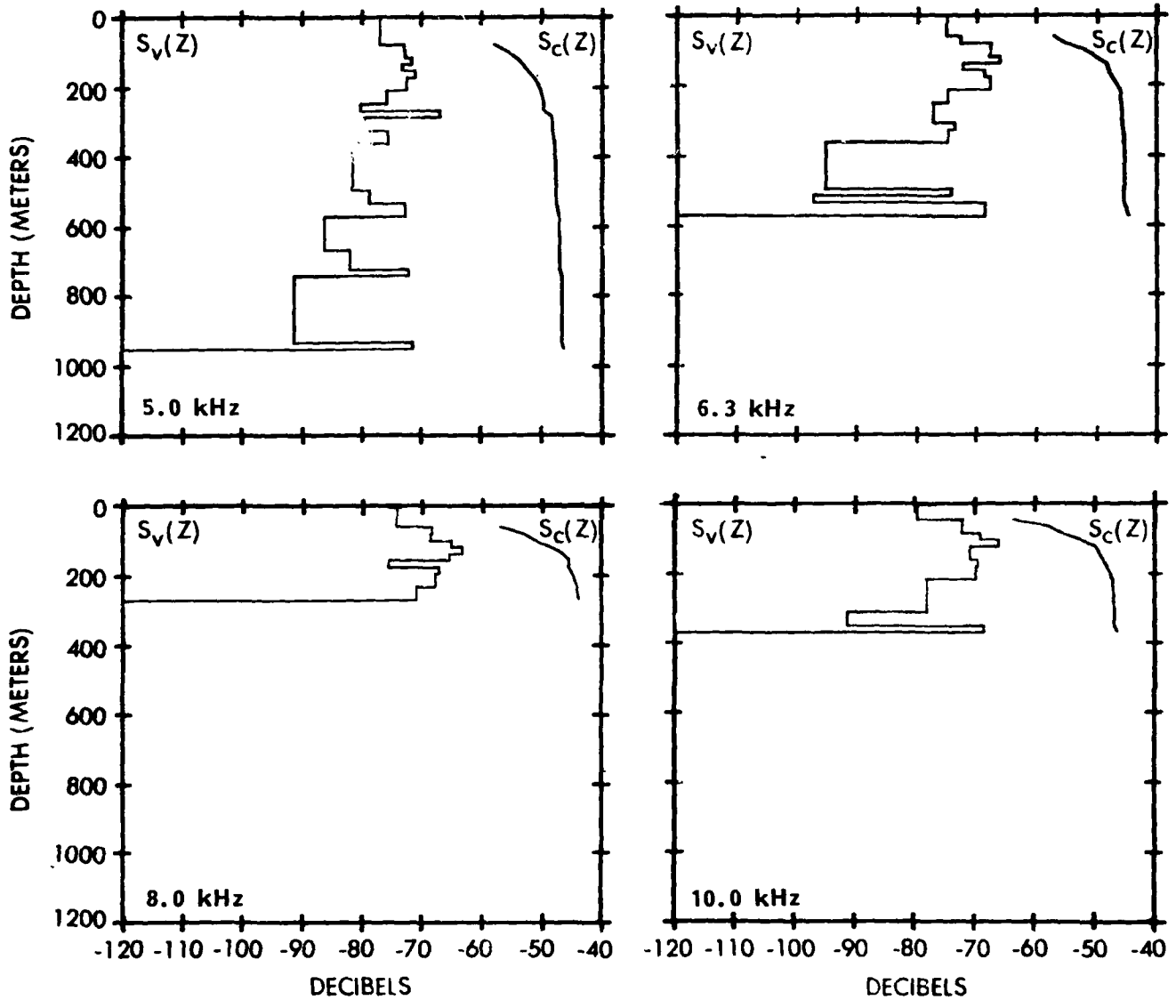

Figure B-40. CARIBCAP II, $S_v(z)$ and $S_c(z)$, 5 to 10 kHz, Station 2, night

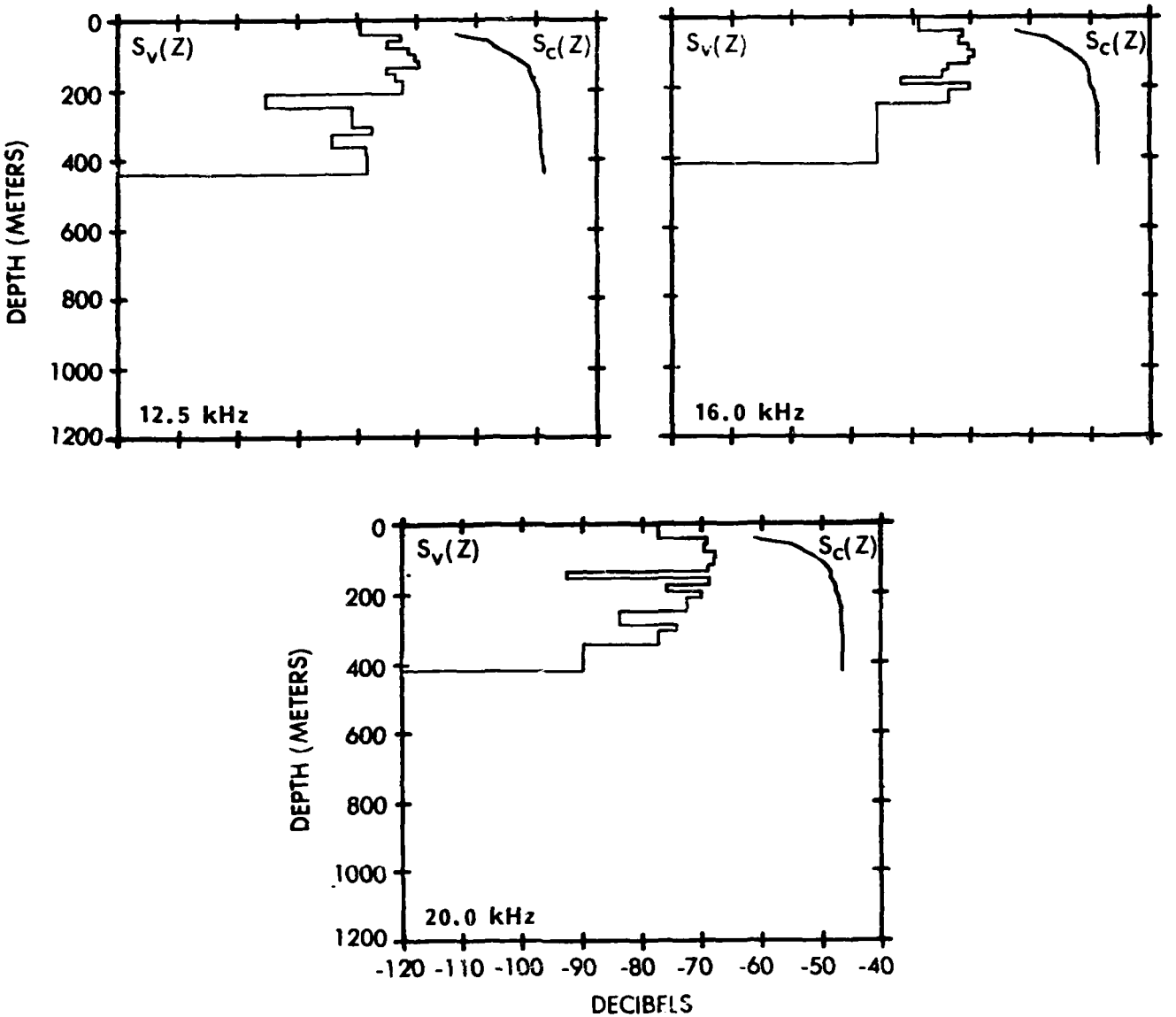

Figure B-41. CARIBCAP II, $S_v(z)$ and $S_c(z)$, 12.5 to 20 kHz, Station 2, night

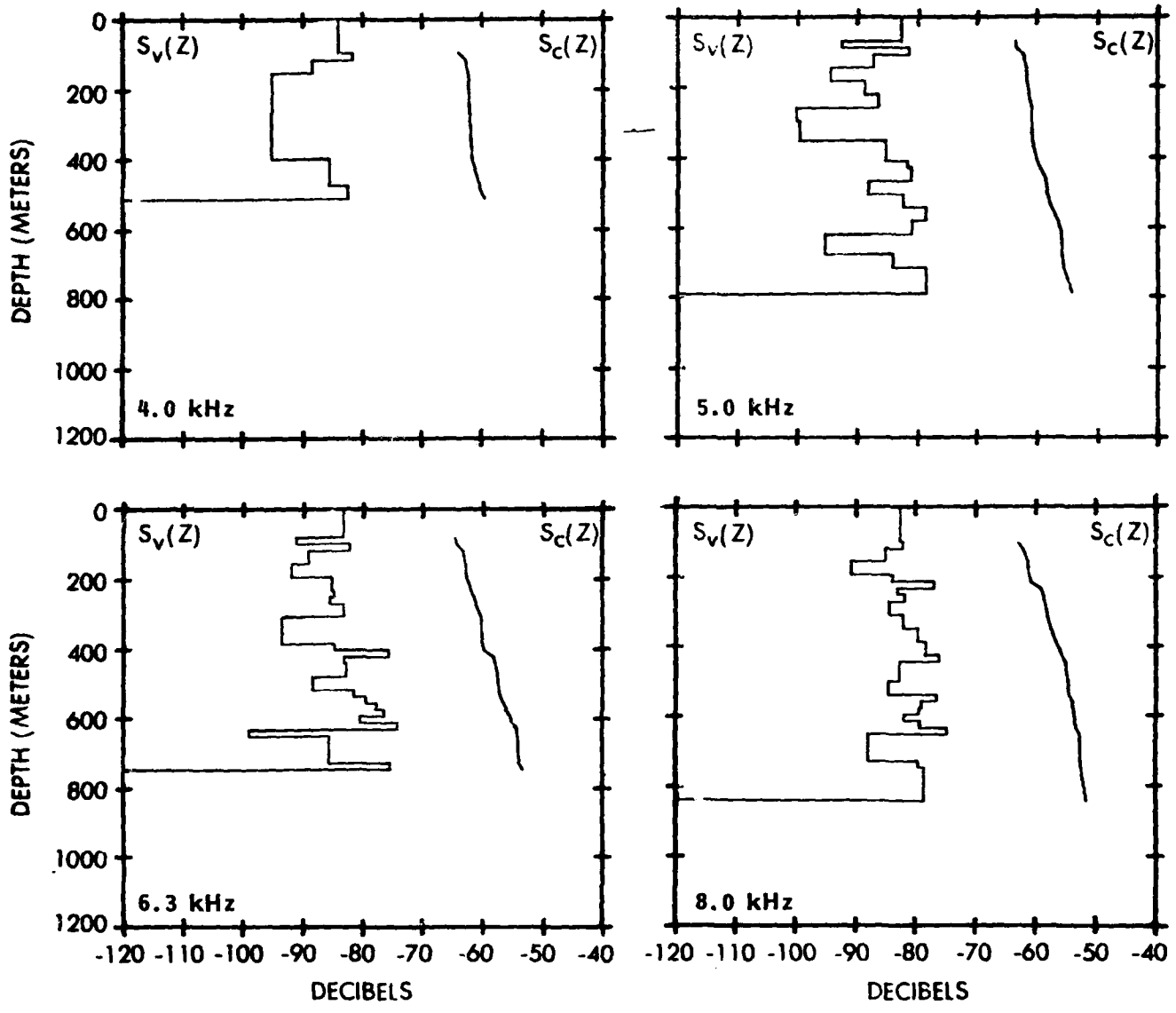

Figure B-42. CARIBCAP II, $S_v(z)$ and $S_c(z)$, 4 to 8 kHz, Station 3, day

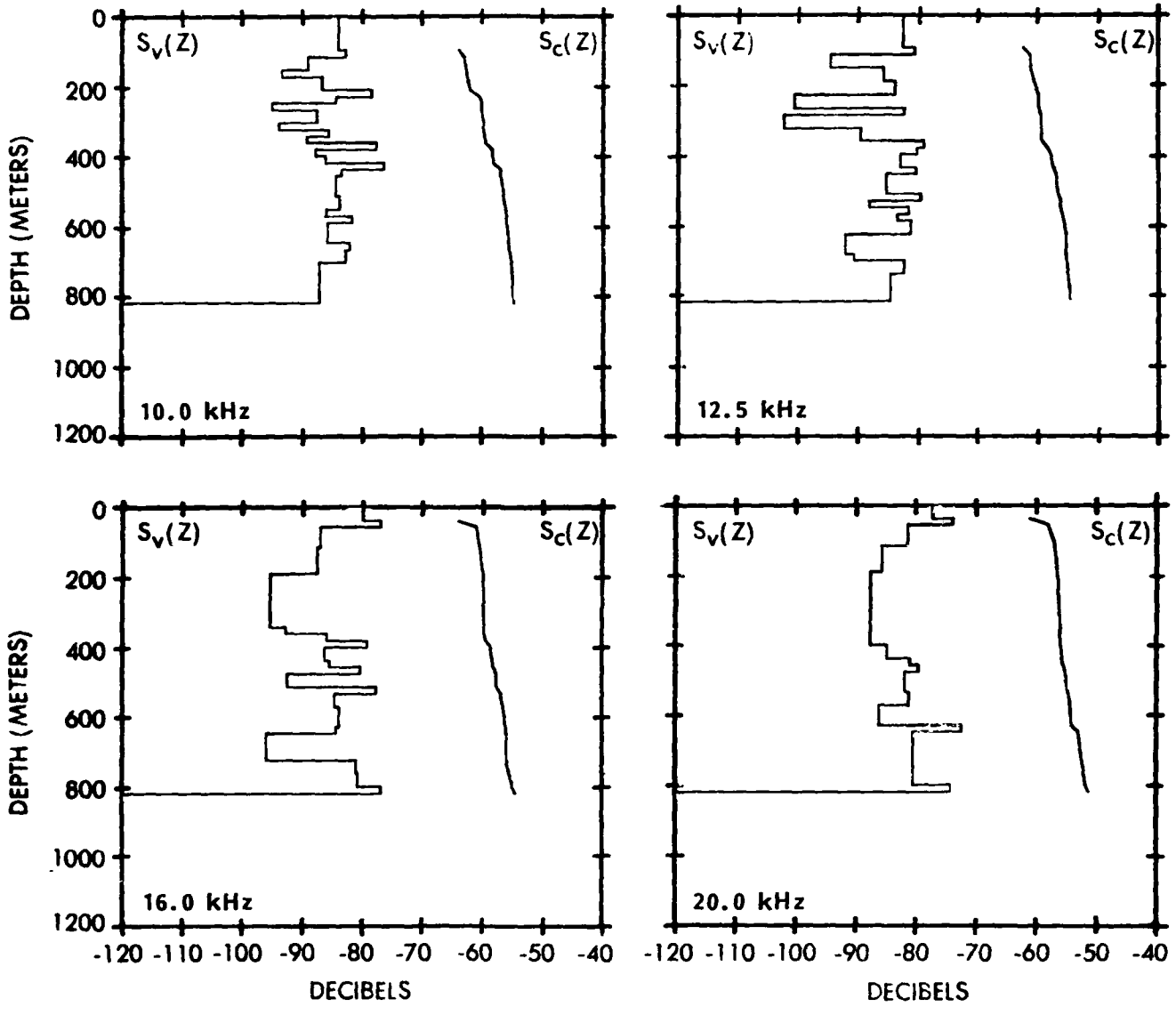

Figure B-43. CARIBCAP II, $S_v(z)$ and $S_c(z)$, 10 to 20 kHz, Station 3. day

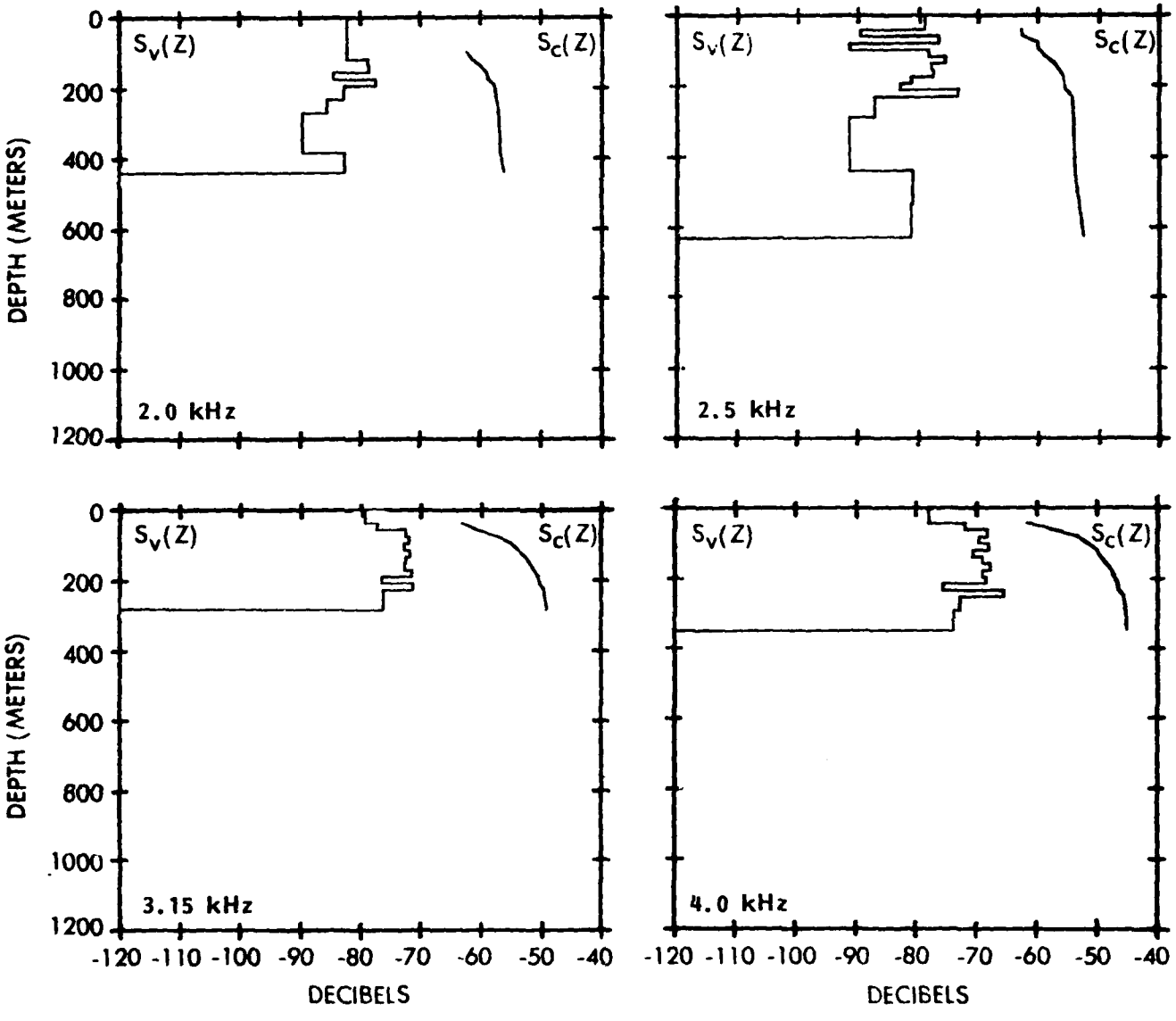

Figure B-44. CARIBCAP II, $S_v(z)$ and $S_c(z)$, 2 to 4 kHz, Station 3, night

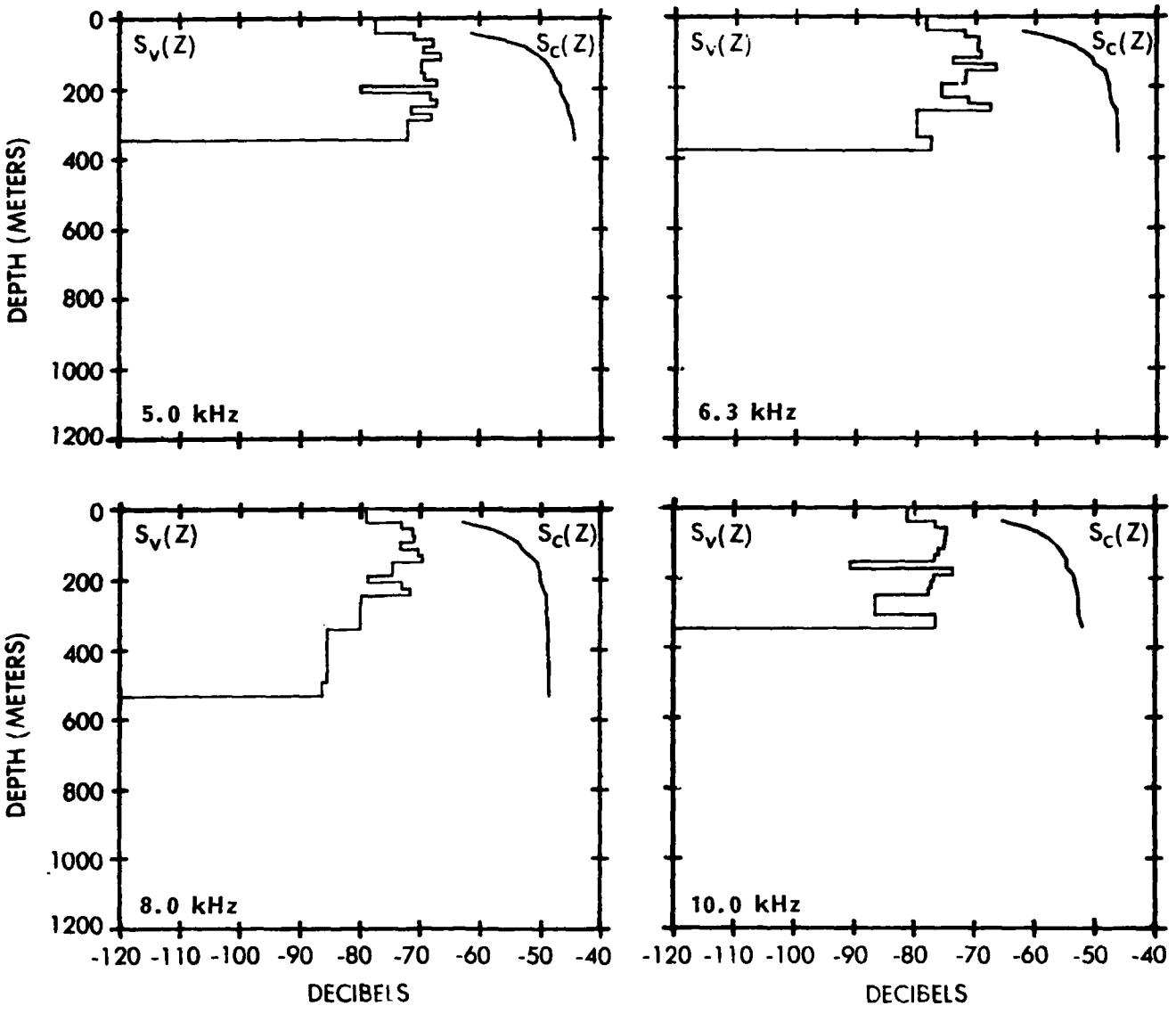

Figure B-45. CARIBCAP II, $S_v(z)$ and $S_c(z)$, 5 to 10 kHz, Station 3, night

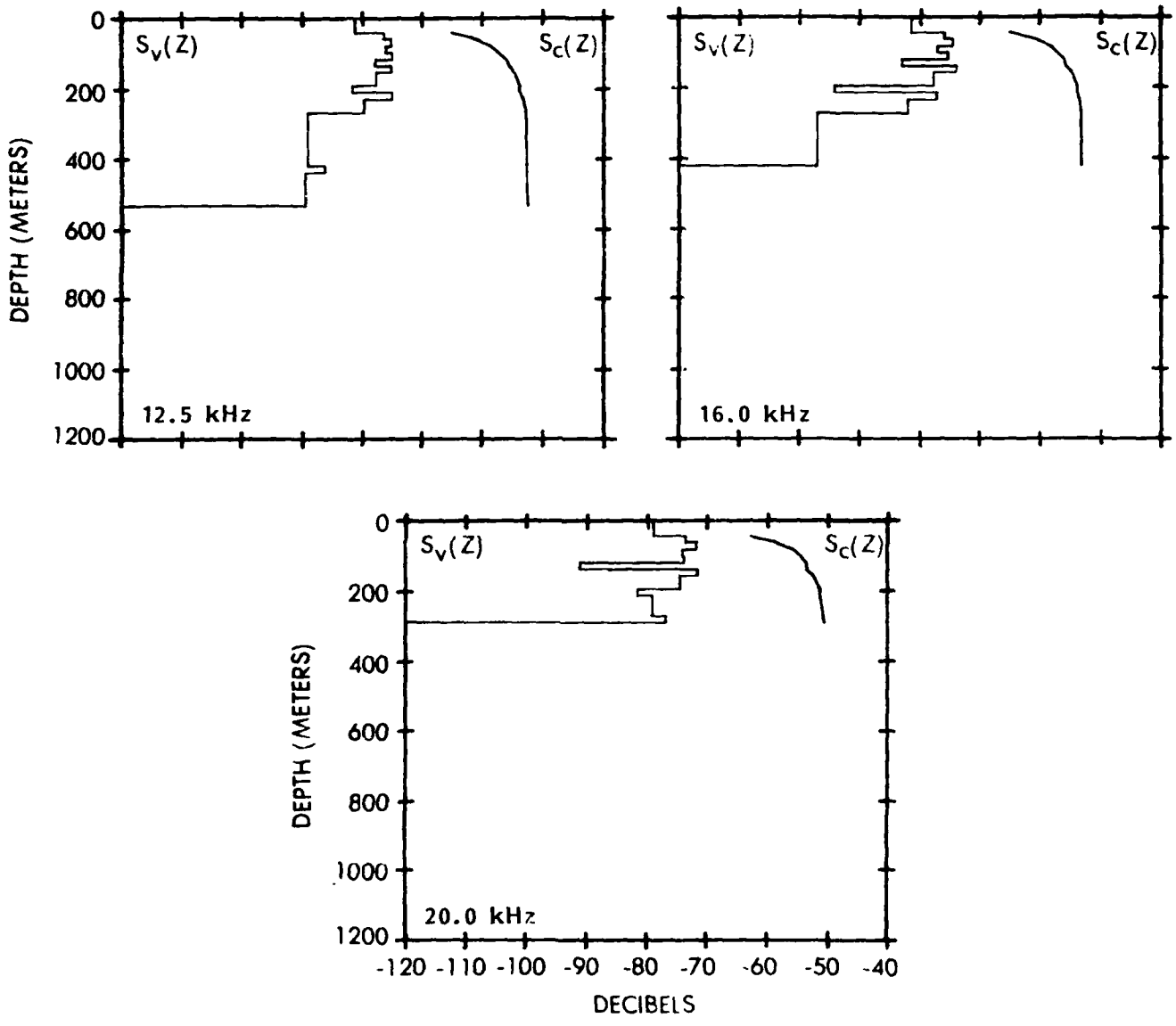

Figure B-46. CARTBCAP II, $S_v(z)$ and $S_c(z)$, 12.5 to 20 kHz, Station 3, night

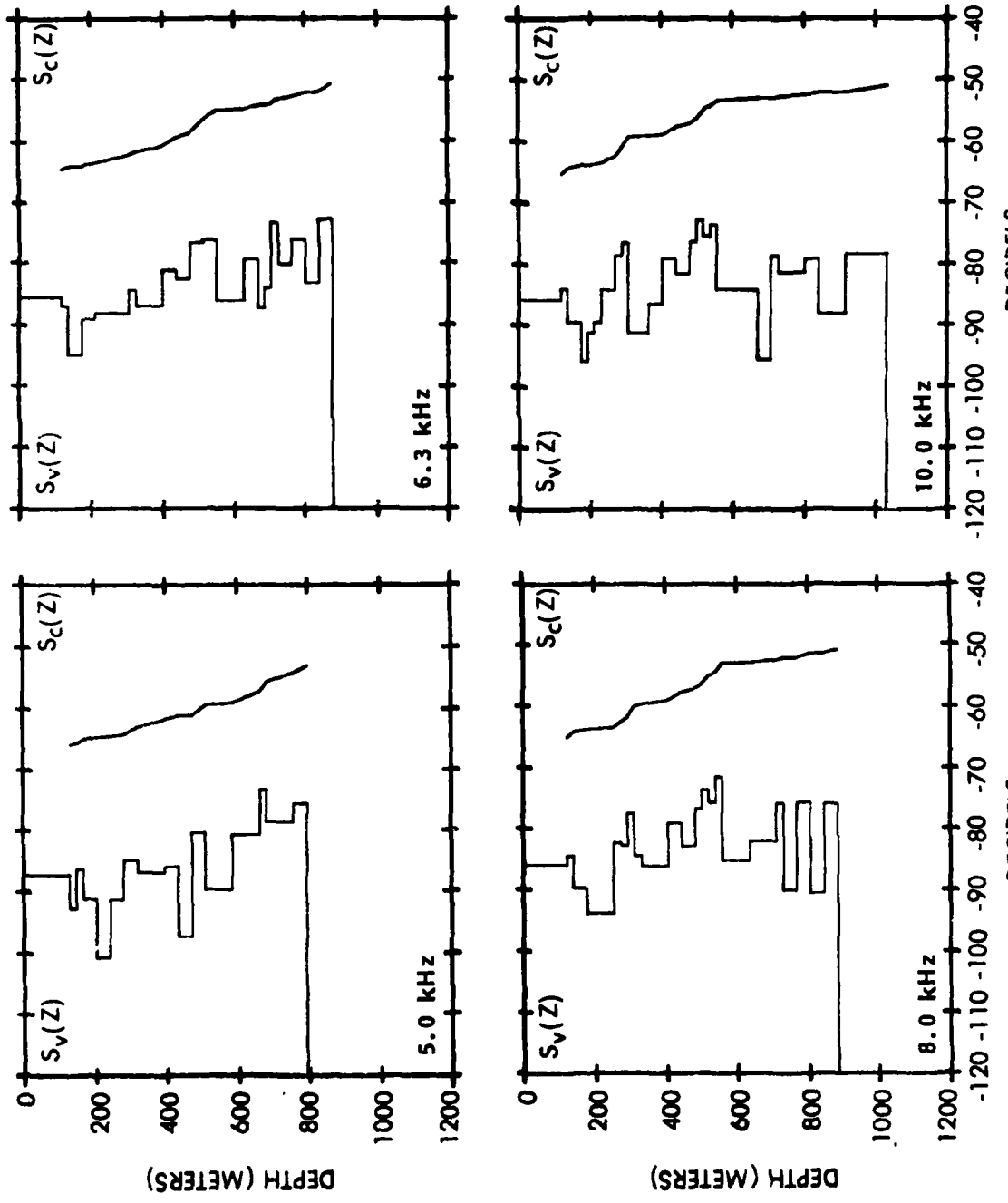

Figure B-47. CARIBCAP II, $S_v(z)$ and $S_c(z)$, 5 to 10 kHz, Station 4, day

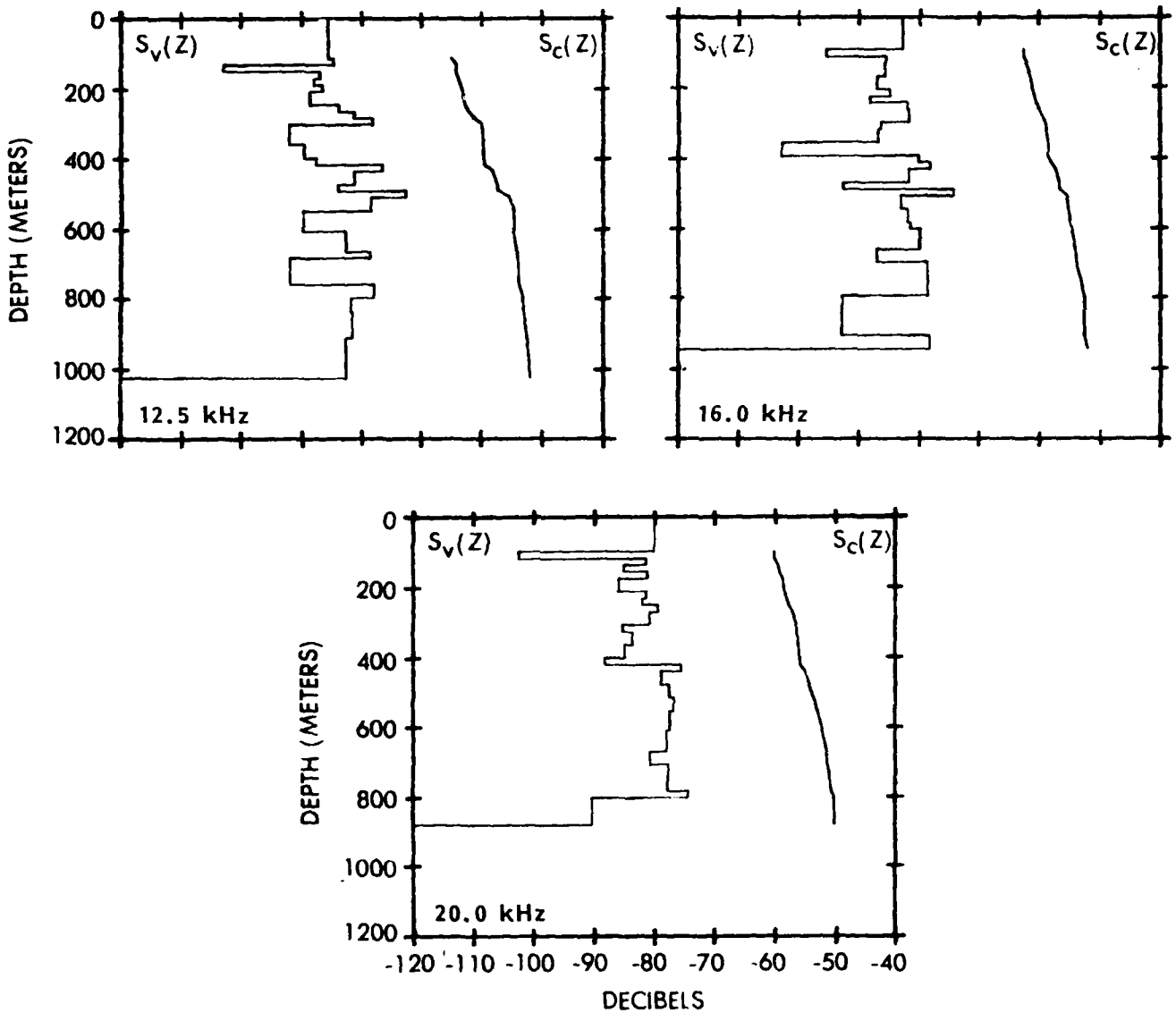

Figure B-48. CARIBCAP II, $S_v(z)$ and $S_c(z)$, 12.5 to 20 kHz, Station 4, day

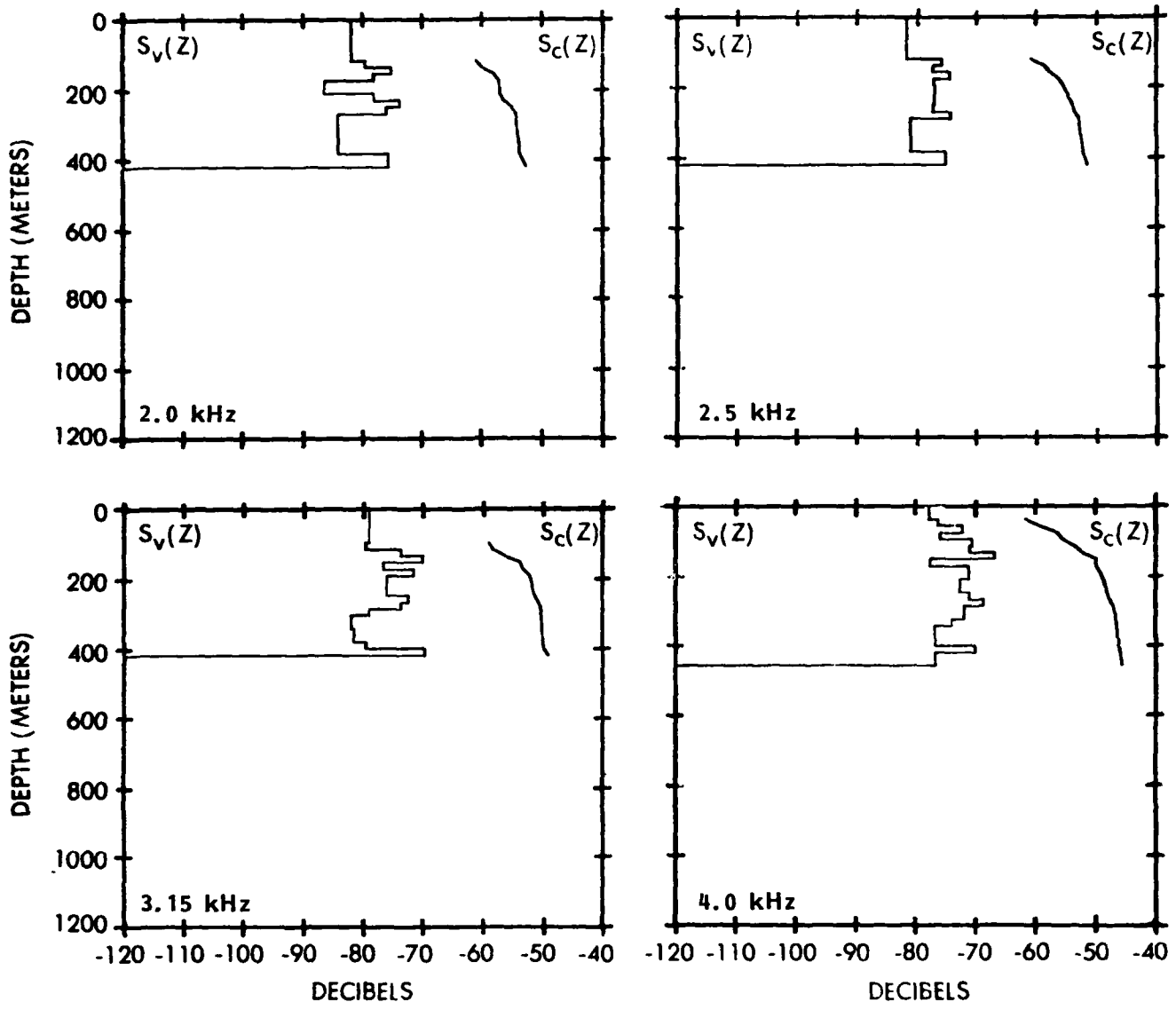

Figure B-49. CARIBCAP II, $S_V(z)$ and $S_C(z)$, 2 to 4 kHz, Station 4, night

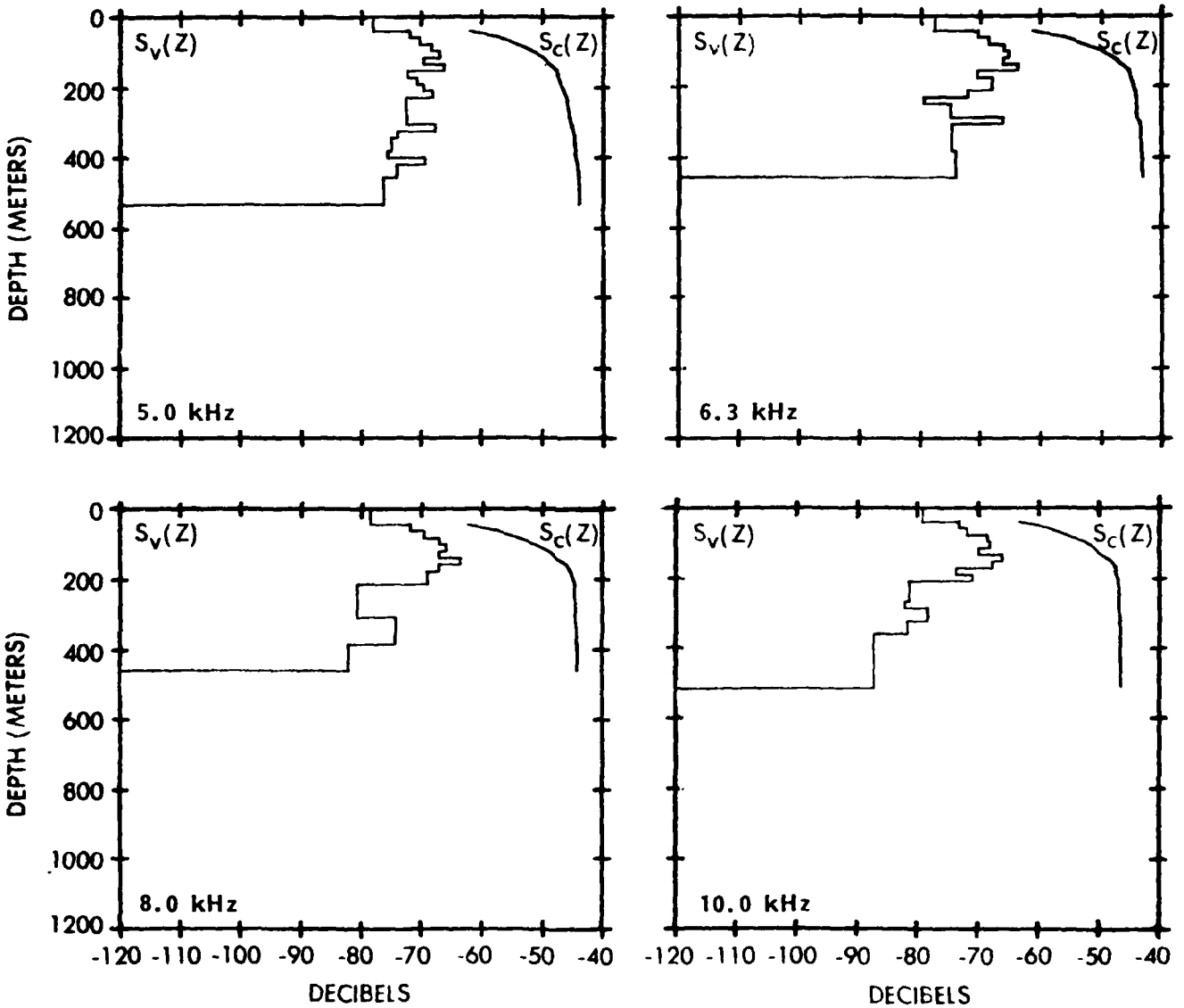

Figure B-50. CARIBCAP II, $S_V(z)$ and $S_C(z)$, 5 to 10 kHz, Station 4, night

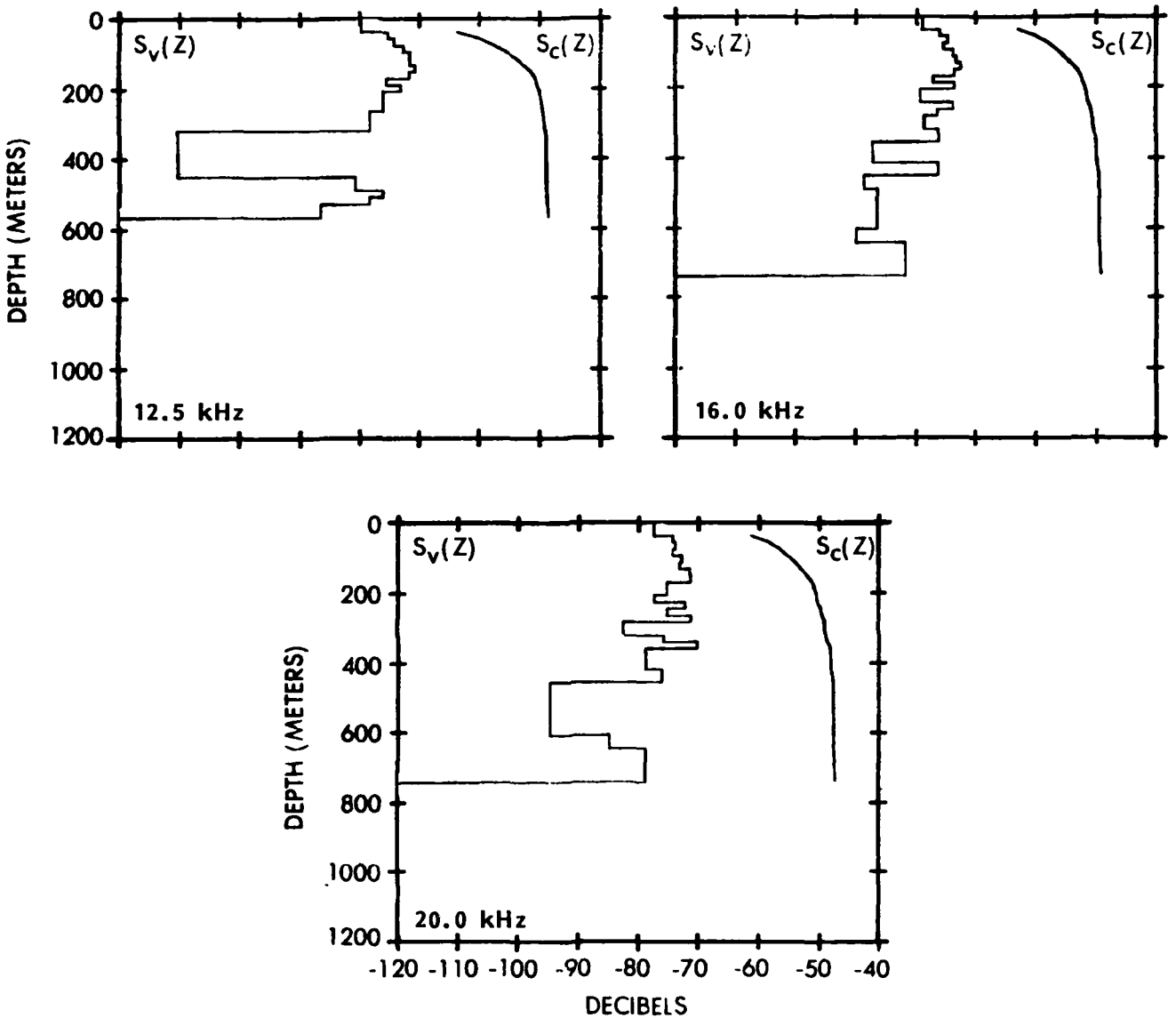

Figure B-51. CARIBCAP II, $S_V(z)$ and $S_C(z)$, 12.5 to 20 kHz, Station 4, night

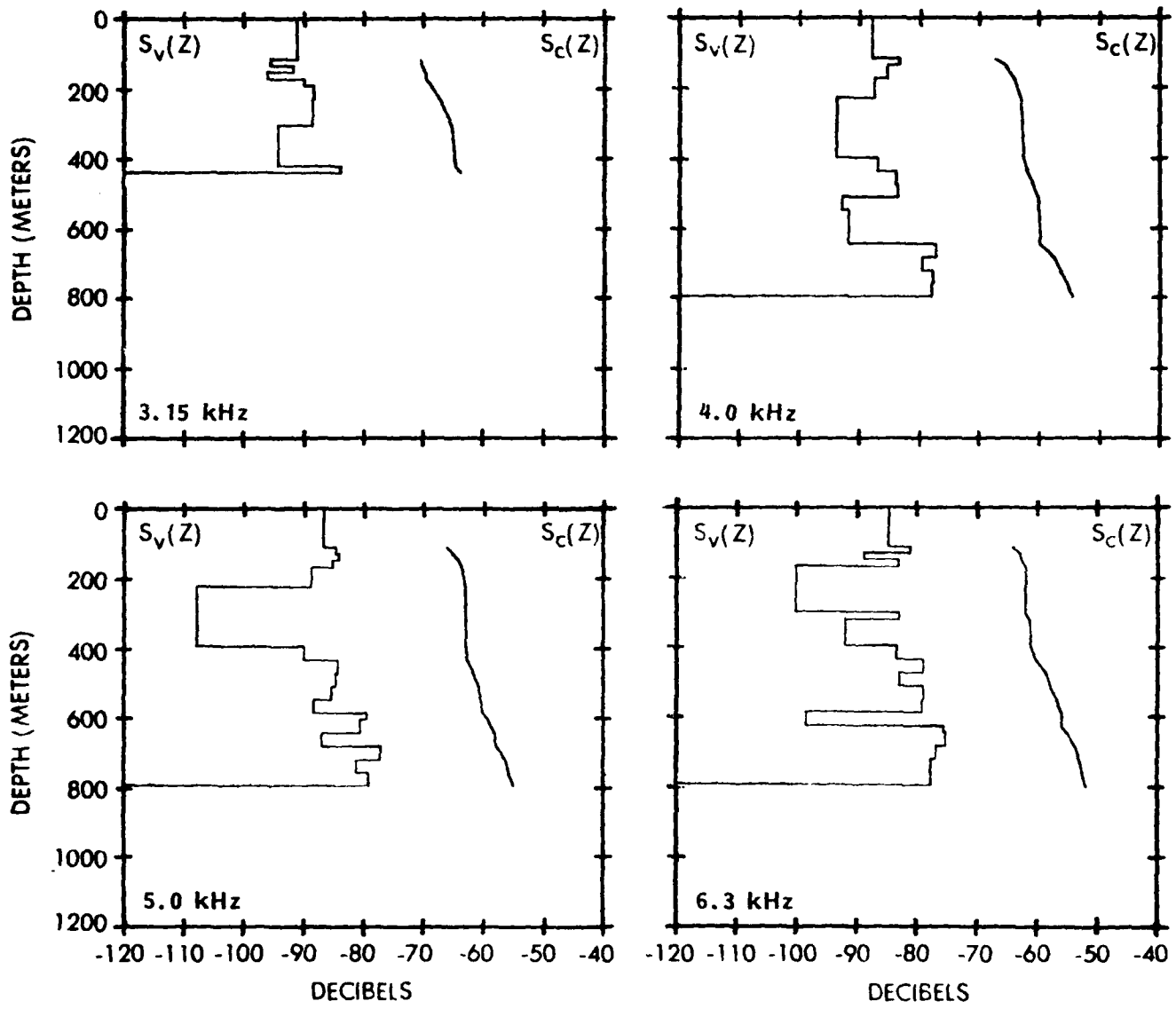

Figure B-52. CARIBCAP II, $S_v(z)$ and $S_c(z)$, 3.15 to 6.3 kHz, Station 5, day

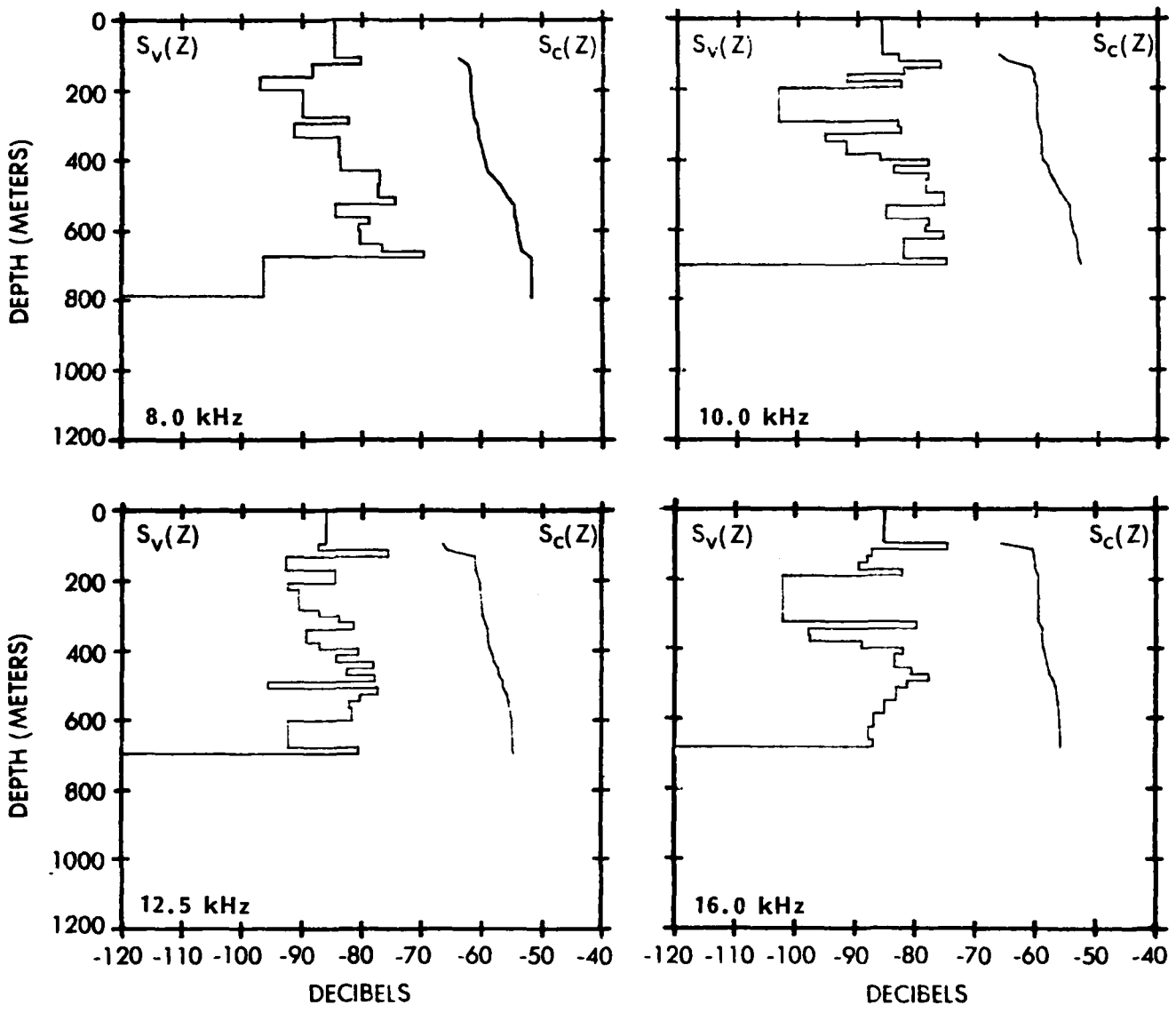

Figure B-53. CARIBCAP II, $S_V(z)$ and $S_C(z)$, 8 to 16 kHz, Station 5, day

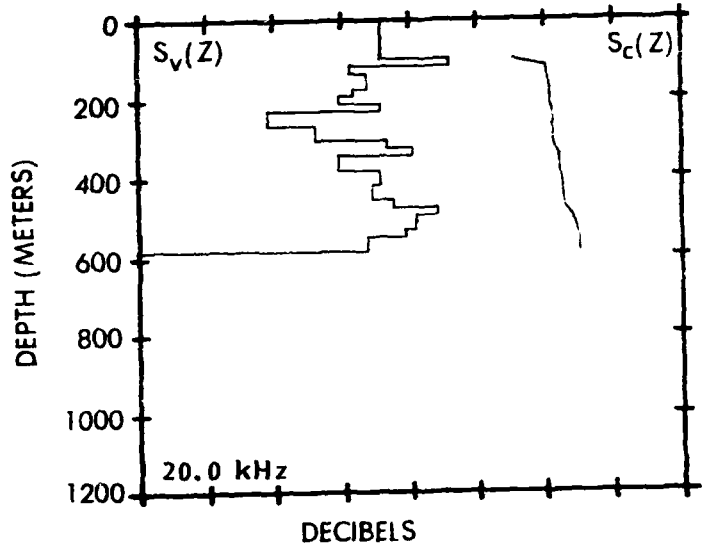

Figure B-54. CARIBCAP II, $S_v(z)$ and $S_c(z)$, 20 kHz, Station 5, day

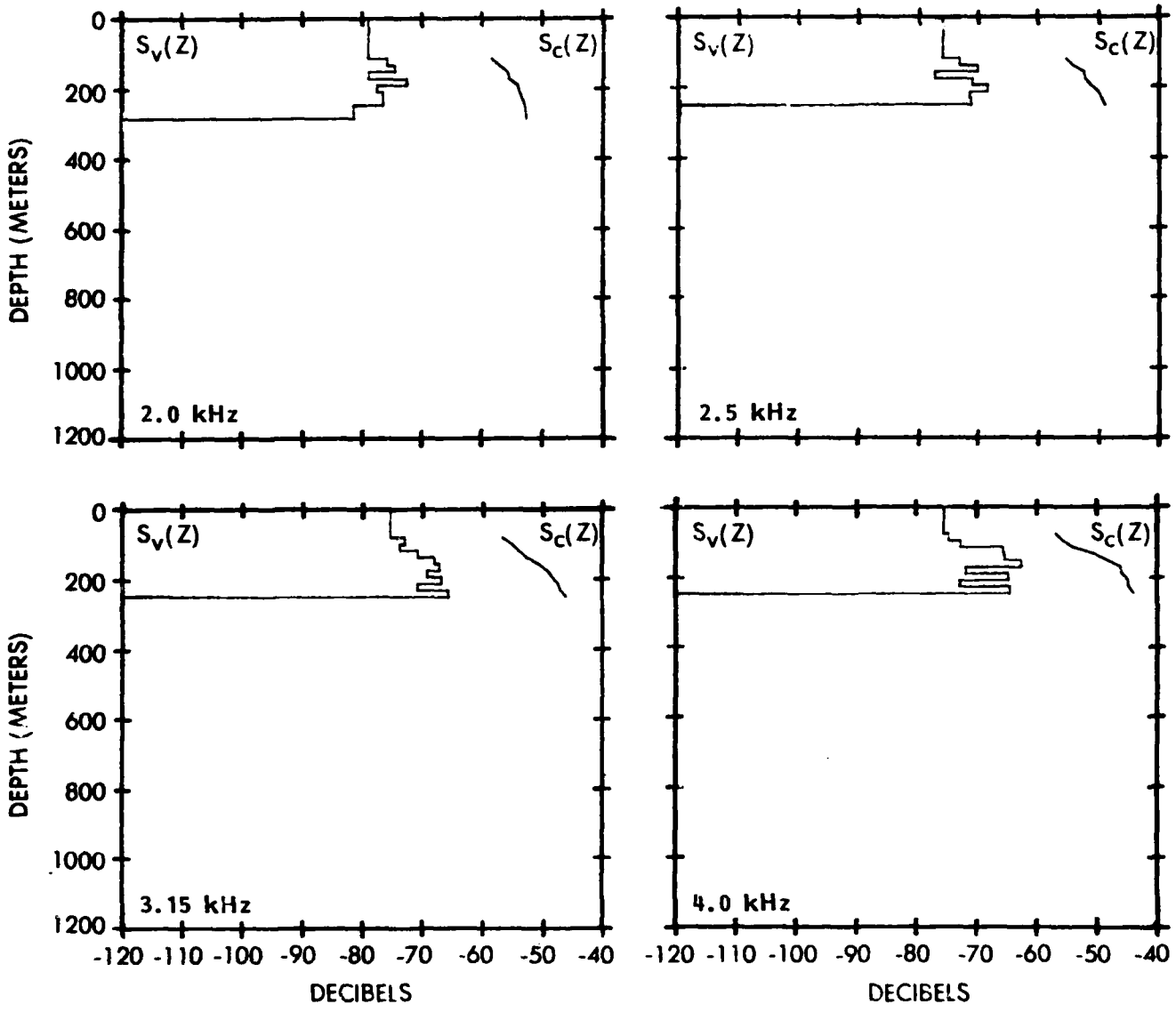

Figure B-55. CARIBCAP II, $S_v(z)$ and $S_c(z)$, 2 to 4 kHz, Station 5, night

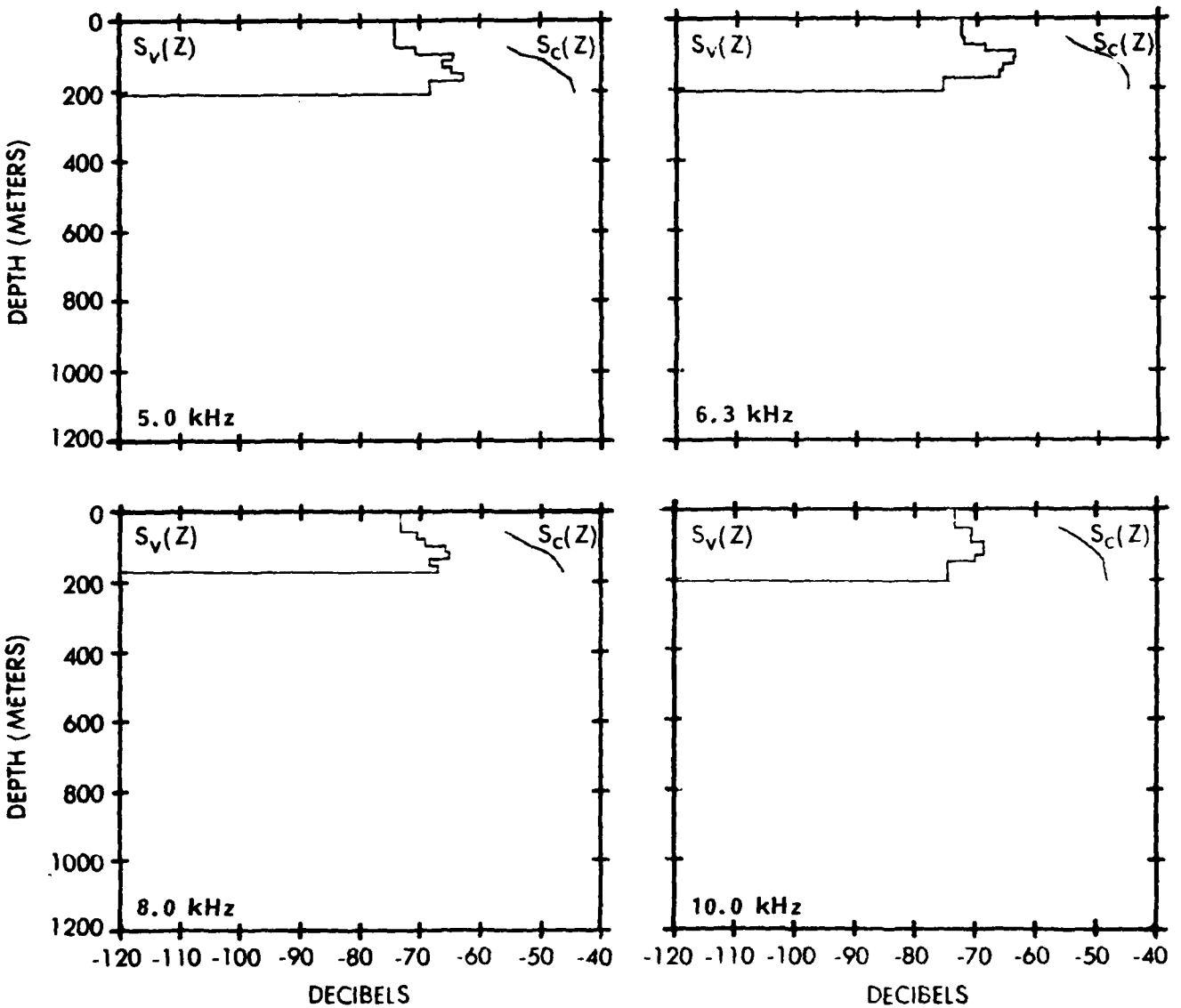

Figure B-56. CARIBCAP II, $S_v(z)$ and $S_c(z)$, 5 to 10 kHz, Station 5, night

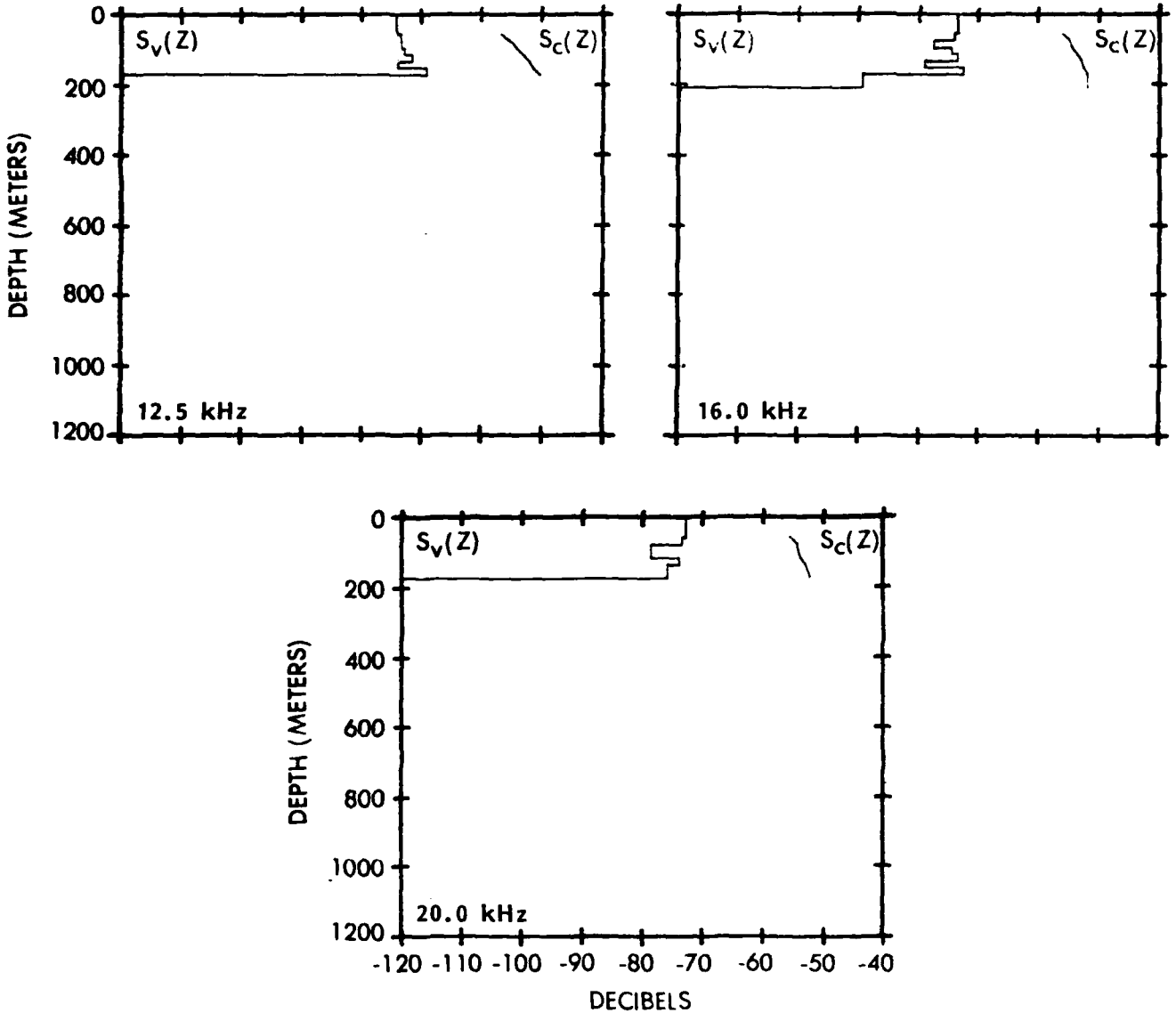

Figure B-57. CARIBCAP II, $S_v(z)$ and $S_c(z)$, 12.5 to 20 kHz, Station 5, night

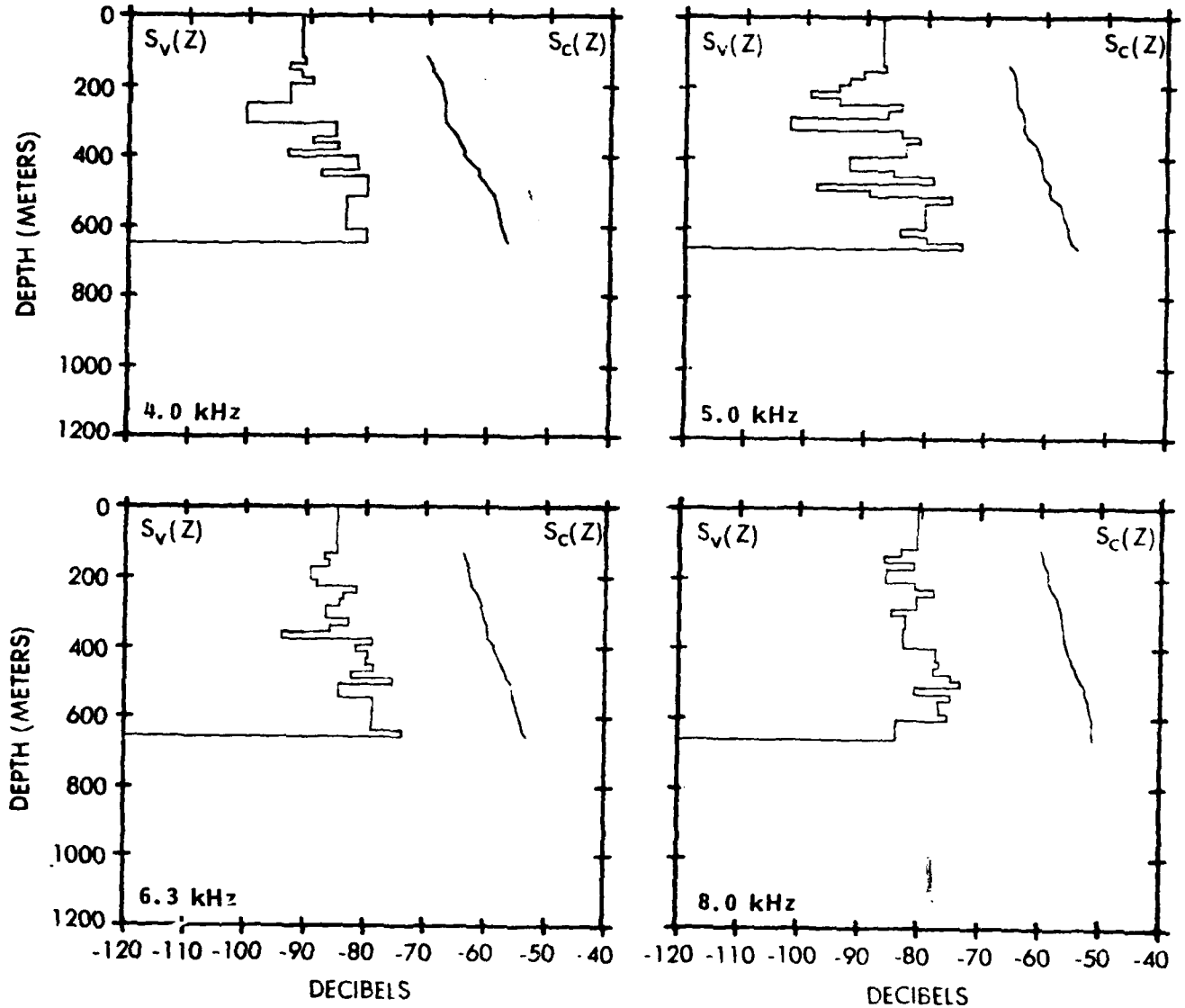

Figure B-58. CARIBCAP II, $S_v(z)$ and $S_c(z)$, 4 to 8 kHz, Station 6, day

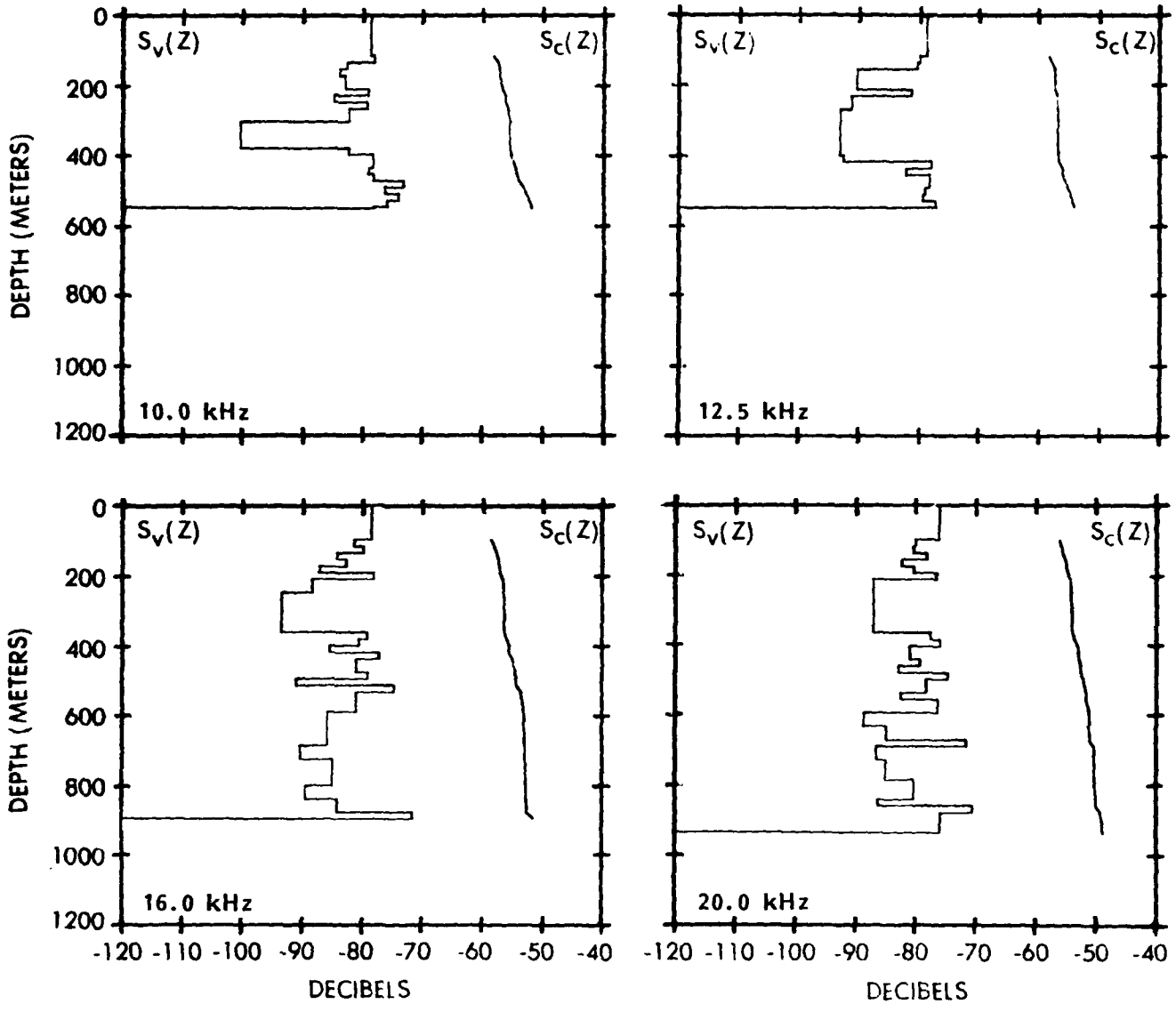

Figure B-59. CARIBCAP II, $S_v(z)$ and $S_c(z)$, 10 to 20 kHz, Station 6, day

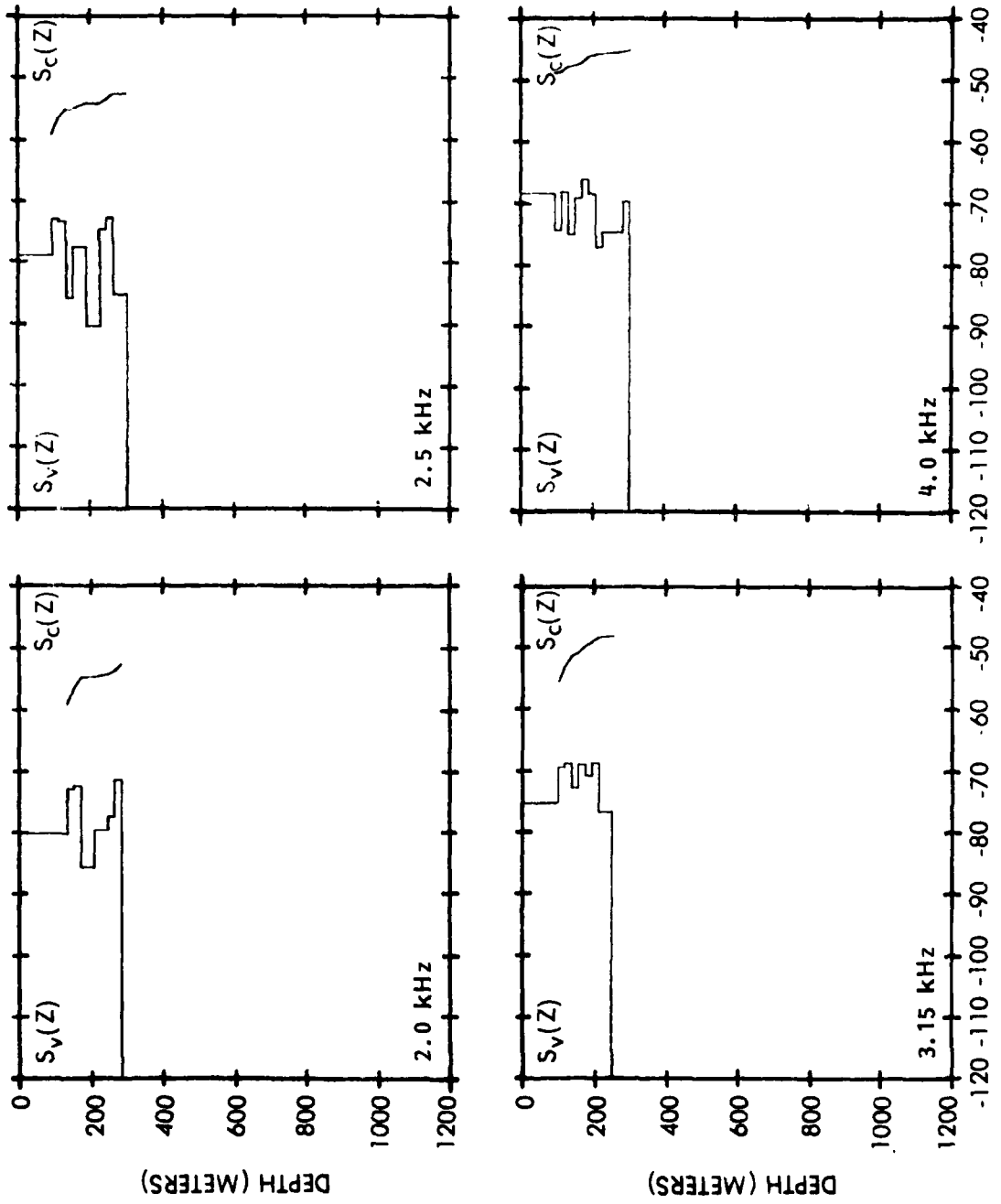

Figure B-60. CARIBCAP II, $S_v(z)$ and $S_c(z)$, 2 to 4 kHz, Station 6 night

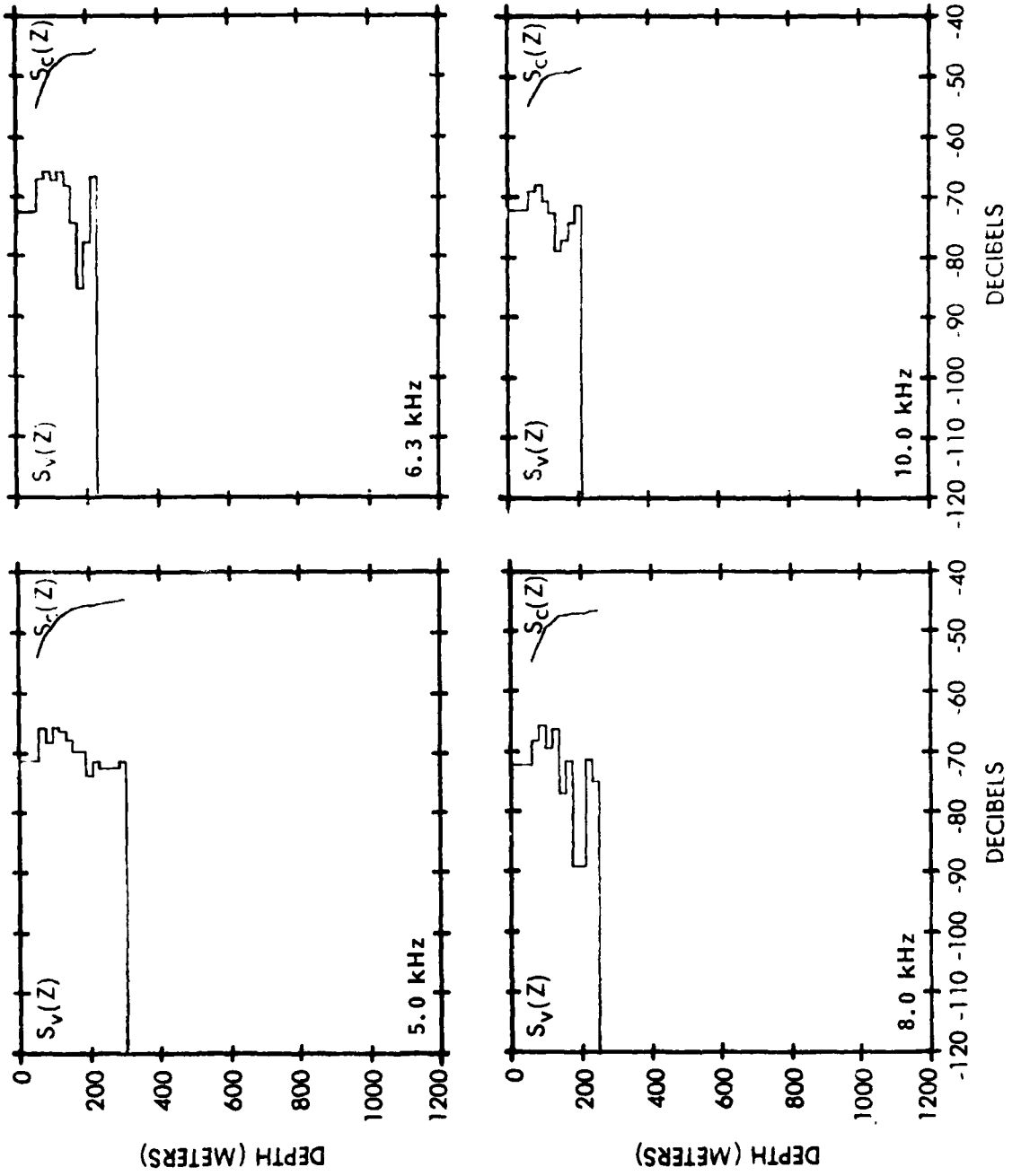

Figure B-61. CARIBCAP II, $S_v(z)$ and $S_c(z)$, 5 to 10 kHz, Station 6, night

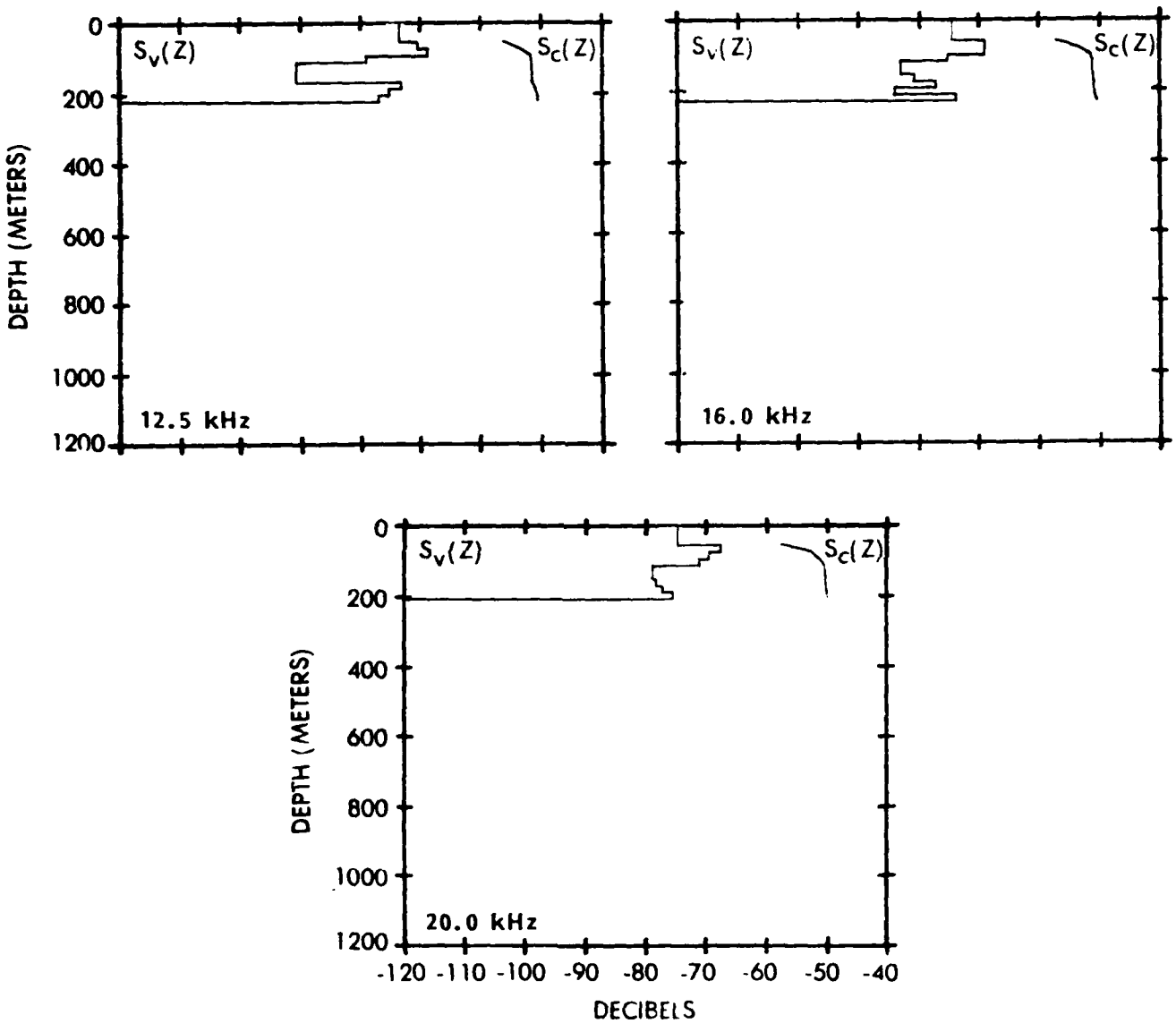

Figure B-62. CARIBCAP II, $S_v(z)$ and $S_c(z)$, 12.5 to 20 kHz, Station 6, night

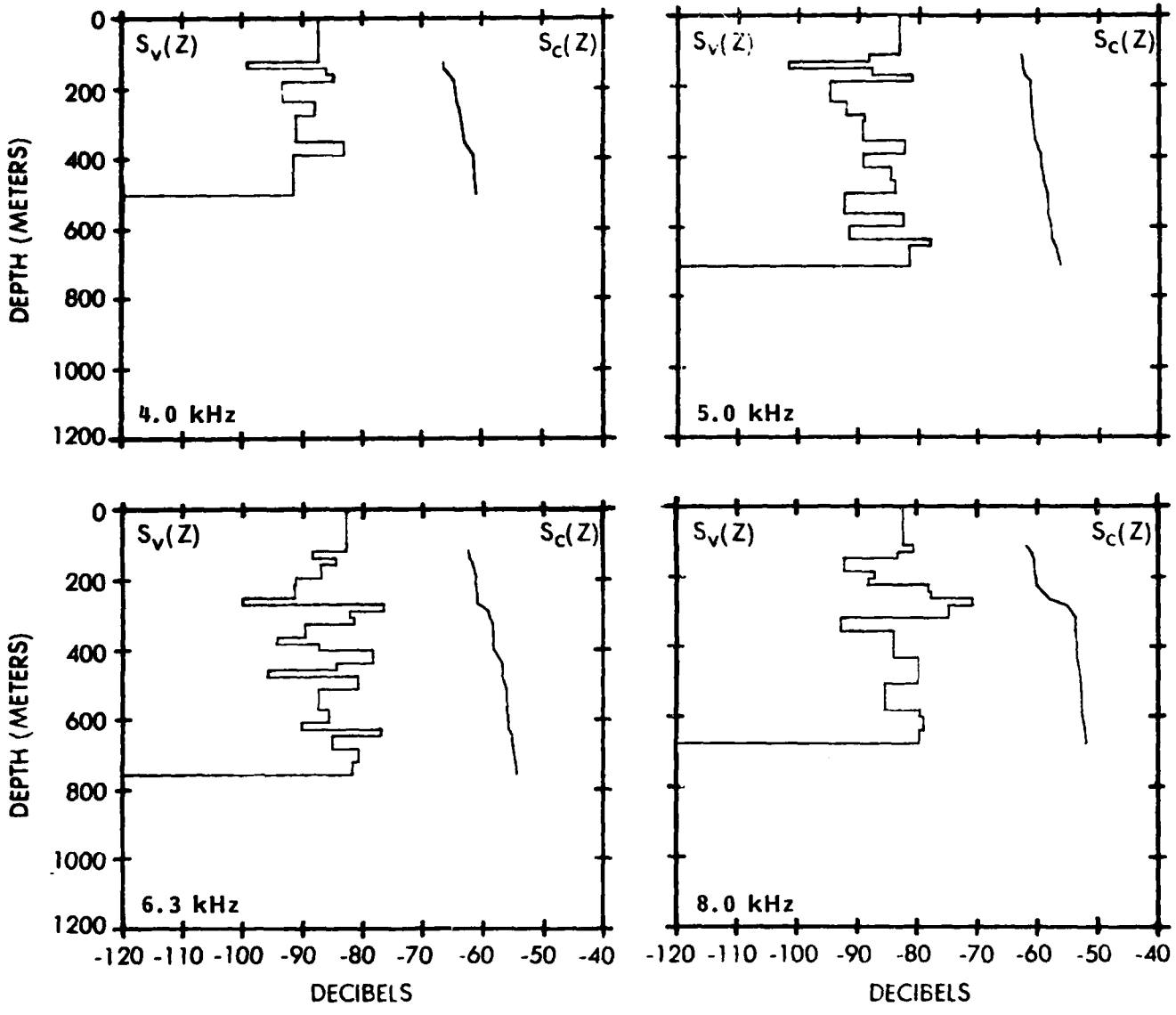

Figure B-63. CARIBCAP II, $S_v(z)$ and $S_c(z)$, 4 to 8 kHz, Station 7, day

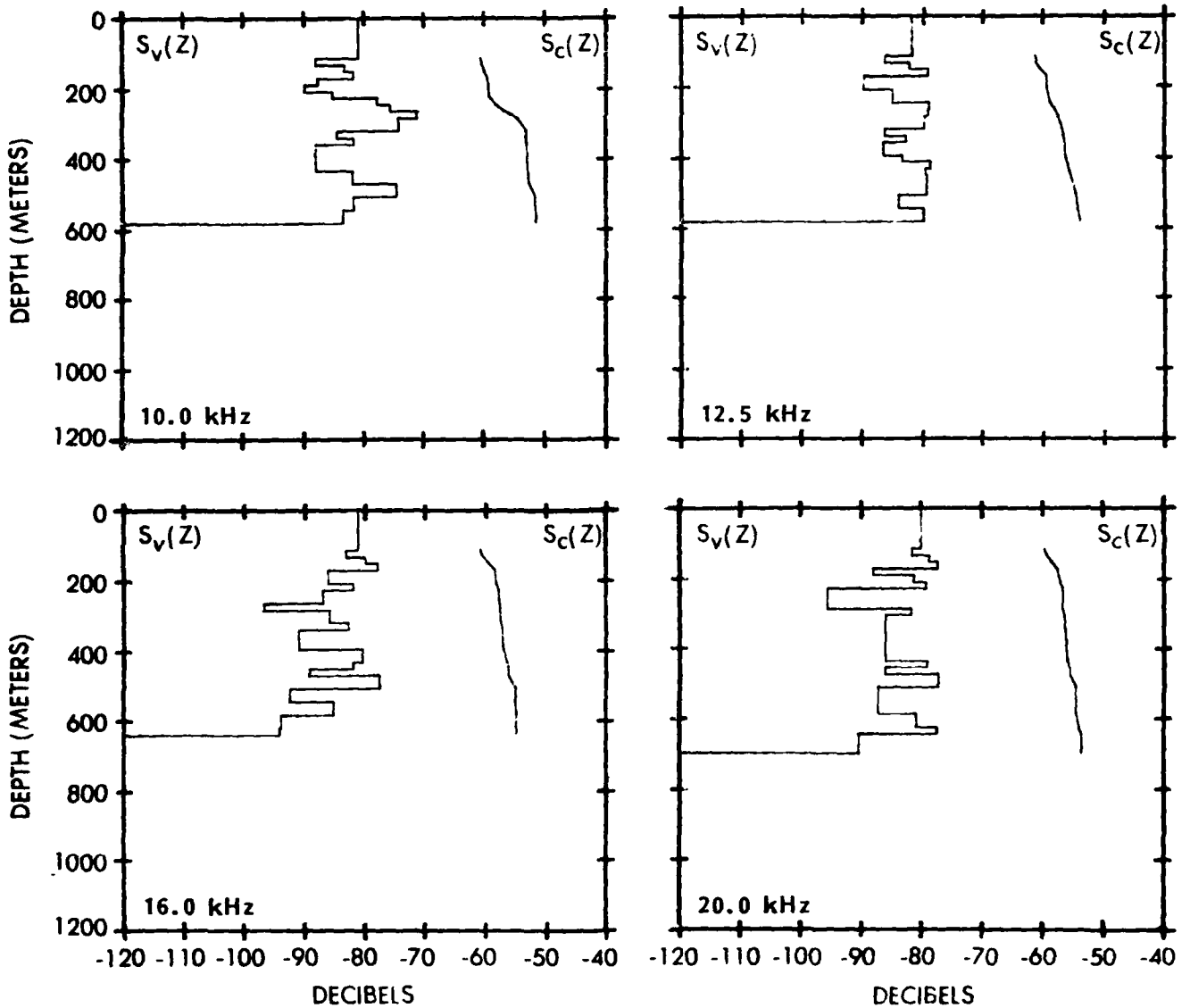

Figure B-64. CARIBCAP II, $S_V(z)$ and $S_C(z)$, 10 to 20 kHz, Station 7, day

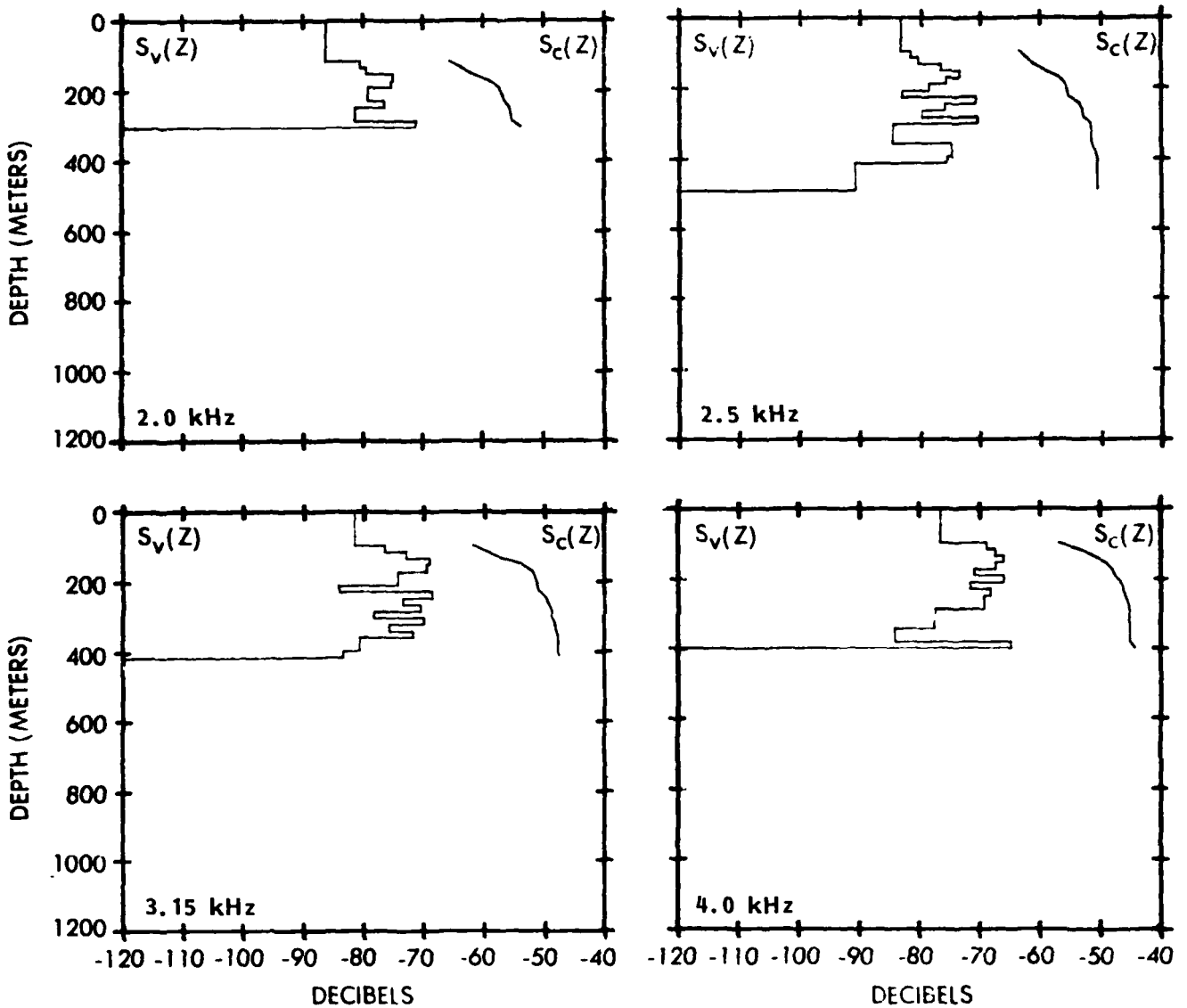

Figure B-65. CARIBCAP II, $S_v(z)$ and $Sc(z)$, 2 to 4 kHz, Station 7, night

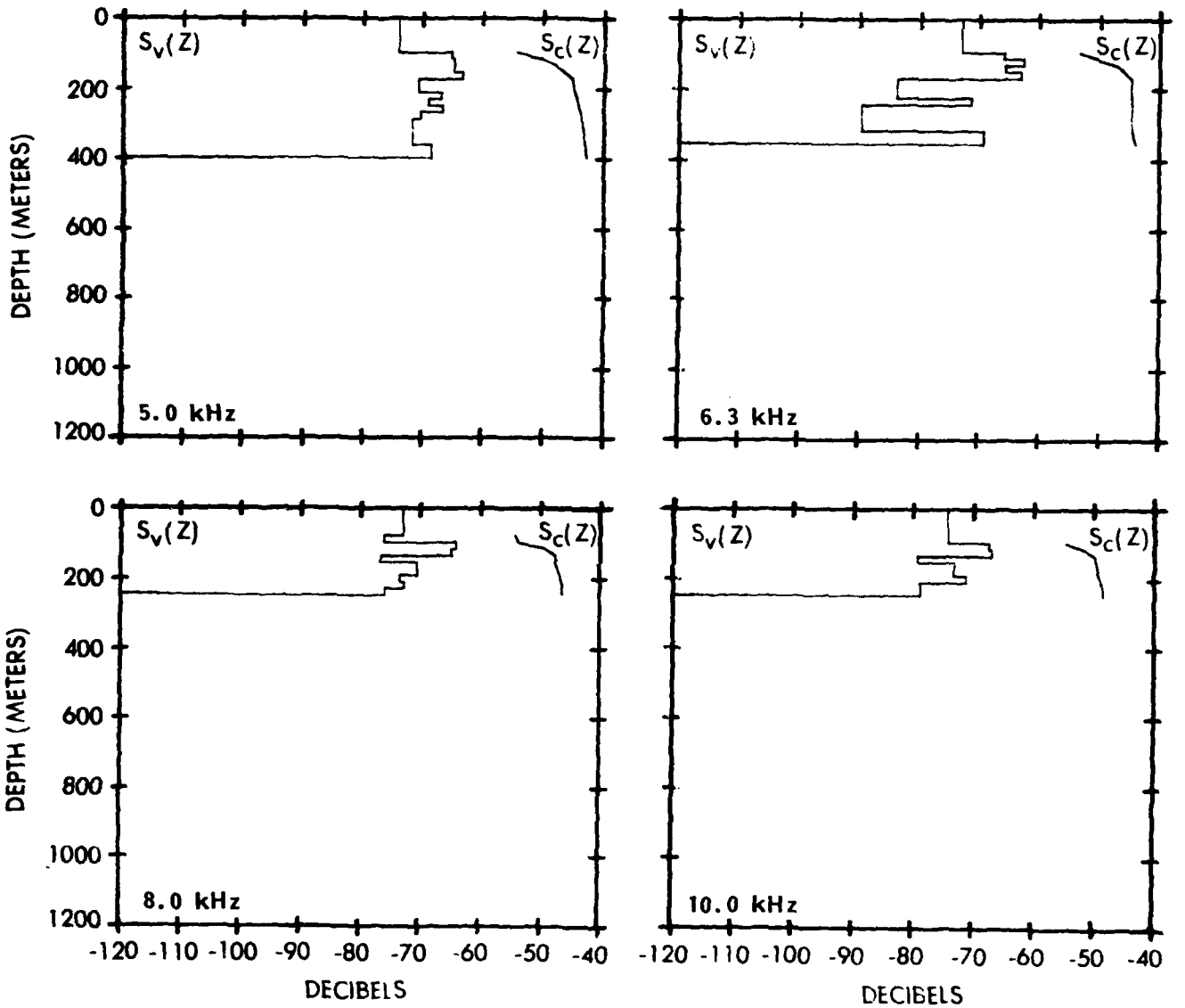

Figure B-66. CARIBCAP II, $S_v(z)$ and $S_c(z)$, 5 to 10 kHz, Station 7, night

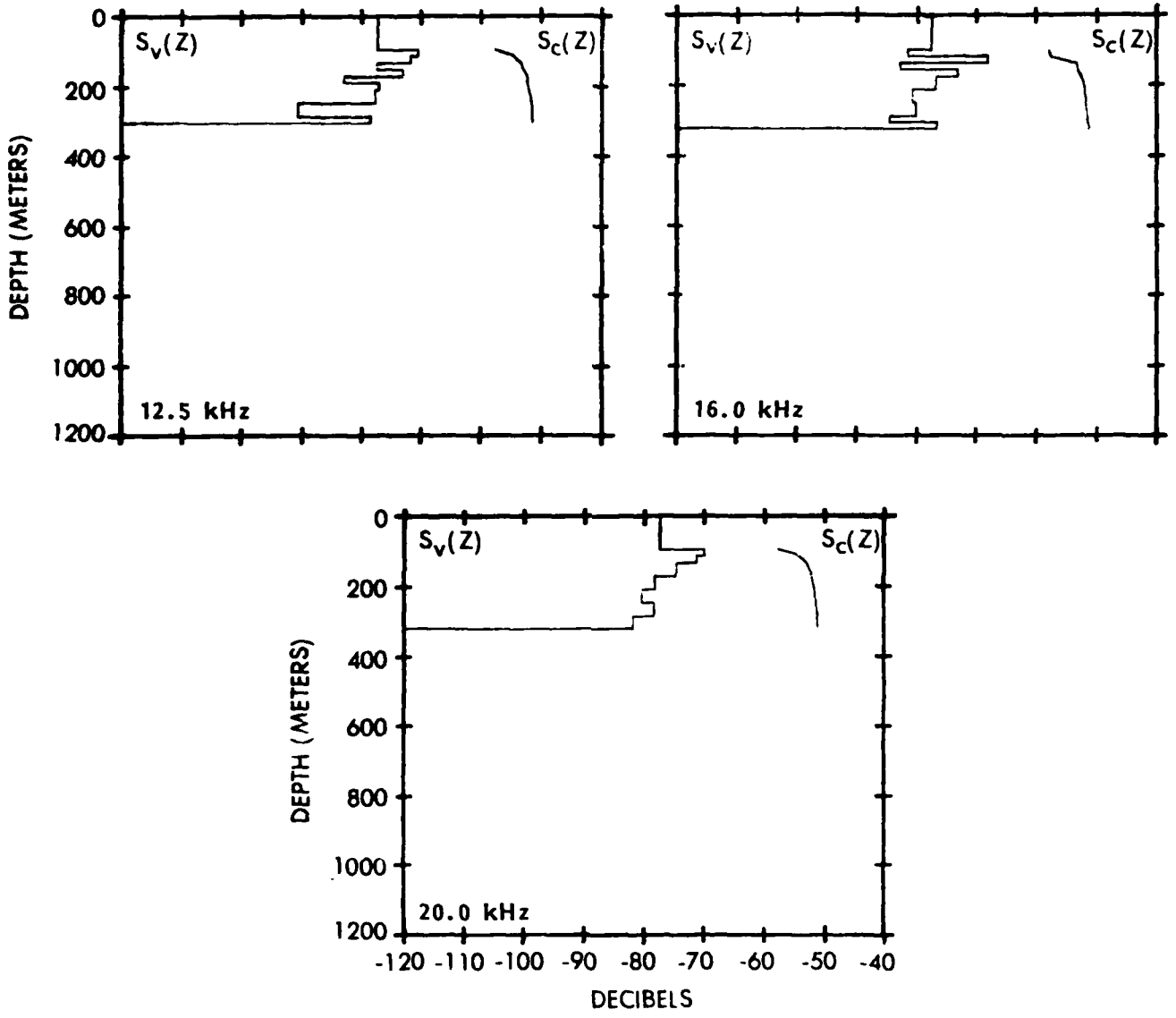

Figure B-67. CARIBCAP II, $S_V(z)$ and $S_C(z)$, 12.5 to 20 kHz, Station 7, night

UNCLASSIFIED

SECURITY CLASSIFICATION OF THIS PAGE (When Data Entered)

REPORT DOCUMENTATION PAGE

READ INSTRUCTIONS BEFORE COMPLETING FORM

1. REPORT NUMBER: NORDA Technical Note 128	2. GOVT ACCESSION NO.: AD-A118165
3. RECIPIENT'S CATALOG NUMBER:	
4. TITLE (and Subtitle): Volume Reverberation Measurements in the Eastern Caribbean Sea	5. TYPE OF REPORT & PERIOD COVERED: Final
	6. PERFORMING ORG. REPORT NUMBER:
7. AUTHOR(s): Coleman Levenson, Marcia A. Wilson, Richard H. Love, Robert A. Fisher	8. CONTRACT OR GRANT NUMBER(s):
9. PERFORMING ORGANIZATION NAME AND ADDRESS: Ocean Acoustics Division, Naval Ocean Research and Development Activity, NSTL Station, Mississippi 39529	10. PROGRAM ELEMENT, PROJECT, TASK AREA & WORK UNIT NUMBERS:
11. CONTROLLING OFFICE NAME AND ADDRESS: Ocean Acoustics Division, Naval Ocean Research and Development Activity, NSTL Station, Mississippi 39529	12. REPORT DATE: November 1981
	13. NUMBER OF PAGES: 122
14. MONITORING AGENCY NAME & ADDRESS(if different from Controlling Office):	15. SECURITY CLASS. (of this report): Unclassified
	15a. DECLASSIFICATION/DOWNGRADING SCHEDULE:

16. DISTRIBUTION STATEMENT (of this Report)

Unlimited

DISTRIBUTION STATEMENT A
Approved for public release;
Distribution Unlimited

17. DISTRIBUTION STATEMENT (of the abstract entered in Block 20, if different from Report)

18. SUPPLEMENTARY NOTES

19. KEY WORDS (Continue on reverse side if necessary and identify by block number)

Volume Reverberation
Column strength

20. ABSTRACT (Continue on reverse side if necessary and identify by block number)

Volume reverberation measurements were made utilizing explosive sources and an omnidirectional receiver in the Caribbean Sea along the Aves Ridge during June 1974 and February through March 1977. This report presents results of those measurements in the form of scattering strength profiles and column strengths for one-third octave bands. Comparisons are made between the two sets of data and previous data taken in the same area. Discrete biological net tows at one station are also compared to peak scattering depths.

DD FORM 1 JAN 73 1473 EDITION OF 1 NOV 65 IS OBSOLETE
S/N 0102-LF-014-6601

UNCLASSIFIED
SECURITY CLASSIFICATION OF THIS PAGE (When Data Entered)